The Role of Sea Urchins and Kelp Loss in Changing the Assemblage Structure and Trait Diversity of shallow Marine Communities

by

© Jasmin Maria Schuster

A Thesis submitted to the School of Graduate Studies
in partial fulfillment of the requirements for the degree of
Doctor of Philosophy, Marine Biology

Department of Ocean Sciences
Memorial University of Newfoundland and Labrador
St. John's, Newfoundland, Canada

January, 2023

Abstract

Coastal habitats, such as kelp forests, are declining in many areas of the ocean. Change is driven by various factors, including increases in sea urchins, which are kelp consumers (grazers) that can rapidly remove kelp forests and create barrens devoid of macroalgae. At the same time, warming and cooling trends and extreme heat events due to anthropogenic climate change are restructuring reef communities around the globe. Biological assemblages found on shallow reefs are thus responding to the loss of complex habitat and ocean temperature changes simultaneously. The aims of this thesis were to: I) examine responses of shallow marine populations and communities to kelp loss, with a focus on urchin-driven kelp loss; and II) assess whether kelp loss alters assemblage vulnerability to anthropogenic temperature change. In my thesis I utilized measures of an organisms' fundamental physiological response, and global biodiversity data from kelp ecosystems, to assess assemblage change at multiple levels of biological organization and from local to global spatiotemporal scales. I found that neighbouring kelp and sea urchin barren habitats have populations and communities with different physiological characteristics that relate to energetics. For example, green sea urchin (*Strongylocentrotus droebachiensis*) populations from kelp forests had higher routine metabolic rates across the range of temperatures tested than those from adjacent barrens. Sea urchins from kelp forests were also less sensitive to temperature increases than their barrens counterparts. Findings from subsequent experiments suggest that metabolic

differences among sea urchin populations relate to the availability of kelp as a food source. At the community level, I report that kelp and barren habitats also host fish communities with distinct realized thermal affinities and geographic range sizes, with more warm-affinity species in regions close to the tropics present at barrens than in kelp habitats. Sea urchins, thus, facilitate tropicalization processes on rocky reefs in temperate regions. Similar tropicalization signals also emerged in a kelp forest ecosystem during two severe heat events in the Pacific Northwest, with stronger signals of tropicalization in urchin barrens than at kelp forested sites. Overall, loss of kelp (as habitat and food source) leads to a reorganization of reef assemblages, moving assemblages towards greater sensitivity to warming. My findings highlight the importance of protecting and restoring complex habitats to maintain the functioning and diversity of marine biological assemblages.

Acknowledgements

Dr. Amanda Bates has supported me in so many ways that I am grateful for, as a supervisor, mentor, collaborator, connector, cheerleader and friend. I am just as inspired by her brilliant science and passion as I was 9 years ago, when I was a first year undergraduate. I appreciate Amanda's trust for me to lead our Reef Life Survey team, a task full of joy and opportunity. As a supervisor, Amanda has supported my growth as a scientist, pushed me intellectually, inspired curiosity and creativity, cared for my physical, mental and financial health, and above all, has refused to stop believing in me. This last part has meant the most. The biggest, heartfelt thanks therefore extend to you, Amanda.

My Ph.D. work was supported and improved by many valued collaborators, that shared their knowledge, time and resources. Thank you to Drs. Rick Stuart-Smith and Graham Edgar, who welcomed me into the Reef Life Survey world, sharing their passion for the underwater world and infectiously spreading the gospel of monitoring. It has been a pleasure collaborating and working with them both. My gratitude also goes to Dr. David Kushner for sharing his in-depth knowledge of the ecosystems in the Channel Islands, and his generosity with time for discussions.

Thanks to the members of my supervisory committee, Drs. Kurt Gamperl and Patrick Gagnon, for providing thoughtful and helpful input during the development stage of this thesis, and being constructive and detailed collaborators. A special

thanks also to Dr. Kurt Gamperl for sharing equipment and expert advice on running respirometry experiments. I am also grateful to Dr. Paul Snelgrove, for sharing lab space at the Ocean Science Centre.

Thanks to the entire community of staff, educators and researchers at the Bamfield Marine Science Centre. BMSC was a sanctuary where I could complete my final experiments and field surveys, while shielded from the Covid-19 pandemic. Many people at BMSC have supported this thesis through inspiring conversations, helping problem-solve and providing resources – thank you! I also want to thank Tao Eastham and Siobhan Gray especially, for going above and beyond.

I am immensely grateful to all the Reef Life Survey and KFMP divers, who dedicate so much time, skill and effort to generating the biodiversity data presented in this thesis. Their contributions will positively benefit researchers and society at large for many years to come.

Thanks to the most amazing lab mates from the MUN and UVic melting pot of Bates students. They have enriched this Ph.D. experience by making it fun, balanced and not-too-serious. A special thanks to Cerren, who was my most supportive academic sister from day one. Valesca, Brandy and Jackson, a massive thank you, for helping with fieldwork and data collection for this thesis.

I’m ever grateful to my friends who shared the ups and downs of this journey with me. Lilli Mayerhofer, thank you for always listening.

Thank you Julek, my unwavering cheerleader, problem-solver and defender of my well-being. Thanks for running off into the sun, water or mountains with me, when it was needed. Our tandem-Ph.Ds have benefited so much from the solidarity and humor shared along the journey.

For a lifetime of optimism, encouragement, love and Urvertrauen, I thank my family. Mama, none of it is possible without you. Julia and Jana, thank you for always being proud of me.

Thank you, Papa, for planting and watering the marine biology seed.

I acknowledge that the waters and lands where this PhD research was conducted are the ancestral and unceded territories of the of the Mi'kmaq and Beothuk (*island of Newfoundland*) and of the Huu-ay-aht and Tseshaht First Nations (Vancouver island: *Barkley Sound*). I am grateful for their past and present stewardship of the life around us, and for the opportunity to learn and grow on their lands and waters.

Funding for this research was provided by the Canada Research Chairs program, an NSERC Discovery grant awarded to Dr. Amanda Bates, and the School of Graduate Studies at Memorial University of Newfoundland and Labrador. A PADI Foundation grant also supported this work.

Table of Contents

Abstract……ii

Acknowledgements……iv

List of Tables……ix

List of Figures……xi

List of Common Abbreviations……xviii

Co-authorship Statement……xx

Chapter 1 - Introduction *1*

1.1 Seascape change 2

1.2 A traits perspective of assemblage change 6
1.2.1 Why traits approaches are useful 7
1.2.2 The environmental niche and derived traits 8
1.2.3 From individuals to species – environmental impacts across levels of biological organization 12

1.3 The underwater forest as a study system 15
1.3.1 Kelps are foundational habitat formers 16
1.3.2 Sea urchins drive seascape change in underwater forests 17
1.3.3 Temperature drives seascape change in underwater forests 20

1.4 Thesis chapter overview 21

1.5 Literature cited 24

Chapter 2 - Distinct Realized Physiologies in Green Sea Urchin (Strongylocentrotus droebachiensis) Populations from Barren and Kelp Habitats *41*

2.1 Abstract 42

2.2 Introduction 43

2.3 Methods 47
2.3.1 Sea urchin collections 47
2.3.2 Experimental system for measuring oxygen consumption 50
2.3.3 Oxygen consumption measurements 51
2.3.3.1 Pre-measurement procedures and containment of sea urchins 51
2.3.3.2 'Acute' temperature exposure protocol (Assay Method 1) 52
2.3.3.3 Temperature 'ramping' exposure protocol (Assay Method 2) 53
2.3.4 Ash-free dry mass 54
2.3.5 Data Processing and Analyses 54

2.4 Results 57

2.5 Discussion 65

2.6 References 74

2.7 Appendix A – Supplementary figures and tables for Chapter 2 83

Chapter 3 - The Role of Kelp Availability and Type on the Energetic State and Thermal Tolerance of Sea Urchin and Gastropod Grazers. 105

3.1 Abstract 106

3.2 Introduction 108

3.3 Methods 114
3.3.1 Organism collection 114
3.3.2 Food treatments and cage set-up 115
3.3.3 Experimental assay system for measuring oxygen consumption 118
3.3.4 Pre-measurement procedures and treatment of grazers 119
3.3.5 Oxygen consumption measurements 120
3.3.6 Heat resistance experiment 121
3.3.7 Calculation of $\dot{M}O_2$ 122
3.3.8 Ash-free dry mass 123
3.3.9 Statistical analyses 124

3.4 Results 125

3.5 Discussion 133

3.6 Conclusion 139

3.7 References 139

3.8 Appendix B – Supplementary figures and tables for Chapter 3 150

Chapter 4 - Tropicalization of Temperate Reef Fish Communities Facilitated by Urchin Grazing and Diversity of Thermal Affinities. 169

4.1 Abstract 170

4.2 Introduction 171

4.3 Methods 177
4.3.1 Survey data 177
4.3.2 Community temperature metrics and thermal affinity 179
4.3.3 Statistical modelling 182

4.4 Results 183

4.5 Discussion 189

4.6 References 197

4.7 Appendix C – Supplementary analysis for Chapter 4 204
C1 Supplementary Methods 204
C1.1 Functional richness 204
C2 Supplementary Results 204
C3 Supplementary Discussion 205
C4 References 206

4.8 Appendix D – Supplementary figures and tables for Chapter 4 207

Chapter 5 - Rapid Fish Community Response to Two Severe Marine Heat Events in the Pacific. *242*

5.1 Abstract **242**

5.2 Introduction **244**

5.3 Methods **251**

5.3.1 Channel Islands National Park's kelp forest monitoring program (KFMP) 251

5.3.2. Community temperature metrics and thermal affinity 255

5.3.3 Functional trait classification 257

5.3.4 Statistical modelling 257

5.4 Results **258**

5.4.1 Community thermal diversity 258

5.4.2 Individual species responses 264

5.4.2.1 Fish indicator species and sea urchins 265

5.4.3 Habitat-specific tropicalization signals 270

5.4.4 Trait change 274

5.5 Discussion **274**

5.6 References **281**

5.7 Appendix E – Supplementary figures and tables for Chapter 5 ..... **288**

Chapter 6 – Overview, Synthesis and Future Directions *323*

6.1 Overview **323**

6.2 Chapter summaries **325**

6.3 Synthesis **328**

6.3.1 Future directions 336

6.4 Final remarks **338**

6.5 References **339**

Appendix F – Biodiversity Surveys of Shallow Rocky Reefs *347*

Reef Life Survey Canada – standardized biodiversity surveys **347**

List of Tables

Table 1.1 Definitions for fundamental and realized niche that span levels of biological organization, as applied throughout this thesis. Limited examples are given for levels not considered in this body of work. The final column ('Thesis application') indicates which traits/levels are addressed in the thesis chapters. . 14

Table 2.1 Details on the green sea urchin collection sites used in these experiments. The 'Protocol' column indicates in which experiment a given group of sea urchins was used. Two experimental protocols were used; an 'acute' temperature protocol and a 'ramping' protocol (see methods). The latter was used for the construction of individual thermal response curves (TRCs). 'SW Temp.' indicates ambient seawater temperature (ºC) at the time of collection. ... 48

Table 2.2 Temperature sensitivity (Q_{10} values) of absolute oxygen consumption, and parameters of metabolic performance, for green sea urchins collected from barren and kelp habitats at Bauline, Biscayan Cove and Tors Cove, Newfoundland. Two separate Q_{10} values were calculated: i.e., 4 – 14 ºC and 14 – 26 ºC. Fourteen ºC was the average water temperature during the summer. For the 'acute' protocol, Q_{10} values were calculated based on the mean absolute $\dot{M}O_2$ values for each site/habitat combination, whereas Q_{10} values during the 'ramping' protocol were calculated for individual urchins from Biscayan Cove. MMR_T is the maximum absolute $\dot{M}O_2$ recorded. For the 'acute' protocol, the individual with the highest absolute $\dot{M}O_2$ for each site and habitat is indicated. The temperature at which absolute $\dot{M}O_2$ was maximum is indicated by T_{max}. AS_T is temperature-induced metabolic scope (MMR_T – MR at 4 ºC). One Q_{10} value in the cold range (4 – 14 ºC) was excluded from the analysis after being confirmed as an outlier (marked by an * in the table) using a Grubb's test (G = 1.852, U = 0.518, p = 0.171). 64

Table 3.1 Behavioural response sequence of grazing invertebrate species to acute heat exposure (35°C). LOE = loss of equilibrium ('functional mortality' occurs). The time of LOE (see 2 and 3) was recorded for each individual using species-specific criteria..... 123

Table 4.1 Vulnerability of fish communities to thermal diversity change with urchin driven seascape change (barren formation) in temperate ecoregions. Exposure to warming based on NOAA dOISST.v2.1 (1982-2019), calculated as mean±sd degree change for each ecoregion (updated from 30). The most vulnerable ecoregions to urchin-associated tropicalization signals are indicated by grey shading..... 192

Table 5.1 In situ temperatures recorded before (3-years), during and after (3-years) two severe marine heat events in the Channel Islands National Park, CA, USA. Daily temperature values were averaged across each event phase. Sd = standard deviations. Temperature changes were calculated from event phase

averages (event rise = change in mean temperature during event, relative to the three years prior; event fall = change in mean temperature in the three years after the event, relative to the event). 260

List of Figures

Figure 1.1 Upscaling of biological processes that are influenced by the environment. Environmental drivers (e.g., temperature or habitat change) unfold hierarchically from molecular mechanisms to whole organism performance, and then from individuals to populations, communities and ecosystems. Evolution creates an important feedback loop because selection operating at the level of the individual can, over time, change the gene pool. Physiology spans molecular to individual scales and beyond, while ecology spans individual to biosphere scales. The green box highlights levels of organization and processes addressed in this thesis. Adapted from Cooke et al. 2014..... 13

Figure 1.2 Conceptual diagram of the themes and questions addressed in this thesis. Sea urchin overgrazing of kelp forests restructures habitats, leading to changes in assemblage structure (A-B). Kelp forests and sea urchin barrens present distinct environmental filters (C) due to their unique physicochemical characteristics. Chapter outlines (D-F) and implications of overall thesis work (G). 22

Figure 2.1 The map shows green sea urchin collection sites along the easternmost side of the Avalon Peninsula, Newfoundland, Canada (plot inset shows the province of Newfoundland (NL), with the red box outlining the Avalon Peninsula). Sea urchins were hand collected from Biscayan Cove, Tors Cove and Bauline (see Table 2.1 for further details). Panels on the right (A-D) show kelp beds (A, B) and sea urchin barrens (C, D) on the Avalon Peninsula. Pictures were taken by snorkelers at ~4m depth in August 2020. B and C show count quadrats with a size of 0.5 x 0.5 m, placed in a kelp bed and barren, respectively. 49

Figure 2.2 Ash-free dry mass (AFDM) to wet mass ratios for green sea urchins collected from barren and kelp habitats in Newfoundland. The temperatures on the x-axis indicate the temperature steps each set of urchins was exposed to during oxygen consumption measurements. Data for each habitat and temperature combination represent 27 sea urchins, N=216 in total. Boxplots show maximum, minimum and median values, as well as 25th and 75th percentile values. 58

Figure 2.3 Absolute (A) oxygen consumption ($\dot{M}O_2$) and mass-independent (B) oxygen consumption of green sea urchins collected from barren and kelp habitats as a function of experimental seawater temperature, and measured using the 'acute' protocol. Individuals were collected from three sites in Newfoundland and for each site, nine fresh sea urchins were acutely exposed to each temperature (N=27 sea urchins per temperature). Boxplots show maximum, minimum and median values, as well as 25th and 75th percentile values. N=216 sea urchins across all sites. Note: sea urchins from Bauline (N=9 urchins) were mistakenly

measured at 8ºC instead of 6ºC, thus boxplots at 6ºC represent sea urchins from Biscayan Cove and Tors Cove only (N=18 urchins). 59

Figure 2.4 Absolute oxygen consumption ($\dot{M}O_2$) of green sea urchins from barren and kelp habitats in Biscayan Cove when exposed to the 'ramping' protocol. Boxplots (A) show maximum, minimum and median absolute $\dot{M}O_2$ values, as well as 25th and 75th percentile values. (B) Shows thermal response curves for each sea urchin (N=9 urchins), with dashed lines and triangles denoting sea urchins from kelp habitats, and solid lines and circles indicating those from sea urchin barrens. 60

Figure 2.5 Temperature sensitivity (Q_{10}) of absolute oxygen consumption ($\dot{M}O_2$) in green sea urchins collected from barren and kelp habitats (A-D). Q_{10} values were calculated from 4 – 14 ºC and 14 – 26 ºC based on mean $\dot{M}O_2$ values for each site and habitat measured during the 'acute' protocol (A-B, N=3), and for each individual sea urchin using the 'ramping' protocol (C-D, Biscayan Cove, see data in Fig 2.4: N=9). Note: mean summer water temperature was ~14ºC. (E) Shows the difference in maximum oxygen consumption (MMR_T) between sea urchins from barren and kelp habitats, and (F) shows the difference in temperature-induced metabolic scope (AS_T). Both of these parameters were calculated using data from the 'ramping' protocol. N=9 sea urchins per habitat type. Boxplots show maximum, minimum and median values, as well as 25th and 75th percentile values for each habitat type. Asterisks indicate a significant difference (* = $p < 0.05$, ** = p <0.01, *** $p < 0.001$) between values for sea urchins collected from barren and kelp habitats. 62

Figure 2.6 Comparison of temperature-dependent changes in $\dot{M}O_2$ when measured using the 'acute' (red) vs. the temperature 'ramping' protocol (blue). (A) Absolute $\dot{M}O_2$ and (B) mass-independent $\dot{M}O_2$. Boxplots show maximum, minimum and median values, as well as 25th and 75th percentile values, for each temperature exposure protocol ('acute' and 'ramping'). N=72 sea urchins across both protocols..... 63

Figure 3.1 Location and set-up of caging experiment. For 7 weeks, nine cages were suspended in the water column at ~5 m depth off the South docks at the Bamfield Marine Science Centre (BMSC) foreshore, in Bamfield (A), Vancouver Island, Canada (see cage location pins in B). Three different food treatments (C) were administered throughout the caging period: a) Macrocystis pyrifera (giant kelp; N = 3 cages); b) Saccharina latissima (sugar kelp; N = 3 cages) and c) no macroalgae (N = 3 cages). Each cage contained a polyculture (D) of four grazing invertebrate species: Mesocentrotus franciscanus, Strongylocentrotus purpuratus, Pomaulax gibberosus and Tegula pulligo (N = 12 individuals per species per cage). Invertebrate illustrations by Cerren Richards..... 116

Figure 3.2 Absolute oxygen consumption ($\dot{M}O_2$) of four grazing invertebrate species at two measurement time-points (Week 2 and Week 7) along a 7-week food treatment (Macrocystis pyrifera, Saccharina latissima and no macroalgae).

$\dot{M}O_2$ measurements were made at ambient seawater temperatures at time of measurement (9.0°C at Week 2; 10.5°C at Week 7). Boxplots show maximum, minimum and median values, as well as 25th and 75th percentile values. N=432 individuals across all species and treatments. Grey shaded boxplots indicate significant difference of a treatment from the Macrocystis treatment. 128

Figure 3.3 Mass-independent oxygen consumption ($\dot{M}O_2$) of four grazing invertebrate species (A-D) at two measurement time-points (Week 2 and 7) along a 7-week food treatment (Macrocystis pyrifera, Saccharina latissima and no macroalgae). $\dot{M}O_2$ measurements were made at ambient seawater temperatures at time of measurement (9.0°C at Week 2; 10.5°C at Week 7). Boxplots show maximum, minimum and median values, as well as 25th and 75th percentile values. Grey shaded boxplots indicate significant difference of a treatment from the Macrocystis treatment. 129

Figure 3.4 Functional survival (time until loss of equilibrium; LOE) probability of four grazing invertebrate species during acute exposure to near-lethal heat stress (35°C). All food treatment data were pooled for each species. Curves show Kaplan-Meier survival functions with mean estimated functional survival and 95% confidence intervals (shaded areas). Dashed lines indicate the time where 50% of the population of each species was predicted to be functionally moribund. The boxplot inset shows the time until LOE in seconds for each species, with species codes and colours corresponding to full species names in the legend. Boxplots show maximum, minimum and median values, as well as 25^{th} and 75^{th} percentile values for each species. 131

Figure 3.5 Functional survival (time until loss of equilibrium; LOE) probability of four grazing invertebrate species (A-D) across three food treatments during acute exposure to near-lethal heat stress (35°C). Curves show Kaplan-Meier survival functions with mean estimated functional survival and 95% confidence intervals (shaded areas). Dashed lines indicate the time where 50% of the population of each treatment was predicted to be functionally moribund. N = 216. 132

Figure 4.1 Conceptual illustration of Community Temperature Index (CTI; box a), community thermal diversity (CTDiv; box b) and community thermal range (CTR; box c). CTI is calculated as the average thermal affinity (STI) of all species in a local community. The CTDiv (Burrows et al. 2019) score indicates the variation of thermal affinities among species in a community and is calculated as the standard deviation (SD) of STIs. Communities with a mix of cold- (blue) and warm-affinity (red) species have a high score and those containing species with similar thermal affinities have a low score. The CTR represents the average breadth of species' thermal ranges (STRs). 176

Figure 4.2 Map of temperate ecoregions (23.5 - 50° latitude) with surveyed shallow rocky reef sites hosting sea urchin barrens or kelp beds. Polygons on the map show the ecoregions included in this analysis, with colours indicating their relative CTI sensitivity. A CTI sensitivity score (high, medium or low) was

assigned based on the composition of the ecoregional species pool (average species' thermal range (STR) and diversity of thermal affinities (sdSTI); see methods; (Burrows et al. 2019)). Plots on the left and right side of the map show differences in community temperature index in kelp beds (green solid lines) and sea urchin barrens (purple dotted lines) under four simulated scenarios of CTI sensitivity. 185

Figure 4.3 Differences in community temperature index (CTI), community thermal diversity (CTDiv) and community thermal range (CTR) for fish communities at barrens and in kelp beds across temperate rocky reefs spanning a temperature gradient. Trends are modelled separately for ecoregions with high CTI sensitivity (left column; a-c) and medium CTI sensitivity (right column, d-f). The CTI sensitivity score was assigned to each ecoregion on the basis of its sdSTI and STR (see methods). Lines indicate trends of barrens (dotted purple line) vs kelp (solid green line) relative to the mean. A symbol is included in the top or bottom right corner of each panel when trends are significant, relative to the mean, i.e., purple dots indicating a significant difference at barrens, and green asterisks indicate kelp sites are significantly different. Shaded areas are 95% confidence intervals predicted by GAMMs. All fixed effects are scaled for coefficient comparison. CTI values differed significantly across ecoregions which masked local CTI differences due to habitat. Raw values are shown in supplementary figure S5. See supplementary material table S5 for model summary tables..... 187

Figure 4.4 Differences in species richness of warm (a) and cold (b) affinity fishes (relative to the mean) contrasted for barren and kelp sites across temperate rocky reefs. Differences in richness at sites with high CTI sensitivity (matching Fig 4.3a-c) are shown here. Lines indicate trends of barrens (dotted purple line) vs kelp (solid green line) relative to the mean. A symbol is included in the bottom left corner of each panel when trends are significant, relative to the mean, i.e., purple dots indicating a significant difference at barrens, and green asterisks indicate kelp sites are significantly different. Shaded areas are 95% confidence intervals predicted by GAMMs. All fixed effects are scaled for coefficient comparison. Richness values differed significantly across ecoregions which masked local richness differences due to habitat. See supplementary material table S6 for model summary tables..... 188

Figure 5.1 Time-series of ENSO index values (A) and in situ daily mean temperatures (B) recorded in the Channel Islands (CI) National Park, California, USA. The multivariate ENSO index tracks shifts between warm El Niño oceanographic conditions (positive values; red) and cold La Niña years (negative values; blue). Daily mean temperatures (black line), as well as daily maximum (red dots) and daily minimum (blue dots) are shown in B, starting in 1993 when in situ temperature monitoring began (marked by vertical dashed line). Grey shaded areas mark two extreme marine heat events that occurred in the Park since monitoring began. 249

Figure 5.2 Non-metric multidimensional scaling (NMDS) ordination plots illustrating substrate-cover differences among 16 permanent monitoring sites in the Channel Islands National Park. Substrate composition (% cover of rock, sand, cobble, bare substrate, coralline algae, macroalgae and kelp) across sites is shown for two marine heat events: the 1997 – 98 El Niño (top row) and 2014 – 16 Heat Blob (bottom row), before (A, D), during (B, E) and after (C, F) each event. Each site was classified as a sea urchin barren (brown shading) or kelp forest (green shading) based on both sea urchin densities and kelp densities in the three years prior to each event. Sites that are barren are distinct from sites that are forested based on substrate NMDS plots (see A and D), although some sites undergo changes (i.e., kelp loss) during and after the event, reducing differences between barrens and kelp classified sites. 255

Figure 5.3 Differences in community temperature index (CTI; first row), community thermal diversity (CTDiv; second row) and community thermal range (CTR; third row) for fish communities observed before, during and after the 1997 – 98 El Niño. Community thermal diversity was contrasted for a 3-year period prior to the event, the event years (red shading) and a 3-year period after to the event. The first column (A-C) shows CTI, CTDiv and CTR values of indicator fish species assemblages (13 species monitored). The second column (D-F) shows CTI, CTDiv and CTR values of all fish species observed at the Channel Islands (note: monitoring of the whole fish community started in 1996, i.e., only one year prior to the El Niño event). Boxplots show maximum, minimum and median values, as well as 25th and 75th percentile values. 261

Figure 5.4 Differences in community temperature index (CTI; first row), community thermal diversity (CTDiv; second row) and community thermal range (CTR; third row) for fish communities observed before, during and after the 2014 – 16 Heat Blob. Community thermal diversity was contrasted for a 3-year period prior to the event, the event years (red shading) and a 3-year period after to the event. The first column (A-C) shows CTI, CTDiv and CTR values of indicator fish species assemblages (13 species monitored). The second column (D-F) shows CTI, CTDiv and CTR values of all fish species observed at the Channel Islands. Boxplots show maximum, minimum and median values, as well as 25th and 75th percentile values. 262

Figure 5.5 Heatmap of the occurrence frequency of 13 indicator fish species across 16 sites in the Channel Islands before, during and after two marine heat events: the 1997 – 98 El Niño (A) and the 2014 – 16 Heat Blob (B). Individual fish species are organized by thermal affinity, with the warmest-affinity species near the top, and coolest affinity species at the bottom. Occurrence frequencies three years prior and three years after each event are shown. Tile shading indicates the percentage of sites (out of 16) a species was observed at in a given year, with occurrences bins for occurrences at 0-25% of sites, 25-50% of sites, 50-75% of sites and 75-100% of sites. Grey shaded tiles indicate a species was absent at all sites during that year. 266

Figure 5.6 Percentage change in warm-affinity and cold-affinity fishes, 13 individual indicator fish species and four sea urchin species across all islands, and for individual islands. Percent change was calculated for each location from the pre-event period to the event period (first column, A and C) and from the event period to the post-event period (second column, B and D). Abundance responses to two marine heat events are shown: the 1997 – 98 El Niño (A-B) and the 2014 – 16 Heat Blob (C-D). Individual fish species are organized by thermal affinity, with the warmest-affinity species near the top, and coolest affinity species at the bottom. Percent change was calculated from model estimates of individual fish abundances across event periods, using linear mixed effects models. Tile colours indicate binned % abundance change values, with little change (-20 to 20% change) in white, moderate declines in light orange (-20 to -100), moderate increases in light purple (20 to 100), strong declines (greater than -100%) in orange and strong increases (greater than 100%) in purple. Tiles are shaded in grey where abundance data was insufficient for model fitting (mostly zeros or complete absence at a given island). 269

Figure 5.7 Annual differences in community temperature index (CTI) between kelp forested sites (green) and sea urchin barren sites (brown) in the Channel Islands National Park before, during and after the 1997 – 98 El Niño (A, B) and the 2014 – 16 Heat Blob (C, D). Event years are highlighted by the grey boxes. CTI was calculated for assemblages of 13 indicator fishes (top row) and for the whole fish community (bottom row, >120 fish species observed). Note: monitoring of the whole fish community started in 1996, i.e., only one year prior to the El Niño event..... 271

Figure 5.8 Coefficient plots from linear mixed-effect models contrasting the community temperature index (CTI; A), community thermal diversity (CTDiv; B) and community thermal ranges (CTR; C) of the pre-event period (3 years prior to event) and post-event period (3 years after event) to the event period, respectively. CTI, CTDiv and CTR were calculated based on the composition of the whole fish community. Open symbols show model coefficients for the 1997 – 98 El Niño, and filled symbols show coefficients for the 2014 – 16 Heat Blob. An overall (global; black symbols) model was fit for each response, as well as a habitat specific model (brown symbols for sea urchin barrens; green symbols for kelp forests and grey symbols for mixed or patchy habitats). In A, grey shaded areas denote community-level tropicalization signals associated with the event (i.e., lower CTI before the event means a shift towards a more tropical community during the event, and higher CTI after the event, compared to the event period, means further community tropicalization). In B and C, grey shaded areas show a loss in community thermal diversity and contraction of community thermal ranges associated with the event (i.e., higher CTDiv or CTR before the event mean less thermally diverse communities or communities with smaller thermal ranges, on average, during the event. Lower CTDiv or CTR after the event suggest further declines in CTDiv and CTR, or lack of community recovery). Depth was included as a covariate in all models..... 272

Figure 5.9 Coefficient plots from linear mixed-effect models contrasting the community temperature index (CTI; A), community thermal diversity (CTDiv; B) and community thermal ranges (CTR; C) of the pre-event period (3 years prior to event) and post-event period (3 years after event) to the event period, respectively. CTI, CTDiv and CTR were calculated based on the composition of the indicator species assemblage (13 species). Open symbols show model coefficients for the 1997 – 98 El Niño, and filled symbols show coefficients for the 2014 – 16 Heat Blob. An overall (global; black symbols) model was fit for each response, as well as a habitat specific model (brown symbols for sea urchin barrens; green symbols for kelp forests and grey symbols for mixed or patchy habitats). In A, grey shaded areas denote community-level tropicalization signals associated with the event (i.e., lower CTI before the event means a shift towards a more tropical community during the event, and higher CTI after the event, compared to the event period, means further community tropicalization). In B and C, grey shaded areas show a loss in community thermal diversity and contraction of community thermal ranges associated with the event (i.e., higher CTDiv or CTR before the event mean less thermally diverse communities or communities with smaller thermal ranges, on average, during the event. Lower CTDiv or CTR after the event suggest further declines in CTDiv and CTR, or lack of community recovery). Depth was included as a covariate in all models. 273

Figure 6.1 Overview of the main findings reported in this thesis. Sea urchin overgrazing of kelp forests restructures habitats, leading to changes in trait diversity and assemblage structure in shallow marine populations and communities. Traits based on fundamental and realized niches are useful to detect animal responses to habitat and temperature change at different scales of biological organization. Photos of sea urchin barren and kelp forest licenced under CC BY 2.0..... 336

List of Common Abbreviations

AFDM	Ash-free dry mass
AIC	Akaine Information Criterion
ANOVA	Analysis of Variance
AS_T	Temperature-induced metabolic scope
BMSC	Bamfield Marine Sciences Centre
CTI	Community Temperature Index
CTDiv	Community Thermal Diversity
CTR	Community Thermal Range
DM	Dry mass
GAM	Generalized Additive Model
GAMM	Generalized Additive Mixed Model
KFMP	Channel Islands National Park's kelp forest monitoring program
MMR_T	Maximum Metabolic Rate (i.e., maximum oxygen consumption)
$\dot{M}O_2$	Oxygen consumption
MPA(s)	Marine Protected Area(s)
MUN	Memorial University of Newfoundland and Labrador

p	p-value
Q_{10}	Temperature coefficient
RDFC	Roving Diver Fish Counts
RLS	Reef Life Survey
sd	Standard deviations
sdSTI	diversity of STI
sp.	species
spp.	species pluralis
SST	Sea surface temperature
STI	Species Thermal Index
STR	Species Thermal Range
T_{max}	Temperature at which oxygen consumption peaks
TRC	Thermal Response Curve
UVic	University of Victoria
VFT	Visual Fish Transect
WM	Wet mass

Co-authorship Statement

The research described in the present thesis was designed, conceptualized and conducted by Jasmin M. Schuster with guidance from Dr. Amanda Bates and committee members Drs. Kurt Gamperl and Patrick Gagnon. Jasmin Schuster was responsible for field and laboratory data collection and analysis, with assistance from Amanda Bates. All chapters were written by Jasmin Schuster, with intellectual and editorial input from Drs. Amanda Bates, Kurt Gamperl and Patrick Gagnon. Chapter 2 has been published in *FACETS* and Chapter 4 has been published in *Global Ecology and Biogeography* (see complete references below). Chapter 3 is under revision in the *Journal of Experimental Marine Biology and Ecology* and has been resubmitted. Future publications in the primary literature based on work presented in this thesis will be co-authored by Jasmin Schuster and Amanda Bates (Chapter 3), and Dr. David Kushner (Chapter 5).

Schuster, J. M., Gamperl, A. K., Gagnon, P. and Bates, A. E., 2022. Distinct realized physiologies in green sea urchin (Strongylocentrotus droebachiensis) populations from barren and kelp habitats. FACETS, 7, pp.822-842

Schuster, J. M., Stuart-Smith, R. D., Edgar, G. J. and Bates, A. E., 2022. Tropicalization of temperate reef fish communities facilitated by urchin grazing and diversity of thermal affinities. Global Ecology and Biogeography, 31(5), pp.995-1005.

Chapter 1 - Introduction

1.1 Seascape change

Human activities impact all ecosystems on Earth. Local pressures from resource extraction, overexploitation of wild populations, pollution and land- or sea-scape modification are occurring simultaneously with anthropogenic climate change; which together are reshaping the dynamics of life on Earth (Jackson *et al.* 2001; Pereira *et al.* 2010; Newbold *et al.* 2015; Loughlin *et al.* 2018; Warren *et al.* 2018). Because of these multiple stressors, biodiversity (the variety of life) is in decline in many places (Worm *et al.* 2006; Poloczanska *et al.* 2013). Yet, biodiversity ensures the stability and functioning of natural systems and provides a wide range of goods and services, such as food and oxygen provisioning, that are essential for human well-being (Worm *et al.* 2006; Poloczanska *et al.* 2013).

Biodiversity supports human well-being and resources, while also creating greater stability of ecological functions (Oliver *et al.* 2015; Wang & Loreau 2016). Areas with high biodiversity are predicted to be more resilient to environmental change because taxonomic diversity generates greater variation in responses to disturbance or change (i.e., response diversity) leading to greater ecological stability (Yachi & Loreau 1999). Ecological theory and fisheries data suggest that resilience is higher in areas that promote biodiversity, such as those protected from human activities [e.g., Marine Protected Areas (MPAs] where extraction of marine resources is prohibited (Babcock *et al.* 2010; Costello 2014; Bates *et al.* 2019). For example, long-term monitoring data from Australian reefs shows that community composition is more stable (i.e., resists change under environmental change) in protected areas where top predators are present compared to adjacent areas that

are open to fishing (Bates *et al.* 2014; Mellin *et al.* 2016). Several mechanisms can enhance resilience to environmental change in areas protected from human activity by supporting biogenic habitat[1], intact food webs, increased community diversity and increased population diversity (Bates *et al.* 2019).

The potential for warming to alter the dynamics and distributions of species is well recognized (Parmesan & Yohe 2003; Poloczanska *et al.* 2013). Temperatures are changing in multiple dimensions on the planet (Waldock *et al.* 2018), with signals of long-term warming or cooling, shortening or lengthening of seasons, more extreme temperatures, changes in temperature variability, and more frequent extreme events, such as heatwaves (Meehl & Tebaldi 2004; Bates *et al.* 2018). These temperature stressors can lead to changes in the behaviour, performance, growth, reproduction, life history, distribution and survival of organisms (Newell 1966; Gillooly *et al.* 2001; Somero 2010; Poloczanska *et al.* 2013; Michaletz 2018; Blowes *et al.* 2019; Kennedy *et al.* 2019). How organisms respond to stressful temperatures depends on the duration, magnitude, timing and frequency of the stress event (Bates & Morley 2020). In the ocean, where the majority of organisms are ectotherms (i.e., organisms whose body temperature is regulated by external temperatures), temperature stress elicits responses across multiple levels of biological organization. Once temperatures exceed their tolerance limits, ectotherms must ultimately adapt, move or perish (Pinsky *et al.* 2013; Sandblom *et al.* 2016; Harris *et al.* 2018). Yet, accelerating rates of environmental change

[1] Biogenic habitats are habitats created by living organisms (e.g., kelp, seagrass, corals etc.)

make it difficult for organisms to keep track with temperatures, leading to biodiversity loss in many regions (Wang & Loreau 2016).

As temperature changes unfold across the planet, land- and sea-scapes are also being altered by human activities, leading to habitat loss, fragmentation or creation (Pandolfi *et al.* 2003; Williams *et al.* 2019). On land, urbanization and land-use change, for example due to agricultural expansion or deforestation, are driving declines in natural habitats (Laurance 1999; Kreutzweiser *et al.* 2008; Williams & Newbold 2020). In the ocean, trawling, dredging, nutrient pollution and associated deoxygenation, or coastal development can alter or damage foundational taxa[2] and lead to habitat destruction (Thrush & Dayton 2002; Airoldi *et al.* 2008). Both habitat and temperature change can, thus, alter local environments in directions that make them unsuitable for some organisms, potentially leading to a reshuffling of local assemblages and a loss of biodiversity.

In the wild, organisms are challenged to persist in rapidly changing oceans, where temperature and habitat changes modify local environmental conditions (Holbrook *et al.* 2019). Local temperature and land- or sea-scape change (habitat change) are two important 'environmental filters'[3] of individuals and species (Williams & Newbold 2020). This is because a new set of environmental conditions often favours certain individuals or species, for example, with smaller body sizes, faster

[2] Foundational taxa are species that create the physical structure of an ecosystem by forming biogenic habitats, for example, corals and sponges form reefs, macroalgae and mangroves form forests, seagrasses form meadows and mussels form beds.
[3] Abiotic factors that prevent the establishment or persistence of a species in a particular location (Kraft *et al.* 2014).

growth rates, bold/aggressive behaviours or more general diets (Cooke *et al.* 2019; Duncan *et al.* 2019; Richards *et al.* 2021). Temperature is important because it governs the physiological rates of ectotherms (Gillooly *et al.* 2001; Brown *et al.* 2004), and thermal constraints scale up to higher order processes (e.g., behaviour, life-history, distribution). Habitat change is important because species and populations adapt to utilize local resources that may be provided by one habitat type but not another. Loss of natural habitat may selectively target certain physiological and behavioural phenotypes, and shift populations that persist in altered habitats to different physiological states (Williams *et al.* 2019). For example, species within altered land- or sea-scapes (e.g., deforested areas like pastures) are affiliated with higher temperature preferences than species within natural habitats (Clavero *et al.* 2011; Barnagaud *et al.* 2012; Nowakowski *et al.* 2018). Local temperature and habitat change can also interact, for example, ectotherms with low heat tolerances have been linked with greater sensitivity to land-use change (Nowakowski *et al.* 2017).

Environmental filtering and subsequent changes in an organisms' abundance and distribution are non-random and may lead to an overall loss of diversity, which in turn may reduce an assemblage's capacity to respond to climate disturbance (Bates *et al.* 2014). This is because phenotypic plasticity and response diversity offer insurance against changes in function due to species' loss, as well as adaptive potential under environmental change (Bates *et al.* 2019; Beukhof *et al.* 2019; Park & Razafindratsima 2019). Consequently, we might expect that intact,

natural areas (even if not formally protected from human activity) support higher resilience to climate change, compared to areas where natural systems have been altered, disrupted or fragmented. While natural areas may create more resilient biological communities with greater ability to resist and recover from climate events (Carpenter *et al.* 2001; Bates *et al.* 2019), disrupted habitats may have the opposite effect, leaving populations, species and communities more vulnerable to climate disturbance.

1.2 A traits perspective of assemblage change

Identifying general principles that determine the distribution and abundance of organisms across habitats, ecosystems and environmental gradients is a fundamental challenge in ecology. Assemblage organization is complex and multi-faceted, but traits (measurable organismal characteristics) can mediate distribution and abundance patterns, providing a conceptual framework to describe general processes of biodiversity organization (McGill *et al.* 2006). An organisms' morphological, physiological, behavioural and life-history traits influence the effects of environmental filters on biodiversity patterns (Steneck & Dethier 1994; Lavorel *et al.* 1997; Lambers *et al.* 2006; Green *et al.* 2022). Biodiversity is reshuffling due to contemporary climate change, but traditional metrics (e.g., species richness) can fail to capture assemblage change. For example, environmental disturbance may lead to declines in richness (number of species) in some cases, but not others, due to simultaneous species gains and losses, and changes in the composition of species (Dornelas *et al.* 2014, 2019; Gotelli *et al.* 2017). Trait approaches often offer an improvement over traditional species-based metrics.

1.2.1 Why traits approaches are useful

Trait-based approaches are increasingly used to predict assemblage re-organization under environmental changes. Over 800 trait-based studies now exist globally, and the field is growing exponentially (see recent review by Green et al., 2022). A key strength and goal of trait-based approaches is to provide predictions and generalities, enabled by their applicability across broad taxonomic groups, different types of stressors, environmental contexts and research aims (Messier *et al.* 2010; Enright *et al.* 2014; Aguirre-Gutiérrez *et al.* 2016; Richards *et al.* 2021; Green *et al.* 2022). In some cases, trait approaches are more sensitive to detecting change than classical metrics, when for example, environmental filtering alters an assemblage's trait combinations but not the number of species present (Strecker *et al.* 2011; De Palma *et al.* 2017). In addition, traits can provide powerful mechanistic insights: species' traits evolve, in part, as adaptations to a given environment. Thus, traits relate directly to how organisms function in their environment (McGill *et al.* 2006; Gallagher *et al.* 2020), and changes in species presence following environmental disturbance can be understood through traits that explain the underlying mechanism(s). For example, observing declines in three taxonomically distant species from an assemblage after a disturbance may offer limited information about why these particular species were vulnerable, but identifying them all as herbivores can yield useful clues on how the system changed. This is because trait groups are expected to respond to environmental change in a similar way because they share similar environmental adaptations, preferences and vulnerabilities (Cooke *et al.* 2019). As such, response traits can

simplify the many context dependencies that determine a species' relative fitness and presence in an assemblage (McGill *et al.* 2006; Kraft *et al.* 2015). Grouping species by their response traits can also group species within assemblages in smaller units that have ecological importance (e.g., by trophic group).

Trait-approaches do have some limitations, however, with single, often categorical traits sometimes being inadequate descriptors of species-environment relationships. Traits based on environmental niches (i.e., a trait's performance/response across environmental gradients) may offer more useful and predictive insights of assemblage responses to environmental change. For this reason, in the present thesis I focus on approaches which use traits based on environmental niches (i.e., how individuals or species respond to the environment), but also leverage categorical traits that relate to species function (e.g., trophic groups).

1.2.2 The environmental niche and derived traits

Organisms have adapted over evolutionary time scales to a specific set of environmental conditions within which, on average, they function optimally (Pörtner & Knust 2007). The combination of multidimensional environmental conditions that permit or constrain an organism's survival and fitness define environmental niches. The classic niche definition by Hutchinson denotes that the fundamental niche is defined as the set of environmental conditions within which an organism can live in the absence of biotic interactions, and the realized niche is a subunit of the fundamental niche that is constrained by biotic interactions (Hutchinson 1957;

Kearney & Porter 2004). In other words, the fundamental niche represents a potential area of distribution based on environmental tolerances, while the realized niche represents the occupied geographical area, as constrained by environmental conditions and competition, predators and dispersal limitations.

Quantifying environmental niches can be a powerful approach to gain general and predictive insights of assemblage change that relates clearly to environmental drivers. For example, physiological temperature tolerance limits (fundamental niche) and the range of temperatures an organism experiences across the geographic range it occupies (realized niche) allow direct linkages between organism physiology, behaviour, distribution and climate conditions (Stuart-Smith *et al.* 2015; Burrows *et al.* 2019; Bates & Morley 2020). Both classes of niches describe the environmental position an organism occupies in an ecosystem, but each has unique constraints and applications.

Biologists have used physiological response curves to describe the effects of environmental change on animals and map the limits of the fundamental niche for many decades (Vernon 1894; Martin 1903; Snyder 1908; reviewed by Little & Seebacher 2021). Response curves can inform on the implications of changing environments on trait dynamics, and individual response curves describe changes in physiological (or behavioural) rates along an environmental gradient (e.g., temperature, oxygen or salinity levels). The y-axis of a response curve can be processes from molecules (e.g., enzyme kinetics) to whole-organism measures (e.g., metabolic rate, locomotion or feeding rates). Thus, response curves describe

rates as a function of the presented environment. Response curve shapes typically follow a unimodal, inverted U-shape, where performance peaks at some intermediate environmental level and decreases along the environmental gradient in either direction (Dell *et al.* 2011; Englund *et al.* 2011). However, the shape of response curves can vary within and between taxonomic or functional groups, and across environmental contexts.

Mapping a single dimension of a fundamental niche with response curves has several useful applications. Response curves of cellular, organ or whole-organism processes can help understand environmental impacts at higher levels of organization (Harley *et al.* 2017; Little & Seebacher 2021). For example, thermal sensitivity of heart rate can indicate whole-organism and population-level performances, such as migration success (Eliason *et al.* 2011). Comparative approaches can also help identify the plasticity and adaptive capacity of organisms to overcome environmental change. For example, when response curves are compared between populations and species, differences in curve shape can reflect local adaptation(s). In ectotherms, physiological rates are governed by external temperatures, which in turn affect behaviour, fitness and distribution (Bozinovic & Pörtner 2015). Consequently, changes in physiological trait distribution and performance may move populations towards lower resilience to climate change (Hofmann & Todgham 2010). The potential to leverage our understanding of fundamental tolerance limits to environmental conditions, and the physiological

mechanisms that determine them, is highlighted by the renewed research interest in the topic.

Quantifying physiological response curves for whole assemblages is challenging and often limited to small organisms due to equipment and cost limitations. Furthermore, how fundamental tolerances measured in the lab relate to performance in the wild can be ambiguous. A backwards approach, where the environmental niche is constructed based on observed distributions in space, overcomes these limitations (McInerny & Etienne 2012). Quantifying different components of this distribution such as the range of temperatures experienced across a species' range can offer an estimate of the realized niche, and represent the geographic realisation of a species fundamental niche. Using realized niches for the quantification of assemblage change at large spatial scales, and is facilitated by the increasing availability of species occurrence data. For example, the *Global Biodiversity Information Facility* (GBIF; https://www.gbif.org/), *Reef Life Survey* (RLS; https://reeflifesurvey.com/) and the citizen science initiative *iNaturalist* (https://www.inaturalist.org/), collate open and free biodiversity data from around the world. Matching environmental data (e.g., sea surface temperature data derived from satellites) at increasingly fine scales is also fuelling the popularity of realized niche approaches. Species realized niches can explain assemblage change with warming. For example, in shallow reef fish assemblages, warming caused an increase in species with warmer realized thermal niches (warm-affinity), while fishes with colder affinities declined (Bates *et al.* 2014, 2017; Givan *et al.*

2018). Similar approaches have also been successfully applied in terrestrial systems, demonstrating, for example, that the thermal affinities of birds track climate warming (Devictor *et al.* 2008), and that average thermal niche breadths of insects increase with land-use intensity (Kühsel & Blüthgen 2015).

1.2.3 From individuals to species – environmental impacts across levels of biological organization

The impacts of environmental change unfold across biological scales (Cooke *et al.* 2014). Exerted at the molecular and cellular level, environmental change then influences physiological processes and organ function, which in turn impacts whole organism performance, behaviour and ultimately fitness (Figure 1.1). As a result, environmental impacts at the level of the individual traverse up the hierarchy of biological organization. Individual physiological effects translate into effects on population dynamics and distribution patterns, which sum to ecosystem-scale changes by influencing the structure of communities and assemblages (Cooke *et al.* 2014). Most conservation and management issues relate to populations, communities or ecosystems, but it is the individual that is in contact with its local environment, necessitating individual effects to be scaled up. Individual physiology, thus, represents a 'filter' between environmental conditions and population to ecosystem level impacts (Seebacher & Franklin 2012).

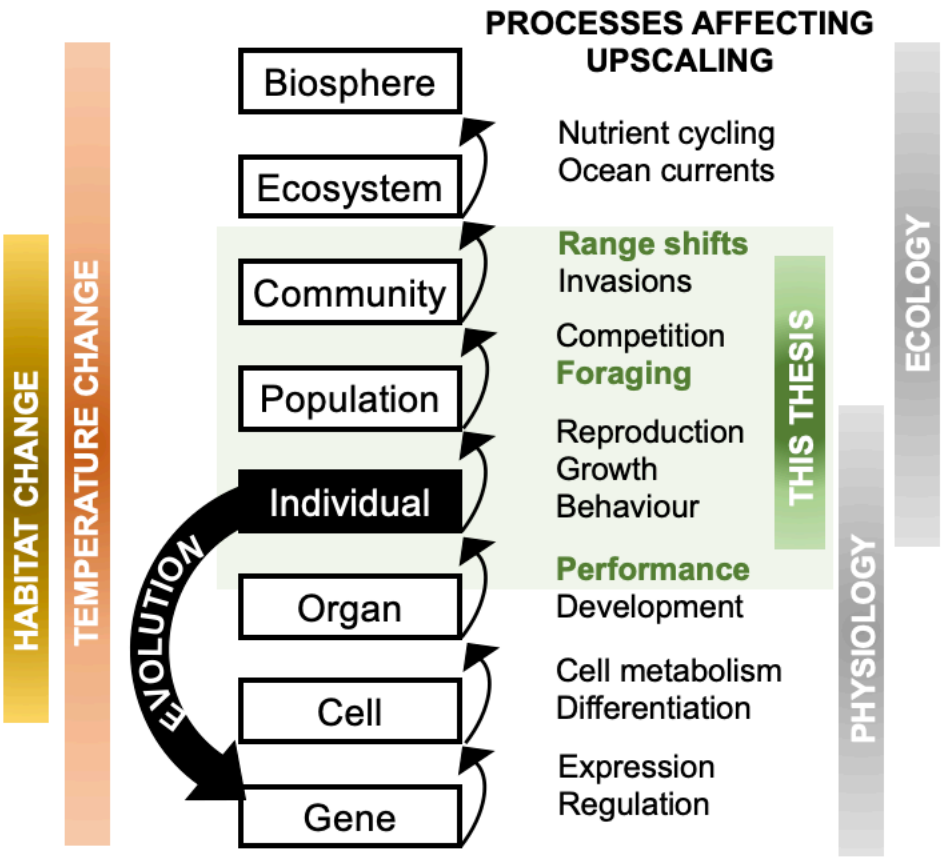

Figure 1.1 Upscaling of biological processes that are influenced by the environment. Environmental drivers (e.g., temperature or habitat change) unfold hierarchically from molecular mechanisms to whole organism performance, and then from individuals to populations, communities and ecosystems. Evolution creates an important feedback loop because selection operating at the level of the individual can, over time, change the gene pool. Physiology spans molecular to individual scales and beyond, while ecology spans individual to biosphere scales. The green box highlights levels of organization and processes addressed in this thesis. Adapted from Cooke *et al.* 2014.

In the present thesis, I quantify trait change across biological levels of organization, applying trait-based approaches from the individual to population (Chapter 2 and Chapter 3) and community (Chapter 4 and Chapter 5) levels. Both fundamental

(Chapter 2 and Chapter 3) and realized niches (Chapter 4 and Chapter 5) can be defined across levels of biological organization. Definitions and how I apply them are provided in Table 1.1.

Table 1.1 Definitions for fundamental and realized niche that span levels of biological organization, as applied throughout this thesis. Limited examples are given for levels not considered in this body of work. The final column ('Thesis application') indicates which traits/levels are addressed in the thesis chapters.

Level of Organization	Fundamental niche	Realized niche	Thesis application
Molecules, Cells, Organs	Enzyme activity or heart rates across a temperature gradient	NA	NA
Individual (Whole organism)	Metabolic rates across a temperature gradient within one individual	Range of local temperatures experienced by an individual, throughout its lifespan (or defined life stage), across its geographic range	Fundamental: Chapter 2 Realized: NA
Population	Average metabolic rates over a temperature gradient. Metabolic rates are averaged across several individuals from a given population	Range of local temperatures experienced across a population's geographic extent. Range defined over specified timeframe (e.g., 1 year)	Fundamental: Chapters 2 & 3 Realized: NA
Species	Average metabolic rates over a temperature gradient. Rates are sampled and averaged across several populations	Range of temperatures experienced across a species' geographic range (Species' Thermal Range; STR)	Fundamental: NA Realized: Chapters 4 & 5
Community	Average metabolic rates over a temperature gradient across all species	Community niche is composed of individual species niches that co-occur at the same time.	Fundamental: NA

	found in a local community	Average breadth of thermal ranges (STRs) across all species in a community (Burrows *et al.* 2019)	Realized: Chapters 4 & 5
Ecosystem	Estimates of ecosystem-wide respiration or photosynthetic rates over a temperature gradient	Average breadth of thermal ranges (STRs) across entire pool of species present in an ecosystem	NA

1.3 The underwater forest as a study system

By volume, the ocean is the largest habitable space on Earth, and coastal areas, albeit small in area relative to open oceans, support a vast amount of diverse marine life. Much of the habitable space in coastal waters is created by biogenic habitat formers. Coral reefs, seagrass beds and mangroves provide key coastal habitat in tropical shallow waters, while kelp forests are arguably the most important habitat formers in cooler, temperate and polar waters (Thomson *et al.* 2015; Wernberg *et al.* 2016). These habitat formers provide structurally complex habitat for diverse food webs, increase productivity and support ecosystem functions and services (Jones *et al.* 1996; Hastings *et al.* 2007; Smale *et al.* 2013). Preserving habitat-forming species can benefit dependent species, and support higher abundances of more species to enrich communities, but also entire ecosystems. As such, habitat-formers underpin the climate change resilience of biological systems because they support greater response diversity, similar to protected areas (Bates *et al.* 2019).

Biogenic habitats that are dynamic and at risk of loss, are thus, valuable study systems to understand the role of natural habitats in building climate resilience. Underwater macroalgae forests are some of the largest shallow-water marine biomes in the world (Krumhansl *et al.* 2016), covering 1.5 to 2 million km^2 and found along 28% of coastal seascapes in temperate and polar regions (Starko *et al.* 2021; Duarte *et al.* 2022). Kelp forests (i.e., with floating surface canopies) and beds (i.e., completely submerged) provide complex habitats that extend from the seafloor into the water column, but are also vulnerable (Steneck *et al.* 2002; Wernberg *et al.* 2018; McPherson *et al.* 2021) and can disappear over short or long timespans due to natural cycles (e.g., seasons, changes in oceanographic conditions) or disturbance (e.g., herbivory, pollution, environmental stress). Due to their dynamic nature and responsiveness to environmental conditions, kelp forests are useful sentinels of change and represent ideal study systems to investigate how organisms respond to habitat loss and environmental stress.

1.3.1 Kelps are foundational habitat formers

'The numbers of living creatures of all Orders whose existence intimately depends on kelp is wonderful … I can only compare these great aquatic forests of the southern hemisphere with the terrestrial ones in the intertropical regions. Yet if in any country a forest was destroyed, I do not believe as many species of animals would perish as would here from the destruction of kelp.' — Darwin 1839

Kelps are foundational species that modify the environment and resources of other organisms. Underwater forests are formed by various species of brown algae, known as kelps (Order Laminariales), which are prolific primary producers

supporting productivity levels that rival tropical rainforests (Dayton 1985; Wernberg *et al.* 2010; Krumhansl *et al.* 2016). Kelps can grow at rapid rates (up to 50 cm per day in some species) and provide ecosystem services valued in the billions of dollars annually (Barbier *et al.* 2011; Krumhansl *et al.* 2016), by producing oxygen, sequestering carbon, cycling nutrients, providing coastal protection and supporting diverse food webs (Beck *et al.* 2001; Cebrian 2002). Kelps also enhance diversity and secondary productivity by forming biogenic habitat that supports diverse assemblages of understory vegetation, invertebrates and fishes that are ecologically and economically important (Haegele & Schweigert 1985; Paddack & Estes 2000; Markel & Shurin 2015). Furthermore, kelps are a significant food source for a myriad of species, with the isotopic signatures of kelp species often found in organisms several kilometres offshore (Hill *et al.* 2006). Because canopy forming kelps create complex 3-dimensional habitat, kelp forests are typically vertically structured, with layers of understory algae and animal communities below the canopy (Goodsell & Connell 2005; Wernberg *et al.* 2005; Flukes *et al.* 2014).

1.3.2 Sea urchins drive seascape change in underwater forests

Apart from environmental stress, the greatest contemporary threat to kelps is grazing pressure by herbivorous sea urchins (Dayton 1985; Filbee-Dexter & Scheibling 2014; Ling *et al.* 2015). Sea urchins can form dense feeding fronts and overgraze entire kelp forests or beds in short time spans, making sea urchins effective drivers of deforestation in coastal oceans. Globally, sea urchin-induced deforestation has been increasing over the past 2-3 decades (Steneck *et al.* 2002), and overfishing and extirpation of apex predators (e.g., sea otters, lobster,

groundfish) has triggered trophic cascades that have led to sea urchin population increases in many regions (Jessup *et al.* 2004; Steneck *et al.* 2004; Pederson & Johnson 2006; Bonaviri *et al.* 2009; Sangil *et al.* 2012). This has resulted in widespread kelp deforestation (Ling 2008; Ling *et al.* 2015). Sea urchin range expansion due to warming oceans has also led to increased deforestation pressure in some regions (Agatsuma & Hoshikawa 2007; Ling 2008; Feng *et al.* 2019). Once sea urchins have destructively overgrazed attached kelps, barren seascapes remain, which are devoid of kelp and macroalgae (Pearse *et al.* 1970; Filbee-Dexter & Scheibling 2014; Ling *et al.* 2015).

Sea urchins can persist in barrens for years or even decades, surviving on drift kelp or encrusting algae and biofilms, while preventing kelp recovery (Harrold & Reed 1985). Consequently, sea urchin grazing can lead to regime shifts, and cause sudden and long-lasting shifts in ecosystem structure and function that are difficult to reverse. Such regime shifts have been documented in the North Atlantic [e.g., Maine (Johnson *et al.* 2013), Nova Scotia (Scheibling *et al.* 1999) and Newfoundland (Keats 1991)], in the Pacific [along coasts from California (Ebeling *et al.* 1985) to Alaska (Konar & Estes 2003)], and in the Indian Ocean (Ling *et al.* 2015; Kriegisch *et al.* 2016). Generally, paths towards kelp forest re-establishment are limited once urchin barrens have formed, but recovery has been documented following disease outbreaks that caused sea urchin mass mortalities (Pearse & Hines 1979; Scheibling 1986), after urchin predator recovery (Estes *et al.* 1998;

Ling 2008), or following human intervention through urchin harvesting or removal (Keats *et al.* 1990; Andrew & Underwood 1993; Leinaas & Christie 1996).

Sea urchin barrens are unique environments because they represent rocky reef areas that would be kelp forested in the absence of urchin disturbance. Furthermore, urchin barrens represent distinct habitats that have lower structural complexity and productivity than kelp beds. The absence of kelp in barrens creates a distinct physical and chemical environment, with reduced shade, increased wave exposure (Reed & Foster 1984; Wernberg *et al.* 2005; Rosman *et al.* 2013), and lower availability of food and three-dimensional structure that provides refugia for reef animals (Harrold & Reed 1985).

The distinct physicochemical characteristics of kelp forests and sea urchin barrens create different environmental conditions which may filter individuals and species. Hence, kelp loss and barrens formation are often associated with a shift in assemblage structure. Contrary to the species-rich environments that kelp forests typically represent, sea urchin barrens are often associated with high abundances of few species. In Southern California, for example, over 200 species of algae, invertebrates, fishes and mammals are commonly observed in giant kelp forests, but 36% of common species occur significantly more often in forested areas than in deforested (barren) areas (Graham 2004). Loss of canopy kelp can also shift understory vegetation communities towards foliose algae-dominated states, with consequences for sessile invertebrates (Flukes *et al.* 2014). The absence of kelp may facilitate colonization by range expanding species that prefer hard substratum.

For example, in Australia, barrens created by the sea urchin *Centrostephanus rodgersii* promoted a tropicalization of the community by attracting warm-affinity species and functional groups typical of lower latitudes (Bates *et al.* 2017).

1.3.3 Temperature drives seascape change in underwater forests

Kelp are cool-water species, and this makes elevated temperatures stressful for them (Kirkman 1984; Wernberg *et al.* 2010). Thus, kelp forests are critically threatened by long-term temperature changes (Filbee-Dexter & Wernberg 2018; Smale 2020; Berry *et al.* 2021). Increasing temperature stress is expected to erode the resilience of kelp beds, drive abundance declines and range contractions towards the tropics, and a reduction of recruitment success (Wernberg *et al.* 2010; Flukes *et al.* 2014; Krumhansl *et al.* 2016). Assemblages present in kelp ecosystems, are thus, challenged by simultaneous kelp loss and warming. Global biodiversity data from kelp systems enable space-for-time substitutes to understand the combined impacts of slow, gradual warming and kelp loss.

By contrast, acute heat events occurring in kelp systems allow insights into temperature-kelp loss interactions at short temporal scales. Marine heatwaves[4], which are increasing in frequency due to climate change, can cause mass die-offs of kelp at rapid time-scales (Wernberg *et al.* 2016; Hughes *et al.* 2018; Babcock *et al.* 2019). In addition, marine heatwaves can cause the mass mortality of invertebrates (Garrabou *et al.* 2009) or fishes (Amatzia *et al.* 2020), change the relative abundance of species and remove or introduce taxa (Vergés *et al.* 2014;

[4] Discrete periods of anomalously warm temperatures.

Wernberg *et al.* 2016; Harris *et al.* 2018; Hughes *et al.* 2018). Consequent changes in assemblage structure, food web dynamics and species relative abundance can amplify negative heatwave effects on kelp, for example when herbivore populations (e.g., sea urchins or fishes) increase after an event, preventing kelp recovery (Wernberg *et al.* 2016).

1.4 Thesis chapter overview

The overarching goal of this thesis was to quantify change in the trait diversity of shallow marine populations and communities due to kelp loss, with a focus on traits that relate to temperature (Figure 1.2). I selected temperature-related traits so that I could link assemblage responses to habitat loss with an organism's capacity to respond to temperature changes (gradual and acute warming). Focusing on thermal niches is well justified for ectotherms in marine ecosystems (Beaugrand 2015; Payne *et al.* 2016). Chapter 2 and Chapter 3 characterize the fundamental thermal responses of individuals and populations, whereas Chapter 4 and Chapter 5 focus on realized niches, scaling from species to whole community responses. For the first two chapters, I selected a physiological trait that is universal across taxa and systems, and underpins all higher order processes: metabolism (Brown *et al.* 2004; Huey & Kingsolver 2019; Norin & Metcalfe 2019; Brandl *et al.* 2022).

The four core chapters of this thesis (Chapters 2-5) are original research, and were written as stand-alone manuscripts for publication in the primary scientific literature. Consequently, some repetition of materials and methods occurs among chapters.

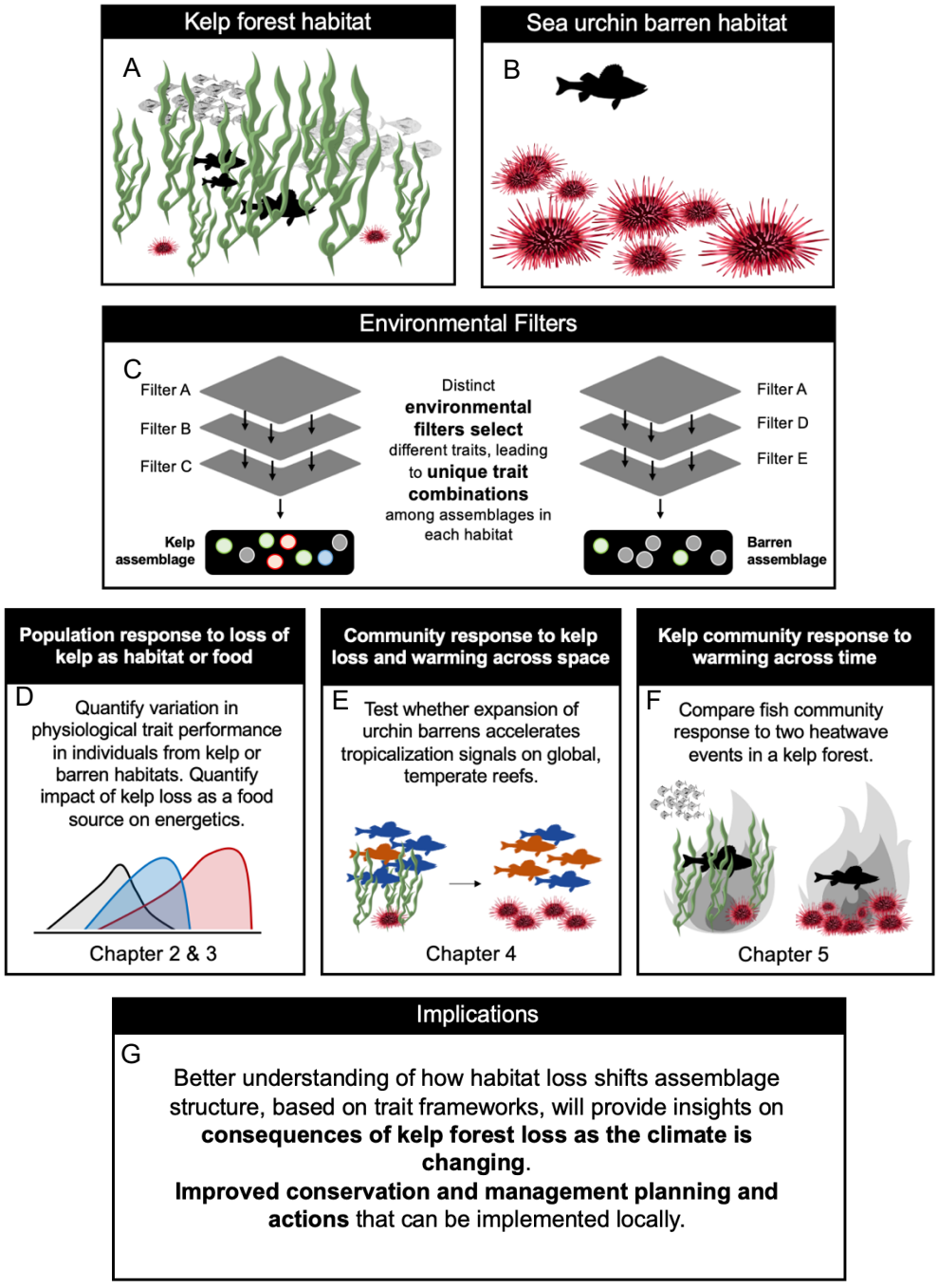

Figure 1.2 Conceptual diagram of the themes and questions addressed in this thesis. Sea urchin overgrazing of kelp forests restructures habitats, leading to changes in assemblage structure (A-B). Kelp forests and sea urchin barrens

present distinct environmental filters (C) due to their unique physicochemical characteristics. Chapter outlines (D-F) and implications of overall thesis work (G).

In Chapter 2, I quantified differences in the temperature-dependent physiological trait performance of sea urchin populations that persist in kelp or barren habitats. Different environmental filters present in kelp and barren habitats may select for distinct phenotypes expressed in the physiological states of populations. I measured the temperature dependence of metabolic rates, as a proxy of realized physiology between urchin populations from neighbouring kelp and barren habitats.

In Chapter 3, I examined how changes in food type and food restriction alter individual grazer physiology to understand the impacts of the loss of kelp as a primary food source on rocky reefs. I quantified mass-independent oxygen consumption of four grazing invertebrate species after seven weeks of treatment with different types of kelp or no kelp. Furthermore, I tested whether prolonged lack of kelp or type of kelp impairs a grazers' ability to respond to environmental stress, by quantifying grazer heat resistance to an acute, near-lethal heat exposure following the three diet treatments.

In Chapter 4, I used Reef Life Survey data (RLS, Edgar et al., 2020) to test whether widespread loss of kelp habitats through sea urchin overgrazing systematically alters the sensitivity of fish communities to warming in temperate latitudes. RLS provides exemplary standardized survey data for thousands of species and locations around the world, and now spans more than 10 years of surveys. These

data, thus, provide a unique opportunity to investigate shifts in community structure with warming across different habitat types.

In Chapter 5, I used unique and comprehensive time-series data from the Channel Islands National Park, California (USA), to test how fish communities respond to two severe marine heat events. The parks' data documents change in the abundance and diversity of organisms in the kelp forest system since 1982.

In Chapter 6, I synthesise the results of this thesis in the context of traits-related assemblage change as a response to environmental change and habitat loss in the ocean. I also discuss the importance, but also the limitations, of the presented work while highlighting how the results of this thesis are relevant for management and conservation in a warming world.

1.5 Literature cited

Agatsuma, Y. & Hoshikawa, H. (2007). Northward extension of geographic range of the sea urchin *Hemicentrotus pulcherrimus* in Hokkaido, Japan. *J. Shellfish Res.*, 26, 629–635.

Aguirre-Gutiérrez, J., Kissling, W.D., Carvalheiro, L.G., WallisDeVries, M.F., Franzén, M. & Biesmeijer, J.C. (2016). Functional traits help to explain half-century long shifts in pollinator distributions. *Sci. Rep.*, 6, 24451.

Airoldi, L., Balata, D. & Beck, M. (2008). The Gray Zone: Relationships between habitat loss and marine diversity and their applications in conservation. *J. Exp. Mar. Bio. Ecol.*, 366, 8–15.

Amatzia, G., Liraz, L., Galit, S., E., R.D. & Arik, D. (2020). Rapid onsets of warming events trigger mass mortality of coral reef fish. *Proc. Natl. Acad.*

Sci., 117, 25378–25385.

Andrew, N.L. & Underwood, A.J. (1993). Density-dependent foraging in the sea urchin *Centrostephanus rodgersii* on shallow subtidal reefs in New South Wales, Australia. *Mar. Ecol. Prog. Ser.*, 99, 89–98.

Babcock, R.C., Bustamante, R.H., Fulton, E.A., Fulton, D.J., Haywood, M.D.E., Hobday, A.J., *et al.* (2019). Severe Continental-Scale Impacts of Climate Change Are Happening Now: Extreme Climate Events Impact Marine Habitat Forming Communities Along 45% of Australia's Coast. *Front. Mar. Sci.*, 6, 1–14.

Babcock, R.C., Shears, N.T., Alcala, A.C., Barrett, N.S., Edgar, G.J., Lafferty, K.D., *et al.* (2010). Decadal trends in marine reserves reveal differential rates of change in direct and indirect effects. *Proc. Natl. Acad. Sci.*, 107, 18256–18261.

Barbier, E.B., Hacker, S.D., Kennedy, C., Koch, E.W., Stier, A.C. & Silliman, B.R. (2011). The value of estuarine and coastal ecosystem services. *Ecol. Monogr.*, 81, 169–193.

Barnagaud, J.-Y., Devictor, V., Jiguet, F., Barbet-Massin, M., Le Viol, I. & Archaux, F. (2012). Relating Habitat and Climatic Niches in Birds. *PLoS One*, 7, e32819.

Bates, A.E., Barrett, N.S., Stuart-Smith, R.D., Holbrook, N.J., Thompson, P.A. & Edgar, G.J. (2014). Resilience and signatures of tropicalization in protected reef fish communities. *Nat. Clim. Chang.*, 4, 62–67.

Bates, A.E., Cooke, R.S.C., Duncan, M.I., Edgar, G.J., Bruno, J.F., Benedetti-Cecchi, L., *et al.* (2019). Climate resilience in marine protected areas and the 'Protection Paradox.' *Biol. Conserv.*, 236, 305–314.

Bates, A.E., Helmuth, B., Burrows, M.T., Duncan, M.I., Garrabou, J., Guy-Haim, T., *et al.* (2018). Biologists ignore ocean weather at their peril. *Nature*, 560, 299–301.

Bates, A.E. & Morley, S.A. (2020). Interpreting empirical estimates of experimentally derived physiological and biological thermal limits in ectotherms. *Can. J. Zool.*, 98, 237–244.

Bates, A.E., Stuart-smith, R.D., Barrett, N.S. & Edgar, G.J. (2017). Biological interactions both facilitate and resist climate-related functional change in temperate reef communities. *Proc. R. Soc. B Biol. Sci.*, 284.

Beaugrand, G. (2015). Theoretical basis for predicting climate-induced abrupt shifts in the oceans. *Philos. Trans. Biol. Sci.*, 370, 1–9.

Beck, M.W., Heck, K.L., Able, K.W., Childers, D.L., Eggleston, D.B., Gillanders, B.M., *et al.* (2001). The Identification, Conservation, and Management of Estuarine and Marine Nurseries for Fish and Invertebrates: A better understanding of the habitats that serve as nurseries for marine species and the factors that create site-specific variability in nurse. *Bioscience*, 51, 633–641.

Berry, H.D., Mumford, T.F., Christiaen, B., Dowty, P., Calloway, M., Ferrier, L., *et al.* (2021). Long-term changes in kelp forests in an inner basin of the Salish Sea. *PLoS One*, 16, e0229703.

Beukhof, E., Dencker, T.S., Pecuchet, L. & Lindegren, M. (2019). Spatio-temporal variation in marine fish traits reveals community-wide responses to environmental change. *Mar. Ecol. Prog. Ser.*, 610, 205–222.

Blowes, S.A., Supp, S.R., Antão, L.H., Bates, A., Bruelheide, H., Chase, J.M., *et al.* (2019). The geography of biodiversity change in marine and terrestrial assemblages. *Science*, 366, 339–345.

Bonaviri, C., T, V.F., Badalamenti, F., Gianguzza, P., M, D.L. & Riggio, S. (2009). Fish versus starfish predation in controlling sea urchin populations in Mediterranean rocky shores. *Mar. Ecol. Prog. Ser.*, 382, 129–138.

Bozinovic, F. & Pörtner, H.-O. (2015). Physiological ecology meets climate change. *Ecol. Evol.*, 5, 1025–1030.

Brandl, S.J., Lefcheck, J.S., Bates, A.E., Rasher, D.B. & Norin, T. (2022). Can metabolic traits explain animal community assembly and functioning? *Biol. Rev.*, n/a.

Brown, J.H., Gillooly, J.F., Allen, A.P., Savage, V.M. & West, G.B. (2004). Toward a metabolic theory of ecology. *Ecology*, 85, 1771–1789.

Burrows, M.T., Bates, A.E., Costello, M.J., Edwards, M., Edgar, G.J., Fox, C.J., *et al.* (2019). Ocean community warming responses explained by thermal affinities and temperature gradients. *Nat. Clim. Chang.*, 9, 959–963.

Carpenter, S., Walker, B., Anderies, J.M. & Abel, N. (2001). From metaphor to measurement: resilience of what to what? *Ecosystems*, 4, 765–781.

Cebrian, J. (2002). Variability and control of carbon consumption, export, and accumulation in marine communities. *Limnol. Oceanogr.*, 47, 11–22.

Clavero, M., Villero, D. & Brotons, L. (2011). Climate change or land use dynamics: do we know what climate change indicators indicate? *PLoS One*, 6, e18581.

Cooke, R., Eigenbrod, F. & Bates, A. (2019). Projected losses of global mammal and bird ecological strategies. *Nat. Commun.*, 10, 2279.

Cooke, S.J., Killen, S.S., Metcalfe, J.D., McKenzie, D.J., Mouillot, D., Jørgensen, C., *et al.* (2014). Conservation physiology across scales: Insights from the marine realm. *Conserv. Physiol.*, 2.

Costello, M.J. (2014). Long live Marine Reserves: A review of experiences and benefits. *Biol. Conserv.*, 176, 289–296.

Dayton, P.K. (1985). Ecology of Kelp Communities. *Annu. Rev. Ecol. Syst.*, 16, 215–245.

Dell, A.I., Pawar, S. & Savage, V.M. (2011). Systematic variation in the temperature dependence of physiological and ecological traits. *Proc. Natl. Acad. Sci.*, 108, 10591 LP – 10596.

Devictor, V., Julliard, R., Denis, C. & Jiguet, F. (2008). Birds are tracking climate warming, but not fast enough. *Proc. Biol. Sci.*, 275, 2743–2748.

Dornelas, M., Gotelli, N.J., McGill, B., Shimadzu, H., Moyes, F., Sievers, C., *et al.* (2014). Assemblage Time Series Reveal Biodiversity Change but Not Systematic Loss. *Science*, 344, 296–299.

Dornelas, M., Gotelli, N.J., Shimadzu, H., Moyes, F., Magurran, A.E. & McGill, B.J. (2019). A balance of winners and losers in the Anthropocene. *Ecol. Lett.*, 22, 847–854.

Duarte, C.M., Gattuso, J., Hancke, K., Gundersen, H., Filbee-Dexter, K., Pedersen, M.F., *et al.* (2022). Global estimates of the extent and production of macroalgal forests. *Glob. Ecol. Biogeogr.*

Duncan, M.I., Bates, A.E., James, N.C. & Potts, W.M. (2019). Exploitation may influence the climate resilience of fish populations through removing high performance metabolic phenotypes. *Sci. Rep.*, 9, 11437.

Ebeling, A.W., Laur, D.R. & Rowley, R.J. (1985). Severe storm disturbances and reversal of community structure in a southern California kelp forest. *Mar. Biol.*, 84, 287–294.

Edgar, G., Cooper, A., Baker, S., Barker, W., Barrett, N., Becerro, M., *et al.* (2020). Reef Life Survey: Establishing the ecological basis for conservation of shallow marine life. *Biol. Conserv.*

Eliason, E.J., Clark, T.D., Hague, M.J., Hanson, L.M., Gallagher, Z.S., Jeffries, K.M., *et al.* (2011). Differences in Thermal Tolerance Among Sockeye Salmon Populations. *Science*, 332, 109–112.

Englund, G., Öhlund, G., Hein, C.L. & Diehl, S. (2011). Temperature dependence of the functional response. *Ecol. Lett.*, 14, 914–921.

Enright, N.J., Fontaine, J.B., Lamont, B.B., Miller, B.P. & Westcott, V.C. (2014). Resistance and resilience to changing climate and fire regime depend on

plant functional traits. *J. Ecol.*, 102, 1572–1581.

Estes, J.A., Tinker, M.T., Williams, T.M. & Doak, D.F. (1998). Killer whale predation on sea otters linking oceanic and nearshore ecosystems. *Science*, 282, 473–476.

Feng, W., Nakabayashi, N., Narita, K., Inomata, E., Aoki, M.N. & Agatsuma, Y. (2019). Reproduction and population structure of the sea urchin *Heliocidaris crassispina* in its newly extended range: The Oga Peninsula in the Sea of Japan, northeastern Japan. *PLoS One*, 14, e0209858.

Filbee-Dexter, K. & Scheibling, R. (2014). Sea urchin barrens as alternative stable states of collapsed kelp ecosystems. *Mar. Ecol. Prog. Ser.*, 495, 1–25.

Filbee-Dexter, K. & Wernberg, T. (2018). Rise of Turfs: A New Battlefront for Globally Declining Kelp Forests. *Bioscience*, 68, 64–76.

Flukes, E., Johnson, C. & Wright, J. (2014). Thinning of kelp canopy modifies understory assemblages: The importance of canopy density. *Mar. Ecol. Prog. Ser.*, 514, 57–70.

Gallagher, R. V, Falster, D.S., Maitner, B.S., Salguero-Gómez, R., Vandvik, V., Pearse, W.D., *et al.* (2020). Open Science principles for accelerating trait-based science across the Tree of Life. *Nat. Ecol. Evol.*, 4, 294–303.

Garrabou, J., Coma, R., Bensoussan, N., Bally, M., Chevaldonne, P., Cigliano, M., *et al.* (2009). Mass mortality in Northwestern Mediterranean rocky benthic communities: effects of the 2003 heat wave. *Glob. Chang. Biol.*, 15, 1090–1103.

Gillooly, J.F., Brown, J.H., West, G.B., Savage, V.M. & Charnov, E.L. (2001). Effects of Size and Temperature on Metabolic Rate. *Science*, 293, 2248–2251.

Givan, O., Edelist, D., Sonin, O. & Belmaker, J. (2018). Thermal affinity as the dominant factor changing Mediterranean fish abundances. *Glob. Chang.*

Biol., 24, e80–e89.

Goodsell, P.J. & Connell, S.D. (2005). Disturbance initiates diversity in recruitment of canopy-forming algae: interactive effects of canopy-thinning and substratum availability. *Phycologia*, 44, 632–639.

Gotelli, N.J., Shimadzu, H., Dornelas, M., McGill, B., Moyes, F. & Magurran, A.E. (2017). Community-level regulation of temporal trends in biodiversity. *Sci. Adv.*, 3, e1700315.

Graham, M.H. (2004). Effects of Local Deforestation on the Diversity and Structure of Southern California Giant Kelp Forest Food Webs. *Ecosystems*, 7, 341–357.

Green, S.J., Brookson, C.B., Hardy, N.A. & Crowder, L.B. (2022). Trait-based approaches to global change ecology: moving from description to prediction. *Proc. R. Soc. B Biol. Sci.*, 289, 20220071.

Haegele, C.W. & Schweigert, J.F. (1985). Estimation of egg numbers in Pacific herring spawns on giant kelp. *North Am. J. Fish. Manag.*, 5, 65–71.

Harley, C.D.G., Connell, S.D., Doubleday, Z.A., Kelaher, B., Russell, B.D., Sarà, G., *et al.* (2017). Conceptualizing ecosystem tipping points within a physiological framework. *Ecol. Evol.*, 7, 6035–6045.

Harris, R.M.B., Beaumont, L.J., Vance, T.R., Tozer, C.R., Remenyi, T.A., Perkins-Kirkpatrick, S.E., *et al.* (2018). Biological responses to the press and pulse of climate trends and extreme events. *Nat. Clim. Chang.*, 8, 579–587.

Harrold, C. & Reed, D.C. (1985). Food Availability, Sea Urchin Grazing, and Kelp Forest Community Structure. *Ecology*, 66, 1160–1169.

Hastings, A., Byers, J.E., Crooks, J.A., Cuddington, K., Jones, C.G., Lambrinos, J.G., *et al.* (2007). Ecosystem engineering in space and time. *Ecol. Lett.*, 10, 153–164.

Hill, J., McQuaid, C. & Kaehler, S. (2006). Biogeographic and nearshore–offshore

trends in isotope ratios of intertidal mussels and their food sources around the coast of southern Africa. *Mar. Ecol. Prog. Ser.*, 318, 63–73.

Hofmann, G.E. & Todgham, A.E. (2010). Living in the Now: Physiological Mechanisms to Tolerate a Rapidly Changing Environment. *Annu. Rev. Physiol.*, 72, 127–145.

Holbrook, N.J., Scannell, H.A., Gupta, A. Sen, Benthuysen, J.A., Feng, M., Oliver, E.C.J., *et al.* (2019). A global assessment of marine heatwaves and their drivers. *Nat. Commun.*, 10, 1–13.

Huey, R.B. & Kingsolver, J.G. (2019). Climate Warming, Resource Availability, and the Metabolic Meltdown of Ectotherms. *Am. Nat.*, 194, E140–E150.

Hughes, T.P., Kerry, J.T., Baird, A.H., Connolly, S.R., Dietzel, A., Eakin, C.M., *et al.* (2018). Global warming transforms coral reef assemblages. *Nature*, 556, 492–496.

Hutchinson, G.E. (1957). Concluding Remarks. *Cold Spring Harb. Symp. Quant. Biol.*

Jackson, J.B.C., Kirby, M.X., Berger, W.H., Bjorndal, K.A., Botsford, L.W., Bourque, B.J., *et al.* (2001). Historical Overfishing and the Recent Collapse of Coastal Ecosystems. *Science*, 293, 629–637.

Jessup, D.A., Miller, M., Ames, J., Harris, M., Kreuder, C., Conrad, P.A., *et al.* (2004). Southern Sea Otter as a Sentinel of Marine Ecosystem Health. *Ecohealth*, 1, 239–245.

Johnson, T., Wilson, J., Cleaver, C., Morehead, G. & Vadas Robert, S. (2013). Modeling fine scale urchin and kelp dynamics: Implications for management of the Maine sea urchin fishery. *Fish. Res.*, 141, 107–117.

Jones, C.G., Lawton, J.H. & Shachak, M. (1996). Organisms as Ecosystem Engineers. In: Ecosystem Management (eds. Samson, F.B. & Knopf, F.L.). Springer New York, New York, NY, pp. 130–147.

Kearney, M. & Porter, W.P. (2004). Mapping the fundamental niche: physiology, climate and the distribution of a nocturnal lizard. *Ecology*, 85, 3119–3131.

Keats, D.W. (1991). Refugial Laminaria Abundance and Reduction in Urchin Grazing in Communities in the North-West Atlantic. *J. Mar. Biol. Assoc. United Kingdom*, 71, 867–876.

Keats, D.W., South, R.G. & Steele, D.H. (1990). Effects of an experimental reduction in grazing by green sea urchins on a benthic macroalgal community in eastern Newfoundland. *Mar. Ecol. Prog. Ser.*, 68, 181–193.

Kennedy, C.M., Oakleaf, J.R., Theobald, D.M., Baruch-Mordo, S. & Kiesecker, J. (2019). Managing the middle: A shift in conservation priorities based on the global human modification gradient. *Glob. Chang. Biol.*, 25, 811–826.

Kirkman, H. (1984). Standing stock and production of Ecklonia radiata (C.Ag.): J. Agardh. *J. Exp. Mar. Bio. Ecol.*, 76, 119–130.

Konar, B. & Estes, J.A. (2003). The stability of boundary regions between kelp beds and deforested areas. *Ecology*, 84, 174–185.

Kraft, N.J.B., Adler, P.B., Godoy, O., James, E.C., Fuller, S. & Levine, J.M. (2015). Community assembly, coexistence and the environmental filtering metaphor. *Funct. Ecol.*, 29, 592–599.

Kreutzweiser, D.P., Hazlett, P.W. & Gunn, J.M. (2008). Logging impacts on the biogeochemistry of boreal forest soils and nutrient export to aquatic systems: A review. *Environ. Rev.*, 16, 157–179.

Kriegisch, N., Reeves, S., Johnson, C.R. & Ling, S.D. (2016). Phase-Shift Dynamics of Sea Urchin Overgrazing on Nutrified Reefs. *PLoS One*, 11, e0168333.

Krumhansl, K.A., Okamoto, D.K., Rassweiler, A., Novak, M., Bolton, J.J., Cavanaugh, K.C., *et al.* (2016). Global patterns of kelp forest change over the past half-century. *Proc. Natl. Acad. Sci.*, 113, 13785 LP – 13790.

Kühsel, S. & Blüthgen, N. (2015). High diversity stabilizes the thermal resilience of pollinator communities in intensively managed grasslands. *Nat. Commun.*, 6, 7989.

Lambers, H., Shane, M.W., Cramer, M.D., Pearse, S.J. & Veneklaas, E.J. (2006). Root Structure and Functioning for Efficient Acquisition of Phosphorus: Matching Morphological and Physiological Traits. *Ann. Bot.*, 98, 693–713.

Laurance, W.F. (1999). Reflections on the tropical deforestation crisis. *Biol. Conserv.*, 91, 109–117.

Lavorel, S., McIntyre, S., Landsberg, J. & Forbes, T.D.A. (1997). Plant functional classifications: from general groups to specific groups based on response to disturbance. *Trends Ecol. Evol.*, 12, 474–478.

Leinaas, H.P. & Christie, H. (1996). Effects of removing sea urchins (*Strongylocentrotus droebachiensis*): Stability of the barren state and succession of kelp forest recovery in the east Atlantic. *Oecologia*, 105, 524–536.

Ling, S.D. (2008). Range expansion of a habitat-modifying species leads to loss of taxonomic diversity: a new and impoverished reef state. *Oecologia*, 156, 883–894.

Ling, S.D., Scheibling, R.E., Rassweiler, A., Johnson, C.R., Shears, N., Connell, S.D., *et al.* (2015). Global regime shift dynamics of catastrophic sea urchin overgrazing. *Philos. Trans. R. Soc. B Biol. Sci.*, 370, 20130269.

Little, A.G. & Seebacher, F. (2021). Physiological Performance Curves: When Are They Useful? *Front. Physiol.*, 12, 805102.

Loughlin, N.J.D., Gosling, W.D., Mothes, P. & Montoya, E. (2018). Ecological consequences of post-Columbian indigenous depopulation in the Andean–Amazonian corridor. *Nat. Ecol. Evol.*, 2, 1233–1236.

Markel, R.W. & Shurin, J.B. (2015). Indirect effects of sea otters on rockfish

(Sebastes spp.) in giant kelp forests. *Ecology*, 96, 2877–2890.

Martin, C.J. (1903). I. Thermal adjustment and respiratory exchange in monotremes and marsupials.—A study in the development of homæothermism. *Philos. Trans. R. Soc. London. Ser. B, Contain. Pap. a Biol. Character*, 195, 1–37.

McGill, B.J., Enquist, B.J., Weiher, E. & Westoby, M. (2006). Rebuilding community ecology from functional traits. *Trends Ecol. Evol.*, 21, 178–185.

McInerny, G.J. & Etienne, R.S. (2012). Ditch the niche – is the niche a useful concept in ecology or species distribution modelling? *J. Biogeogr.*, 39, 2096–2102.

McPherson, M.L., Finger, D.J.I., Houskeeper, H.F., Bell, T.W., Carr, M.H., Rogers-Bennett, L., *et al.* (2021). Large-scale shift in the structure of a kelp forest ecosystem co-occurs with an epizootic and marine heatwave. *Commun. Biol.*, 4, 298.

Meehl, G.A. & Tebaldi, C. (2004). More intense, more frequent, and longer lasting heat waves in the 21st century. *Science (80-.).*, 305, 994–997.

Mellin, C., Aaron MacNeil, M., Cheal, A.J., Emslie, M.J. & Julian Caley, M. (2016). Marine protected areas increase resilience among coral reef communities. *Ecol. Lett.*, 19, 629–637.

Messier, J., McGill, B.J. & Lechowicz, M.J. (2010). How do traits vary across ecological scales? A case for trait-based ecology. *Ecol. Lett.*, 13, 838–848.

Michaletz, S.T. (2018). Evaluating the kinetic basis of plant growth from organs to ecosystems. *New Phytol.*, 219, 37–44.

Newbold, T., Hudson, L.N., Hill, S.L.L., Contu, S., Lysenko, I., Senior, R.A., *et al.* (2015). Global effects of land use on local terrestrial biodiversity. *Nature*, 520, 45–50.

Newell, R.C. (1966). Effect of Temperature on the Metabolism of Poikilotherms.

Nature, 212, 426–428.

Norin, T. & Metcalfe, N.B. (2019). Ecological and evolutionary consequences of metabolic rate plasticity in response to environmental change. *Philos. Trans. R. Soc. B Biol. Sci.*, 374, 20180180.

Nowakowski, A.J., Frishkoff, L.O., Agha, M., Todd, B.D. & Scheffers, B.R. (2018). Changing thermal landscapes: merging climate science and landscape ecology through thermal biology. *Curr. Landsc. Ecol. Reports*, 3, 57–72.

Nowakowski, A.J., Watling, J.I., Whitfield, S.M., Todd, B.D., Kurz, D.J. & Donnelly, M.A. (2017). Tropical amphibians in shifting thermal landscapes under land-use and climate change. *Conserv. Biol.*, 31, 96–105.

Oliver, T.H., Heard, M.S., Isaac, N.J.B., Roy, D.B., Procter, D., Eigenbrod, F., *et al.* (2015). Biodiversity and Resilience of Ecosystem Functions. *Trends Ecol. Evol.*, 30, 673–684.

Paddack, M.J. & Estes, J.A. (2000). Kelp forest fish populations in marine reserves and adjacent exploited areas of central California. *Ecol. Appl.*, 10, 855–870.

De Palma, A., Kuhlmann, M., Bugter, R., Ferrier, S., Hoskins, A.J., Potts, S.G., *et al.* (2017). Dimensions of biodiversity loss: Spatial mismatch in land-use impacts on species, functional and phylogenetic diversity of European bees. *Divers. Distrib.*, 23, 1435–1446.

Pandolfi, J.M., Bradbury, R.H., Sala, E., Hughes, T.P., Bjorndal, K.A., Cooke, R.G., *et al.* (2003). Global Trajectories of the Long-Term Decline of Coral Reef Ecosystems. *Science*, 301, 955–958.

Park, D.S. & Razafindratsima, O.H. (2019). Anthropogenic threats can have cascading homogenizing effects on the phylogenetic and functional diversity of tropical ecosystems. *Ecography (Cop.).*, 42, 148–161.

Parmesan, C. & Yohe, G. (2003). A globally coherent fingerprint of climate

change impacts across natural systems. *Nature*, 421, 37–42.

Payne, N.L., Smith, J.A., van der Meulen, D.E., Taylor, M.D., Watanabe, Y.Y., Takahashi, A., *et al.* (2016). Temperature dependence of fish performance in the wild: links with species biogeography and physiological thermal tolerance. *Funct. Ecol.*, 30, 903–912.

Pearse, J., M.E., C., Leighton, D., C.T., M. & W.J., N. (1970). Marine waste disposal and sea urchin ecology. In: *Kelp Habitat Improvement Project, California Annual Report* (ed. North, W.J.). California Institute of Technology, Pasadena, CA, pp. 1–93.

Pearse, J.S. & Hines, A.H. (1979). Expansion of a central California kelp forest following the mass mortality of sea urchins. *Mar. Biol.*, 51, 83–91.

Pederson, H.G. & Johnson, C.R. (2006). Predation of the sea urchin *Heliocidaris erythrogramma* by rock lobsters (*Jasus edwardsii*) in no-take marine reserves. *J. Exp. Mar. Bio. Ecol.*, 336, 120–134.

Pereira, H., Leadley, P., Proença, V., Alkemade, R., Scharlemann, J., Fernandez, J., *et al.* (2010). Scenarios for Global Biodiversity in the 21st Century. *Science,* 330, 1496–1501.

Pinsky, M.L., Worm, B., Fogarty, M.J., Sarmiento, J.L. & Levin, S.A. (2013). Marine Taxa Track Local Climate Velocities. *Science*, 341, 1239 LP – 1242.

Poloczanska, E.S., Brown, C.J., Sydeman, W.J., Kiessling, W., Schoeman, D.S., Moore, P.J., *et al.* (2013). Global imprint of climate change on marine life. *Nat. Clim. Chang.*, 3, 919–925.

Pörtner, H.O. & Knust, R. (2007). Climate Change Affects Marine Fishes Through the Oxygen Limitation of Thermal Tolerance. *Science*, 315, 95–97.

Reed, D.C. & Foster, M.S. (1984). The Effects of Canopy Shadings on Algal Recruitment and Growth in a Giant Kelp Forest. *Ecology*, 65, 937–948.

Richards, C., Cooke, R.S.C. & Bates, A.E. (2021). Biological traits of seabirds

predict extinction risk and vulnerability to anthropogenic threats. *Glob. Ecol. Biogeogr.*, 30, 973–986.

Rosman, J.H., Denny, M.W., Zeller, R.B., Monismith, S.G. & Koseff, J.R. (2013). Interaction of waves and currents with kelp forests (*Macrocystis pyrifera*): Insights from a dynamically scaled laboratory model. *Limnol. Oceanogr.*, 58, 790–802.

Sandblom, E., Clark, T.D., Gräns, A., Ekström, A., Brijs, J., Sundström, L.F., *et al.* (2016). Physiological constraints to climate warming in fish follow principles of plastic floors and concrete ceilings. *Nat. Commun.*, 7, 11447.

Sangil, C., Clemente, S., Martín-García, L. & Hernández, J.C. (2012). No-take areas as an effective tool to restore urchin barrens on subtropical rocky reefs. *Estuar. Coast. Shelf Sci.*, 112, 207–215.

Scheibling, R. (1986). Increased macroalgal abundance following mass mortalities of sea urchins (*Strongylocentrotus droebachiensis*) along the Atlantic coast of Nova Scotia. *Oecologia*, 68, 186–198.

Scheibling, R., Hennigar, A. & Balch, T. (1999). Destructive grazing, epiphytism, and disease: The dynamics of sea urchin - kelp interactions in Nova Scotia. *Can. J. Fish. Aquat. Sci.*, 56, 2300–2314.

Seebacher, F. & Franklin, C.E. (2012). Determining environmental causes of biological effects: the need for a mechanistic physiological dimension in conservation biology. *Philos. Trans. R. Soc. B Biol. Sci.*, 367, 1607–1614.

Smale, D.A. (2020). Impacts of ocean warming on kelp forest ecosystems. *New Phytol.*, 225, 1447–1454.

Smale, D.A., Burrows, M.T., Moore, P., O'Connor, N. & Hawkins, S.J. (2013). Threats and knowledge gaps for ecosystem services provided by kelp forests: a northeast A tlantic perspective. *Ecol. Evol.*, 3, 4016–4038.

Snyder, C.D. (1908). A comparative study of the temperature coefficients of the

velocities of various physiological actions. *Am. J. Physiol. Content*, 22, 309–334.

Somero, G.N. (2010). The physiology of climate change: how potentials for acclimatization and genetic adaptation will determine 'winners' and 'losers.' *J. Exp. Biol.*, 213, 912 LP – 920.

Starko, S., Wilkinson, D.P. & Bringloe, T.T. (2021). Recent global model underestimates the true extent of Arctic kelp habitat. *Biol. Conserv.*, 257, 109082.

Steneck, R.S. & Dethier, M.N. (1994). A functional group approach to the structure of algal-dominated communities. *Oikos*, 476–498.

Steneck, R.S., Graham, M.H., Bourque, B.J., Corbett, D., Erlandson, J.M., Estes, J.A., *et al.* (2002). Kelp forest ecosystems: biodiversity, stability, resilience and future. *Environ. Conserv.*, 29, 436–459.

Steneck, R.S., Vavrinec, J. & Leland, A. V. (2004). Accelerating Trophic-level Dysfunction in Kelp Forest Ecosystems of the Western North Atlantic. *Ecosystems*, 7, 323–332.

Strecker, A., Olden, J., Whittier, J. & Paukert, C. (2011). Defining conservation priorities for freshwater fishes according to taxonomic, functional, and phylogenetic diversity. *Ecol. Appl.*, 21, 3002–3013.

Stuart-Smith, R.D., Edgar, G.J., Barrett, N.S., Kininmonth, S.J. & Bates, A.E. (2015). Thermal biases and vulnerability to warming in the world's marine fauna. *Nature*, 628, 88–104.

Thomson, J.A., Burkholder, D.A., Heithaus, M.R., Fourqurean, J.W., Fraser, M.W., Statton, J., *et al.* (2015). Extreme temperatures, foundation species, and abrupt ecosystem change: an example from an iconic seagrass ecosystem. *Glob. Chang. Biol.*, 21, 1463–1474.

Thrush, S.F. & Dayton, P.K. (2002). Disturbance to marine benthic habitats by

trawling and dredging: implications for marine biodiversity. *Annu. Rev. Ecol. Syst.*, 449–473.

Vergés, A., Steinberg, P.D., Hay, M.E., Poore, A.G.B., Campbell, A.H., Ballesteros, E., *et al.* (2014). The tropicalization of temperate marine ecosystems: climate-mediated changes in herbivory and community phase shifts. *Proc. R. Soc. B Biol. Sci.*, 281.

Vernon, H.M. (1894). The relation of the respiratory exchange of cold-blooded animals to temperature. *J. Physiol.*, 17, 277.

Waldock, C., Dornelas, M. & Bates, A.E. (2018). Temperature-driven biodiversity change: disentangling space and time. *Bioscience*, online only, 1–12.

Wang, S. & Loreau, M. (2016). Biodiversity and ecosystem stability across scales in metacommunities. *Ecol. Lett.*, 19, 510–518.

Warren, R., Price, J., Graham, E., Forstenhaeusler, N. & VanDerWal, J. (2018). The projected effect on insects, vertebrates, and plants of limiting global warming to 1.5°C rather than 2°C. *Science*, 360, 791–795.

Wernberg, T., Bennett, S., Babcock, R.C., de Bettignies, T., Cure, K., Depczynski, M., *et al.* (2016). Climate-driven regime shift of a temperate marine ecosystem. *Science*, 353, 169–172.

Wernberg, T., Coleman, M.A., Bennett, S., Thomsen, M.S., Tuya, F. & Kelaher, B.P. (2018). Genetic diversity and kelp forest vulnerability to climatic stress. *Sci. Rep.*, 8, 1851.

Wernberg, T., Kendrick, G.A. & Toohey, B.D. (2005). Modification of the physical environment by an *Ecklonia radiata* (Laminariales) canopy and implications for associated foliose algae. *Aquat. Ecol.*, 39, 419–430.

Wernberg, T., Thomsen, M.S., Tuya, F., Kendrick, G.A., Staehr, P.A. & Toohey, B.D. (2010). Decreasing resilience of kelp beds along a latitudinal temperature gradient: potential implications for a warmer future. *Ecol. Lett.*,

13, 685–694.

Williams, J.J., Bates, A.E. & Newbold, T. (2019). Human-dominated land uses favour species affiliated with more extreme climates, especially in the tropics. *Ecography (Cop.).*, 43, 391–405.

Williams, J.J. & Newbold, T. (2020). Local climatic changes affect biodiversity responses to land use: A review. *Divers. Distrib.*, 26, 76–92.

Worm, B., Barbier, E.B., Beaumont, N., Duffy, J.E., Folke, C., Halpern, B.S., *et al.* (2006). Impacts of Biodiversity Loss on Ocean Ecosystem Services. *Science*, 314, 787 LP – 790.

Yachi, S. & Loreau, M. (1999). Biodiversity and ecosystem productivity in a fluctuating environment: The insurance hypothesis. *Proc. Natl. Acad. Sci.*, 96, 1463–1468.

Chapter 2 - Distinct Realized Physiologies in Green Sea Urchin (*Strongylocentrotus droebachiensis*) Populations from Barren and Kelp Habitats

This chapter formed the basis of the publication:

Schuster, J. M., Gamperl, A. K., Gagnon, P. and Bates, A. E., 2022. Distinct realized physiologies in green sea urchin (Strongylocentrotus droebachiensis) populations from barren and kelp habitats. FACETS, 7, pp.822-842.

2.1 Abstract

Overgrazing of habitat-forming kelps by sea urchins is reshaping reef seascapes in many temperate regions. Loss of kelp, in particular as a food source, may alter individual consumer physiology, which in turn may impair ability to respond to climate warming. Here, we measured the temperature dependence of absolute and mass-independent oxygen consumption ($\dot{M}O_2$) using two different exposure protocols (acute exposure and temperature 'ramping'), as proxies of realized physiology, between green sea urchin (*Strongylocentrotus droebachiensis)* populations from neighbouring barren and kelp habitats. Sea urchins from kelp habitats consumed 8-78% more oxygen than sea urchins from barrens, (across a range of temperatures tested [4-32 ºC]), and had higher maximum $\dot{M}O_2$ values (by 26%). This was in part because kelp urchins typically had greater body masses. However, higher mass-independent $\dot{M}O_2$ values of kelp urchins suggest metabolic plasticity in response to habitat per se. In addition, the $\dot{M}O_2$ of sea urchins from kelp habitats was less sensitive to increases in temperature. We conclude that sea urchins from barren and kelp habitats of comparable body mass represent different energetic units. This highlights that habitat type can drive population-level variation which may shape urchins' activities and environmental impact. Such variation should be integrated into energy-based models.

2.2 Introduction

Sea urchin populations are rapidly expanding across shallow rocky reef habitats in many temperate regions (Filbee-Dexter & Scheibling 2014). Urchins can reach high densities and form feeding (grazing) fronts that rapidly overgraze macroalgae, including bioengineering kelps (Filbee-Dexter & Scheibling 2014; Frey & Gagnon 2015; Ling *et al.* 2015). The proliferation of sea urchins, and the associated expansion of barrens, have been primarily linked to the over-exploitation of natural predators such as large groundfish and sea otters (Jessup *et al.* 2004; Pederson & Johnson 2006; Bonaviri *et al.* 2009; Sangil *et al.* 2012), but also to climate perturbations (e.g., heatwaves) and disease-driven food web changes (McPherson *et al.* 2021; Smith *et al.* 2021). As kelp beds transition to barrens, habitat complexity, sediment accumulation and the availability of 3D-structures and shade decrease markedly, whereas wave exposure increases (Reed & Foster 1984; Rosman *et al.* 2007; Watanabe *et al.* 2016; Layton *et al.* 2019; Morris *et al.* 2020), and this limits both food sources and refugia. This shift to a more simplified ecosystem can impose strong 'environmental filters', defined as a set of environmental conditions that select a subset of species from a regional species' pool (Lebrija-Trejos *et al.* 2010). Thus, the presence and absence of kelp may differentially select for subsets of traits or phenotypes (Kraft *et al.* 2015), and hence lead to shifts in assemblage structure, as well as the functional and genetic structure of populations.

The paucity of food (including kelp) in sea urchin barrens suggests that there is a fundamental difference in the selection pressures on sea urchin phenotypes as

compared to those in kelp habitats (Benjamin *et al.* 2010; Hollins *et al.* 2018; Duncan *et al.* 2019). Multiple species of macroalgae are commonly present in kelp habitats, and support preferential and selective feeding by grazers, whilst grazers in barrens often experience prolonged starvation, and rely on drift kelp, filamentous algae and biofilms for their nutrition (Vanderklift & Wernberg 2008; Filbee-Dexter & Scheibling 2014; Renaud *et al.* 2015). The quantity and quality of food influences metabolic rate, which ultimately controls the pace of life and underpins an organism's physiology and functioning (Brown *et al.* 2004; Huey & Kingsolver 2019; Norin & Metcalfe 2019). Metabolic rate is the sum of all life-sustaining chemical reactions that create and use energy, and is typically estimated by measuring oxygen consumption ($\dot{M}O_2$). Metabolic plasticity is often observed under different environmental conditions and in relation to food (Norin & Metcalfe 2019). Therefore, metabolic rates may differ between sea urchins living in kelp and barren habitats because of contrasting food availabilities and quality.

Understanding how metabolic rates are shaped by a species' habitat also has implications in the context of climate change and population-level resilience. Organisms that cannot meet their basic energetic needs because of resource limitations may not be able to regulate and optimize their metabolic response to environmental stress. Metabolic rate can be used as a proxy to estimate an organism's overall physiological state and to characterize its sensitivity to environmental change (Silbiger *et al.* 2019), since metabolic rate fuels all organism functioning and is strongly temperature-dependent (Boltzmann 1872; Gillooly *et al.*

2001; Dell *et al.* 2011). Populations with different physiological trait distributions can respond differently when exposed to challenging thermal conditions, such as heatwaves (Padfield *et al.* 2016; Silbiger *et al.* 2019). For example, two populations with different thermal tolerance ranges, temperature optima (where performance is maximal) and thermal safety margins (i.e., the difference between a species' optimal temperature and its critical upper thermal limit) may respond differently to the same heatwave event, with only one population experiencing adverse effects. Yet, there has been limited research into how habitat shifts may shape physiological trait distribution within coastal populations (but see: Bernhardt & Leslie 2013; Miller & Dowd 2019; Spindel *et al.* 2021), and what the implications are for climate resilience.

The northwest Atlantic represents a model system where green sea urchin (S*trongylocentrotus droebachiensis* [O.F. Müller, 1776]) populations typically reach high densities, and can transform kelp habitats into extensive barrens (Scheibling & Hatcher 2001). Green sea urchins in this region play a key ecological role as consumers, and exert strong top-down control on marine communities by removing foundational kelps (Scheibling *et al.* 1999; Gagnon *et al.* 2004; Scheibling & Lauzon-Guay 2007; Frey & Gagnon 2015). Even so, kelp beds and kelp patches of mainly *Alaria esculenta* and *Laminaria* spp. are present in the northwest Atlantic, in areas where sea urchin populations die-off cyclically because of disease outbreaks or where high currents limit sea urchin grazing (Keats *et al.* 1990; Feehan & Scheibling 2014; Frey & Gagnon 2016). This system provides an

opportunity to directly compare sea urchin populations in terms of their physiology from these adjacent, yet contrasting, habitats.

In the present study, we use a standardized experimental approach to, first, determine whether green sea urchins from barren and kelp habitats differ in their realized physiological state (metabolic rate and thermal sensitivity) by measuring their absolute, mass-independent and mass-specific $\dot{M}O_2$ over a range of temperatures. Absolute $\dot{M}O_2$ estimates the energy required per unit time to maintain biological functions, whilst mass-specific $\dot{M}O_2$ gives metabolic rate scaled to the organisms' mass (Peters 1983; Brown *et al.* 2004). Because absolute $\dot{M}O_2$ and body mass are typically correlated (Brown *et al.* 2004), and because sea urchin mass itself may vary across barrens and kelp habitats, we also calculate mass-independent $\dot{M}O_2$ to compare populations without the confounding effect of body mass. Second, we test whether the thermal sensitivity of metabolism differs between sea urchins from barren and kelp habitats. Third, we compare two experimental approaches to investigate the effects of short-term increases in sea water temperature on urchin metabolism: (Method 1) an 'acute' temperature exposure protocol, where sea urchins are transferred to a novel (stable) temperature, and oxygen consumption is measured at that temperature; and (Method 2) a temperature 'ramping' (dynamic) exposure protocol, in which the same set of individuals are exposed to stepwise increases in temperature (Terblanche *et al.* 2007). The latter experiment allowed us to construct thermal response curves (TRCs) for each individual (Huey & Stevenson 1979), and

enabled us to evaluate an individual's response to a temperature gradient. We used these two approaches to test if the different methods result in similar, or different, temperature-dependent changes in $\dot{M}O_2$, and to examine whether 'heat-hardening' [i.e., an increase in heat tolerance following a sub-lethal exposure to elevated temperatures (Maness & Hutchison 1980)] occurs during temperature ramping.

2.3 Methods

2.3.1 Sea urchin collections

Green sea urchins (N=225) were collected by snorkelers from three sites along the northeastern arm of the Avalon Peninsula: Biscayan Cove, Tors Cove, and Bauline (ordered by collection date; see Fig 2.1 and Table 2.1 for details on the collection sites). Sites were chosen as comparable replicates of barren and kelp habitats with similar depth profiles, extent and exposure to waves, as well as shore access and distance from the laboratory. Sea urchins with test diameters of ~7-8 cm were haphazardly hand collected from habitats within the same depth range (see Table 2.1, Fig S1) that resembled kelp or barrens habitats (i.e., with or without kelp) as assessed visually. Kelp areas were sections of rocky reef, at least 10 x 5 m in size, with dense, continuous kelp cover, whilst barren areas (also at least 10 x 5 m) were rocky reefs devoid of fleshy seaweeds, with bare rock substrate covered in encrusting coralline algae. Prior to collection, sea urchin densities were quantified in kelp and barren areas by counting the number of individuals in a 0.5 x 0.5 m quadrat. Seven quadrats were haphazardly placed in each kelp and barren area of the three sites (N=42 quadrats). Sea urchins collected in each habitat were kept

separate at all times and placed into individual seawater-filled coolers for immediate transport to the Ocean Science Centre (OSC) in Logy Bay, Newfoundland, within 2 hours of collection. At the OSC, the sea urchins were placed into holding tanks with seawater at 14ºC (the average ambient summer temperature) and a 12-hour light: 12-hour dark photoperiod, and left to recover from transport and handling stress for 24 hours. To measure the routine $\dot{M}O_2$ of the urchin populations in a 'field-fresh' physiological state, $\dot{M}O_2$ measurements were started after the initial 24-hour recovery period, and completed within seven days of collection. Sea urchins were not fed at any point to avoid post-feeding increases in metabolic rate (i.e., specific dynamic action).

Table 2.1 Details on the green sea urchin collection sites used in these experiments. The 'Protocol' column indicates in which experiment a given group of sea urchins was used. Two experimental protocols were used; an 'acute' temperature protocol and a 'ramping' protocol (see methods). The latter was used for the construction of individual thermal response curves (TRCs). 'SW Temp.' indicates ambient seawater temperature (ºC) at the time of collection.

Collection Site	º Latitude	º Longitude	Collection depth (m)	Date (DD-MM-YY)	SW Temp.	Protocol	# of sea urchins collected
Biscayan Cove	47.803947	52.787087	1.4-5.6	12-08-20	14ºC	'Acute'	72
Tors Cove	47.212302	52.844915	2.5-4.5	06-09-20	11ºC	'Acute'	72
Bauline	47.722456	52.835011	0.7-3.0	21-09-20	11ºC	'Acute'	72
Biscayan Cove	47.803947	52.787087	2.0-3.0	06-11-20	7ºC	'Ramping'	9

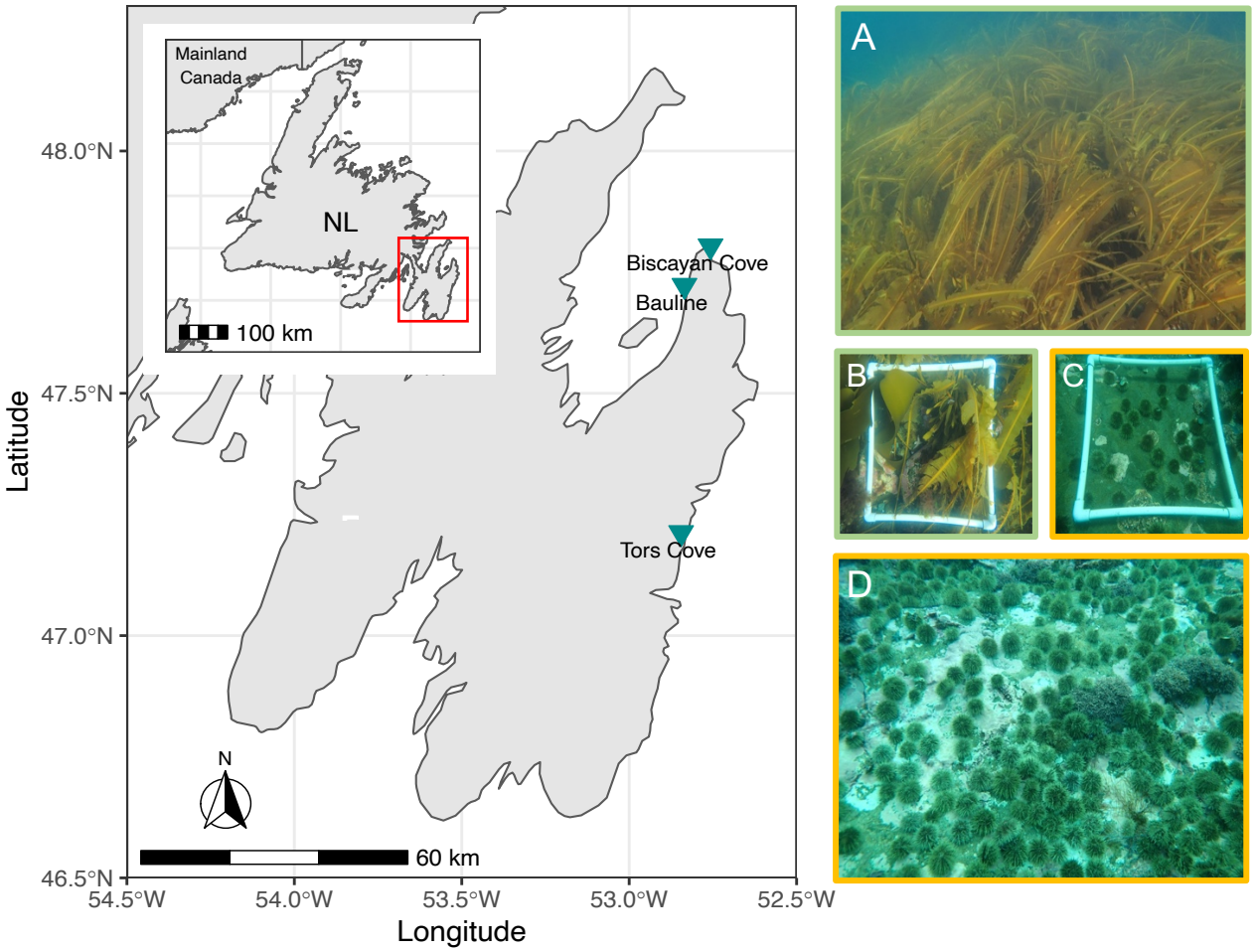

Figure 2.1 The map shows green sea urchin collection sites along the easternmost side of the Avalon Peninsula, Newfoundland, Canada (plot inset shows the province of Newfoundland (NL), with the red box outlining the Avalon Peninsula). Sea urchins were hand collected from Biscayan Cove, Tors Cove and Bauline (see Table 2.1 for further details). Panels on the right (A-D) show kelp beds (A, B) and sea urchin barrens (C, D) on the Avalon Peninsula. Pictures were taken by snorkelers at ~4m depth in August 2020. B and C show count quadrats with a size of 0.5 x 0.5 m, placed in a kelp bed and barren, respectively.

2.3.2 Experimental system for measuring oxygen consumption

We used a custom-built experimental system to measure the $\dot{M}O_2$ of individual sea urchins (see Fig S2). The system built by the Technical Services Department at Memorial University of Newfoundland and Labrador, consists of a table with 10 removable acrylic chambers (each 650 mL in volume and 9 cm in diameter) with magnetic stir plates, located inside an insulated seawater tank (YETI Tundra cooler, 125 L; Austin, Texas, USA). A heater (submersible aquarium heater, 300 Watts; Aqueon, Franklin, Wisconsin, USA) and chiller (Isotemp Model 3016S; Fisher Scientific, Waltham, Massachusetts, USA) controlled by a thermostat (Inkbird ITC-308 Temperature Controller; Inkbird Tech, London, UK) were used to adjust seawater temperatures in the insulated cooler. A water pump connected to the chiller circulated the seawater from one end of the cooler to the other, ensuring consistent temperatures across the 10 chambers. Seawater within the cooler was continuously aerated with an air pump (Top Fin Aquarium, Air-200; PetSmart LLC, Phoenix, Arizona, USA) attached to an air stone. Each chamber was fitted with a temperature (PreSens dipping probe, Pt1000) and a fiber-optic oxygen probe (PreSens dipping probe, DP-PSt7-10-L2.5-ST10-YOP), and measurements of temperature and water oxygen level (in % saturation) were made every second via a computer running PreSens software (PreSens Measurement Studio 2, Version 3.0.3; Precision Sensing GmbH, Regensburg, Germany). Water oxygen level (in mL O_2 / L) was automatically calculated by the PreSens software. Oxygen probes were calibrated prior to each experimental set (sampling site) with air saturated,

room temperature, seawater and sodium sulfite (no O_2; 1 g Na_2SO_3 dissolved in 100 mL of distilled water at room temperature).

2.3.3 Oxygen consumption measurements

2.3.3.1 Pre-measurement procedures and containment of sea urchins

We used a standardized experimental approach to test for differences in the response of metabolism to temperature between sea urchin populations from barren and kelp habitats. To estimate routine metabolic rate at the eight seawater temperatures (4, 6, 10, 14, 18, 22, 26 or 30°C), the $\dot{M}O_2$ of sea urchins was measured using closed respirometry with the system described above. We chose these temperatures to capture the entire response range (increase, peak and decrease in oxygen consumption) of sea urchins, to allow us to compare the response shape and limits across populations. The coldest and warmest temperatures were experimentally constrained by the heater and cooler capacities, and the intervals were chosen based on logistics and feasibility. Twelve (12) hours before the start of each run, nine urchins were selected for measurement (4 barren urchins and 5 kelp urchins, or vice versa). These nine sea urchins were weighed (to the nearest 0.1 g), and had their individual volumetric displacement measured [volumetric displacement = volume of seawater with urchin - volume without urchin]. One individual was placed into each of the nine chambers, with no urchin in the 10^{th} chamber so that background oxygen consumption (i.e., due to microbial respiration) could be measured in a blank control chamber that contained only seawater. The chambers were then covered with fine-mesh netting to prevent the urchins from crawling out of the chamber, and returned to the holding tank

overnight to allow the urchins to adjust to confinement in the chambers and to recover from handling.

2.3.3.2 'Acute' temperature exposure protocol (Assay Method 1)

To examine the temperature-dependent $\dot{M}O_2$ response of sea urchins from all three sites to acute temperature changes, the YETI cooler was filled with fresh, filtered (10 µm), seawater and set to one of eight target temperatures: 4, 6, 10, 14, 18, 22, 26 or 30°C. Each independent assay was conducted on a different day, and target temperatures were randomized for each day so that warmer temperatures did not relate to longer timespans during which the urchins were held in aquaria. For each assay, all 10 chambers (9 urchins, one blank) with mesh tops were moved from the holding tank to the insulated cooler (pre-set to the target temperature for the day) and the urchins were given 1 hour at their new temperature (standardized to 1 hour because this was the maximum time to equilibrium across all temperatures). Then $\dot{M}O_2$ measurements were made by closing the lids on each chamber and allowing oxygen levels in the chambers to fall by 5-10%. This decrease in oxygen concentration allowed reliable estimates of $\dot{M}O_2$ to be obtained. The total measurement time varied from 15 min to ~ 1.5 h, with shorter measurement times at higher temperatures because $\dot{M}O_2$ increases with temperature (Gillooly *et al.* 2001). Once the measurements were completed for each of the 10 chambers, all sea urchins included in the assay were removed from their chambers and immediately frozen prior to ash-free dry mass determination (see below). The cooler and chambers were then emptied, cleaned with warm freshwater, and refilled with seawater for the next assay. The above

procedures were repeated with new urchins until measurements were made at all target temperatures (N=9 sea urchins per measurement; N=72 sea urchins per collection site; N=216 sea urchins in total across all sites and replicates).

2.3.3.3 Temperature 'ramping' exposure protocol (Assay Method 2)

To examine the metabolic response of sea urchins to a temperature 'ramping' protocol, and to assess how comparable values are between this method and the previous protocol (i.e., acute transfer to a new temperature), we constructed thermal response curves (TRC) for individuals from Biscayan Cove (only one site was included due to logistical constraints). Nine sea urchins from a fresh collection were weighed and prepared as detailed in the 'pre-measurement procedures' section. After overnight recovery period, nine urchin-containing chambers and a blank chamber were placed into the cooler with temperature pre-set to 4°C, and 1 hour was allowed before testing began. Oxygen consumption measurements were then made at each of nine temperature steps: 4, 6, 10, 14, 18, 22, 26, 30 and 32°C with a 30-minute period between each temperature during which the next target temperature was reached and maintained (see Fig S3). The final temperature step (32°C) was added to ensure we accurately defined the sea urchins' TRC as completely as possible. The first experiment ('acute' protocol) showed that $\dot{M}O_2$ peaked at around 26°C. The same nine sea urchins had their $\dot{M}O_2$ measured at all temperatures, and the chamber lids were removed and replaced with the mesh lids between measurements to allow for the replacement of seawater from the cooler in which the chambers were held. After the final measurement was taken, the sea urchins were immediately frozen.

2.3.4 Ash-free dry mass

We determined ash-free dry mass to quantify the amount of organic tissue per sea urchin, which corresponds to the amount of metabolically active tissue. To measure ash-free dry mass, empty aluminum weigh boats were first placed in a muffle furnace (500°C) for 12 h to remove any trace of organic matter, and thereafter, stored in a sealed container until use. Sea urchins frozen at the end of both temperature challenges were thawed prior to weighing. The urchins were then placed on pre-weighed (to 0.001 g accuracy) weigh boats, and dried in a combustion oven (at 60°C) for 12 to 24 h until their dry mass stabilized. The sea urchins were then ashed in a muffle furnace at 500°C for 12 h. Ash-free dry mass (i.e., metabolically active tissue) was calculated as dry mass (with boat) minus ashed mass (with boat). Individual dry mass was calculated as dry mass minus the empty weigh boat weight, where dry mass was the total mass of an individual (organic and inorganic) after drying. Finally, an individual's inorganic mass was calculated as ashed mass minus the empty boat weight. This inorganic mass primarily represents an individual's calcified endoskeleton (test), although small traces of sediment or inorganic gut content may also be present in the ashed sample.

2.3.5 Data Processing and Analyses

Values of $\dot{M}O_2$ were calculated for each individual using the respR package in R (Harianto *et al.* 2019). $\dot{M}O_2$ values were adjusted for salinity and water volume in the chamber (i.e., after correction for an individual's volumetric displacement). Mass-independent $\dot{M}O_2$ was calculated by regressing absolute $\dot{M}O_2$ on individual

wet body mass (non-linear regression) and extracting the residuals. Mass-specific values were adjusted for wet-mass or ash-free dry mass (i.e., absolute $\dot{M}O_2$ divided by mass), with the latter accounting for the mass of metabolically active tissue only. All $\dot{M}O_2$ measurements were also corrected for background respiration using the $\dot{M}O_2$ values for the blank chamber of each run. Background respiration values were typically < 0.1 mL / O_2 / h. The $\dot{M}O_2$ data were visually inspected to confirm that a linear decrease in water % air saturation of 5-10% occurred. We set a minimum r^2 of 0.98 (Chabot *et al.* 2021) to identify non-linear measurements and discarded eight measurements (all from Assay Method 1; Fig S6) with an r^2 value below this threshold.

To compare the temperature sensitivity of barren and kelp sea urchins, we calculated temperature coefficients (Q_{10} values) from the 'acute' protocol assays, based on the mean absolute $\dot{M}O_2$ for each site and habitat group, and for the temperature 'ramping' (TRC) protocol, using absolute values of $\dot{M}O_2$ for each individual sea urchin. Q_{10} values were calculated for each group or individual urchin based on the equation:

$$Q_{10} = \frac{R_2}{R_1}^{\left(\frac{10}{T_2 - T_1}\right)}, \qquad \text{(Eqn. 1)}$$

where R_1 = $\dot{M}O_2$ at temperature T_1, R_2 = $\dot{M}O_2$ at temperature T_2. Separate Q_{10} values were calculated for the lower temperature range (cold-range Q_{10}; T_1 = 4ºC and T_2 = 14ºC) and the warm-range (i.e., temperatures above the average summer

/holding temperature (warm-range Q_{10}; T_1 = 14ºC and T_2 = 26ºC)). We calculated these Q_{10} values separately because temperature sensitivity may change at more stressful temperatures that lie outside the sea urchins' realized range. Additionally, we determined the maximum metabolic rate and estimated the T_{max} (temperature at which $\dot{M}O_2$ peaked) from each thermal response curve, by identifying the maximum $\dot{M}O_2$ achieved by each individual across temperatures, and the temperature that corresponded with this maximum value. Finally, temperature-induced metabolic scope (AS_T) was calculated as the difference between the maximum recorded metabolic rate (MMR_T; $\dot{M}O_2$ at 26ºC) and the lowest metabolic rate measured (LMR_T; the $\dot{M}O_2$ at 4ºC).

To test for differences in the urchins' $\dot{M}O_2$ between barren and kelp sites using Assay Method 1, we used generalized additive mixed models within the package 'mgcv' in R (R Core Team 2014) using the 'gamm' function (Wood 2011; Pinheiro *et al.* 2015). The random effect of site was included to account for variation in the response variables due to site. A random effect of 'individual' was also used in models resulting from Assay Method 2 (the 'ramping' protocol), since temperature ramping led to repeated measurements on the same individuals. Habitat (barrens vs. kelp) was included as a fixed effect in all models to test for habitat-dependent variation in the $\dot{M}O_2$ responses of the sea urchins, with temperature included as a covariate. For models with absolute $\dot{M}O_2$ as the response variable, we also included body mass as a covariate, to account for the potentially confounding effect of individual mass.

We visually inspected Gaussian model fits to ensure test assumptions were met (normality of residuals and homogenous error structure), and compared model results across different distribution families (Poisson and quasi-Poisson, both with a log-link function) to ensure the results were consistent. Additionally, we compared gamm results with results from linear mixed-model fits with a polynomial term (function 'lme' in R package 'nlme'), again ensuring reported model results were robust (Zuur *et al.* 2009).

To compare sea urchin mass (wet mass, ash-free dry mass, inorganic mass and AFDM to wet mass ratio), metabolic parameters (MMR_T and AS_T), and the thermal sensitivity of $\dot{M}O_2$ (i.e., Q_{10} values), we fit one-way or two-way ANOVAs using the function 'aov' in the R 'stats' package (R Core Team 2014) with habitat, or habitat and site as main effects, and with an interaction term, as appropriate. We visually checked that test assumptions were met, and ran a Shapiro-Wilk normality test using the function 'shapiro.test' in the R 'stats' package (Team 2014). We performed Tukey's HSD post-hoc tests to compare data between the three sites using the function 'tukeyHSD' in the R 'stats' package.

2.4 Results

Sea urchin density averaged 25 ± 9 individuals per 0.25 m^2 in barrens, and 7 ± 5 individuals per 0.25 m^2 in areas with kelp across the three sites (26 ± 7 vs. 6 ± 7 at Biscayan Cove, 22 ± 13 vs. 8 ± 4 at Tors Cove and 26 ± 9 vs. 7 ± 5 at Bauline, in kelp vs. barrens, respectively). Across the three sites, green sea urchins from kelp habitats had a greater overall mass (by 8 %; two-way ANOVA, $F(1,2) = 17.80$, p

<0.01), more metabolically active tissue [i.e., higher AFDM values by 48 % (two-way ANOVA, $F(1,2) = 138.24$, $p < 0.01$)] and more inorganic mass (by 16 %; two-way ANOVA, $F(1,2) = 23.66$, $p < 0.01$) than sea urchins from barrens (Fig S4, Tables S5-S6). Green sea urchin masses ranged across the sites from 23.3-113.4 g (wet mass) and 0.9-8.5 g (AFDM) in kelp and 15.2-99.0 g (wet mass and) and 0.8-5.3 g (AFDM) in barrens. Sea urchins from kelp habitats also had significantly higher AFDM to wet mass ratios (two-way ANOVA, $F(1,2) = 47.15$, $p < 0.01$, Table S5, Fig 2.2, Fig S5) than individuals from barrens.

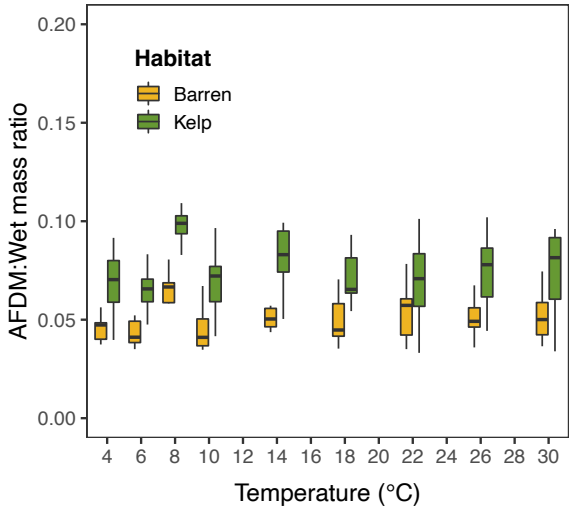

Figure 2.2 Ash-free dry mass (AFDM) to wet mass ratios for green sea urchins collected from barren and kelp habitats in Newfoundland. The temperatures on the x-axis indicate the temperature steps each set of urchins was exposed to during oxygen consumption measurements. Data for each habitat and temperature combination represent 27 sea urchins, N=216 in total. Boxplots show maximum, minimum and median values, as well as 25th and 75th percentile values.

Green sea urchin populations from barren and kelp habitats differed in their oxygen consumption (Figs 2.3-2.4). Overall, sea urchins from kelp habitats had significantly higher absolute $\dot{M}O_2$ values (by 8-78 %) than sea urchins from

adjacent barrens (Figs 2.3-2.4; Table S1; Fig S7) across the three study sites (Fig 2.1), and this pattern was generally consistent across temperatures (Figs 2.3-2.4). This was in part due to body mass (Table S1), as urchins from kelp habitats having a higher wet mass and a greater AFDM: wet mass ratio (Fig 2.2; Figs S4-5), as their $\dot{M}O_2$ per g of AFDM was, in fact, lower as compared to sea urchins from barren habitats (Figs S9-10). However, after accounting for body mass, the mass-independent $\dot{M}O_2$ of sea urchins from kelp habitats was still significantly higher than that of sea urchins from barrens (Fig 2.3 A-B; Table S1; Fig S7 C-D).

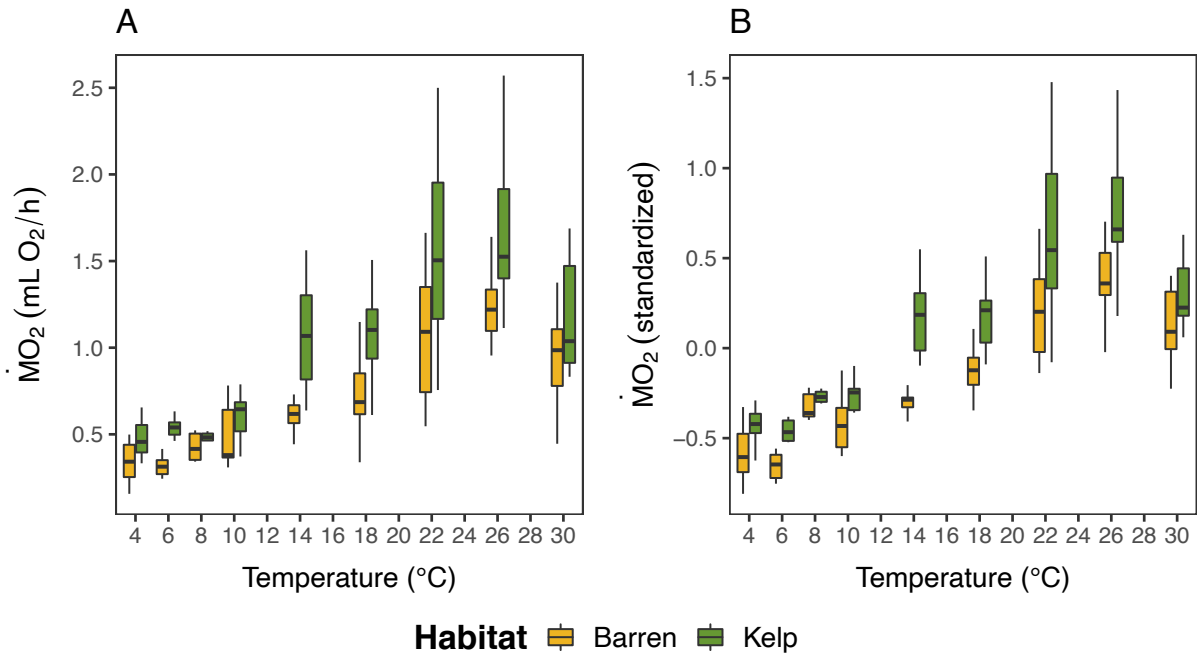

Figure 2.3 Absolute (A) oxygen consumption ($\dot{M}O_2$) and mass-independent (B) oxygen consumption of green sea urchins collected from barren and kelp habitats as a function of experimental seawater temperature, and measured using the 'acute' protocol. Individuals were collected from three sites in Newfoundland and for each site, nine fresh sea urchins were acutely exposed to each temperature (N=27 sea urchins per temperature). Boxplots show maximum, minimum and median values, as well as 25th and 75th percentile values. N=216 sea urchins across all sites. Note: sea urchins from Bauline (N=9 urchins) were mistakenly

measured at 8ºC instead of 6ºC, thus boxplots at 6ºC represent sea urchins from Biscayan Cove and Tors Cove only (N=18 urchins).

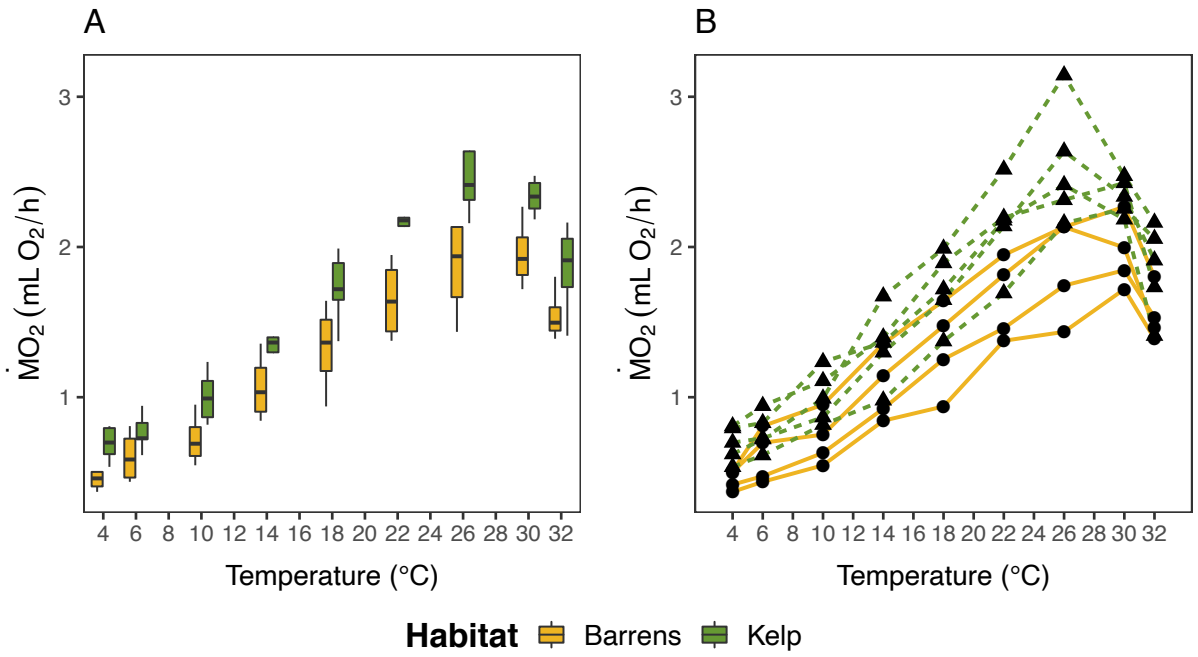

Figure 2.4 Absolute oxygen consumption ($\dot{M}O_2$) of green sea urchins from barren and kelp habitats in Biscayan Cove when exposed to the 'ramping' protocol. Boxplots (A) show maximum, minimum and median absolute $\dot{M}O_2$ values, as well as 25th and 75th percentile values. (B) Shows thermal response curves for each sea urchin (N=9 urchins), with dashed lines and triangles denoting sea urchins from kelp habitats, and solid lines and circles indicating those from sea urchin barrens.

The temperature sensitivity (i.e., Q_{10} value) of sea urchin $\dot{M}O_2$ was significantly higher in animals from barrens than those from kelp habitats over the cold temperature range (Q_{10} 4-14ºC; one-way ANOVA; $F(1,6) = 27.47$, $p = 0.002$, Table S3), but only when assessed using the temperature 'ramping' protocol (Table 2.2, Fig 2.5A, C). Similarly, the temperature sensitivity of $\dot{M}O_2$ in sea urchins from barrens was significantly higher in the warm temperature range (Q_{10} 14-26ºC) when measured using the 'acute' protocol (one-way ANOVA; $F(1,4) = 11.35$, p =

0.028, Table S3). Mean Q_{10} values ranged from 1.50 to 3.14, and from 1.31 to 1.84 across the two temperature ranges (4-14ºC and 14-26ºC, respectively) when sea urchins were exposed to the 'acute' protocol. These values were similar to those measured using the 'ramping' protocol, where Q_{10} values ranged from 1.72 to 2.69 and from 1.46 to 1.93, respectively.

$\dot{M}O_2$ generally peaked between 26-30ºC when considering all site by habitat combinations (Table 2.2), with urchins inhabiting areas with kelp having significantly (by 26 %) higher maximum $\dot{M}O_2$ values (one-way ANOVA; $F(1,7) = 8.008$, $p = 0.025$; Fig 2.5E; Table S3) than sea urchins from barrens. Despite the finding that sea urchins from kelp habitats had higher values for MMR_T, there was no significant difference in the temperature-induced metabolic scope (AS_T; $p = 0.254$; Table S3; Fig 2.5F; Table 2.2). There were also no significant differences in values of MMR_T or AS_T when standardized for wet mass (MMR_T; $p = 0.946$; AS_T; $p = 0.397$) or ash-free dry mass (MMR_T; $p = 0.090$; AS_T; $p = 0.123$), although sea urchins from kelp habitats had lower MMR_T and AS_T values than sea urchins from barren habitats when standardized for ash-free dry mass (Fig S11). Overall, the $\dot{M}O_2$ of Biscayan Cove urchins did not differ significantly when measured using the two methods ('acute' temperature protocol vs. the 'ramping' protocol: Fig 2.6, Table S2, Fig S8).

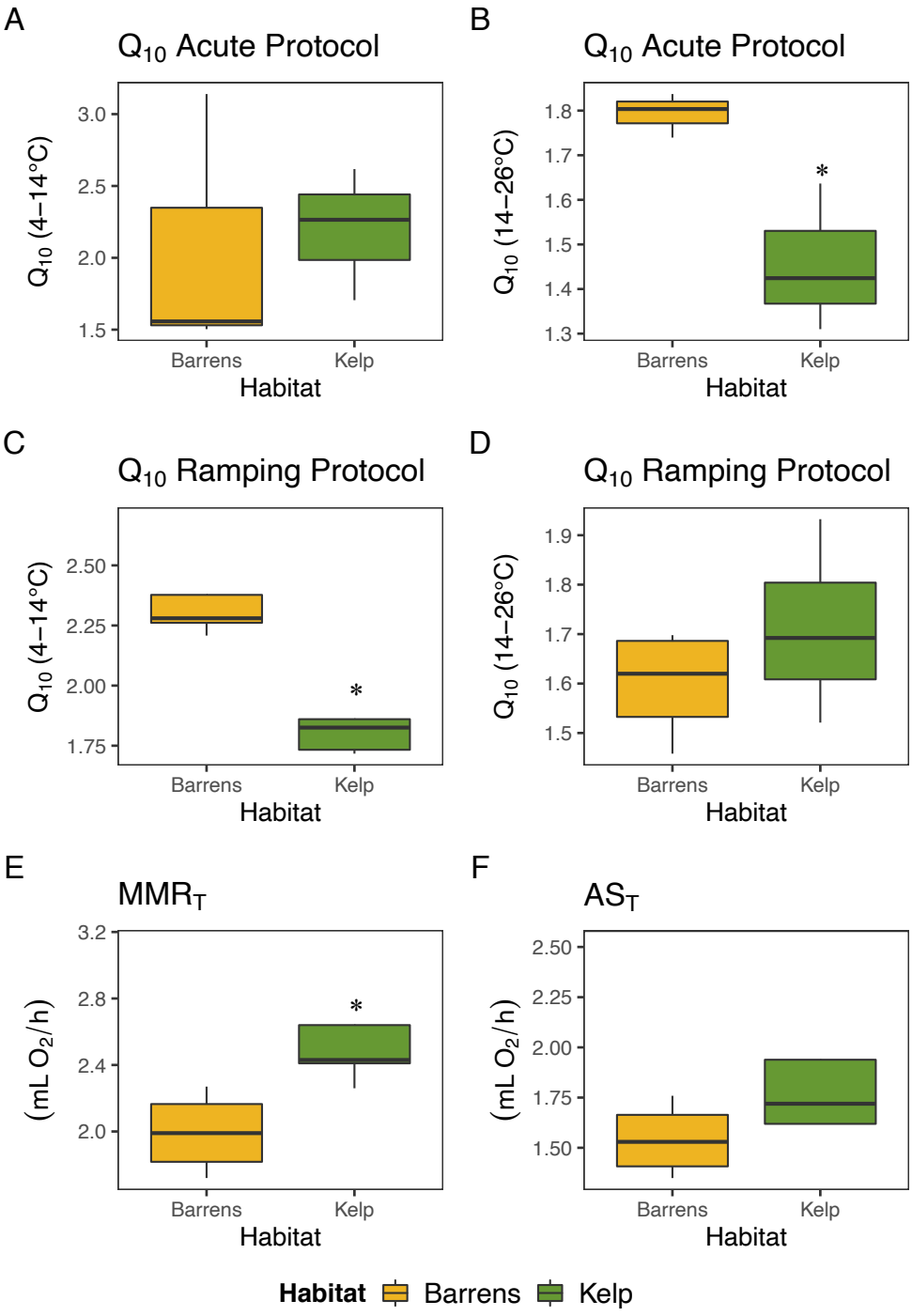

Figure 2.5 Temperature sensitivity (Q_{10}) of absolute oxygen consumption ($\dot{M}O_2$) in green sea urchins collected from barren and kelp habitats (A-D). Q_{10} values were calculated from 4 – 14 ºC and 14 – 26 ºC based on mean $\dot{M}O_2$ values for each site

and habitat measured during the 'acute' protocol (A-B, N=3), and for each individual sea urchin using the 'ramping' protocol (C-D, Biscayan Cove, see data in Fig 2.4: N=9). Note: mean summer water temperature was ~14°C. (E) Shows the difference in maximum oxygen consumption (MMR_T) between sea urchins from barren and kelp habitats, and (F) shows the difference in temperature-induced metabolic scope (AS_T). Both of these parameters were calculated using data from the 'ramping' protocol. N=9 sea urchins per habitat type. Boxplots show maximum, minimum and median values, as well as 25th and 75th percentile values for each habitat type. Asterisks indicate a significant difference (* = p < 0.05, ** = p <0.01, *** p < 0.001) between values for sea urchins collected from barren and kelp habitats.

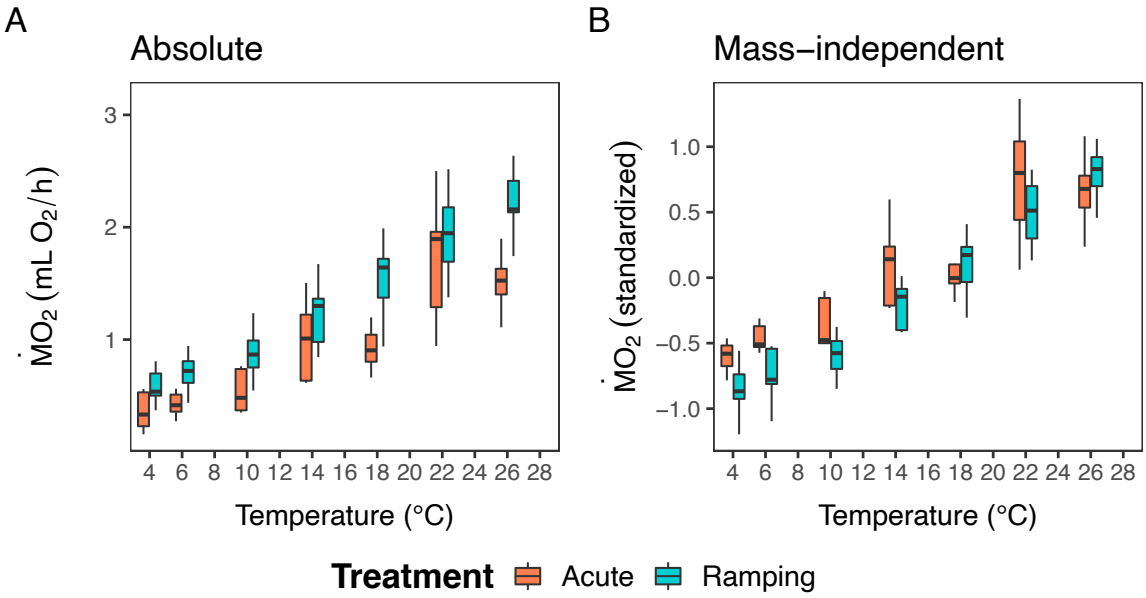

Figure 2.6 Comparison of temperature-dependent changes in $\dot{M}O_2$ when measured using the 'acute' (red) vs. the temperature 'ramping' protocol (blue). (A) Absolute $\dot{M}O_2$ and (B) mass-independent $\dot{M}O_2$. Boxplots show maximum, minimum and median values, as well as 25th and 75th percentile values, for each temperature exposure protocol ('acute' and 'ramping'). N=72 sea urchins across both protocols.

Table 2.2 Temperature sensitivity (Q_{10} values) of absolute oxygen consumption, and parameters of metabolic performance, for green sea urchins collected from barren and kelp habitats at Bauline, Biscayan Cove and Tors Cove, Newfoundland. Two separate Q_{10} values were calculated: i.e., 4 – 14 ºC and 14 – 26 ºC. Fourteen ºC was the average water temperature during the summer. For the 'acute' protocol, Q_{10} values were calculated based on the mean absolute $\dot{M}O_2$ values for each site/habitat combination, whereas Q_{10} values during the 'ramping' protocol were calculated for individual urchins from Biscayan Cove. MMR_T is the maximum absolute $\dot{M}O_2$ recorded. For the 'acute' protocol, the individual with the highest absolute $\dot{M}O_2$ for each site and habitat is indicated. The temperature at which absolute $\dot{M}O_2$ was maximum is indicated by T_{max}. AS_T is temperature-induced metabolic scope (MMR_T – MR at 4 ºC). One Q_{10} value in the cold range (4 – 14 ºC) was excluded from the analysis after being confirmed as an outlier (marked by an * in the table) using a Grubb's test (G = 1.852, U = 0.518, p = 0.171).

Experiment	Population or Replicate	Q_{10} (4-14 ºC)	Q_{10} (14-26 ºC)	MMR_T (mL O_2 / h)	T_{max} (ºC)	AS_T (mL O_2 / h)
'Acute'	Barrens Bauline	1.56	1.80	1.31	26	NA
'Acute'	Kelp Bauline	1.81	1.64	1.42	26	NA
'Acute'	Barrens Biscayan Cove	3.14	1.84	1.63	26	NA
'Acute'	Kelp Biscayan Cove	2.62	1.31	2.50	22	NA
'Acute'	Barrens Tors Cove	1.50	1.74	1.80	22	NA
'Acute'	Kelp Tors Cove	2.26	1.42	2.57	26	NA
'Ramping'	Barrens #1	2.28	1.68	2.13	26	1.63
'Ramping'	Barrens #2	2.67	1.45	2.27	30	1.76
'Ramping'	Barrens #3	2.28	1.56	1.72	30	1.35
'Ramping'	Barrens #4	2.21	1.70	1.85	30	1.43
'Ramping'	Kelp #1	1.86	1.80	2.64	26	1.94
'Ramping'	Kelp #2	1.83	1.93	2.26	30	1.72

'Ramping'	Kelp #3	1.73	1.52	2.43	30	1.62
'Ramping'	Kelp #4	1.72	1.61	2.41	26	1.62
'Ramping'	Kelp #5	2.69*	1.69	3.14	26	2.52

2.5 Discussion

We showed that green sea urchins from barren and kelp habitats in Newfoundland differ in their realized physiological states, with those from kelp habitats having higher metabolic rates, but reduced temperature sensitivity, compared to urchins from barren areas. The average urchin from areas with kelp consumed 8-78% more oxygen than urchins from areas without kelp (i.e., barrens), across the range of typical ocean temperatures. The higher overall energetic requirements of sea urchins in kelp habitats was in part due to their greater mass. Yet, significant differences remained between sea urchins from areas with and without kelp when their mass-independent oxygen consumption rates were compared, which indicates that metabolic plasticity exists between habitat types regardless of mass-effects. In contrast, when considering metabolism standardized per gram of animal, sea urchins from kelp habitats consumed less oxygen than barren urchins, which suggests a larger investment in energy-storing tissues with low oxygen demand in populations from areas with kelp. We conclude that sea urchin populations from kelp and barren habitats have fundamentally different mass-specific and mass-independent energy requirements, and hence, represent ecologically distinctive

"units". Such distinct populations may respond to, and interact with, their environment in unique but predictable ways.

Variation in individual energy requirements is ecologically important because biomass-energy relationships and the energetic status of a population form the basis of an organisms' ability to respond to environmental variability. Energetic models, such as the metabolic theory of ecology (Brown *et al.* 2004) or dynamic energy budget models (Kooijman 1986), are built upon mass-energy scaling laws and are commonly used to predict organismal responses to environmental variability. Yet, most energetic models are average-based, and predict a species' mean response (rather than population specific responses) with unexplained, but often substantial, variation around the mean (Saito *et al.* 2021). This can lead to inaccurate predictions. Integrating habitat-based energy relationships into energetic models could explain some of this variation, and improve the forecasting of a species' vulnerability to environmental change.

The differences we detected in the metabolic performance of green sea urchins from barrens and kelp habitats presumably relate to habitat characteristics, and the physical challenges and environmental filters that each habitat presents (as summarized in the introduction). Yet, differences in food availability/quality emerges amongst a number of abiotic and biotic differences as the most likely driver of differences in the energetic demand and physiology of sea urchins (Mueller & Diamond 2001; Huey & Kingsolver 2019). This is because populations in kelp habitats have access to nutritious and rich food sources, whilst high density

sea urchin barren populations experience prolonged periods of starvation, and compete for scarce food sources such as drift kelp, encrusting algae, and biofilms (Norderhaug *et al.* 2003; Vanderklift & Wernberg 2008; Filbee-Dexter & Scheibling 2014; Renaud *et al.* 2015; Wells *et al.* 2017). Increased competition for scarce food resources in barrens intensifies food shortages, and this also appeared to be the case in the present study. Sea urchin densities were over three-fold higher in barren areas than in kelp areas across all sites.

Organisms that cannot meet their basic energetic demands because of reduced food availability or quality, or starvation, have limited capacity to regulate and optimize their metabolic response to environmental change (Boersma *et al.* 2008; O'Connor *et al.* 2009). Compared to sea urchins from kelp habitats, sea urchins from barrens in our experiments had lower absolute MMR_T values (by 26 %), and their $\dot{M}O_2$ was also more sensitive to increasing temperature (i.e., they had higher Q_{10} values). Perhaps green sea urchins from barrens are more sensitive to temperature change because prolonged starvation reduces their ability to maintain homeostasis as a lower underlying plasticity of cellular traits cannot buffer for environmental change, and this leads to stronger temperature-induced metabolic responses (Brett *et al.* 1969; Huey & Kingsolver 2019). Although data on the longevity of the barrens-state at these specific sites is not available, personal observations indicate that these barrens have existed at least since 2019, and sea urchin barrens are a persistent community state across the majority of the northwest North Atlantic (Adey & Hayek 2011; Frey & Gagnon 2015), suggesting

extended starvation is likely. Additional studies on differences in protein expression in response to heat stress (e.g., heat shock proteins) between barren and kelp populations could prove insightful. It has been previously reported that various ectotherms lower their preferred body temperatures (reviewed in Angilletta 2009) and metabolic rates (Schuster *et al.* 2019) under starvation or reduced food regimes.

Green sea urchins in kelp habitats had larger body masses, more metabolically active tissue, and more inorganic (ashed) mass in comparison to sea urchins of the same test size from barrens (which contain relatively more water for a given body mass) across our study sites. Limited food availability in sea urchin barrens may limit urchins from shunting energy into tissue growth and storage. Sea urchins in areas with kelp, by contrast, may invest more energy into the growth of metabolically active tissues, but also the development of robust and larger body structures (e.g. ossicles or jaw length) and gonad growth (Meidel & Scheibling 1998; DeVries *et al.* 2019). This hypothesis is supported by our findings of relatively lower $\dot{M}O_2$, MMR_T and AS_T values in sea urchins from kelp compared to barren sea urchins when standardized to the mass of metabolically active tissue (i.e., AFDM). Greater investment in energy stores (e.g., lipids and glycogen) that consume little oxygen would explain why sea urchins from kelp habitats consume less oxygen per unit mass. Evidently, the internal structures of sea urchins from barren and kelp habitats are different, even though the populations appear visually similar (at a macroscopic level).

Variation in the body structure of green sea urchins from barrens and kelp may also emerge because of differing abiotic conditions across the two habitats. For example, kelp forests can alter local pH and dissolved oxygen (Cornwall *et al.* 2013; Krause-Jensen *et al.* 2016), and influence hydrodynamics which in turn changes the residence time of chemically altered seawater (Gaylord *et al.* 2012; Hirsh *et al.* 2020). Thus, kelp forests present unique biochemical habitats compared to areas where kelp are absent. As such, areas with productive kelp have been suggested to act as deoxygenation and acidification refugia relative to surrounding waters (Frieder *et al.* 2012). Thus, our finding that barren urchins have lower inorganic masses than kelp urchins suggests that a compelling direction for future investigations is whether differences in seawater biochemistry between barrens and kelp beds affect calcification processes in sea urchins (e.g., Hoshijima & Hofmann 2019).

We also report that the temperature at which oxygen consumption ($\dot{M}O_2$) of green sea urchins peaks (T_{max}; 26 - 30ºC) exceeds summer maximal coastal temperatures in Newfoundland, where sea temperatures typically reach 14ºC, and rarely exceed 20ºC (Frey & Gagnon 2015; Bélanger & Gagnon 2020). Thus, it is unlikely that $\geq$26ºC represents the realized maximum performance for this species, as longer-term experiments with green sea urchins show signs of deterioration at temperatures greater than 15ºC, and grazing rates rapidly decline above 12ºC (Frey & Gagnon 2015). Instead, the temperatures where aerobic scope is highest would give a better indication of the optimum for sea urchin physiological

performance, and would likely lie well below the temperature where $\dot{M}O_2$ peaks. In addition, the impact of disease dynamics on sea urchin performance under warming scenarios needs to be evaluated to predict how populations will fare in the future (but see: Scheibling *et al.* 1999; Lafferty *et al.* 2004; Lester *et al.* 2007). Disease dynamics in high density sea urchin barrens may interact with the heightened temperature sensitivity of barren urchins (i.e., impaired physiological states due to disease may further modify the shape of thermal response curves, or increased temperature sensitivity may increase disease vulnerability), leading to reduced population performance. Collectively, these data show that TRCs alone (and the T_{max} value) have limited capacity to predict population performance in the wild, or at what temperatures sea urchins begin to be impacted under slower rates of warming then our experimental protocols. We advise caution with regards to applying temperature tolerance data from rapid, short-term exposures to species' population models that predict species' success in future climates and inform conservation decisions.

In this study, we also found that exposure to an 'acute' temperature protocol versus a 'ramping' temperature protocol yielded similar $\dot{M}O_2$ values (for this sea urchin species and ecological context). This was unexpected as there is much debate about which physiological assay designs are most suited to particular lines of investigation, and different assay protocols can lead to different physiological responses (Terblanche *et al.* 2007; Bates & Morley 2020). In the 'acute' protocol, individuals were moved from the ambient holding temperature to a target

temperature, and, each individual was used for one independent measurement. Consequently, there was a greater temperature "shock" at increasingly warmer temperatures. Acute approaches are also both time and replication intensive, as each individual organism is only exposed to a single temperature challenge. By contrast, 'ramping' approaches repeatedly measure the same individuals across multiple temperature steps. In such approaches, cumulative temperature effects as organisms are exposed to longer durations of heat stress can limit the inferences from the results of ramping approaches (Overgaard *et al.* 2012).

Accumulated temperature effects may also lead to 'heat-hardening', where thermal tolerance is impacted by previous sub-lethal heat exposures during ramping, which can impact rate measurements (Dahlgaard *et al.* 1998; Kelty & Lee 2001). However, many researchers now recognize that 'ramping' protocols that use 'ecologically-relevant' rates of heating (e.g., that reflect acute temperature changes in smaller water bodies or tide pools, or seasonal changes in coastal water temperatures) are the most appropriate method when the question relates to species in their natural environment, and the goal of the study is not specifically to study the maximum or minimum temperature at which a particular physiological mechanism fails (e.g. Leeuwis *et al.* 2019; Zanuzzo *et al.* 2019; Gamperl *et al.* 2020). Further, in this study there was no evidence of 'heat-hardening' (when sea urchins were exposed to increasing temperature steps), or a time/cumulative heat load effect on $\dot{M}O_2$. The slightly higher $\dot{M}O_2$ values with the 'ramping' protocol may have been related to differences in ambient seawater temperature at the time of

sea urchin collection (urchins collected for the 'acute' protocol in mid-August [~13ºC ambient seawater] versus collection for the 'ramping' protocol during early November [~7ºC ambient seawater]). This interpretation is supported by rate differences at the first temperature step (4ºC), where stress resulting from incremental temperature ramping had not accumulated yet (i.e., the first temperature step of a 'ramping' protocol is equivalent to that of an 'acute' protocol). Impacts of 'heat-hardening', would manifest in diverging $\dot{M}O_2$ values at higher temperatures during the 'ramping' protocol, relative to $\dot{M}O_2$ values recorded during the 'acute' protocol, but we found no evidence of this in the present study.

Our results suggest that, at least for green sea urchins, the 'acute' and 'ramping' protocols provide comparable data, and do not lead to different oxygen consumption values when the same equipment is used. Even so, researchers should match their experimental design to their research question, in particular when laboratory assays are used to infer or predict climate vulnerability, and when 'heat-hardening', acclimation and adaptation are fundamentally important and ecologically-relevant (Bates & Morley 2020). Therefore, in some cases faster 'ramping' approaches, which require less time and fewer replicates, may be a practical choice for comparison when the goal is to compare amongst many individuals and species. Developing realistic temperature 'ramping' protocols that reflect current rates of change experienced by wild populations, or those predicted in the future (e.g. Zanuzzo *et al.* 2019; Gamperl *et al.* 2020) are crucial to produce accurate bounds on which to base predictions.

Overall, habitat type emerged as a driver of population-level variations in realized physiology. Green sea urchins (and likely other sea urchin species) from barrens are ecologically different 'units' than those from kelp habitats in terms of their metabolic responses to temperature change. Our findings have important implications for the application of energy-based models (e.g., metabolic theory of ecology or dynamic energy budget models) that aim to understand and predict a species' vulnerability under climate change. We show that habitat may play a fundamental role when considering organisms as energetic units, and in explaining differences between individuals. Testing our observations in different species that occupy several distinct habitats (including species occurring in both forests and deforested areas on land) could reveal whether habitat complexity produces consistent energetic sub-units within species that can be integrated into forecasting approaches.

2.6 References

Adey, W.H. & Hayek, L.-A.C. (2011). Elucidating Marine Biogeography with Macrophytes: Quantitative Analysis of the North Atlantic Supports the Thermogeographic Model and Demonstrates a Distinct Subarctic Region in the Northwestern Atlantic. *Northeast. Nat.*, 18, 1–128.

Angilletta, J. (2009). Thermal Adaptation: A Theoretical and Empirical Synthesis. *Therm. Adapt. A Theor. Empir. Synth.*, 1–302.

Bates, A.E. & Morley, S.A. (2020). Interpreting empirical estimates of experimentally derived physiological and biological thermal limits in ectotherms. *Can. J. Zool.*, 98, 237–244.

Bélanger, D. & Gagnon, P. (2020). Low growth resilience of subarctic rhodoliths (*Lithothamnion glaciale*) to coastal eutrophication. *Mar. Ecol. Prog. Ser.*, 642, 117–132.

Benjamin, P., Fromentin, J.-M., Cury, P., Drinkwater, K., Jennings, S., Perry, R., *et al.* (2010). How does fishing alter marine populations and ecosystem sensitivity to climate? *J. Mar. Syst.*, 79, 403–417.

Bernhardt, J.R. & Leslie, H.M. (2013). Resilience to Climate Change in Coastal Marine Ecosystems. *Ann. Rev. Mar. Sci.*, 5, 371–392.

Boersma, M., Aberle, N., Hantzsche, F., Schoo, K., Wiltshire, K. & Malzahn, A. (2008). Nutritional Limitation Travels up the Food Chain. *Int. Rev. Hydrobiol.*, 93, 479–488.

Boltzmann, L. (1872). Weitere Studien über das Wärmegleichgewicht unter Gasmolekülen. *Sitzungsberichte der Math. Cl. der Kais. Akad. der Wissenschaften Wien*, 66, 275–370.

Bonaviri, C., T, V.F., Badalamenti, F., Gianguzza, P., M, D.L. & Riggio, S. (2009). Fish versus starfish predation in controlling sea urchin populations in Mediterranean rocky shores . *Mar. Ecol. Prog. Ser.*, 382, 129–138.

Brett, J.R., Shelbourn, J.E. & Shoop, C.T. (1969). Growth Rate and Body Composition of Fingerling Sockeye Salmon, *Oncorhynchus nerka*, in relation to Temperature and Ration Size. *J. Fish. Res. Board Canada*, 26, 2363–2394.

Brown, J.H., Gillooly, J.F., Allen, A.P., Savage, V.M. & West, G.B. (2004). Toward a metabolic theory of ecology. *Ecology*, 85, 1771–1789.

Chabot, D., Zhang, Y. & Farrell, A.P. (2021). Valid oxygen uptake measurements: using high r2 values with good intentions can bias upward the determination of standard metabolic rate. *J. Fish Biol.*, 98, 1206–1216.

Cornwall, C.E., Hepburn, C.D., McGraw, C.M., Currie, K.I., Pilditch, C.A., Hunter, K.A., *et al.* (2013). Diurnal fluctuations in seawater pH influence the response of a calcifying macroalga to ocean acidification. *Proc. R. Soc. B Biol. Sci.*, 280, 20132201.

Dahlgaard, J., Loeschcke, V., Michalak, P. & Justesen, J. (1998). Induced thermotolerance and associated expression of the heat-shock protein Hsp70 in adult *Drosophila melanogaster*. *Funct. Ecol.*, 12, 786–793.

Dell, A.I., Pawar, S. & Savage, V.M. (2011). Systematic variation in the temperature dependence of physiological and ecological traits. *Proc. Natl. Acad. Sci.*, 108, 10591 LP – 10596.

DeVries, M., Webb, S. & Taylor, J. (2019). Re-examination of the effects of food abundance on jaw plasticity in purple sea urchins. *Mar. Biol.*, 166.

Duncan, M.I., Bates, A.E., James, N.C. & Potts, W.M. (2019). Exploitation may influence the climate resilience of fish populations through removing high performance metabolic phenotypes. *Sci. Rep.*, 9, 11437.

Feehan, C. & Scheibling, R. (2014). Disease as a control of sea urchin populations in Nova Scotian kelp beds. *Mar. Ecol. Prog. Ser.*, 500, 149–158.

Filbee-Dexter, K. & Scheibling, R. (2014). Sea urchin barrens as alternative

stable states of collapsed kelp ecosystems. *Mar. Ecol. Prog. Ser.*, 495, 1–25.

Frey, D. & Gagnon, P. (2016). Spatial dynamics of the green sea urchin, *Strongylocentrotus droebachiensis*, in food-depleted habitats. *Mar. Ecol. Prog. Ser.*, 552.

Frey, D.L. & Gagnon, P. (2015). Thermal and Hydrodynamic Environments Mediate Individual and Aggregative Feeding of a Functionally Important Omnivore in Reef Communities. *PLoS One*, 10, 1–28.

Frieder, C.A., Nam, S.H., Martz, T.R. & Levin, L.A. (2012). High temporal and spatial variability of dissolved oxygen and pH in a nearshore California kelp forest. *Biogeosciences*, 9, 3917–3930.

Gagnon, P., Himmelman, J.H. & Johnson, L. (2004). Temporal variation in community interfaces: Kelp-bed boundary dynamics adjacent to persistent urchin barrens. *Mar. Biol.*, 144, 1191–1203.

Gamperl, A., Ajiboye, O., Zanuzzo, F., Sandrelli, R., Peroni, E., Peroni, C., *et al.* (2020). The impacts of increasing temperature and moderate hypoxia on the production characteristics, cardiac morphology and haematology of Atlantic Salmon (*Salmo salar*). *Aquaculture*, 519, 1–14.

Gaylord, B., Nickols, K.J. & Jurgens, L. (2012). Roles of transport and mixing processes in kelp forest ecology. *J. Exp. Biol.*, 215, 997–1007.

Gillooly, J.F., Brown, J.H., West, G.B., Savage, V.M. & Charnov, E.L. (2001). Effects of Size and Temperature on Metabolic Rate. *Science (80-.).*, 293, 2248 LP – 2251.

Harianto, J., Carey, N. & Byrne, M. (2019). respR - An R package for the manipulation and analysis of respirometry data. *Methods Ecol. Evol.*

Hirsh, H.K., Nickols, K.J., Takeshita, Y., Traiger, S.B., Mucciarone, D.A., Monismith, S., *et al.* (2020). Drivers of Biogeochemical Variability in a Central California Kelp Forest: Implications for Local Amelioration of Ocean

Acidification. *J. Geophys. Res. Ocean.*, 125, e2020JC016320.

Hollins, J., Thambithurai, D., Koeck, B., Crespel, A., Bailey, D.M., Cooke, S.J., *et al.* (2018). A physiological perspective on fisheries-induced evolution. *Evol. Appl.*, 11, 561–576.

Hoshijima, U. & Hofmann, G.E. (2019). Variability of Seawater Chemistry in a Kelp Forest Environment Is Linked to in situ Transgenerational Effects in the Purple Sea Urchin, *Strongylocentrotus purpuratus*. *Front. Mar. Sci.*

Huey, R. & Stevenson, R. (1979). Integrating Thermal Physiology and Ecology of Ectotherms: A Discussion of Approaches. *Am. Zool.*, 19.

Huey, R.B. & Kingsolver, J.G. (2019). Climate Warming, Resource Availability, and the Metabolic Meltdown of Ectotherms. *Am. Nat.*, 194, E140–E150.

Jessup, D.A., Miller, M., Ames, J., Harris, M., Kreuder, C., Conrad, P.A., *et al.* (2004). Southern Sea Otter as a Sentinel of Marine Ecosystem Health. *Ecohealth*, 1, 239–245.

Keats, D.W., South, R.G. & Steele, D.H. (1990). Effects of an experimental reduction in grazing by green sea urchins on a benthic macroalgal community in eastern Newfoundland. *Mar. Ecol. Prog. Ser.*, 68, 181–193.

Kelty, J.D. & Lee, R.E. (2001). Rapid cold-hardening of *Drosophila melanogaster* (Diptera: Drosophiladae) during ecologically based thermoperiodic cycles. *J. Exp. Biol.*, 204, 1659–1666.

Kooijman, S.A.L.M. (1986). Energy budgets can explain body size relations. *J. Theor. Biol.*, 121, 269–282.

Kraft, N.J.B., Adler, P.B., Godoy, O., James, E.C., Fuller, S. & Levine, J.M. (2015). Community assembly, coexistence and the environmental filtering metaphor. *Funct. Ecol.*, 29, 592–599.

Krause-Jensen, D., Marbà, N., Sanz-Martin, M., Hendriks, I.E., Thyrring, J., Carstensen, J., *et al.* (2016). Long photoperiods sustain high pH in Arctic

kelp forests. *Sci. Adv.*, 2.

Lafferty, K.D., Porter, J.W. & Ford, S.E. (2004). Are Diseases Increasing in the Ocean? *Annu. Rev. Ecol. Evol. Syst.*, 35, 31–54.

Layton, C., Shelamoff, V., Cameron, M.J., Tatsumi, M., Wright, J.T. & Johnson, C.R. (2019). Resilience and stability of kelp forests: The importance of patch dynamics and environment-engineer feedbacks. *PLoS One*, 14, e0210220.

Lebrija-Trejos, E., Pérez-García, E.A., Meave, J.A., Bongers, F. & Poorter, L. (2010). Functional traits and environmental filtering drive community assembly in a species-rich tropical system. *Ecology*, 91, 386–398.

Leeuwis, R., Nash, G., Sandrelli, R., Zanuzzo, F. & Gamperl, A. (2019). The Environmental Tolerances and Metabolic Physiology of Sablefish (*Anoplopoma fimbria*). *Comp. Biochem. Physiol. Part A Mol. Integr. Physiol.*, 231.

Lester, S.E., Tobin, E.D. & Behrens, M.D. (2007). Disease dynamics and the potential role of thermal stress in the sea urchin, *Strongylocentrotus purpuratus*. *Can. J. Fish. Aquat. Sci.*, 64, 314–323.

Ling, S.D., Scheibling, R.E., Rassweiler, A., Johnson, C.R., Shears, N., Connell, S.D., *et al.* (2015). Global regime shift dynamics of catastrophic sea urchin overgrazing. *Philos. Trans. R. Soc. B Biol. Sci.*, 370, 20130269.

Maness, J.D. & Hutchison, V.H. (1980). Acute adjustment of thermal tolerance in vertebrate ectotherms following exposure to critical thermal maxima. *J. Therm. Biol.*, 5, 225–233.

McPherson, M.L., Finger, D.J.I., Houskeeper, H.F., Bell, T.W., Carr, M.H., Rogers-Bennett, L., *et al.* (2021). Large-scale shift in the structure of a kelp forest ecosystem co-occurs with an epizootic and marine heatwave. *Commun. Biol.*, 4, 298.

Meidel, S.K. & Scheibling, R.E. (1998). Annual reproductive cycle of the green

sea urchin, *Strongylocentrotus droebachiensis*, in differing habitats in Nova Scotia, Canada. *Mar. Biol.*, 131, 461–478.

Miller, L.P. & Dowd, W.W. (2019). Repeatable patterns of small-scale spatial variation in intertidal mussel beds and their implications for responses to climate change. *Comp. Biochem. Physiol. A. Mol. Integr. Physiol.*, 236, 110516.

Morris, R.L., Graham, T.D.J., Kelvin, J., Ghisalberti, M. & Swearer, S.E. (2020). Kelp beds as coastal protection: wave attenuation of Ecklonia radiata in a shallow coastal bay. *Ann. Bot.*, 125, 235–246.

Mueller, P. & Diamond, J. (2001). Metabolic rate and environmental productivity: Well-provisioned animals evolved to run and idle fast. *Proc. Natl. Acad. Sci.*, 98, 12550 LP – 12554.

Norderhaug, K.M., Fredriksen, S. & Nygaard, K. (2003). Trophic importance of Laminaria hyperborea to kelp forest consumers and the importance of bacterial degradation to food quality. *Mar. Ecol. Prog. Ser.*, 255, 135–144.

Norin, T. & Metcalfe, N.B. (2019). Ecological and evolutionary consequences of metabolic rate plasticity in response to environmental change. *Philos. Trans. R. Soc. B Biol. Sci.*, 374, 20180180.

O'Connor, M.I., Piehler, M.F., Leech, D.M., Anton, A. & Bruno, J.F. (2009). Warming and Resource Availability Shift Food Web Structure and Metabolism. *PLOS Biol.*, 7, e1000178.

Overgaard, J., Kristensen, T.N. & Sørensen, J.G. (2012). Validity of Thermal Ramping Assays Used to Assess Thermal Tolerance in Arthropods. *PLoS One*, 7, e32758.

Padfield, D., Yvon-Durocher, G., Buckling, A., Jennings, S. & Yvon-Durocher, G. (2016). Rapid evolution of metabolic traits explains thermal adaptation in phytoplankton. *Ecol. Lett.*, 19, 133–142.

Pederson, H.G. & Johnson, C.R. (2006). Predation of the sea urchin *Heliocidaris erythrogramma* by rock lobsters (*Jasus edwardsii*) in no-take marine reserves. *J. Exp. Mar. Bio. Ecol.*, 336, 120–134.

Peters, R.H. (1983). *The Ecological Implications of Body Size*. *Cambridge Stud. Ecol.* Cambridge University Press, Cambridge.

Pinheiro, J., Bates, D., DebRoy, S., Sarkar, D. & Team, R. (2015). nlme: linear and nonlinear mixed effects models.

Reed, D.C. & Foster, M.S. (1984). The Effects of Canopy Shadings on Algal Recruitment and Growth in a Giant Kelp Forest. *Ecology*, 65, 937–948.

Renaud, P.E., Løkken, T.S., Jørgensen, L.L., Berge, J. & Johnson, B.J. (2015). Macroalgal detritus and food-web subsidies along an Arctic fjord depth-gradient. *Front. Mar. Sci.*, 2, 31.

Rosman, J.H., Koseff, J.R., Monismith, S.G. & Grover, J. (2007). A field investigation into the effects of a kelp forest (*Macrocystis pyrifera*) on coastal hydrodynamics and transport. *J. Geophys. Res. Ocean.*, 112.

Saito, V.S., Perkins, D.M. & Kratina, P. (2021). A Metabolic Perspective of Stochastic Community Assembly. *Trends Ecol. Evol.*, 36, 280–283.

Sangil, C., Clemente, S., Martín-García, L. & Hernández, J.C. (2012). No-take areas as an effective tool to restore urchin barrens on subtropical rocky reefs. *Estuar. Coast. Shelf Sci.*, 112, 207–215.

Scheibling, R. & Hatcher, B. (2001). The ecology of *Strongylocentrotus droebachiensis*. In: *Edible Sea Urchins: Biology and Ecology* (ed. Lawrence, J.M.). Elsevier Science, Amsterdam, pp. 271–306.

Scheibling, R., Hennigar, A. & Balch, T. (1999). Destructive grazing, epiphytism, and disease: The dynamics of sea urchin - kelp interactions in Nova Scotia. *Can. J. Fish. Aquat. Sci.*, 56, 2300–2314.

Scheibling, R. & Lauzon-Guay, J.-S. (2007). Feeding aggregations of sea stars

(*Asterias* spp. and *Henricia sanguinolenta*) associated with sea urchin (*Strongylocentrotus droebachiensis*) grazing fronts in Nova Scotia. *Mar. Biol.*, 151, 1175–1183.

Schuster, L., White, C.R. & Marshall, D.J. (2019). Influence of food, body size, and fragmentation on metabolic rate in a sessile marine invertebrate. *Invertebr. Biol.*, 138, 55–66.

Silbiger, N.J., Goodbody-Gringley, G., Bruno, J.F. & Putnam, H.M. (2019). Comparative thermal performance of the reef-building coral *Orbicella franksi* at its latitudinal range limits. *Mar. Biol.*, 166, 126.

Smith, J.G., Tomoleoni, J., Staedler, M., Lyon, S., Fujii, J. & Tinker, M.T. (2021). Behavioral responses across a mosaic of ecosystem states restructure a sea otter-urchin trophic cascade. *Proc. Natl. Acad. Sci. U. S. A.*, 118.

Spindel, N.B., Lee, L.C. & Okamoto, D.K. (2021). Metabolic depression in sea urchin barrens associated with food deprivation. *Ecology*, 102, e03463.

Team, R.C. (2014). R: a language and environment for statistical computing.

Terblanche, J.S., Deere, J.A., Clusella-Trullas, S., Janion, C. & Chown, S.L. (2007). Critical thermal limits depend on methodological context. *Proc. R. Soc. B Biol. Sci.*, 274, 2935–2943.

Vanderklift, M.A. & Wernberg, T. (2008). Detached kelps from distant sources are a food subsidy for sea urchins. *Oecologia*, 157, 327–335.

Watanabe, H., Ito, M., Matsumoto, A. & Arakawa, H. (2016). Effects of sediment influx on the settlement and survival of canopy-forming macrophytes. *Sci. Rep.*, 6, 18677.

Wells, M.L., Potin, P., Craigie, J.S., Raven, J.A., Merchant, S.S., Helliwell, K.E., *et al.* (2017). Algae as nutritional and functional food sources: revisiting our understanding. *J. Appl. Phycol.*, 29, 949–982.

Wood, S.N. (2011). Fast stable restricted maximum likelihood and marginal

likelihood estimation of semiparametric generalized linear models. *J. R. Stat. Soc. Ser. B (Statistical Methodol.*, 73, 3–36.

Zanuzzo, F.S., Bailey, J.A., Garber, A.F. & Gamperl, A.K. (2019). The acute and incremental thermal tolerance of Atlantic cod (Gadus morhua) families under normoxia and mild hypoxia. *Comp. Biochem. Physiol. A. Mol. Integr. Physiol.*, 233, 30–38.

Zuur, A., Ieno, E.N., Walker, N., Saveliev, A.A. & Smith, G.M. (2009). *Mixed effects models and extensions in ecology with R*. Springer Science & Business Media.

2.7 Appendix A – Supplementary figures and tables for Chapter 2

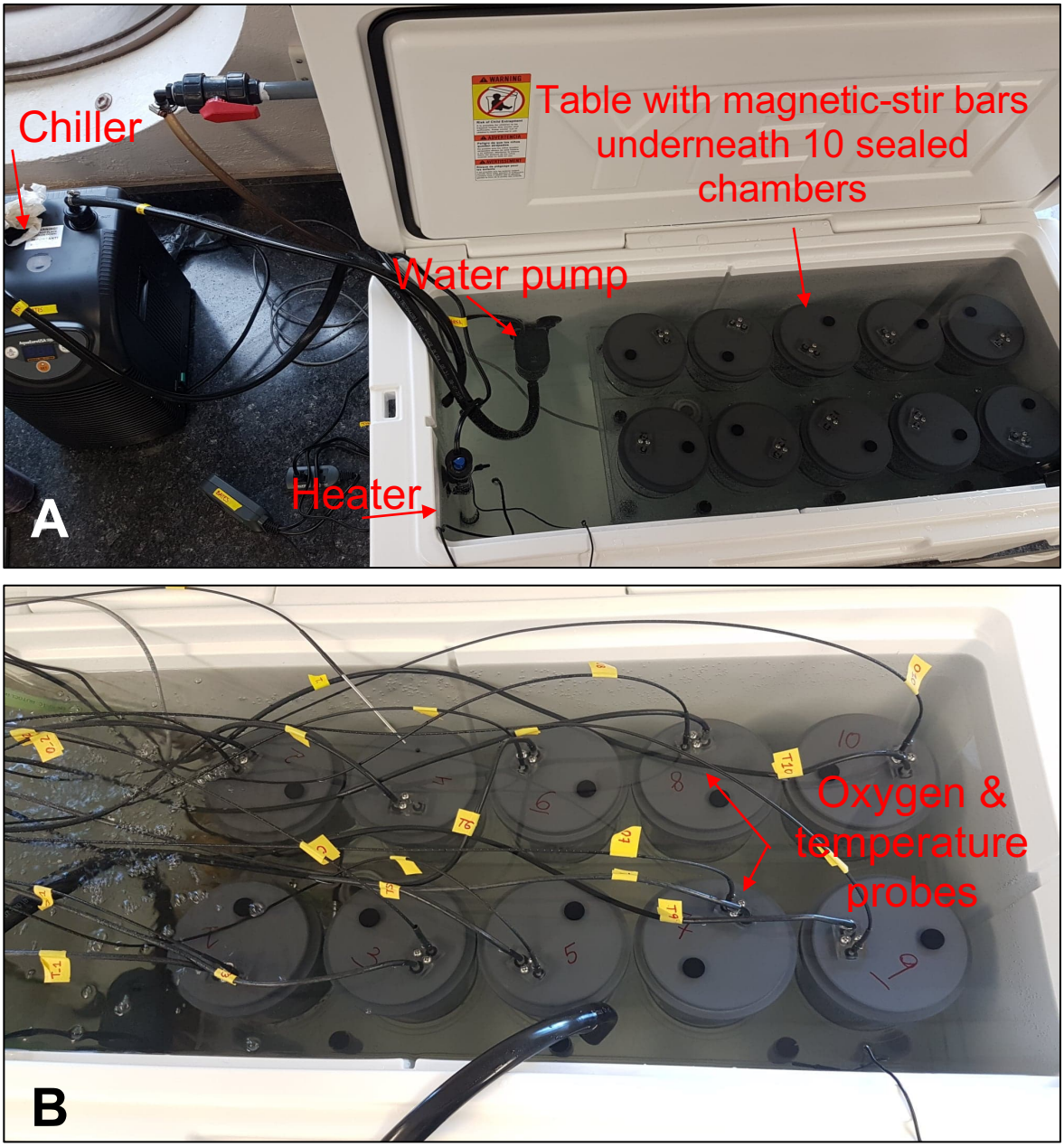

Figure S1. Experimental set-up to measure oxygen consumption in 10 chambers simultaneously (each chamber has a volume of 650 mL). The chambers sit inside a cooler (A) on top of a table with motor-powered magnetic stir plates. A stir bar located beneath a perforated stage inside each chamber keeps the seawater mixed during measurements. Oxygen and temperature probes are inserted into each chamber through ports in the lids (B). One chamber is used as a 'control', and allows for the measurement of background (microorganism) respiration.

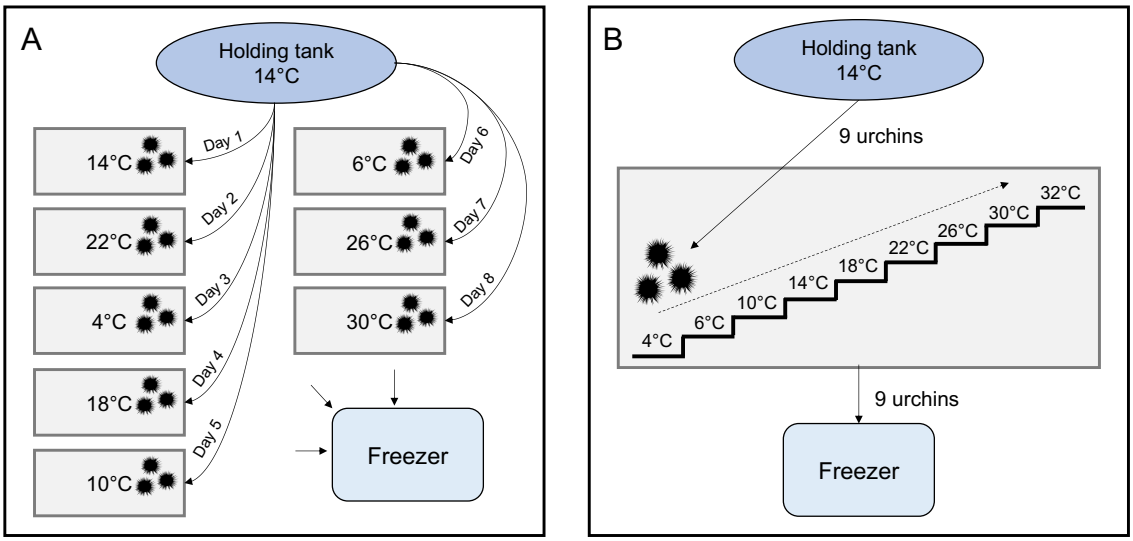

Figure S2. Schematic representation of the 'acute' (A) and 'ramping' protocols (B) used to measure the temperature-dependent oxygen consumption of green sea urchins. In the 'acute' protocol, nine sea urchins were moved directly from their holding tank (at 14 ºC; blue oval) into the cooler (grey box) each day. The seawater temperature in the cooler was pre-set to the test temperature, and temperatures were randomized across days as indicated in (A). The oxygen consumption of the nine urchins was measured after 1 hour in the cooler, and all urchins were frozen after each day's assay (i.e., each urchin was only tested at one temperature). In the 'ramping' protocol (B), nine urchins were placed into the cooler at 4 ºC, and oxygen consumption was measured at each temperature step, with a 30-minute period between each target temperature during which temperature was ramped to the next target temperature. After the 'ramping' protocol was completed the nine urchins were immediately frozen.

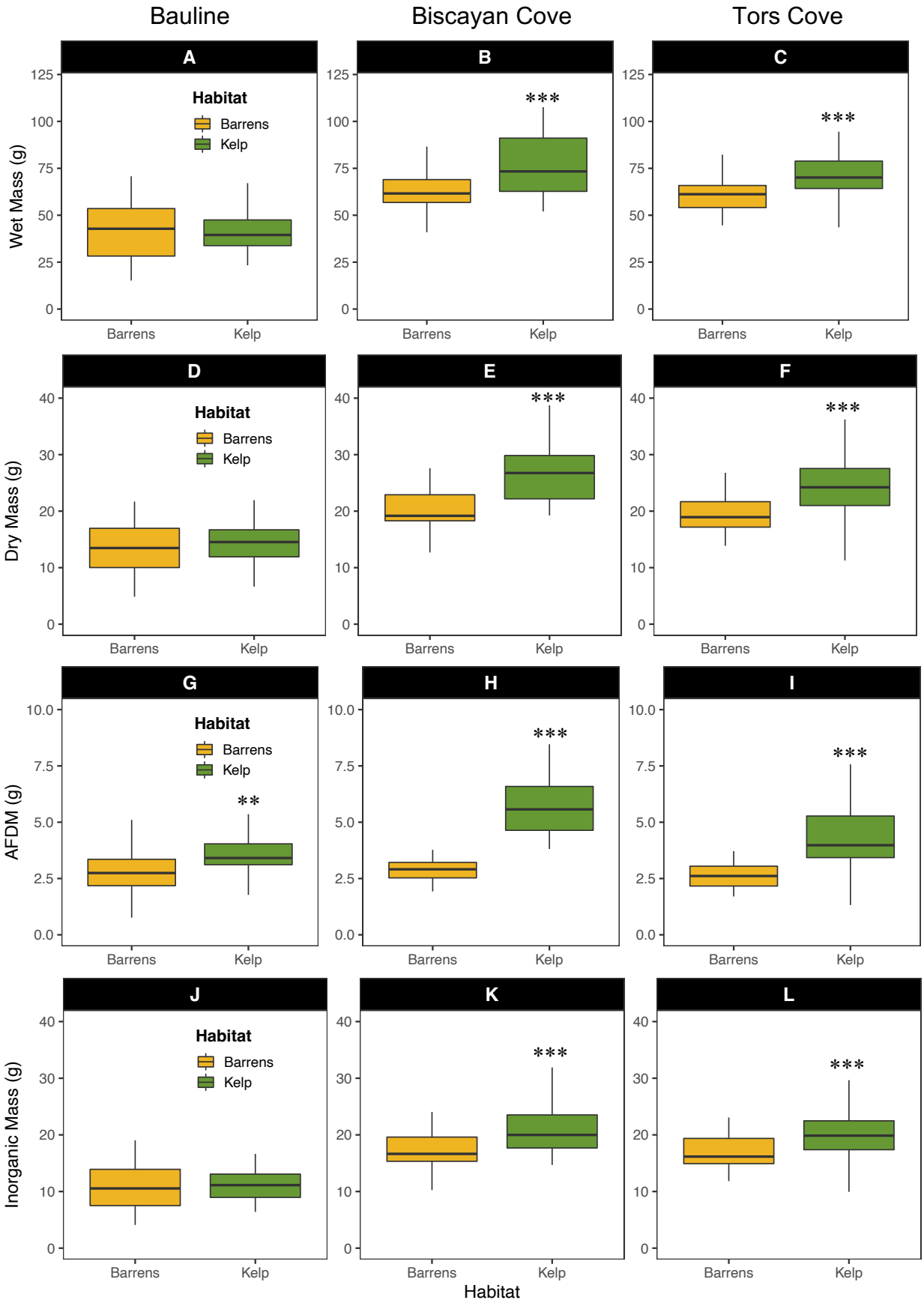
Bauline
Biscayan Cove
Tors Cove
A
B
C
D
E
F
G
H
I
J
K
L
Habitat
Barrens
Kelp
***
**
Wet Mass (g)
Dry Mass (g)
AFDM (g)
Inorganic Mass (g)
Habitat

Figure S3. Wet mass (top row, A-C), dry mass (2nd row, D-F), ash-free dry mass (ADFM; 3rd row, G-I) and inorganic (ash) mass (bottom row, J-L) of green sea urchins used during the 'acute' temperature trials. Urchins were collected from three sites (Bauline, left column; Biscayan Cove, middle column; Tors Cove, right column). Boxplots show maximum, minimum and median values, and 25th and 75th percentile values. Asterisks above the boxplots indicate a significant difference (* = p < 0.05, ** = p <0.01, *** p < 0.001) between urchins from barren and kelp habitats.

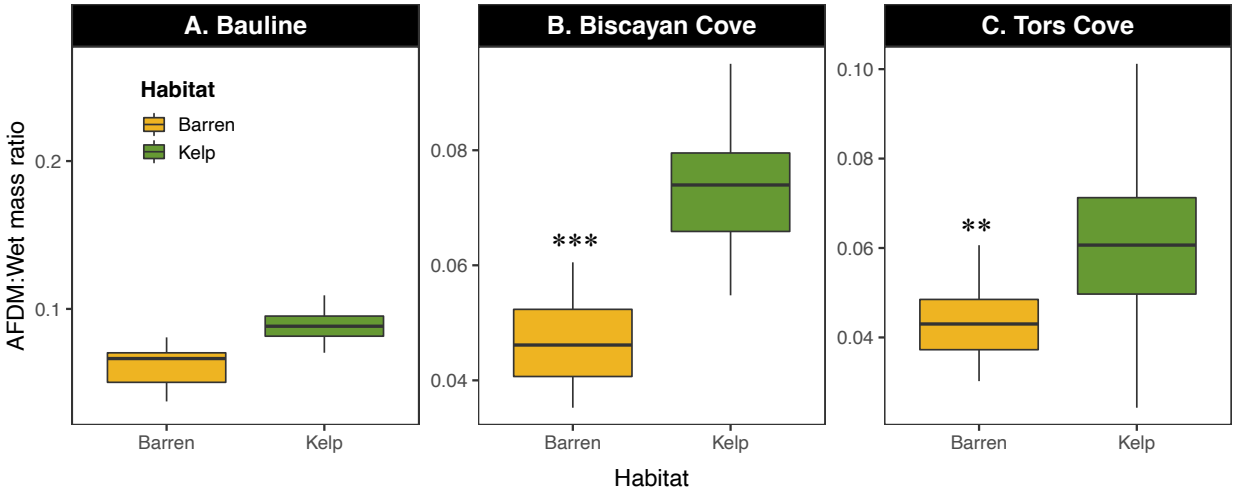

Figure S4. Ash-free dry mass (AFDM) to wet mass ratios for sea urchins from barren and kelp habitats at three sites in Newfoundland. These green sea urchins were used in the 'acute' temperature experiment (Experiment 1; N=220). Boxplots show maximum, minimum and median values, and 25th and 75th percentile values, for both habitat types. Asterisks above the boxplots indicate a significant difference (* = p < 0.05, ** = p <0.01, *** p < 0.001) between urchins from barren and kelp habitats.

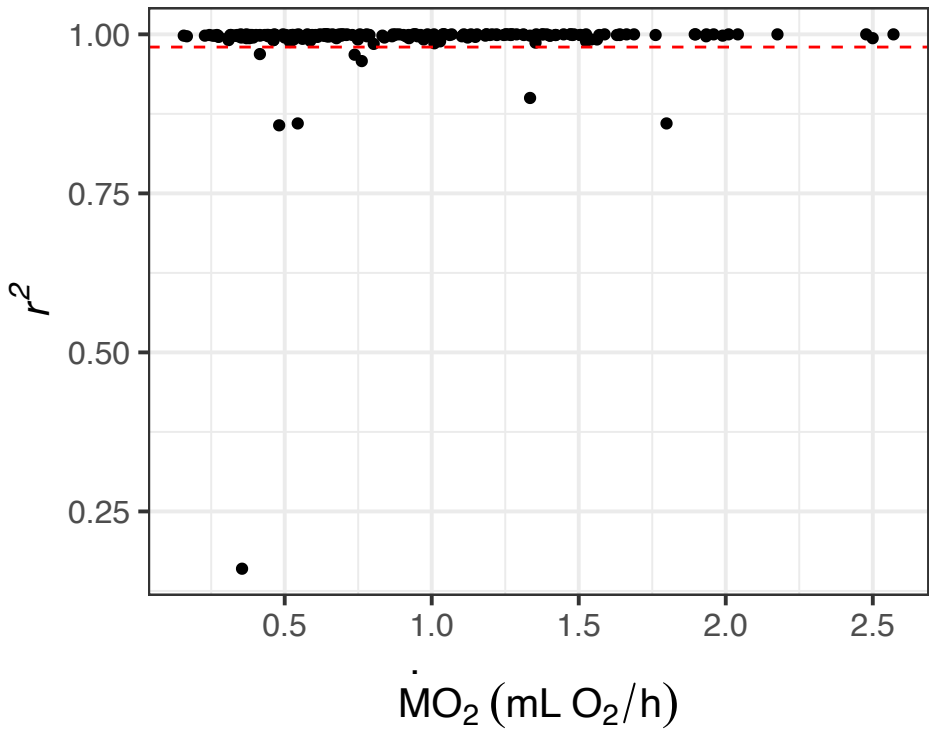

Figure S5. Plot of the r^2 for the relationship between time and water [oxygen] level, and the calculated oxygen consumption ($\dot{M}O_2$) of green sea urchins. The dotted red line indicates an $r^2 = 0.98$. All measurements with an r^2 below this value (N=8) were removed from analysis.

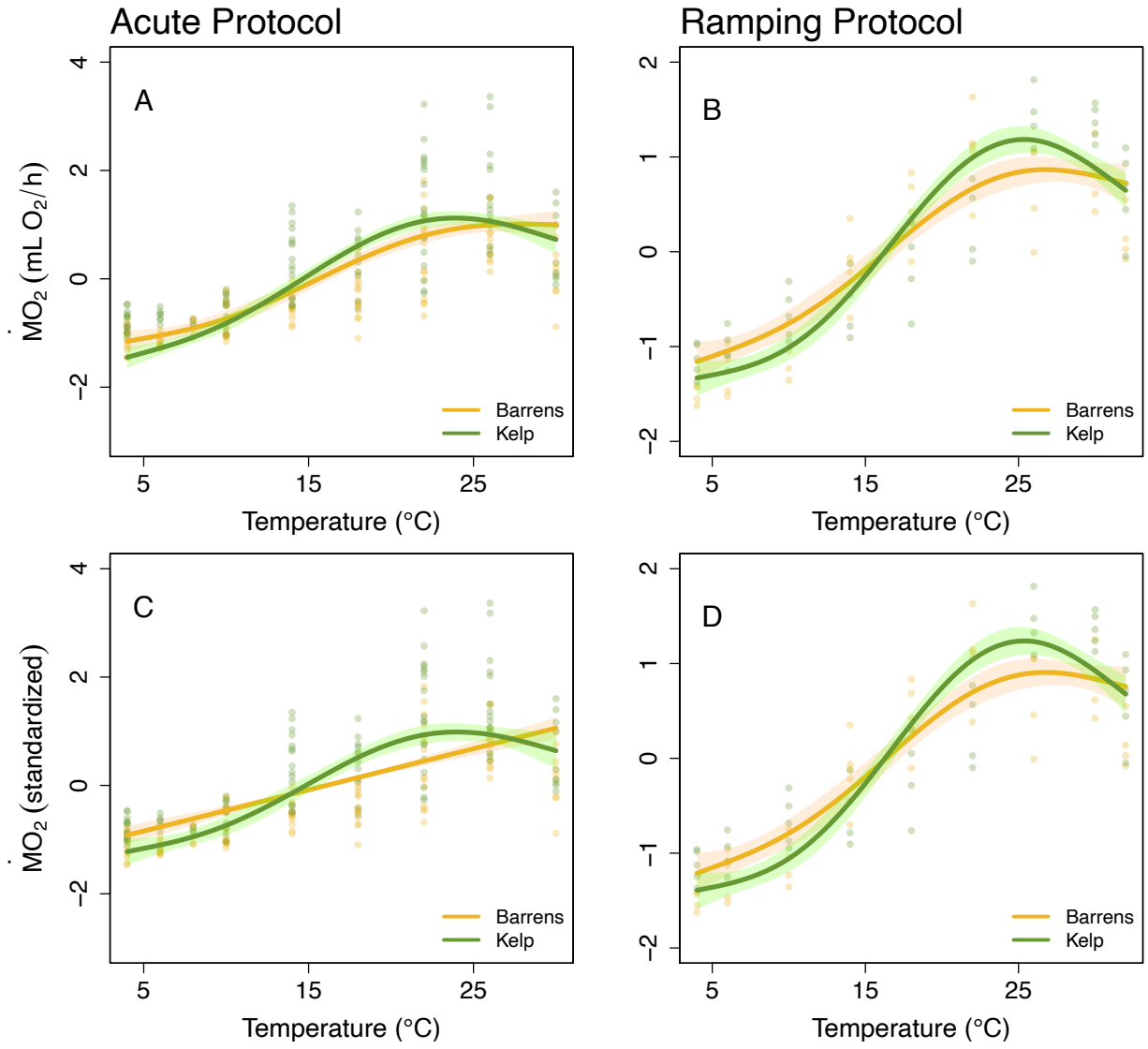

Figure S6. Temperature-dependent changes in absolute (A, B) oxygen consumption ($\dot{M}O_2$) and mass-independent oxygen consumption (C, D) in green sea urchins from kelp (green lines) and barren (yellow lines) habitats. $\dot{M}O_2$ was measured using an 'acute' temperature protocol (A, C) and a protocol where urchins were incrementally exposed to higher temperatures (i.e., a 'ramping' protocol; B, D). Lines indicate the $\dot{M}O_2$-temperature relationships for urchins from kelp vs. barren habitats relative to the mean (horizontal zero-intercept line), shaded areas are 95% confidence intervals predicted by GAMMs. A mass-covariate was included in models of absolute oxygen consumption (A, B). Points are scaled raw data. All fixed effects are scaled for coefficient comparison. See Table S1 for the summary of GAMM model results.

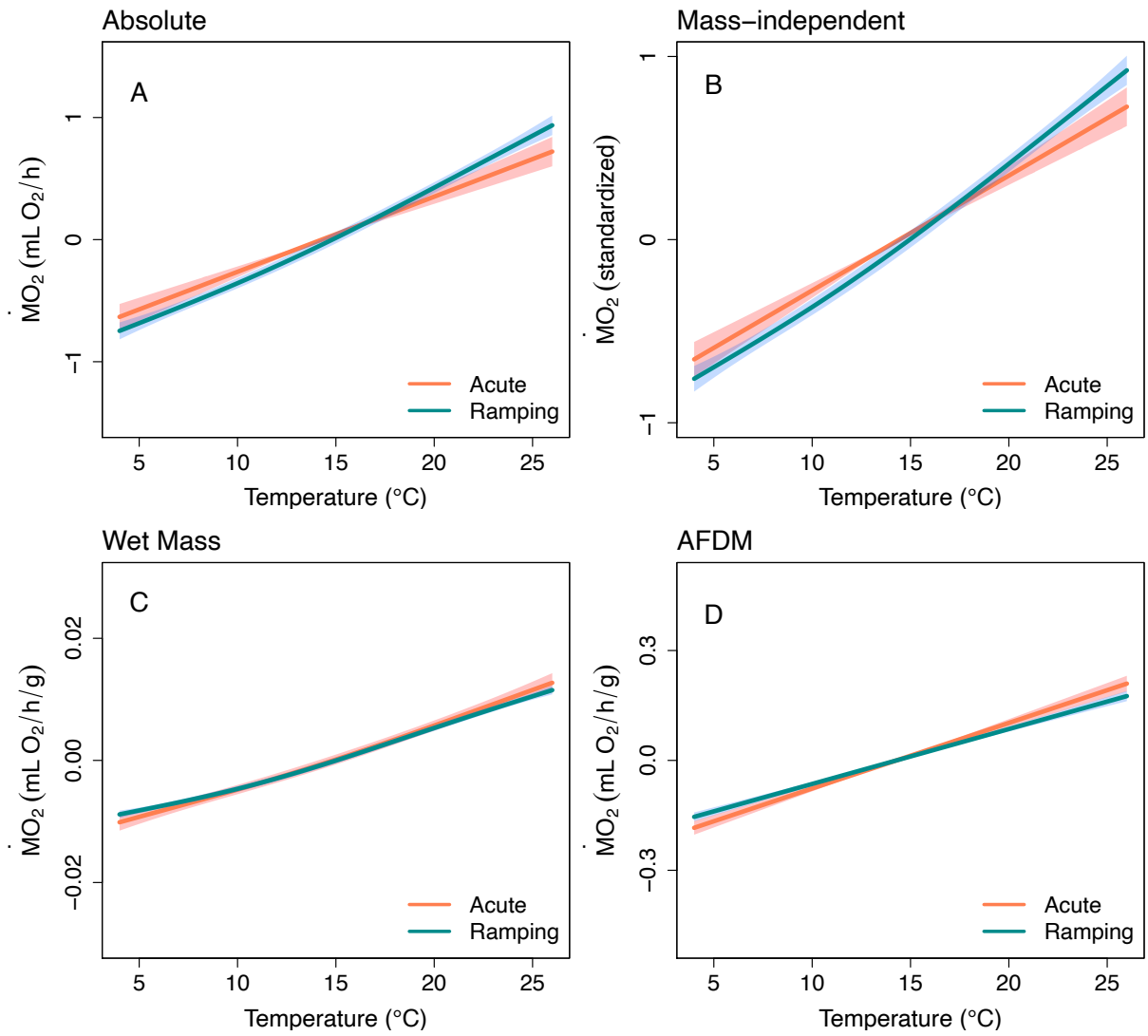

Figure S7. Oxygen consumption ($\dot{M}O_2$) [absolute values (A); mass-independent (B); relative to wet mass, (C); and relative to ash-free dry mass (AFDM), (D)] in green sea urchins exposed to an acute increase in temperature vs. those exposed to a 'ramping' protocol. Lines indicate rate-temperature relationships measured during the two protocols, relative to the mean (horizontal zero-intercept line). Shaded areas are 95% confidence intervals predicted by GAMMs. All fixed effects are scaled for coefficient comparison. See Table S2 for the summary of GAMM model results.

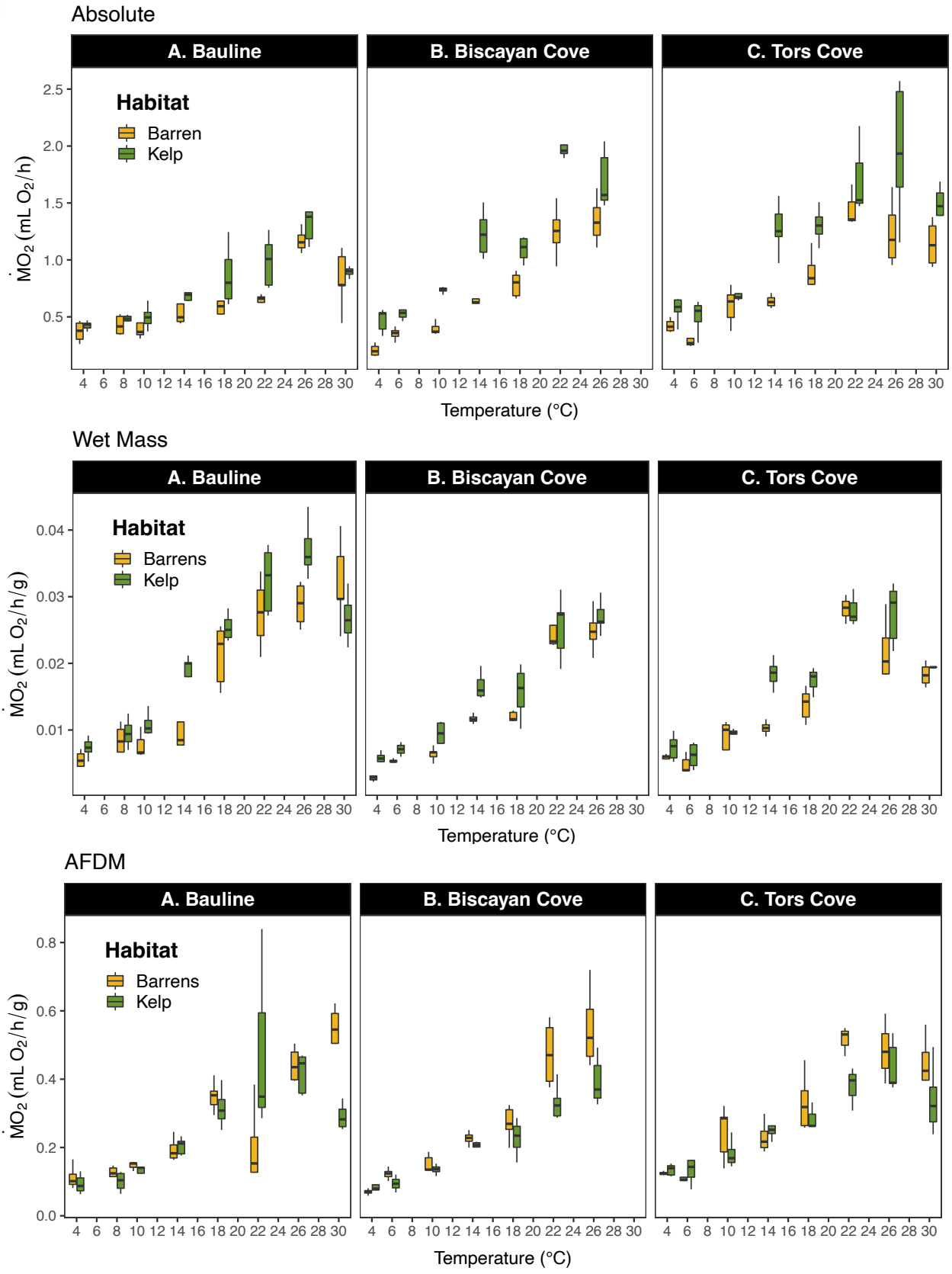
Absolute
A. Bauline
B. Biscayan Cove
C. Tors Cove
Habitat
Barren
Kelp
$\dot{M}O_2$ (mL O_2/h)
Temperature (°C)
Wet Mass
Habitat
Barrens
Kelp
$\dot{M}O_2$ (mL O_2/h/g)
Temperature (°C)
AFDM
Habitat
Barrens
Kelp
$\dot{M}O_2$ (mL O_2/h/g)
Temperature (°C)

Figure S8. Boxplots of oxygen consumption ($\dot{M}O_2$) vs. temperature for green sea urchins collected from kelp and barren habitats at three sites on the Avalon peninsula [absolute oxygen consumption, top panel; wet mass-specific values, middle panel; and relative to the mass of metabolically active tissue (AFDM), bottom panel]. Boxplots show maximum, minimum and median values, and 25th and 75th percentile values. Nine urchins were individually exposed to each temperature using the 'acute' protocol (see Methods). Note: sea urchins from Bauline (N=9) were mistakenly measured at 8ºC instead of 6ºC, thus boxplots at 6 ºC represent sea urchins from Biscayan Cove and Tors Cove only (N=18).

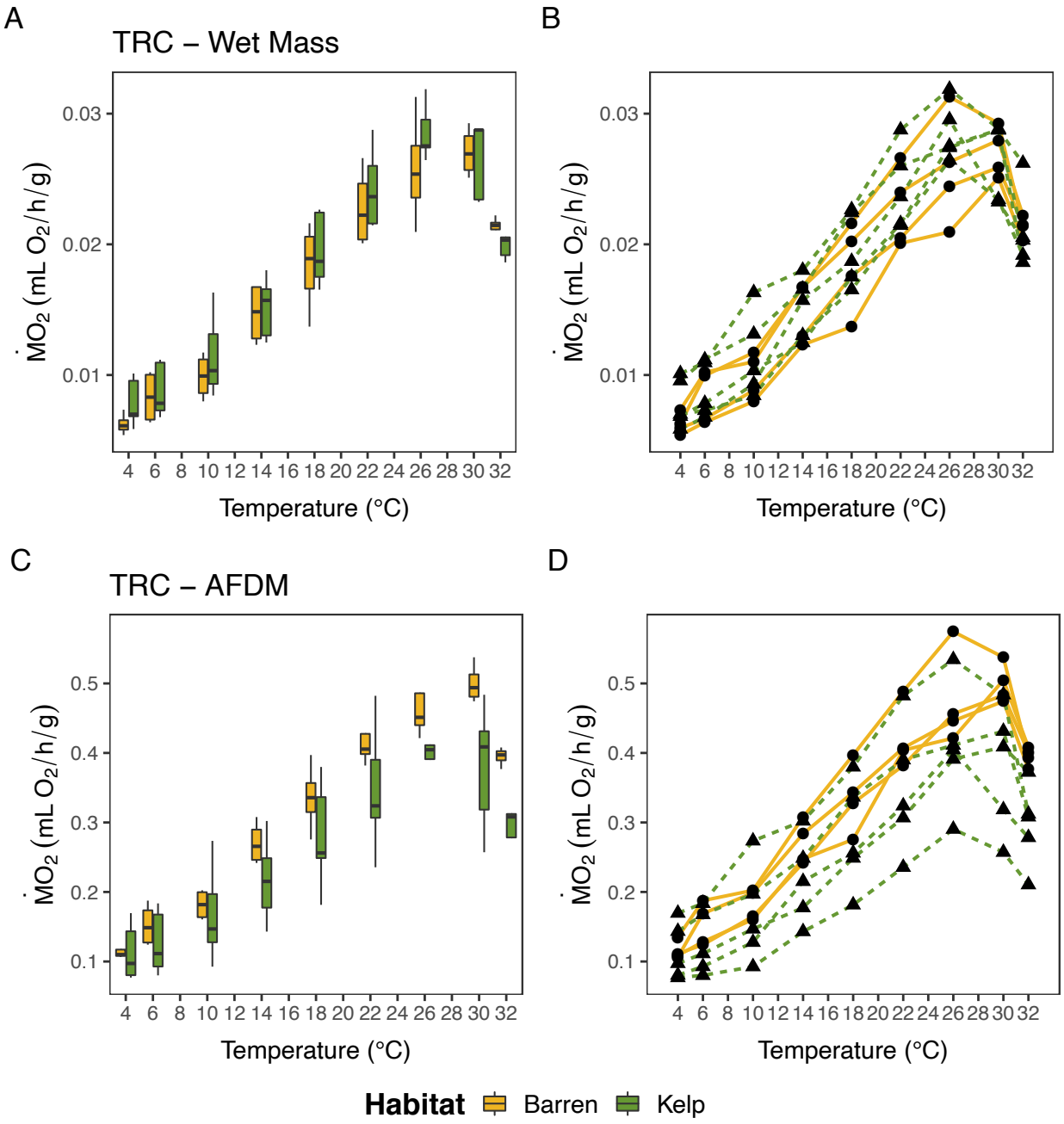

Figure S9. Oxygen consumption ($\dot{M}O_2$) of green sea urchins from Biscayan Cove exposed to an incremental increase in water temperature (i.e., the 'ramping' protocol). In the top panels (A and B) $\dot{M}O_2$ is standardized to wet mass. In the bottom panels (C and D) $\dot{M}O_2$ values are standardized to ash-free dry mass (AFDM). Boxplots show maximum, minimum and median values, and 25th and 75th percentile values. B and D show thermal response curves (TRCs) for individual urchins (dashed lines and triangles represent urchins from kelp habitats (N=5), whereas solid lines and circles represent urchins from barrens (N=4).

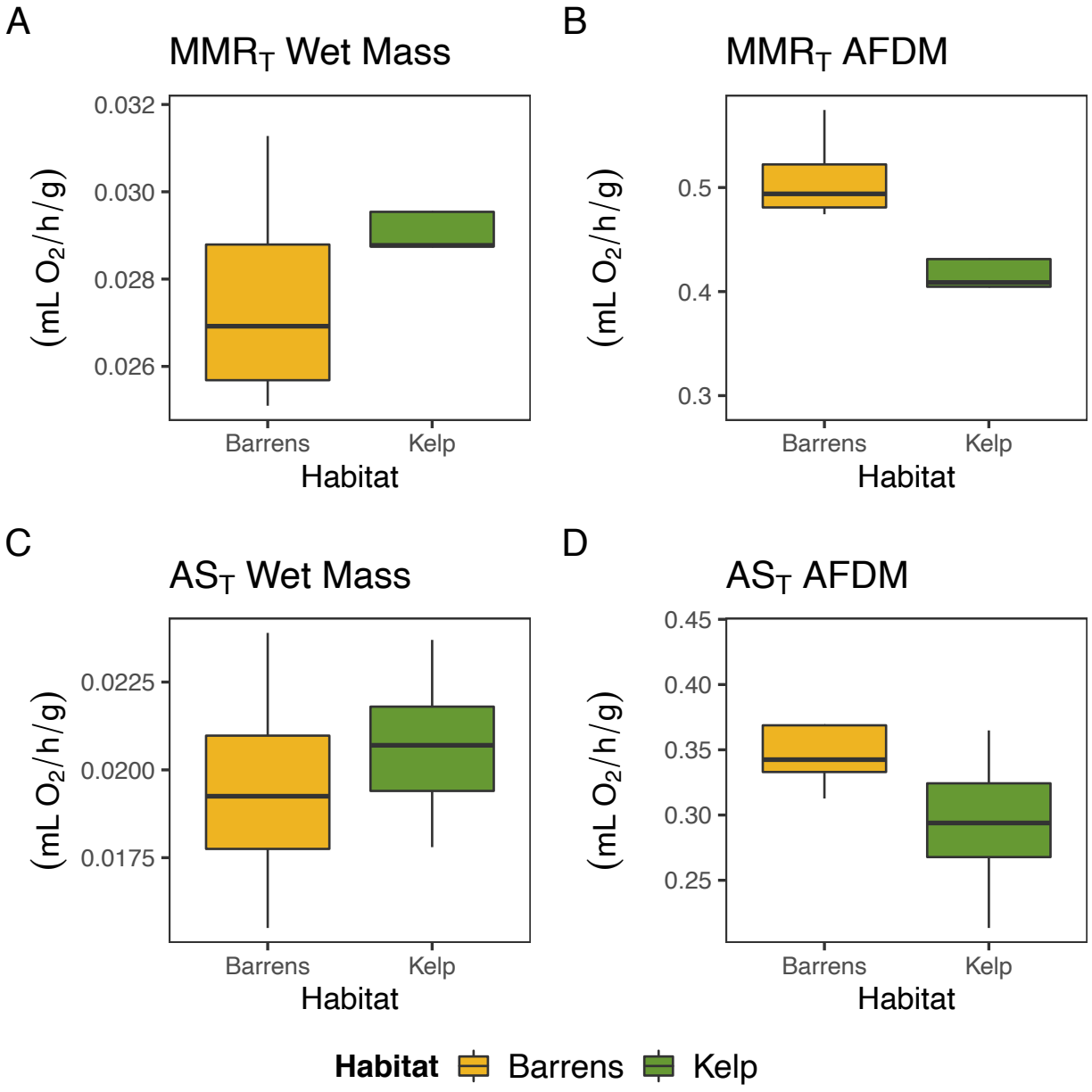

Figure S10. Maximum oxygen consumption (MMR_T), standardized to wet mass (A) and ash-free dry mass (AFDM; B), of green sea urchins from barren and kelp habitats. C and D show the difference in temperature-induced aerobic scope (AS_T), standardized for wet mass and AFDM, respectively. N=9 per habitat type. Boxplots show maximum, minimum and median values, as well as 25th and 75th percentile values.

Table S1. Summary table for statistical tests of absolute oxygen consumption (A, B), oxygen consumption rates independent of mass (C, D) and rates relative to wet mass (E, F) and ash-free dry mass (G, H) as affected by temperature in green sea urchins from two contrasting habitats (barrens and kelps). We fit generalized additive mixed models (GAMM, mgcv package (R Core Team 2014)) with the function gamm in R. Random effects of site are included to account for the spatial structure of the data in models for the 'acute' temperature protocol (A, C, E, G). Random effects of individual are included to account for repeated measurements on the same individuals during the 'ramping' protocol (TRCs; B, D, F, H). 's' indicates fixed effects (Temperature at which oxygen consumption was measured), modelled with penalized regression splines (GAM component) for barren and kelp sites, and wet mass was included as a covariate for models with absolute oxygen consumption as the response variable. Data were scaled for coefficient comparison. AIC = Akaine information criterion; Std. error = standard error; Edf = Estimated degrees of freedom; Ref. df = reference degree of freedom (prior to deductions). We ran models with different distribution families (gaussian, quasi-poisson), and a linear mixed effects model with a polynomial term to ensure patterns are consistent.

A) Absolute oxygen consumption rates during 'acute' exposures

Random effects

~1| Site:	<0.001
Residual:	0.464
AIC:	301.28
R^2:	0.78

LME	**Estimated value**	**Std. Error**	**DF**	**t-value**	**p-value**
Intercept	-1.544	0.114	199	-13.59	<0.001
Wet mass	0.026	0.002	199	14.16	<0.001
GAM	**Edf**	**Ref. df**		**F-value**	**p-value**
s(Temperature:Barren)	2.78	2.78		104.6	<0.001
s(Temperature:Kelp)	2.92	2.92		154.6	<0.001

B) Absolute oxygen consumption rates during 'ramping' (TRC) exposures

Random effects

~1| Individual:	0.193
Residual:	0.280
AIC:	75.08
R^2:	0.88

LME	**Estimated value**	**Std. Error**	**DF**	**t-value**	**p-value**
Intercept	-1.872	0.476	70	-3.94	<0.001

Wet mass	0.023	0.006	7	3.985	0.005
GAM	**Edf**	**Ref. df**		**F- value**	**p-value**
s(Temperature:Barren)	2.82	2.82		99.25	<0.001
s(Temperature:Kelp)	2.96	2.96		178.33	<0.001

C) Mass-independent metabolic rates during 'acute' exposures

Random effects	
~1| Site:	0.278
Residual:	0.592
AIC:	397.89
R^2:	0.56

LME	**Estimated value**	**Std. Error**	**DF**	**t-value**	**p-value**
Intercept	0.002	0.167	200	0.01	0.990
GAM	**Edf**	**Ref. df**		**F-value**	**p-value**
s(Temperature:Barren)	1.00	1.00		114.4	<0.001
s(Temperature:Kelp)	2.85	2.85		73.26	<0.001

D) Mass-independent metabolic rates during 'ramping' (TRC) exposures

Random effects	
~1| Individual:	0.202
Residual:	0.293
AIC:	80.38
R^2:	0.87

LME	**Estimated value**	**Std. Error**	**DF**	**t-value**	**p-value**
Intercept	0.000	0.076	70	0.000	1.000
GAM	**Edf**	**Ref. df**		**F-value**	**p-value**
s(Temperature:Barren)	2.82	2.82		100.5	<0.001
s(Temperature:Kelp)	2.96	2.96		180.6	<0.001

E) Wet mass-specific metabolic rates during 'acute' exposures

Random effects	
~1| Site:	0.200
Residual:	0.436
AIC:	284.99
R^2:	0.77

LME	Estimated value	Std. Error	DF	t-value	p-value
Intercept	-0.006	0.120	200	-0.053	0.958
GAM	**Edf**	**Ref. df**		**F-value**	**p-value**
s(Temperature:Barren)	2.89	2.89		127.8	<0.001
s(Temperature:Kelp)	2.95	2.95		145.0	<0.001

F) Wet mass-specific metabolic rates during 'ramping' (TRC) exposures

Random effects
~1| Individual: 0.226
Residual: 0.271
AIC: 71.85
R^2: 0.87

LME	Estimated value	Std. Error	DF	t-value	p-value
Intercept	0.000	0.083	70	0.000	1.000
GAM	**Edf**	**Ref. df**		**F-value**	**p-value**
s(Temperature:Barren)	2.89	2.89		147.1	<0.001
s(Temperature:Kelp)	2.95	2.95		179.0	<0.001

G) Ash-free dry mass-specific metabolic rates during 'acute' exposures

Random effects
~1| Site: 0.127
Residual: 0.525
AIC: 343.67
R^2: 0.76

LME	Estimated value	Std. Error	DF	t-value	p-value
Intercept	-0.007	0.083	198	-0.087	0.931
GAM	**Edf**	**Ref. df**		**F-value**	**p-value**
s(Temperature:Barren)	1.00	1.00		286.3	<0.001
s(Temperature:Kelp)	2.92	2.92		71.86	<0.001

H) Ash-free dry mass-specific metabolic rates during 'ramping' (TRC) exposures

Random effects
~1| Individual: 0.397
Residual: 0.268

AIC: 78.83
R^2: 0.75

LME	Estimated value	Std. Error	DF	t-value	p-value
Intercept	0.000	0.138	70	0.000	1.000
GAM	**Edf**	**Ref. df**		**F-value**	**p-value**
s(Temperature:Barren)	2.91	2.91		171.4	<0.001
s(Temperature:Kelp)	2.93	2.93		123.5	<0.001

Table S2. Summary table for statistical tests of oxygen consumption ($\dot{M}O_2$) as affected by temperature when using two contrasting measurement methods ('acute' vs. 'ramping'). Oxygen consumption values are expressed as absolute $\dot{M}O_2$ (A), mass-independent (B), wet mass-specific $\dot{M}O_2$ (C) and ash-free dry mass-specific $\dot{M}O_2$ (D); this corresponds with plots A-D in Fig. S8. We fit generalized additive mixed models (GAMM, mgcv package, (R Core Team 2014)) with the function gamm in R. Random effects of individual, nested within measurement approach, are included to account for repeated measurements on the same individuals during the 'ramping' protocol. 's' indicates fixed effects (Temperature at which oxygen consumption was measured) modelled with penalized regression splines (GAM component) for the 'acute' and 'ramping' approaches. Data were scaled for coefficient comparison. AIC = Akaine Information Criterion; Std. error = standard error; Edf = Estimated degrees of freedom; Ref. df = reference degree of freedom (prior to deductions). We ran models with different distribution families (gaussian, quasi-poisson), and a linear mixed effects model with a polynomial term to ensure patterns are consistent.

A) Absolute oxygen consumption rates

Random effects

~1| Treatment:	0.172
~1| Individual:	0.263
Residual:	0.161
AIC:	29.62
R^2:	0.69

LME	**Estimated value**	**Std. Error**	**DF**	**t-value**	**p-value**
Intercept	1.09	0.13	69	8.25	0.000
GAM	**Edf**	**Ref. df**		**F-value**	**p-value**
s(Temperature:Acute)	1.00	1.00		143.2	<0.001
s(Temperature:Ramping)	1.86	1.86		454.2	<0.001

B) Mass-independent rates

Random effects

~1| Treatment:	0.052
~1| Individual:	0.216
Residual:	0.163
AIC:	6.83
R^2:	0.80

LME	**Estimated value**	**Std. Error**	**DF**	**t-value**	**p-value**
Intercept	-0.02	0.05	65	-0.34	0.733
GAM	**Edf**	**Ref. df**		**F-value**	**p-value**

s(Temperature:Acute)	1.00	1.00		189.5	<0.001
s(Temperature:Ramping)	1.84	1.84		448.3	<0.001

C) Wet mass-specific rates

Random effects

~1| Treatment:	<0.001
~1| Individual:	0.003
Residual:	0.001
AIC:	-1143.81
R^2:	0.85

LME	**Estimated value**	**Std. Error**	**DF**	**t-value**	**p-value**
Intercept	0.01	<0.001	69	35.77	0.000
GAM	**Edf**	**Ref. df**		**F-value**	**p-value**
s(Temperature:Acute)	1.60	1.60		225.6	<0.001
s(Temperature:Ramping)	2.71	2.71		754.0	<0.001

D) Ash-free dry mass-specific rates

Random effects

~1| Treatment:	1.07
~1| Individual	0.06
Residual:	0.03
AIC:	-388.5
R^2:	0.79

LME	**Estimated value**	**Std. Error**	**DF**	**t-value**	**p-value**
Intercept	0.24	0.01	69	31.25	0.000
GAM	**Edf**	**Ref. df**		**F-value**	**p-value**
s(Temperature:Acute)	1.91	1.91		148	<0.001
s(Temperature:Ramping)	2.05	2.05		546.2	<0.001

Table S3. Summary of the statistical results from the one-way ANOVAs used to test for differences in parameters between green sea urchins from the two different habitats. Q_{10} values were calculated based on mean $\dot{M}O_2$ values for barren and kelp bed urchins at each site in the 'acute' experiment, and on individual $\dot{M}O_2$ values in urchins tested using the 'ramping' protocol. One Q_{10} value (4-14ºC) from the 'ramping' protocol was excluded after being identified as an outlier by a Grubb's test. MMR_T and AS_T are temperature-dependent maximum metabolic rate and aerobic scope, respectively.

			DF	Sum of Squares	Mean Squares	F-value	p-value
'Acute' Protocol	**Q_{10} 4 – 14 ºC**	Habitat	1	0.025	0.025	0.046	0.840
		Residuals	4	2.152	0.538		
	Q_{10} 14 - 26 ºC	Habitat	1	0.170	0.170	11.35	0.028
		Residuals	4	0.060	0.015		
'Ramping' Protocol	**Q_{10} 4 – 14 ºC**	Habitat	1	0.660	0.660	27.47	0.002
		Residuals	6	0.144	0.024		
	Q_{10} 14 - 26 ºC	Habitat	1	0.028	0.028	1.382	0.278
		Residuals	7	0.143	0.020		
	MMR_T	Habitat	1	0.757	0.757	8.008	0.025
		Residuals	7	0.661	0.095		
	AS_T	Habitat	1	0.259	0.259	2.657	0.147
		Residuals	7	0.684	0.098		

Table S4. Summary of the statistical results from a Mann-Whitney test used to identify differences in Q_{10} values between the two habitat types. Q_{10} values were calculated based on $\dot{M}O_2$ values from the 'ramping' protocol.

	W-value	p-value
Q_{10} cold range	16	0.191

Table S5. Summary of the statistical results for comparisons of wet mass, dry mass, ash-free dry mass (AFDM), inorganic (ash) mass, and the AFDM to wet mass ratios for green sea urchins between two habitat types and three sites. We ran a two-way ANOVA for each of the five response variables with habitat and site as explanatory variables. Test statistics were calculated for urchins from the experiment using the 'acute' protocol.

		DF	Sum of Squares	Mean Squares	F-value	p-value
Ratio	Habitat	1	0.019	0.019	47.15	<0.000
	Site	2	0.028	0.014	33.32	<0.000
	Habitat * Site	2	0.001	0.001	1.88	0.155
	Residuals	205	0.084	0.0004		
Wet mass	Habitat	1	3575	3575	17.80	<0.000
	Site	2	31150	15580	77.58	<0.000
	Habitat * Site	2	2310	1155	5.75	0.004
	Residuals	205	41148	201		
Dry mass	Habitat	1	1018	1017.9	46.65	<0.000
	Site	2	3196	1598.1	73.24	<0.000
	Habitat * Site	2	271	135.6	6.21	0.002

	Residuals	205	4473	21.8		
Ash-free dry mass	Habitat	1	162.41	162.41	138.24	<0.000
	Site	2	38.81	19.40	16.52	<0.000
	Habitat * Site	2	31.67	15.83	13.48	<0.000
	Residuals	205	240.83	1.17		
Inorganic mass	Habitat	1	367	367.1	23.66	<0.000
	Site	2	2666	1333.2	85.92	<0.000
	Habitat * Site	2	123	61.6	3.97	0.02
	Residuals	205	3181	15.5		

Table S6. Summary table of the results of the Tukey HSD post-hoc tests conducted after the models shown in Table S5 were performed.

		Mean diff	Lower CI	Upper CI	p-value
Ratio	Biscayan Cove - Bauline	-0.019	-0.027	-1.042	<0.000
	Tors Cove - Bauline	-0.027	-0.035	-1.894	<0.000
	Tors Cove – Biscayan Cove	-0.008	-0.016	4.017	0.051
Wet mass	Biscayan Cove - Bauline	27.42	21.61	33.23	<0.000
	Tors Cove - Bauline	24.26	18.74	29.75	<0.000
	Tors Cove – Biscayan Cove	-3.17	-8.83	2.50	0.39
Dry mass	Biscayan Cove - Bauline	8.95	7.03	10.86	<0.000
	Tors Cove - Bauline	7.56	5.74	9.37	<0.000
	Tors Cove – Biscayan Cove	-1.39	-3.26	0.48	0.19
Ash-free dry mass	Biscayan Cove - Bauline	1.06	0.61	1.50	<0.000
	Tors Cove - Bauline	0.32	-0.10	0.74	0.18
	Tors Cove – Biscayan Cove	-0.74	-1.17	-0.31	<0.001
Inorganic mass	Biscayan Cove - Bauline	7.89	6.27	9.50	<0.000
	Tors Cove - Bauline	7.24	5.71	8.77	<0.000
	Tors Cove – Biscayan Cove	-0.65	-2.22	0.93	0.595

Chapter 3 - The Role of Kelp Availability and Type on the Energetic State and Thermal Tolerance of Sea Urchin and Gastropod Grazers.

This chapter has been reviewed, revised, and re-submitted for consideration as a publication:

Schuster, J. M. and Bates, A. E., (in review). The role of kelp availability and type on the energetic state and thermal tolerance of sea urchin and gastropod grazers. Journal of Experimental Marine Biology and Ecology.

3.1 Abstract

Environmental and anthropogenic stressors are driving widespread declines in underwater forests, formed by kelps and macroalgae, around the world. The loss of vulnerable kelp species that form the surface canopy typically leads to alternate rocky reef states, dominated by substrate-near understory vegetation or reefs where large fleshy algae (macroalgae) are entirely absent, as, for example, in sea urchin barrens. Such alternate reef states are expected to be more commonplace in the future, due to warming-related declines in canopy kelp, and could represent a major shift in food availability and quality. In particular, grazers that prefer kelp may be negatively affected by the loss of canopy kelp if they must switch to less nutritious food sources to avoid starvation. Here, we investigate if changes in food resource type or starvation alter grazer physiology, and whether prolonged lack of higher-quality foods impairs an organism's ability to respond to temperature stress. We quantified the mass-independent oxygen consumption ($\dot{M}O_2$), as a proxy of whole-organism physiology, of four grazing invertebrate species [two sea urchin species (*Mesocentrotus franciscanus* and *Strongylocentrotus purpuratus*) and two gastropod species (*Pomaulax gibberosus* and *Tegula pulligo*)] that were given one of three diets over seven weeks: 1) giant kelp: *Macrocystis pyrifera*; 2) sugar kelp: *Saccharina latissima*; or 3) no kelp. We further tested for differences in the heat resistance of these four grazers using an acute, near-lethal, heat exposure after provisioning the three diets for seven-weeks. We found that the two sea urchins had values for mass-independent $\dot{M}O_2$ that were lower by 26-78% after macroalgae restrictions, while the two gastropod grazers did not display food-related metabolic

responses when presented with macroalgae versus no food. While the effects of food restriction in the two urchin species were large, the effects of kelp type were small and variable. The urchins were also distinguished in terms of their heat resistance, and both urchin species could withstand acute, extreme, heat stress twice as long as the gastropod species. While a lack of macroalgae has clear physiological consequences for sea urchins that are detectable at the whole-organism level, overall, the type of macroalgae provisioned (*Macrocystis* versus *Saccharina*) had limited impacts on grazer physiology after seven weeks.

3.2 Introduction

Kelps, large brown macroalgae, are declining around the world (Wernberg *et al.* 2019). The loss of kelp species that extend to the water surface and form floating canopies (canopy kelps, hereafter) is of particular concern because canopy kelps influence and structure entire understory communities. These canopy kelps form underwater forests that provide complex habitat, primary production and ecosystem services, and support coastal food webs and fisheries (Graham *et al.* 2007; Schiel & Foster 2015). However, the abundance, distribution and health of canopy kelp forests are threatened by stress associated with changing temperatures, more frequent extreme weather events (e.g., marine heatwaves or high-intensity storms) and poor water quality (Meehl *et al.* 2000; Krause-Jensen *et al.* 2012; Duarte *et al.* 2018; Wernberg *et al.* 2018). For example, canopy kelps such as the giant kelp (*Macrocystis pyrifera*) are highly vulnerable to climate change-related impacts, with growth and survival negatively impacted by warm and nutrient poor waters typical of predicted future ocean conditions (Graham 2004; Graham *et al.* 2007; Schiel & Foster 2015). In addition, sea urchin populations are expanding in many regions, where they rapidly overgraze kelps and intensify herbivory pressure (Filbee-Dexter & Scheibling 2014; Ling *et al.* 2015; Rogers-Bennett & Catton 2019).

Environmental and biological stressors can act simultaneously, and are changing kelp forests at a range of temporal and spatial scales (Krumhansl *et al.* 2016; Pfister *et al.* 2018). However, the impacts of such disturbance can vary across distinct vegetational layers. For example, some stressors impact floating canopy

kelps more severely than understory kelps (i.e., kelp and macroalgae growing beneath the canopy). Floating canopy kelps are also more vulnerable to wave damage by increasingly frequent extreme storm events than subsurface, understory, vegetation (Graham *et al.* 2007; Schiel & Foster 2015). Moreover, surface seawater temperatures are often several degrees warmer than subsurface waters, exposing floating canopy kelps to more extreme temperature highs than understory kelps. While other environmental stressors (e.g., long-term warming, nutrient limitation) are similar across vegetation layers, the stress tolerance and response of understory macroalgal species is often more variable, with some species benefiting from surface canopy removal through increased light availability and decreased competition (Schiel & Foster 2015; Castorani *et al.* 2018). The few species of kelp that form floating surface canopies [*Macrocystis pyrifera, Eualaria fistulosa, Nereocystis luetkeana* and *Ecklonia maxima* (Steneck *et al.* 2002)] appear vulnerable to ocean conditions predicted for the future (Graham 2004; Graham *et al.* 2007; Schiel & Foster 2015). Some understory kelps and macroalgae are also vulnerable, but the diversity of understory algae provides functional redundancy (i.e., multiple species contribute in similar ways, and species can be substituted), while surface canopy formers are often functionally unique, and thus, irreplaceable (Graham *et al.* 2007; Teagle *et al.* 2017). Overall, there is substantial evidence that many ecosystem functions in temperate marine systems are directly, and indirectly, dependent on canopy forming kelps (Stachowicz *et al.* 2008; Tait & Schiel 2018; Castorani *et al.* 2021).

The consequences of kelp loss are wide-ranging, and include shifts in food resources for associated species. When multiple species of kelp are present in a forest, grazers can preferentially, and selectively, feed to optimize fitness outcomes. However, when canopy kelps are lost, some grazers must switch to alternative food sources (e.g., understory algae, drift kelp, or even filamentous algae and biofilms) to avoid starvation (Vanderklift & Wernberg 2008; Filbee-Dexter & Scheibling 2014; Renaud *et al.* 2015). Given the heightened vulnerability of floating canopy kelps, a shift away from canopy kelps as a primary food source may be expected in the future, as has occurred in areas which are rapidly warming such as the large-scale decline of *Macrocystis* in Australia (Johnson *et al.* 2011; Wernberg *et al.* 2016; Layton *et al.* 2020).

The quantity and quality of food influences metabolic rate, a key process that underpins organism physiology and fitness across taxa (McNab 1986; Brown *et al.* 2004; Huey & Kingsolver 2019; Norin & Metcalfe 2019). The chemical reactions that regulate metabolic rates are largely universal across life forms, and the sum of these metabolic reactions is typically estimated by measuring oxygen consumption ($\dot{M}O_2$). Metabolic rate varies across environments: $\dot{M}O_2$ is strongly and universally temperature-dependent (Gillooly *et al.* 2001; Dell *et al.* 2011), and metabolic plasticity has been linked to habitat type (Bernhardt & Leslie 2013; Spindel *et al.* 2021; Schuster *et al.* 2022) and food limitation (Norin & Metcalfe 2019). Resource limitation (i.e., the quality and quantity of food) may constrain an organisms' ability to meet its energetic needs and regulate or optimize its response

to environmental challenges such as heatwaves (Padfield *et al.* 2016; Silbiger *et al.* 2019). Such an effect has been reported for green sea urchin (*Strongylocentrotus droebachiensis*) populations from kelp beds which consume 8-78% more oxygen, and show less sensitivity to temperature increases (based on Q_{10} values) than urchins from barrens (Schuster *et al.* 2022). Reductions in diet quantity during development can also lower routine metabolic rate, a response that would conserve energy when food is limiting (O'Connor *et al.* 2000; Moe *et al.* 2004; Roark & Bjorndal 2009). Persistent food limitations can also reduce a species' mobility, and reduce growth and the capacity for fitness enhancing functions (Bennett & Ruben 1979; Nilsson 2002). Individuals with high metabolic rates, by contrast, tend to be bolder and more aggressive, and dominate over those with low metabolic rates in terms of food access (Metcalfe *et al.* 1995; Biro & Stamps 2010). However, the benefits or costs of a relatively high versus low metabolic rate are often context dependent (reviewed in: Burton et al., 2011).

Loss of canopy kelp as a nutritious food source occurs simultaneously with ocean warming (Steneck *et al.* 2002; Wernberg *et al.* 2019). Both climate change and shifts in food resources could potentially alter net energy gain, which in turn influences an organisms' growth, reproduction and fitness (Huey & Kingsolver 2019). Thus, an initial challenge is to identify which grazing species are most vulnerable to heat stress. Moreover, changes in food resources may drive population-level variation in the ability to thermoregulate and resist heat stress. If so, populations with continuous access to high quality foods may be better able to

respond to, resist, and recover from challenging thermal conditions, such as heatwaves (Padfield *et al.* 2016; Huey & Kingsolver 2019; Silbiger *et al.* 2019), as compared to populations that have experienced prolonged resource limitations. Because metabolic rate (and thus energetic demand) increases with temperature (Gillooly *et al.* 2001), concurrent declines in food resources and warming may create multiplicative challenges, leading to 'metabolic meltdown' where organisms are energetically less heat tolerant (Huey & Kingsolver 2019).

Expansive kelp forests characterize the coastlines of Barkley Sound, a species rich region in the Northeast Pacific. As in other kelp systems, giant kelp (*Macrocystis pyrifera*) harbor many fishes and invertebrates, including gastropods, echinoderms and crustaceans that rely on kelp for their diet (Steneck *et al.* 2002; Graham 2004). However, as has been observed in many regions, *Macrocystis* forests have also declined in the Barkley Sound region, due to broad-scale changes in ocean conditions, and in response to the 2013-2016 heatwave (Bond *et al.* 2015; Starko *et al.* 2019). By contrast, *Saccharina* understory kelps have been relatively stable over the same two decades (Starko *et al.* 2019; Diehl *et al.* 2021). In addition to varying environmental tolerances, *Macrocystis* and *Saccharina* kelps also have well-documented differences (on average) in their nutritional values (see supplementary table S1; Zimmerman & Kremer 1986; Smith *et al.* 2010; Biancarosa *et al.* 2018; Sharma *et al.* 2018; Corino *et al.* 2019; Krogdahl *et al.* 2021). *M. pyrifera* is also a preferred food source for many marine herbivores (Leighton 1966) due to its low levels of phenolics - compounds that deter

herbivores (Anderson & Velimirov 1982; Watanabe 1984; Steinberg 1985). Diverging trends in canopy and understory kelps in Barkley Sound, and a possible future where canopy kelps decline, thus offer an ideal study system to investigate the impact of shifts in kelp species, and food restriction, on organismal energetics.

Here, we quantify changes in the energetic state of four grazing invertebrates in response to macroalgae food type and macroalgae exclusion. First, we determined whether access to a higher quality (on average) canopy kelp (*Macrocystis pyrifera*) versus lower quality understory kelp (*Saccharina latissima*), as compared to a lack of kelp provisioning modifies the realized energetic state (routine metabolic rate) of these grazers by measuring their absolute, mass-independent and mass-specific $\dot{M}O_2$ at ambient seawater temperatures. Absolute $\dot{M}O_2$ estimates whole-organism metabolic rate per unit time, whereas mass-specific $\dot{M}O_2$ represents metabolic rate scaled to the organism' body mass (Peters 1983; Brown *et al.* 2004). Because body mass and absolute $\dot{M}O_2$ are often correlated (Brown *et al.* 2004), and because of variation in body mass across treatments, we calculate mass-independent $\dot{M}O_2$ to compare populations across food treatments without the confounding effects of body mass. Second, we tested for differences in the heat resistance between the four grazers using an acute, near-lethal, heat exposure. Finally, we compared the heat resistance in all species that received the different food treatments for seven weeks. We selected ecologically important urchin species (*Mesocentrotus franciscanus* and *Strongylocentrotus purpuratus)* that are well known to persist in both food rich (kelp forest) and food deprived (urchin

barren) environments to understand the energetic consequences of food limitation and quality. In addition, we included two gastropod grazers (*Pomaulax gibberosus* and *Tegula pulligo*) which are ubiquitous in Barkley Sound, and commonly found feeding on blades of giant kelp.

The preferred diet of the two sea urchin species is live kelp, and *M. pyrifera* in particular (Leighton 1966; Foster *et al.* 2015), but they also rely on drift kelp, and can switch to feeding on filamentous or encrusting algae and biofilms in the absence of kelp (Lawrence 1975; Lawrence & Sammarco 1982; Filbee-Dexter & Scheibling 2014; Renaud *et al.* 2015). Although urchin diets are relatively flexible, absorption efficiency, growth and reproduction are maximal when fed their preferred diet (Vadas 1977). *Tegula* and *Pomaulax* gastropods are less selective/ generalist herbivores (Steinberg 1985), that consume a wide array of macro- and microalgae, as well as biofilms, filamentous algae and epiphytes, but overall prefer *M. pyrifera* (Leighton 1966; Watanabe 1984; Durante & Chia 1991; Mazzillo *et al.* 2013). These four grazers are important members of the local food web, as they move kelp derived carbon to higher trophic levels. However, their resource dependent energetics and thermal vulnerability are unknown.

3.3 Methods

3.3.1 Organism collection

Grazing invertebrates were collected by scuba divers during two successive dives on the 23rd of March 2021 at Eagle Bay (48°50'04.4"N, 125°08'48.2"W) and Ohiat (48°51'11.4"N, 125°10'58.6"W) in Barkley Sound (Vancouver Island, B.C., Canada). Organisms were collected by hand from rocky reef habitat at both sites,

at 5-10 m depth using mesh collection bags. We collected 108 individuals per species, for the following four grazer species: red sea urchins (*Mesocentrotus franciscanus*), purple sea urchins (*Strongylocentrotus purpuratus*), red turban snails (*Pomaulax gibberosus*) and dusky turban snails (*Tegula pulligo*). Individuals with a diameter under 9 cm were selected due to respirometer size constraints. The organisms were placed in seawater filled coolers for immediate transport to the Bamfield Marine Science Centre (BMSC), Bamfield, British Columbia. The transport time by boat from the collection sites to BMSC was 45 minutes. At BMSC, all grazers were weighed to determine their wet mass (0.01 g accuracy) and placed into holding tanks with seawater at 9ºC (the average ambient water temperature at the time of collection; see supplementary figure S1).

3.3.2 Food treatments and cage set-up

On March 24th, nine metal grid cages (35 x 35 x 35 cm [W x L x H]) were prepared for the *in situ* food treatments (N = 3 cages per treatment); each cage fitted with a 7 m rope and weighed with a 1 kg rock to stabilize and suspend it in an upright position in the water column. The insides of the cage walls were also fitted with mesh fabric (1000 µm) to prevent animal escapes or intrusions into the cages, and to restrict introduction of food items larger than plankton. A temperature logger (EnvLogger v2.4, 0.1°C resolution, ELECTRICBLUE, Portugal) was attached to the inner wall of three cages (#1, 4 and 7) to continuously record *in situ* seawater temperatures at 30-minute intervals throughout the study (see supplementary figure S1). All nine cages were then tied to a floating dock (BMSC foreshore: Fig 3.1) with a 1.5 m spacing between each cage. The cages remained fully

submerged in the water column (without touching the bottom) at all times, except during feeding, when all cages were lifted onto the docks, so that all individuals were exposed to air for the same duration of time.

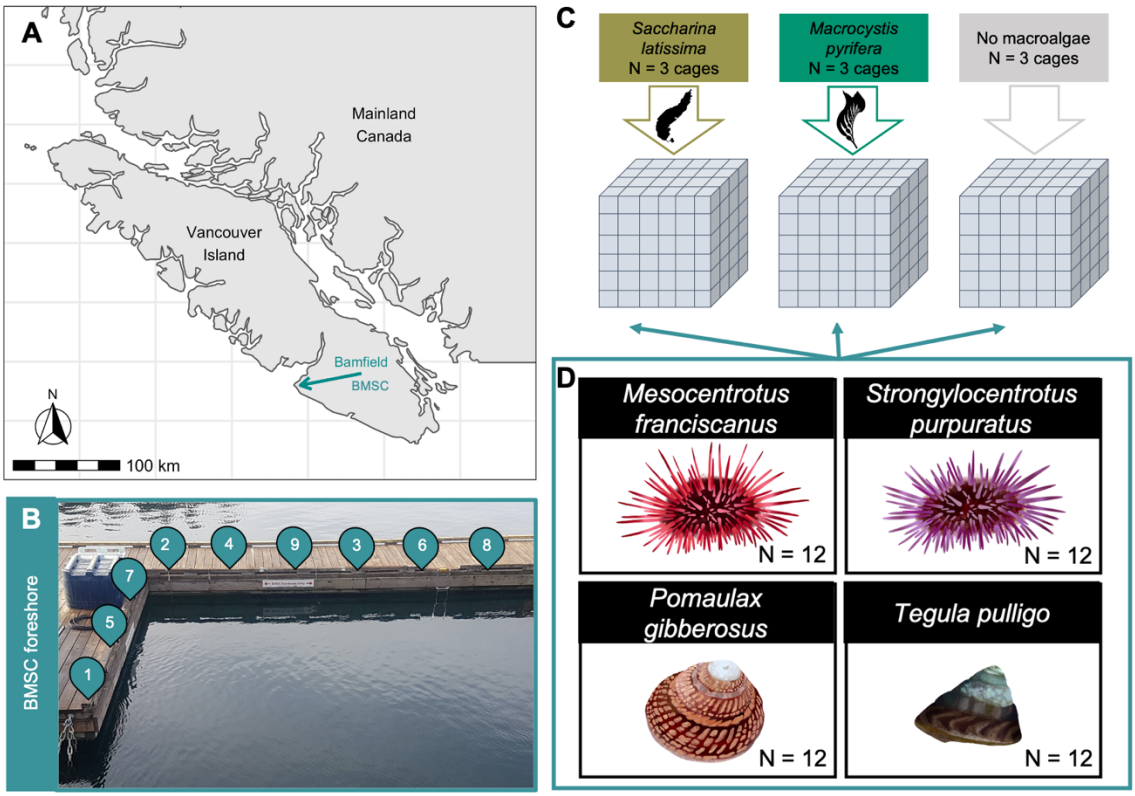

Figure 3.1 Location and set-up of caging experiment. For 7 weeks, nine cages were suspended in the water column at ~5 m depth off the South docks at the Bamfield Marine Science Centre (BMSC) foreshore, in Bamfield (A), Vancouver Island, Canada (see cage location pins in B). Three different food treatments (C) were administered throughout the caging period: a) *Macrocystis pyrifera* (giant kelp; N = 3 cages); b) *Saccharina latissima* (sugar kelp; N = 3 cages) and c) no macroalgae (N = 3 cages). Each cage contained a polyculture (D) of four grazing invertebrate species: *Mesocentrotus franciscanus, Strongylocentrotus purpuratus, Pomaulax gibberosus* and *Tegula pulligo* (N = 12 individuals per species per cage). Invertebrate illustrations by Cerren Richards.

After the animals were weighed, they were transported from the holding tanks back down to the BMSC foreshore in seawater-filled coolers (transport time was less than 10 minutes). At the foreshore, specimens were haphazardly divided into the nine cages, with twelve individuals of each species per cage (N = 48 individuals per polyculture cage; N = 36 individuals per species per treatment; N = 432 individuals across all cages, species and treatments). After the animals were placed inside the cages, lids were immediately secured and each cage was submerged into the water column and fixed to the dock (as described above).

In total, the experiment ran for seven weeks: March 24th to May 15th, 2021. Three cages were assigned to each food treatment (i.e., three cage replicates, with N = 144 individuals in total per treatment): a) *Macrocystis pyrifera*, commonly known as giant kelp; b) *Saccharina latissima*, or sugar kelp; and c) no macroalgae. It is well established that *M. pyrifera* has higher nutritional value, on average, than *S. latissima* (see supplementary table S1). Food for the first two treatments was administered *ad libidum* every 5 days, using freshly harvested blades and stipes of *Macrocystis and Saccharina* kelp. All remaining kelp was removed from the cages and replaced with fresh kelp on feeding days. Seasonal shifts over the course of the experiment resulted *in situ* seawater temperatures increasing from 9.0°C to 10.5°C, on average (see supplementary figure S1).

3.3.3 Experimental assay system for measuring oxygen consumption

A custom-built experimental system was used to measure the oxygen consumption ($\dot{M}O_2$) of grazers. The system consisted of a table with 10 removable acrylic chambers with magnetic stir plates contained within a cooler (custom built at the Technical Services Unit, Memorial University of Newfoundland, St. John's, Newfoundland, Canada). Two sets of 10 chambers of different sizes were used; one set of small chambers (240 mL, 6.5 cm in diameter) for measurements of $\dot{M}O_2$ in red turban and dusky turban snails, and a set of large chambers (650 mL, 9 cm in diameter) for use with sea urchins. The experimental system is described in more detail in Schuster *et al.* (2022) (Chapter 2). In brief, the system consists of an insulated cooler equipped with a heater, chiller and water pump that circulates temperature-controlled seawater across the cooler to ensure consistent temperatures across the 10 chambers. An air pump attached to an air stone continuously aerated the seawater in the cooler, and each chamber was fitted with a temperature probe and a fiber-optic oxygen dipping probe (PreSens Pt1000 and DP-PSt7-10-L2.5-ST10-YOP; Precision Sensing GmbH, Regensburg, Germany). Measurements of temperature and oxygen level (% saturation) were made every second using PreSens software (PreSens Measurement Studio 2, Version 3.0.3), with oxygen measurements automatically temperature-corrected by the software. Oxygen probes were calibrated prior to each assay set (Week 2 and Week 7) with air saturated, room temperature, sea water (100 % O_2) and sodium sulfite (no O_2; 1 g Na_2SO_3 dissolved in 100 mL of room temperature distilled water).

3.3.4 Pre-measurement procedures and treatment of grazers

To estimate routine metabolic rate after 2 and 7 weeks, the $\dot{M}O_2$ of the four grazing invertebrate species was measured using closed respirometry with the system described above. Initial $\dot{M}O_2$ measurements were made at Week 2 to allow the animals to adjust to the cage environment. To quantify the $\dot{M}O_2$ of all individuals (N = 432) at each time-point, measurements were staged over three subsequent assay days (see supplementary figure S2 and table S2). On each assay day, 13 independent $\dot{M}O_2$ measurement runs were completed, comprising all individuals from three different polyculture cages. Preliminary trials determined that *Tegula pulligo* had very low rates of oxygen consumption, and thus, three individuals were placed together in each chamber, so that all runs could be completed each day. On the evening before a given assay day, three cages (one from each treatment group) were brought to the laboratory and placed into a holding tank overnight. The holding tank was supplied with filtered (10 µm) flow-through seawater at ambient temperature (9.0°C in Week 2 and 10.5°C in Week 7; see supplementary figure S1). For each run on a given assay day, nine individuals were selected at a time for measurement, and the mass and volume [measured by displacement (volumetric displacement = volume of seawater with grazer - volume without grazer)] of each individual were recorded. The nine specimens were then distributed amongst the nine chambers, with the tenth chamber remaining empty to account for background respiration (i.e., $\dot{M}O_2$ due to microorganisms). These chambers were initially covered with mesh-fabric to prevent escape of the invertebrates prior to the start of measurements. Measurement runs were repeated

with a new set of nine individuals until all grazers across the three cages were measured.

3.3.5 Oxygen consumption measurements

To make $\dot{M}O_2$ measurements, the insulated cooler was filled with fresh filtered (10 µm) seawater and maintained at ambient temperature for each run. To initiate a measurement run, the tops were put onto each chamber (9 grazers, one blank) and sealed, and the drop in water oxygen levels (in % air saturation) was recorded until oxygen levels dropped by 5 to 10%. The total measurement time varied from 15 min. to approximately 1.5 hours, with longer measurement times for individuals that have lower masses of metabolically active tissue. Once the measurements were completed for each of the 10 chambers, all grazers included in the measurement run were removed from the chambers and returned to a separate holding tank (maintained at the same conditions as the first) until all measurement runs of a day were completed. The chambers were then emptied and cleaned, and nine new grazers were placed into the chambers (after having their mass and volume measured), repeating the same measurement procedure as before. Once all 13 measurement runs in a day were completed, the grazers were returned to their respective cages (that were cleaned with freshwater from a high pressure hose) and fed *ad libidum* according to their assigned treatment. The seawater tank was emptied, rinsed with warm freshwater and refilled with fresh seawater to prepare for the next assay day. The above procedures were repeated with grazers from all nine cages over three subsequent days (N = 3 cages per day; N = 12 individuals per species per cage; N = 432 grazers in total across all cages and

days). After the final oxygen consumption measurement (Week 7), all organisms were returned to their respective cages and left to recover from handling *in situ* for 48 hours before their heat resistance was measured (see below).

3.3.6 Heat resistance experiment

To quantify the heat resistance of the four grazing invertebrate species following the 7-week feeding experiment, we measured the time until loss of equilibrium, which is analogous to 'functional mortality' (e.g., Bates and Morley, 2020), during an acute, static heat exposure. All organisms were removed from their cages on the morning of May 18th, 2021 and placed in flow-through holding tanks supplied with filtered seawater at ambient temperature. For each heat resistance trial, an individual was placed into a temperature-controlled seawater bath maintained at 35°C and a stopwatch was started immediately. This temperature was chosen to prompt a rapid heat stress response without incurring mortality, and the upper limit of sublethal heat tolerance typically lies between 30-45°C for marine invertebrates (Bates *et al.* 2013). We measured the time of 'functional survival' until an individual reached loss of equilibrium, and subsequently the individual was returned to an ambient-temperature water tank, where the organism was assessed for recovery (no mortalities occurred). Due to capacity related time-constraints, we only included half of the individuals from each treatment and species to quantify heat resistance (N = 18 individuals per species x treatment combination; N = 216 total), acknowledging that this decision limited our power to detect significant trends. Loss of equilibrium was defined as the time (seconds) until the organism no longer responded to probing with a blunt metal probe and had ceased all movement (see

Table 3.1 for a description of behavioural responses to heat exposure). After the final measurement, all recovered grazers were immediately frozen.

3.3.7 Calculation of $\dot{M}O_2$

Values of $\dot{M}O_2$ at ambient temperature were calculated for each grazer using the respR package in R (Harianto *et al.* 2019), with values adjusted for salinity and accounting for an individuals' volumetric displacement. In addition, all $\dot{M}O_2$ measurements were corrected for background respiration using the $\dot{M}O_2$ values for the blank chamber of each run. Microbial background respiration values were typically < 0.1 mL O_2 h^{-1}. The $\dot{M}O_2$ data were visually inspected to confirm that a linear decrease in water % air saturation of 5-10% occurred, and that the water O_2 – time relationship had a minimum r^2 of 0.9 (Chabot *et al.* 2021). We removed 34 measurements with an r^2 value below this threshold from subsequent analyses. To calculate mass-independent $\dot{M}O_2$, we regressed absolute $\dot{M}O_2$ against individual wet body mass (non-linear regression) and extracted the residuals, yielding mass standardized $\dot{M}O_2$ values. Because seawater temperatures were 1.5°C higher in Week 7 than in Week 2 due to seasonal shifts (see supplementary figure S1), we calculated the expected change in $\dot{M}O_2$ for a 1.5°C temperature increase based on a Q_{10} temperature coefficient before comparing values. Q_{10} values indicate the temperature sensitivity (fold-change) of biological rates based on chemical reactions. We use an average Q_{10} value of 2.5, as Q_{10} values lie between 2-3 for most biological systems. This Q_{10} value also corresponds well with the temperature sensitivity of metabolic rates observed in sea urchins (Schuster *et al.* 2022). We

compare observed changes in $\dot{M}O_2$ from Week 2 to Week 7 with expected changes in $\dot{M}O_2$ based on Q_{10}.

3.3.8 Ash-free dry mass

At the end of the experiment we determined each individual's ash-free dry mass to quantify the amount of organic, metabolically-active, tissue. First, empty aluminum weigh boats were placed in a muffle furnace (500°C) for 12 hours to remove traces of organic matter and stored in a sealed container until use. Frozen grazers were then thawed prior to weighing, and placed onto the pre-weighed (to 0.001 g accuracy) weigh boats, and then dried in a combustion oven (at 60°C) for 12 to 24 hours until their dry mass stabilized. Then, the grazers were ashed in a muffle furnace at 500°C for 2 hours, to remove all organic material. Ash-free dry mass (i.e., that corresponding to metabolically active tissue) was calculated as dry (organic) mass (with boat) minus ashed (inorganic) mass (with boat). Individual dry mass was calculated as dry mass minus the mass of the empty weigh boat.

Table 3.1 Behavioural response sequence of grazing invertebrate species to acute heat exposure (35°C). LOE = loss of equilibrium ('functional mortality' occurs). The time of LOE (see 2 and 3) was recorded for each individual using species-specific criteria.

Behavioural sequence	*Mesocentrotus franciscanus*	*Strongylocentrotus purpuratus*	*Pomaulax gibberosus*	*Tegula pulligo*
(1)	Sea urchin is active and mobile. Spines move and rotate erratically. Responds defensively to probing by 'closing' spines over probed	Sea urchin is highly active and mobile. Spines move and rotate erratically. Responds defensively to probing by 'closing'	Foot moving around as if undergoing sensory activities. When probed, foot	Snail is active and mobile. Retracts foot and shuts operculum in

	spot. Attachment observed in some cases.	spines over probed spot. May attach to tank surface.	retracts into shell.	response to probing.
(2)	Spines droop. Movement slows.	Spines droop. Movement slows.	Foot mostly retracted into shell. Foot unresponsive to probing.	Foot unresponsive to probing. All movement ceased. **LOE reached.**
(3)	Movement stops. Loss of attachment. Unresponsive to probing. **LOE reached.**	Movement stops. Loss of attachment. Unresponsive to probing. **LOE reached.**	Foot no longer retracted; hangs out of the shell. Unresponsive to probing. **LOE reached.**	

3.3.9 Statistical analyses

To test for differences in grazer $\dot{M}O_2$ across the food treatments, we fit one-way ANOVAs using the function 'aov' in the R 'stats' package (R Core Team 2014) for each species and time-period (Week 2 or Week 7) with food treatment as a main effect. We visually inspected the data to check assumptions, and ran a Shapiro-Wilk normality test (supplementary table S3) using the function 'shapiro.test' in the R 'stats' package (R Core Team 2014). If test assumptions were met, we performed a Tukey's HSD post-hoc test (function 'tukeyHSD in R 'stats' package) to identify differences across the three food treatments following the ANOVA test. If ANOVA test assumptions were not met, we performed a non-parametric Kruskal-Wallis test using the function 'kruskal.test', followed by a Wilcoxon rank test with Bonferroni adjustment (using the function 'wilcox_test') to identify statistically different treatment levels, in the R 'stats' package. For red sea urchins and red turban snails,

we ran a sensitivity test, which involved repeating the analysis procedure outlined above, but with the largest individuals removed. We ran this sensitivity test for the subset of smaller individuals because of initial differences in wet mass across treatments for the red sea urchins and red turban snails before the experiment began (see supplementary figure S3 and table S4). Differences in absolute $\dot{M}O_2$ across treatments using this 'small individual' subset agree well with mass-independent $\dot{M}O_2$ differences across treatments of the whole dataset. We thus proceeded with comparisons of mass-independent $\dot{M}O_2$ values, without the confounding effect of body mass.

We quantified organismal heat resistance using Kaplan-Meier survival analysis, where a survival model was built for each species and treatment using the functions 'Surv' and 'survfit' in the R 'survival' package (Therneau 2021). The time until loss of equilibrium was used as an indicator of 'functional survival', and the Kaplan-Meier function predicted survival probability over time for each species and treatment. Because no significant treatment effects on functional survival were evident, we pooled all treatment data and compared functional survival across species. Finally, we tested for statistical differences between food treatments and species using the function 'survdiff' in the R 'survival' package (Therneau 2021). No censored observations were present in the data.

3.4 Results

Both sea urchin species and red turban snails lowered their absolute oxygen consumption ($\dot{M}O_2$) in response to macroalgae restrictions (Fig 3.2a-c,

supplementary table S5-8), however, in the red turban snails this was due to initial body mass differences across the food treatments (supplementary figure S4). No differences remained across food treatments in the gastropods when considering mass-independent (Fig 3.3c-d) or wet mass-specific $\dot{M}O_2$ (supplementary figure S5). Food-related differences in red turban snail $\dot{M}O_2$ were driven by the largest snails (i.e., in our sensitivity analysis using a subset of small snails (<40 g body mass), no differences in absolute $\dot{M}O_2$ remained. See supplementary figure S3 and table S4).

We found sea urchins lowered their mass-independent oxygen consumption ($\dot{M}O_2$) in response to prolonged macroalgae restriction (Fig 3.3a-b). By contrast, the mass-independent oxygen consumption of two gastropod grazers did not respond to macroalgae provisioning restrictions (Fig 3.3c-d). Unfed individuals of both species of sea urchin had significantly lower mass-independent $\dot{M}O_2$ values after seven weeks compared to macroalgae fed individuals (one-way ANOVA; F = 90.42, d.f. = 2, p = <0.001 for *Mesocentrotus franciscanus;* and Kruskal-Wallis test; X^2 (2, N = 103) = 57.54, p = <0.001 for *Strongylocentrotus purpuratus*; supplementary table S5-8), with mass-independent $\dot{M}O_2$ values that were depressed by 26% and 78% in unfed individuals of *M. franciscanus* and *S. purpuratus*, respectively. Sea urchin individuals that received regular macroalgae supplements raised their mass-independent $\dot{M}O_2$ in response to a 1.5°C *in situ* temperature increase ($\dot{M}O_2$ values at Week 2 [*in situ* & experimental temperature = 9.0°C] versus Week 7 [*in situ* & experimental temperature = 10.5°C], see

supplementary figure S1), whilst unfed individuals displayed a consistently depressed metabolism even when temperature increased (see Fig 3.3). Specifically, $\dot{M}O_2$ values were lower than expected for a 1.5°C temperature increase (based on Q_{10} = 2.5) in unfed individuals of *M. franciscanus* (observed median $\dot{M}O_2$ at 10.5°C was 0.18 ml O_2 h^{-1} vs. expected $\dot{M}O_2$ of 0.25 ml O_2 h^{-1} at 10.5°C, based on Q_{10}) and *S. purpuratus* (observed median $\dot{M}O_2$ = 0.57 vs. expected median $\dot{M}O_2$ = 0.70 ml O_2 h^{-1} at 10.5°C). The influence of food type varied between the two sea urchin species, but was small compared to the food restriction effect (2-18 % difference in $\dot{M}O_2$ between sea urchins receiving *Macrocystis* and *Saccharina* kelp, see Fig 3.3 and supplementary table S5-8). In contrast to the responses in sea urchins, no change in the mass-independent oxygen consumption of two gastropod grazers (*Pomaulax gibberosus* and *Tegula pulligo*, Fig 3.3c-d), was detected in response to the availability or type of macroalgae over the seven weeks of experimental duration (Kruskal-Wallis test; X^2(2, N = 98) = 3.46, p = 0.177 for *P. gibberosus* and one-way ANOVA; F = 1.02, d.f. = 2, p = 0.378 for *T. pulligo*; supplementary table S5-8).

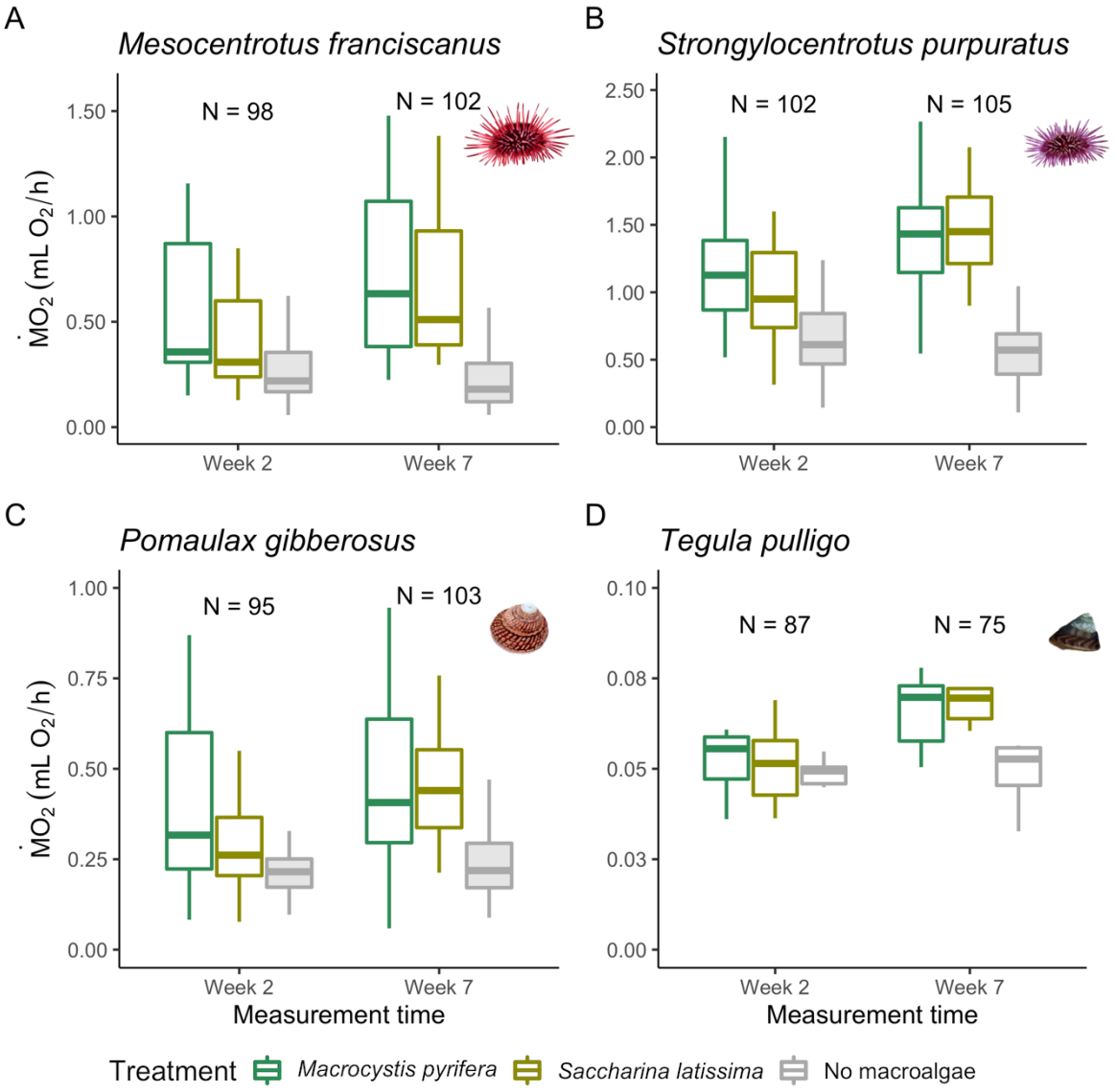

Figure 3.2 Absolute oxygen consumption ($\dot{M}O_2$) of four grazing invertebrate species at two measurement time-points (Week 2 and Week 7) along a 7-week food treatment (*Macrocystis pyrifera*, *Saccharina latissima* and no macroalgae). $\dot{M}O_2$ measurements were made at ambient seawater temperatures at time of measurement (9.0°C at Week 2; 10.5°C at Week 7). Boxplots show maximum, minimum and median values, as well as 25th and 75th percentile values. N=432 individuals across all species and treatments. Grey shaded boxplots indicate significant difference of a treatment from the *Macrocystis* treatment.

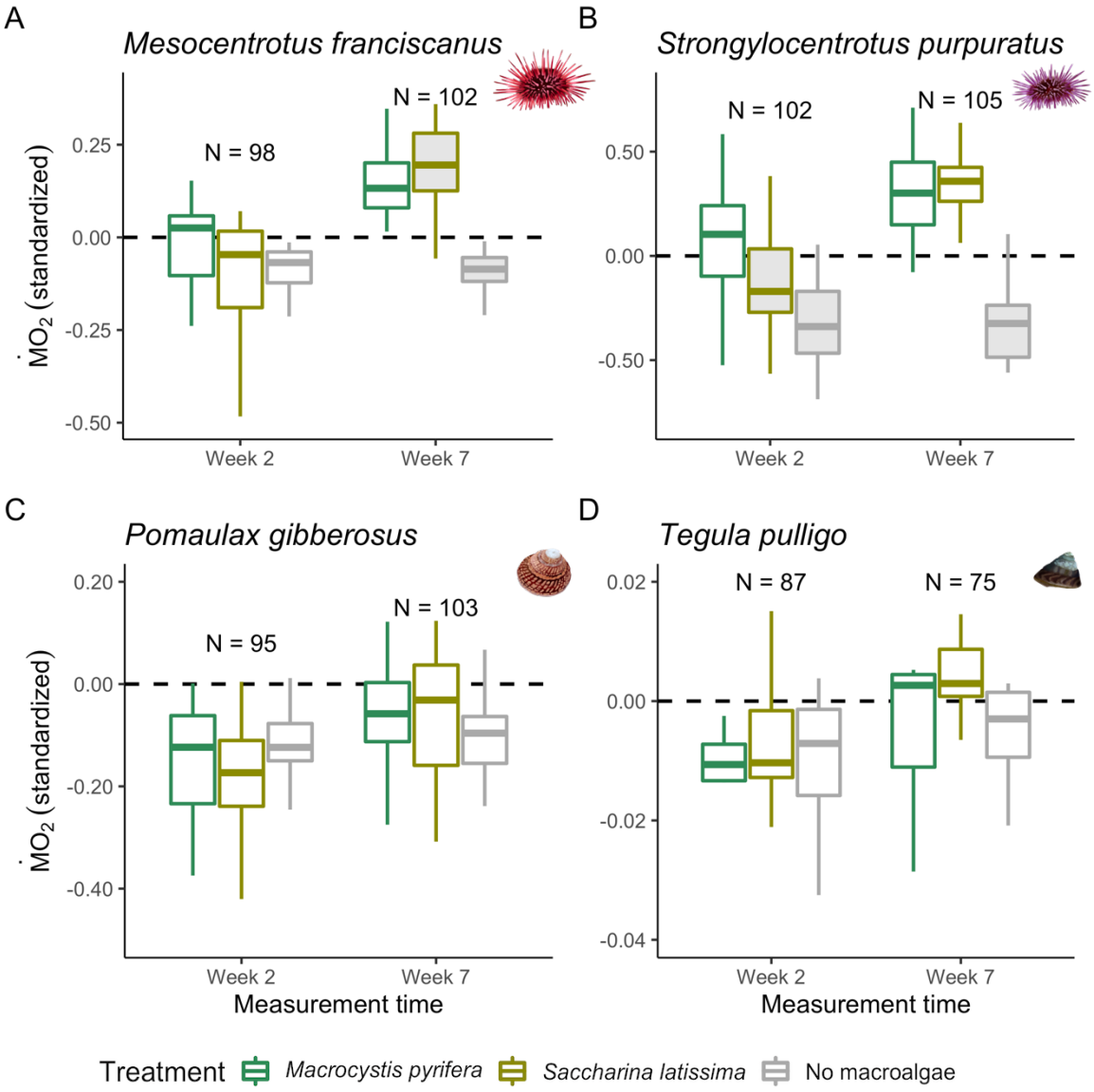

Figure 3.3 Mass-independent oxygen consumption ($\dot{M}O_2$) of four grazing invertebrate species (A-D) at two measurement time-points (Week 2 and 7) along a 7-week food treatment (*Macrocystis pyrifera*, *Saccharina latissima* and no macroalgae). $\dot{M}O_2$ measurements were made at ambient seawater temperatures at time of measurement (9.0°C at Week 2; 10.5°C at Week 7). Boxplots show maximum, minimum and median values, as well as 25th and 75th percentile values. Grey shaded boxplots indicate significant difference of a treatment from the *Macrocystis* treatment.

The temperature sensitivity to extreme heat stress of four grazing invertebrate species differed significantly. The time until 50% population functional mortality (quantified as loss of equilibrium) was twice as long in urchins than in gastropod species (Fig 3.4, Kaplan-Meier survival probability; X^2(3, N = 212) = 86.7, p < 0.001). Red and purple sea urchins had similar functional survival times (median time to LOE = 150 seconds and 152 seconds for *M. franciscanus* and *S. purpuratus*, respectively), however, variation in survival times was larger in *M. franciscanus* (ranging from 29 to 600 seconds) compared to *S. purpuratus* (26 to 355 seconds). By contrast, the time of functional survival under heat was much shorter in the two gastropods (median time to LOE = 90 seconds and 58 seconds in *P. gibberosus* and *T. pulligo*, respectively). In addition, the variation in the heat response of *T. pulligo* was much lower (range of response time to LOE was 33 to 170 seconds) than in the three other species (Fig 3.4).

Functional survival time under extreme heat stress was not significantly different across three food treatments in all four species for our sample sizes. However, across all four species, we observed that individuals without macroalgae provisions reached 50% mortality up to 35% faster than individuals that received macroalgae provisions (Fig 3.5a-d), a pattern that appears consistent. Moreover, the differences between fed and unfed individuals was borderline (p = 0.06) for *Mesocentrotus franciscanus* (X^2(2, N = 18 per treatment) = 5.5, p = 0.06).

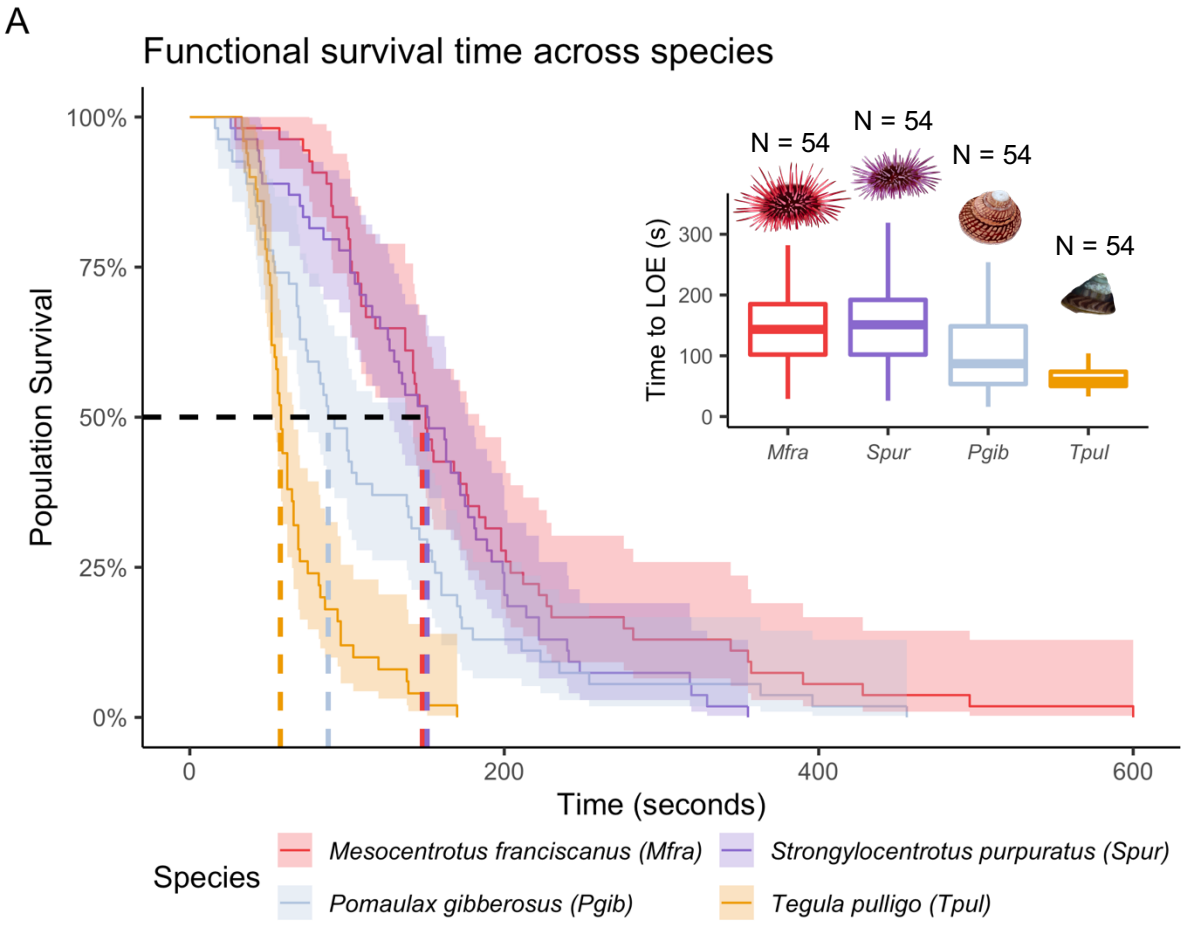

Figure 3.4 Functional survival (time until loss of equilibrium; LOE) probability of four grazing invertebrate species during acute exposure to near-lethal heat stress (35°C). All food treatment data were pooled for each species. Curves show Kaplan-Meier survival functions with mean estimated functional survival and 95% confidence intervals (shaded areas). Dashed lines indicate the time where 50% of the population of each species was predicted to be functionally moribund. The boxplot inset shows the time until LOE in seconds for each species, with species codes and colours corresponding to full species names in the legend. Boxplots show maximum, minimum and median values, as well as 25th and 75th percentile values for each species.

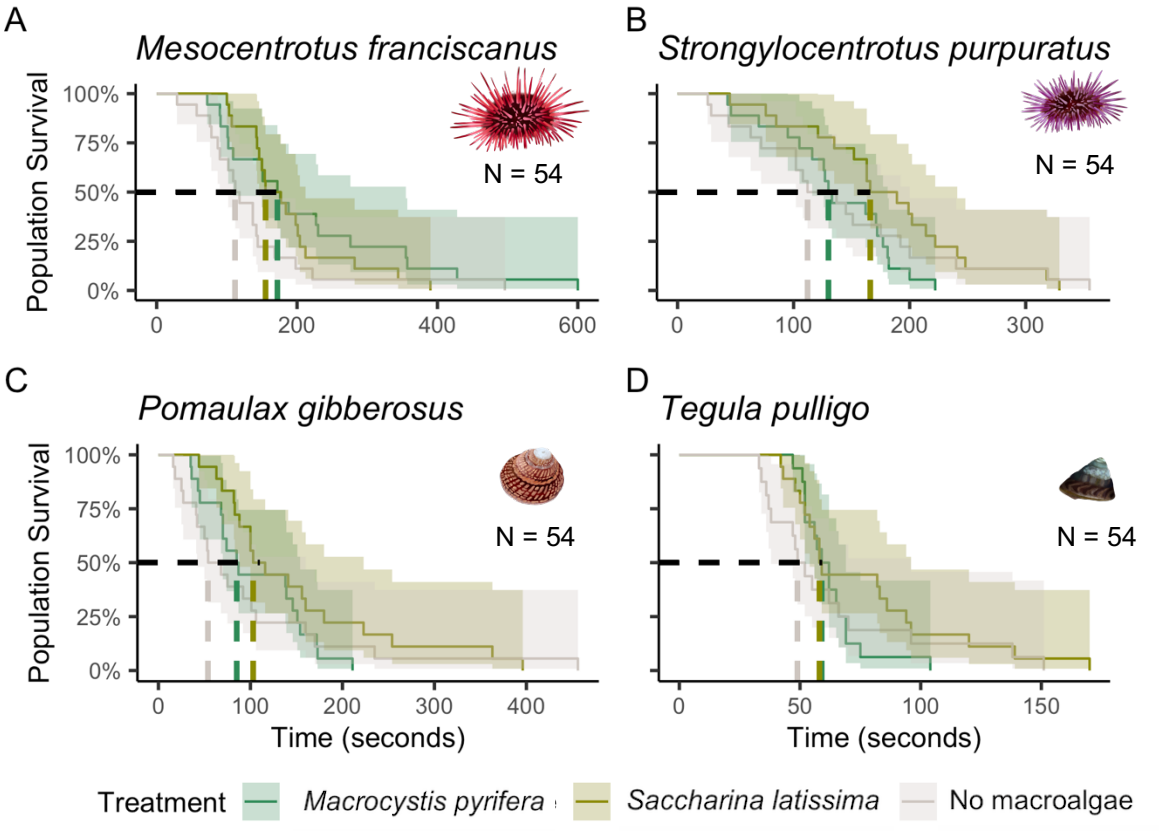

Figure 3.5 Functional survival (time until loss of equilibrium; LOE) probability of four grazing invertebrate species (A-D) across three food treatments during acute exposure to near-lethal heat stress (35°C). Curves show Kaplan-Meier survival functions with mean estimated functional survival and 95% confidence intervals (shaded areas). Dashed lines indicate the time where 50% of the population of each treatment was predicted to be functionally moribund. N = 216.

We found differences at the end of the experiment in body mass across fed and unfed individuals in four grazing invertebrate species. Following the seven week experimental duration, the wet mass of all grazing invertebrate species differed across fed and unfed individuals (by 20-63%), except in purple sea urchins (supplementary figure S4 and table S9-10). However, although animals were haphazardly assigned to treatment cages, in *M. franciscanus* and *P. gibberosus*,

the initial wet mass differed (at Week 0) across food treatments, therefore, these two species were excluded from the dry and ash-free mass comparisons. In *S. purpuratus* and *T. pulligo* significant differences in dry mass (by 9-51%) and ash-free dry mass (by 23-94%) across food treatments were evident (supplementary figure S6-7 and table S9-10) at the end of the treatment period. When comparing individuals that received different macroalgae species (higher and lower quality, on average), no differences in wet, dry or ash-free dry mass were evident at any measurement time-point throughout the experiment (supplementary figures S4, S6-7, supplementary table S9-10).

3.5 Discussion

Overall, we found two sea urchin species with macroalgae-dependent diets responded strongly to macroalgae limitations by lowering their mass-independent oxygen consumption. Sea urchins are known to persist in food deprived, barren environments for years and even decades, and our results support the emerging notion (Dolinar & Edwards 2021; Spindel *et al.* 2021) that metabolic depression is the energetic adaptation allowing prolonged survival during starvation. Indeed, sea urchins from food rich environments (kelp forests) and food deprived environments (urchin barrens) are energetically distinct units, with population-level variation in metabolic performance, mass and heat resilience emerging across these habitat types in green sea urchins (Schuster *et al.* 2022) and red sea urchins (Spindel *et al.* 2021). Our results demonstrate that red and purple sea urchins dramatically reduce their mass-independent oxygen consumption values (by 26-78%) when macroalgae is restricted, mirroring differences detected in $\dot{M}O_2$ from populations of

urchins from forested and barren habitats (Schuster *et al.* 2022). Thus, our experimental results provide mechanistic support that the availability of macroalgal food (but not necessarily kelp species) *per se* drives energetic differences across habitats. Sea urchins' capacity to shift to a state of reduced metabolism is a key adaptation that likely facilitates the stability and persistence of sea urchin barrens.

In contrast to the sea urchins' strong metabolic response to macroalgae exclusion, we found the mass-independent oxygen consumption of two gastropod grazers was unaffected by the same food restrictions. The two gastropod grazers maintained relatively stable energetic states across the three treatments, with uniform increases in mass-independent $\dot{M}O_2$ during a seasonally driven 1.5°C temperature rise across all treatments. This may be explained by the degree to which different grazers rely on macroalgae for food. Grazing gastropods consume a variety of resources, including macroalgae, but also microalgae, filamentous algae and biofilms (Watanabe 1984; Mazzillo *et al.* 2013). The biofilms and planktonic algae that were present on the cage walls may have provided sufficient nutrients and energy to maintain consistent metabolic rates in the two turban snail species, implicating the role of diet diversity as a mechanism to resist warming. Even though sea urchins can also feed on biofilms, filamentous or encrusting algae in the absence of macroalgae (Lawrence 1975; Lawrence & Sammarco 1982; Filbee-Dexter & Scheibling 2014; Renaud *et al.* 2015), these food subsidies appear insufficient to sustain steady rates of oxygen consumption in urchins. Our finding overall suggests that a varied diet (i.e., not being dependent on one food source)

and the ability to effectively absorb nutrients from different resources could be critical in preserving an organisms' physiological state in environments where resource availability is variable.

Against our expectations, we found metabolic performance was not impaired by a dietary shift towards a species of understory kelp over multiple weeks. One explanation for why grazer performance remained similar despite different nutrient compositions (e.g., protein content and C:N ratios) and quality of *Macrocystis* and *Saccharina* kelps (Biancarosa *et al.* 2018; Lowman *et al.* 2021), is that urchins compensate by adjusting absorption efficiencies (Leighton 1968; Foster *et al.* 2015). In addition, sea urchins may adjust their gut microbiome in response to the quality of food received (e.g., Miller et al., 2021). Given the apparent decline in nutritional quality of *Macrocystis* with warming (Lowman *et al.* 2021), an interesting future direction would be to test whether diets of *Macrocystis* with high or low C:N ratios (i.e., low or high nutritional quality *Macrocystis*, respectively) elicit similar results to our comparison of diets composed of different macroalgae species. Another explanation may be that the differences in nutritional qualities of the two kelp species considered were lower at the time of collection than they are on average. Thus our findings implicate future investigations into physiological responses to a diet that is much lower in quality, such as turf species which are replacing canopy kelps in many regions (Filbee-Dexter & Wernberg 2018). Even so, it is also possible that differences in diets comprised of *Macrocystis* versus *Saccharina* may drive physiological changes that were not investigated here, such

as at the cellular level, or changes in reproductive output or growth rates. For example, green sea urchins fed high quality *Laminaria* kelp have larger gonads and body sizes than urchins fed lower quality *Codium* seaweed after 42 weeks (Lyons & Scheibling 2007).

Sea urchins were overall more resilient to acute heat stress than the two gastropods. The ability to withstand heat stress is of paramount ecological importance, especially in light of increasingly frequent temperature challenges (e.g., heatwaves). Measures of extreme heat tolerance are widely used as indicators of overall thermal sensitivity (Fraenkel 1961; Huey *et al.* 1992; Miranda *et al.* 2019; Bates & Morley 2020). Indeed, rocky intertidal systems and mudflats often experience acute and severe heat exposures exceeding 30°C in the summer (Nguyen *et al.* 2011) and nearshore ocean temperatures can shift by 10°C or more in one tidal cycle (Bates *et al.* 2018). Thus, even though heat challenges of the magnitude applied in our experiment are unlikely to occur in the subtidal, such experiments provide useful insights on how different species may cope with acute thermal stress. Based on our survival analysis, red sea urchins are most tolerant to acute heat stress, followed by purple sea urchins, red turban snails and lastly, dusky turban snails. The survival time of red sea urchins was five-fold longer than that of dusky turban snails. The longer survival time of the urchin populations under heat may simply be due to their larger body masses, relative to the gastropods. On very short, acute time-scales, larger body masses may simply provide better buffering against heat stress. The urchins' relative robustness to heat stress, paired

with their ability to endure starvation, are likely a key aspect of their physiology that allow them to persist in resource-limited environments and prevent the re-establishment of macroalgae-dominated rocky reefs.

Despite clear changes in mass-independent oxygen consumption values in the absence of macroalgal food, we found little difference in heat resistance across the two kelp type treatments. This was surprising but could suggest that acute heat response is only weakly coupled with the energetic cost of living and decoupled from food restriction-induced low metabolic rates. Another observation supporting this weak coupling is the lack of response in oxygen consumption to a 1.5°C temperature increase in unfed urchins, as documented here. Metabolic theory predicts clear increases in oxygen consumption with increasing temperatures (Gillooly *et al.* 2001; Brown *et al.* 2004), and this was observed as predicted in fed individuals of all species, but not in unfed urchins. Even so, our ability to detect differences in the grazers ability to withstand heat stress between fed and unfed individuals may have been confounded by a small sample size or because of the severity of the heat stress where an effect may have emerged under milder stress. In addition, differences may have manifested at the cellular level, but were not captured through our whole-organism response measures. For example, the combination of fasting and heat stress resulted in oxidative damage and decreased activity of some key enzymes in mussels (Delorme *et al.* 2020).

We did observe some differences across food treatments, where, in all four species, individuals receiving no macroalgae generally had the shortest survival

times until 50% functional mortality. Indeed, the capacity to withstand heat stress was compromised by macroalgae limitation in red sea urchins, as supported by a borderline significant effect. Thus, food type and starvation may be a driver of differences in heat responses that are biologically meaningful and requires follow up experiments with greater sample sizes or alternative experimental protocols to better tease apart differences.

The mass of metabolically active tissue (ash-free dry mass) was lower in unfed individuals than fed individuals in *S. purpuratus* and *T. pulligo* after seven weeks of treatment. Purple sea urchins had similar wet masses across the treatments throughout the seven weeks but showed clear differences in metabolic tissue mass across fed and unfed individuals at the end of the study period, suggesting food related metabolic mass differences in urchins. During metabolic depression and limited food intake, urchins utilize their energy stores (i.e., lipids and glycogen) that consume little oxygen, leading to tissue declines (Azeez *et al.* 2014). Our finding suggests that although entering metabolic depression may enable sea urchins to survive prolonged periods without macroalgae foods, there is an energetic cost (i.e., tissue loss) to this adaptation, and thus time-limits for how long it can be endured must exist. Sea urchins have been documented to persist in food-deprived barrens for years and even decades (Harrold & Reed 1985; Vanderklift & Wernberg 2008; Filbee-Dexter & Scheibling 2014), but based on our findings, we expect opportunistic feeding on drift kelp or other algae will be critical to replenish and

restore tissues before re-entering periods of metabolic depression to avoid mortality.

3.6 Conclusion

Organisms persist in dynamic environments where food resources are variable. Here, we implicate macroalgae availability as a driver of population-level variation in realized physiology. We demonstrate that restricting macroalgae food has physiological consequences in sea urchins, but not in two gastropod grazers. We show that sea urchins shift to a new physiological state with lower metabolic rates when experiencing prolonged macroalgae restrictions. Macroalgae restrictions had clear metabolic consequences in the urchins, but differences between diets comprised of *Macrocystis* versus *Saccharina* kelps were limited in all four grazers, highlighting that understory macroalgae are a viable and important food alternative for kelp communities. Ability to lower metabolic rates and diet diversity thus appear to be important strategies for organisms to persist in variable, food limited environments. Metabolic performance underpins all organism functioning, thus energy-based forecasting approaches should consider present and future availabilities of food resources and how they modify biomass-energy relationships.

3.7 References

Anderson, R.J. & Velimirov, B. (1982). An Experimental Investigation of the Palatability of Kelp Bed Algae to the Sea Urchin *Parechinus angulosus* LESKE. *Mar. Ecol.*, 3, 357–373.

Azeez, O.I., Meintjes, R. & Chamunorwa, J.P. (2014). Fat body, fat pad and

adipose tissues in invertebrates and vertebrates: the nexus. *Lipids Health Dis.*, 13, 71.

Bates, A.E., Helmuth, B., Burrows, M.T., Duncan, M.I., Garrabou, J., Guy-Haim, T., *et al.* (2018). Biologists ignore ocean weather at their peril. *Nature*, 560, 299–301.

Bates, A.E., McKelvie, C.M., Sorte, C.J.B., Morley, S.A., Jones, N.A.R., Mondon, J.A., *et al.* (2013). Geographical range, heat tolerance and invasion success in aquatic species. *Proc. R. Soc. B Biol. Sci.*, 280, 20131958.

Bates, A.E. & Morley, S.A. (2020). Interpreting empirical estimates of experimentally derived physiological and biological thermal limits in ectotherms. *Can. J. Zool.*, 98, 237–244.

Bennett, A.F. & Ruben, J.A. (1979). Endothermy and Activity in Vertebrates. *Science*, 206, 649–654.

Bernhardt, J.R. & Leslie, H.M. (2013). Resilience to Climate Change in Coastal Marine Ecosystems. *Ann. Rev. Mar. Sci.*, 5, 371–392.

Biancarosa, I., Belghit, I., Bruckner, C.G., Liland, N.S., Waagbø, R., Amlund, H., *et al.* (2018). Chemical characterization of 21 species of marine macroalgae common in Norwegian waters: benefits of and limitations to their potential use in food and feed. *J. Sci. Food Agric.*, 98, 2035–2042.

Biro, P.A. & Stamps, J.A. (2010). Do consistent individual differences in metabolic rate promote consistent individual differences in behavior? *Trends Ecol. Evol.*, 25, 653–659.

Bond, N.A., Cronin, M.F., Freeland, H. & Mantua, N. (2015). Causes and impacts

of the 2014 warm anomaly in the NE Pacific. *Geophys. Res. Lett.*, 42, 3414–3420.

Brown, J.H., Gillooly, J.F., Allen, A.P., Savage, V.M. & West, G.B. (2004). Toward a metabolic theory of ecology. *Ecology*, 85, 1771–1789.

Burton, T., Killen, S.S., Armstrong, J.D. & Metcalfe, B.N. (2011). What causes intraspecific variation in resting metabolic rate and what are its ecological consequences? *Proc. R. Soc. B Biol. Sci.*, 278, 3465–3473.

Castorani, M.C.N., Harrer, S.L., Miller, R.J. & Reed, D.C. (2021). Disturbance structures canopy and understory productivity along an environmental gradient. *Ecol. Lett.*, 24, 2192–2206.

Castorani, M.C.N., Reed, D.C. & Miller, R.J. (2018). Loss of foundation species: disturbance frequency outweighs severity in structuring kelp forest communities. *Ecology*, 99, 2442–2454.

Chabot, D., Zhang, Y. & Farrell, A.P. (2021). Valid oxygen uptake measurements: using high r2 values with good intentions can bias upward the determination of standard metabolic rate. *J. Fish Biol.*, 98, 1206–1216.

Corino, C., Modina, S.C., Di Giancamillo, A., Chiapparini, S. & Rossi, R. (2019). Seaweeds in Pig Nutrition. *Animals*, 9, 1126.

Dell, A.I., Pawar, S. & Savage, V.M. (2011). Systematic variation in the temperature dependence of physiological and ecological traits. *Proc. Natl. Acad. Sci.*, 108, 10591 LP – 10596.

Delorme, N.J., Biessy, L., South, P.M., Zamora, L.N., Ragg, N.L.C. & D, B.J. (2020). Stress-on-stress responses of a marine mussel, *Perna canaliculus*:

food limitation reduces the ability to cope with heat stress in juveniles. *Mar. Ecol. Prog. Ser.*, 644, 105–117.

Diehl, N., Roleda, M.Y., Bartsch, I., Karsten, U. & Bischof, K. (2021). Summer Heatwave Impacts on the European Kelp *Saccharina latissima* Across Its Latitudinal Distribution Gradient. *Front. Mar. Sci.*

Dolinar, D. & Edwards, M. (2021). The metabolic depression and revival of purple urchins (*Strongylocentrotus purpuratus*) in response to macroalgal availability. *J. Exp. Mar. Bio. Ecol.*, 545, 151646.

Duarte, B., Martins, I., Rosa, R., Matos, A.R., Roleda, M.Y., Reusch, T.B.H., *et al.* (2018). Climate Change Impacts on Seagrass Meadows and Macroalgal Forests: An Integrative Perspective on Acclimation and Adaptation Potential. *Front. Mar. Sci.*

Durante, K.M. & Chia, F.-S. (1991). Epiphytism on Agarum fimbriatum: can herbivore preferences explain distributions of epiphytic bryozoans? *Mar. Ecol. Prog. Ser.*, 77, 279–287.

Filbee-Dexter, K. & Scheibling, R. (2014). Sea urchin barrens as alternative stable states of collapsed kelp ecosystems. *Mar. Ecol. Prog. Ser.*, 495, 1–25.

Filbee-Dexter, K. & Wernberg, T. (2018). Rise of Turfs: A New Battlefront for Globally Declining Kelp Forests. *Bioscience*, 68, 64–76.

Foster, M.C., Byrnes, J.E.K. & Reed, D.C. (2015). Effects of five southern California macroalgal diets on consumption, growth, and gonad weight, in the purple sea urchin *Strongylocentrotus purpuratus*. *PeerJ*, 3, e719.

Fraenkel, G. (1961). Resistance to High Temperatures in a Mediterranean Snail,

Littoria neritoides. *Ecology*, 42, 604–606.

Gillooly, J.F., Brown, J.H., West, G.B., Savage, V.M. & Charnov, E.L. (2001). Effects of Size and Temperature on Metabolic Rate. *Science*, 293, 2248–2251.

Graham, M.H. (2004). Effects of Local Deforestation on the Diversity and Structure of Southern California Giant Kelp Forest Food Webs. *Ecosystems*, 7, 341–357.

Graham, M.H., Vasquez, J.A. & Buschmann, A.H. (2007). Global ecology of the giant kelp *Macrocystis*: from ecotypes to ecosystems. *Oceanogr. Mar. Biol.*, 45, 39.

Harianto, J., Carey, N. & Byrne, M. (2019). respR - An R package for the manipulation and analysis of respirometry data. *Methods Ecol. Evol.*

Harrold, C. & Reed, D.C. (1985). Food Availability, Sea Urchin Grazing, and Kelp Forest Community Structure. *Ecology*, 66, 1160–1169.

Huey, R.B., Crill, W.D., Kingsolver, J.G. & Weber, K.E. (1992). A Method for Rapid Measurement of Heat or Cold Resistance of Small Insects. *Funct. Ecol.*, 6, 489–494.

Huey, R.B. & Kingsolver, J.G. (2019). Climate Warming, Resource Availability, and the Metabolic Meltdown of Ectotherms. *Am. Nat.*, 194, E140–E150.

Johnson, C.R., Banks, S.C., Barrett, N.S., Cazassus, F., Dunstan, P.K., Edgar, G.J., *et al.* (2011). Climate change cascades: Shifts in oceanography, species' ranges and subtidal marine community dynamics in eastern Tasmania. *J. Exp. Mar. Bio. Ecol.*, 400, 17–32.

Krause-Jensen, D., Markager, S. & Dalsgaard, T. (2012). Benthic and Pelagic Primary Production in Different Nutrient Regimes. *Estuaries and Coasts*, 35, 527–545.

Krogdahl, Å., Jaramillo-Torres, A., Ahlstrøm, Ø., Chikwati, E., Aasen, I.-M. & Kortner, T.M. (2021). Protein value and health aspects of the seaweeds *Saccharina latissima* and *Palmaria palmata* evaluated with mink as model for monogastric animals. *Anim. Feed Sci. Technol.*, 276, 114902.

Krumhansl, K.A., Okamoto, D.K., Rassweiler, A., Novak, M., Bolton, J.J., Cavanaugh, K.C., *et al.* (2016). Global patterns of kelp forest change over the past half-century. *Proc. Natl. Acad. Sci.*, 113, 13785 LP – 13790.

Lawrence, J.M. (1975). On the Relationships Between Marine Plants and Sea Urchins. *Oceanogr. Mar. Biol. Annu. Rev.*, 13, 213–286.

Lawrence, J.M. & Sammarco, P. (1982). Effect of feeding: Echinoidea. *Echinoderm Nutr.*, 499–519.

Layton, C., Coleman, M.A., Marzinelli, E.M., Steinberg, P.D., Swearer, S.E., Vergés, A., *et al.* (2020). Kelp Forest Restoration in Australia. *Front. Mar. Sci.*, 7, 1–15.

Leighton, D. (1966). Studies of Food Preference in Algivorous Invertebrates of Southern California Kelp Beds. *Pacific Sci.*, 20, 104–113.

Leighton, D.L. (1968). *A comparative study of food selection and nutrition in the abalone, Haliotis rufescens (Swainson), and the sea urchin,* Strongylocentrotus purpuratus *(Stimpson)*. University of California, San Diego.

Ling, S.D., Scheibling, R.E., Rassweiler, A., Johnson, C.R., Shears, N., Connell, S.D., *et al.* (2015). Global regime shift dynamics of catastrophic sea urchin overgrazing. *Philos. Trans. R. Soc. B Biol. Sci.*, 370, 20130269.

Lowman, H.E., Emery, K.A., Dugan, J.E. & Miller, R.J. (2021). Nutritional quality of giant kelp declines due to warming ocean temperatures. *Oikos*, 1–14.

Lyons, D.A. & Scheibling, R.E. (2007). Differences in somatic and gonadic growth of sea urchins (*Stronglyocentrotus droebachiensis*) fed kelp (*Laminaria longicruris*) or the invasive alga *Codium fragile* ssp. tomentosoides are related to energy acquisition. *Mar. Biol.*, 152, 285–295.

Mazzillo, F.F.M., Shapiro, K. & Silver, M.W. (2013). A new pathogen transmission mechanism in the ocean: the case of sea otter exposure to the land-parasite *Toxoplasma gondii*. *PLoS One*, 8, e82477–e82477.

McNab, B.K. (1986). Food habits, energetics, and the reproduction of marsupials. *J. Zool.*, 208, 595–614.

Meehl, G.A., Zwiers, F., Evans, J., Knutson, T., Mearns, L. & Whetton, P. (2000). Trends in extreme weather and climate events: issues related to modeling extremes in projections of future climate change. *Bull. Am. Meteorol. Soc.*, 81, 427–436.

Metcalfe, N.B., Taylor, A.C. & Thorpe, J.E. (1995). Metabolic rate, social status and life-history strategies in Atlantic salmon. *Anim. Behav.*, 49, 431–436.

Miller, P.M., Lamy, T., Page, H.M. & Miller, R.J. (2021). Sea urchin microbiomes vary with habitat and resource availability. *Limnol. Oceanogr. Lett.*, 6, 119–126.

Miranda, N.A.F., Peer, N., Ishak, M.Z.B. & Marshall, D.J. (2019). Heat-wave tolerance in tropical intertidal animals: accounting for thermal and desiccation tolerances. *Ecol. Indic.*, 107, 105561.

Moe, B., Brunvoll, S., Mork, D., Brobakk, T.E. & Bech, C. (2004). Developmental plasticity of physiology and morphology in diet-restricted European shag nestlings (*Phalacrocorax aristotelis*). *J. Exp. Biol.*, 207, 4067–4076.

Nguyen, K.D.T., Morley, S.A., Lai, C.-H., Clark, M.S., Tan, K.S., Bates, A.E., *et al.* (2011). Upper Temperature Limits of Tropical Marine Ectotherms: Global Warming Implications. *PLoS One*, 6, e29340.

Nilsson, J. (2002). Metabolic consequences of hard work. *Proc. R. Soc. London. Ser. B Biol. Sci.*, 269, 1735–1739.

Norin, T. & Metcalfe, N.B. (2019). Ecological and evolutionary consequences of metabolic rate plasticity in response to environmental change. *Philos. Trans. R. Soc. B Biol. Sci.*, 374, 20180180.

O'connor, K.I., Taylor, A.C. & Metcalfe, N.B. (2000). The stability of standard metabolic rate during a period of food deprivation in juvenile Atlantic salmon. *J. Fish Biol.*, 57, 41–51.

Padfield, D., Yvon-Durocher, G., Buckling, A., Jennings, S. & Yvon-Durocher, G. (2016). Rapid evolution of metabolic traits explains thermal adaptation in phytoplankton. *Ecol. Lett.*, 19, 133–142.

Peters, R.H. (1983). *The Ecological Implications of Body Size*. *Cambridge Stud. Ecol.* Cambridge University Press, Cambridge.

Pfister, C.A., Berry, H.D. & Mumford, T. (2018). The dynamics of Kelp Forests in

the Northeast Pacific Ocean and the relationship with environmental drivers. *J. Ecol.*, 106, 1520–1533.

R Core Team. (2014). R: a language and environment for statistical computing.

Renaud, P.E., Løkken, T.S., Jørgensen, L.L., Berge, J. & Johnson, B.J. (2015). Macroalgal detritus and food-web subsidies along an Arctic fjord depth-gradient. *Front. Mar. Sci.*, 2, 31.

Roark, A.M. & Bjorndal, K.A. (2009). Metabolic rate depression is induced by caloric restriction and correlates with rate of development and lifespan in a parthenogenetic insect. *Exp. Gerontol.*, 44, 413–419.

Rogers-Bennett, L. & Catton, C.A. (2019). Marine heat wave and multiple stressors tip bull kelp forest to sea urchin barrens. *Sci. Rep.*, 9, 15050.

Schiel, D.R. & Foster, M.S. (2015). *The biology and ecology of giant kelp forests*. University of California Press.

Schuster, J.M., Gamperl, A.K., Gagnon, P. & Bates, A.E. (2022). Distinct realized physiologies in green sea urchin (*Strongylocentrotus droebachiensis*) populations from barren and kelp habitats. *FACETS*.

Sharma, S., Neves, L., Funderud, J., Mydland, L.T., Øverland, M. & Horn, S.J. (2018). Seasonal and depth variations in the chemical composition of cultivated *Saccharina latissima*. *Algal Res.*, 32, 107–112.

Silbiger, N.J., Goodbody-Gringley, G., Bruno, J.F. & Putnam, H.M. (2019). Comparative thermal performance of the reef-building coral *Orbicella franksi* at its latitudinal range limits. *Mar. Biol.*, 166, 126.

Smith, J.L., Summers, G. & Wong, R. (2010). Nutrient and heavy metal content of

edible seaweeds in New Zealand. *New Zeal. J. Crop Hortic. Sci.*, 38, 19–28.

Spindel, N.B., Lee, L.C. & Okamoto, D.K. (2021). Metabolic depression in sea urchin barrens associated with food deprivation. *Ecology*, 102, e03463.

Stachowicz, J.J., Best, R.J., Bracken, M.E.S. & Graham, M.H. (2008). Complementarity in marine biodiversity manipulations: reconciling divergent evidence from field and mesocosm experiments. *Proc. Natl. Acad. Sci.*, 105, 18842–18847.

Starko, S., Bailey, L.A., Creviston, E., James, K.A., Warren, A., Brophy, M.K., *et al.* (2019). Environmental heterogeneity mediates scale-dependent declines in kelp diversity on intertidal rocky shores. *PLoS One*, 14, e0213191.

Steinberg, P.D. (1985). Feeding Preferences of *Tegula Funebralis* and Chemical Defenses of Marine Brown Algae. *Ecol. Monogr.*, 55, 333–349.

Steneck, R.S., Graham, M.H., Bourque, B.J., Corbett, D., Erlandson, J.M., Estes, J.A., *et al.* (2002). Kelp forest ecosystems: biodiversity, stability, resilience and future. *Environ. Conserv.*, 29, 436–459.

Tait, L.W. & Schiel, D.R. (2018). Ecophysiology of Layered Macroalgal Assemblages: Importance of Subcanopy Species Biodiversity in Buffering Primary Production . *Front. Mar. Sci.* .

Teagle, H., Hawkins, S.J., Moore, P.J. & Smale, D.A. (2017). The role of kelp species as biogenic habitat formers in coastal marine ecosystems. *J. Exp. Mar. Bio. Ecol.*, 492, 81–98.

Therneau, T.M. (2021). A package for survival analysis in R.

Vadas, R.L. (1977). Preferential Feeding: An Optimization Strategy in Sea

Urchins. *Ecol. Monogr.*, 47, 337–371.

Vanderklift, M.A. & Wernberg, T. (2008). Detached kelps from distant sources are a food subsidy for sea urchins. *Oecologia*, 157, 327–335.

Watanabe, J.M. (1984). Food Preference, Food Quality and Diets of Three Herbivorous Gastropods (Trochidae: *Tegula*) in a Temperate Kelp Forest Habitat. *Oecologia*, 62, 47–52.

Wernberg, T., Bennett, S., Babcock, R.C., de Bettignies, T., Cure, K., Depczynski, M., *et al.* (2016). Climate-driven regime shift of a temperate marine ecosystem. *Science*, 353, 169–172.

Wernberg, T., Coleman, M.A., Bennett, S., Thomsen, M.S., Tuya, F. & Kelaher, B.P. (2018). Genetic diversity and kelp forest vulnerability to climatic stress. *Sci. Rep.*, 8, 1851.

Wernberg, T., Krumhansl, K., Filbee-Dexter, K. & Pedersen, M.F. (2019). Chapter 3 - Status and Trends for the World's Kelp Forests. In: (ed. Sheppard, C.B.T.-W.S. an E.E. (Second E.). Academic Press, pp. 57–78.

Zimmerman, R.C. & Kremer, J.N. (1986). In situ growth and chemical composition of the giant kelp, *Macrocystis pyrifera*: response to temporal changes in ambient nutrient availability. *Mar. Ecol. Prog. Ser.*, 27, 277–285.

3.8 Appendix B – Supplementary figures and tables for Chapter 3

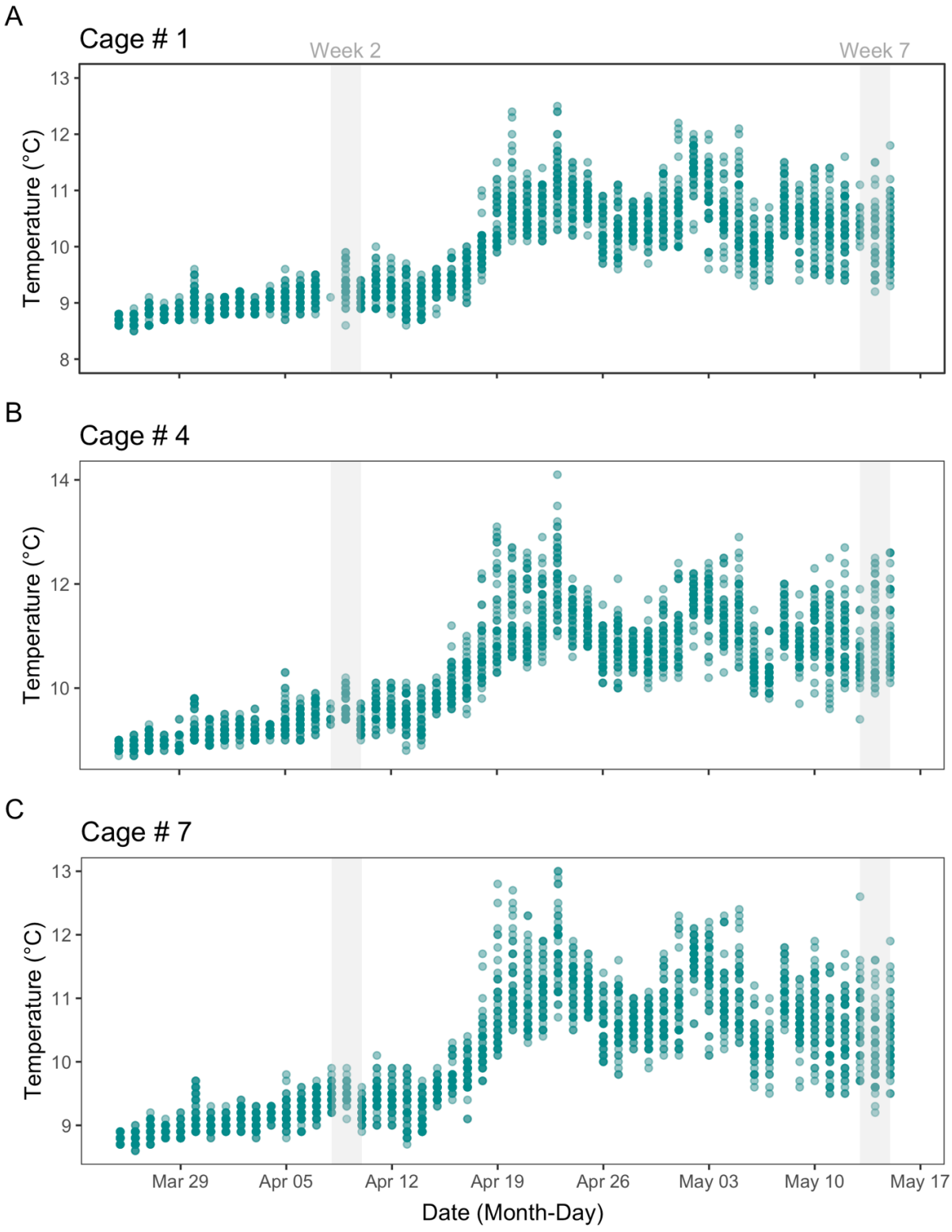

Figure S1. *In situ* seawater temperatures recorded from three temperature loggers (EnvLogger v2.4, 0.1°C resolution, ELECTRICBLUE, Portugal), each placed in a separate cage (# 1, 4 and 7) deployed off the Bamfield Marine Science Centre (BMSC) foreshore. Cages were suspended off a floating dock in the water at 5m depth and remained there over the 7-week food treatment period (24th of March – 15th of May 2021). Grey shaded areas indicate the respective time-periods (3 days at Week 2 and Week 7, respectively) where cages were removed from the water and grazers were brought to the laboratory for physiological assays.

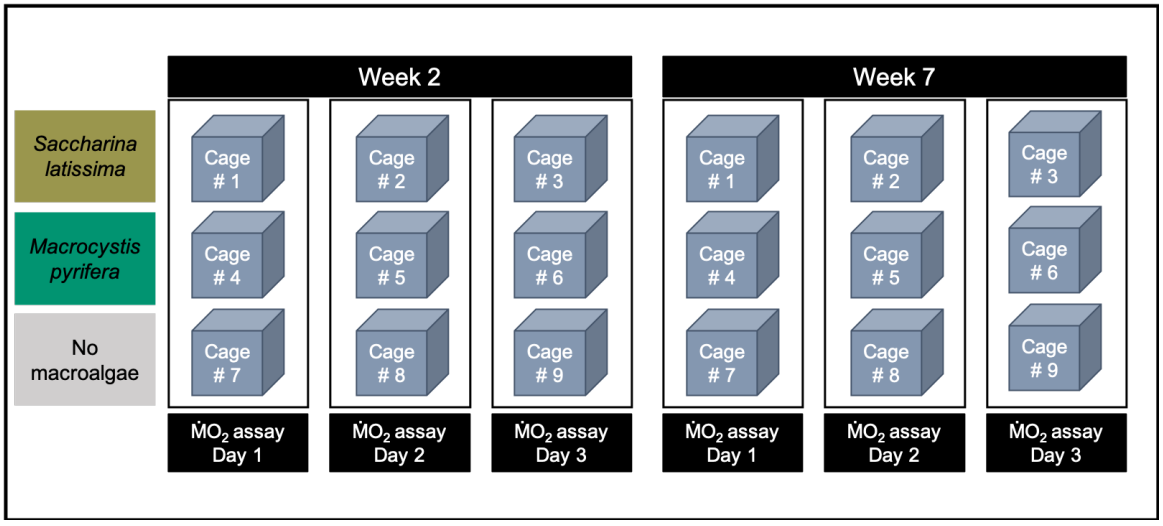

Figure S2. Staged design of oxygen consumption ($\dot{M}O_2$) runs completed after two weeks of *in situ* food treatment (Week 2) and the end of treatment (Week 7). To measure $\dot{M}O_2$ of all 432 individuals (N = 108 per species; 4 species) with a 10-chamber respirometry kit, measurements were split over three assay days during each block (Week 2 and Week 7). Each day, $\dot{M}O_2$ of all individuals from three selected cages was quantified, i.e., 13 measurement runs per day. One cage from each food treatment was included during each assay day. The food treatments consisted of *Macrocystis pyrifera* (giant kelp), *Saccharina latissima* (sugar kelp), and no macroalgae in the final treatment.

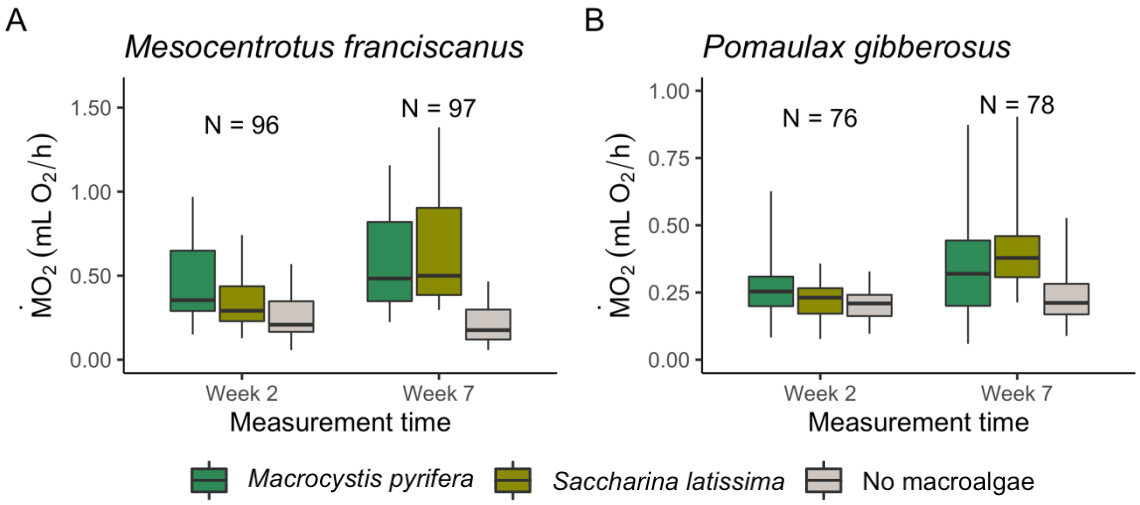

Figure S3. Sensitivity test of absolute oxygen consumption ($\dot{M}O_2$) of two grazing invertebrate species at two measurement time-points (Week 2 and Week 7) along a 7-week food treatment period (*Macrocystis pyrifera*, *Saccharina latissima* and no macroalgae). Because initial wet mass distributions across assigned treatments were uneven before the feeding period started (Week 0; see supplementary figure S4) in these two species, a subset with the largest individuals removed (Wet mass <70 g for *M. franciscanus* and <40 g for *P. gibberosus)* was used to verify treatment differences in $\dot{M}O_2$. Boxplots show maximum, minimum and median values, as well as 25th and 75th percentile values. Number of individuals included across treatments for each time-period are indicated above the boxplots.

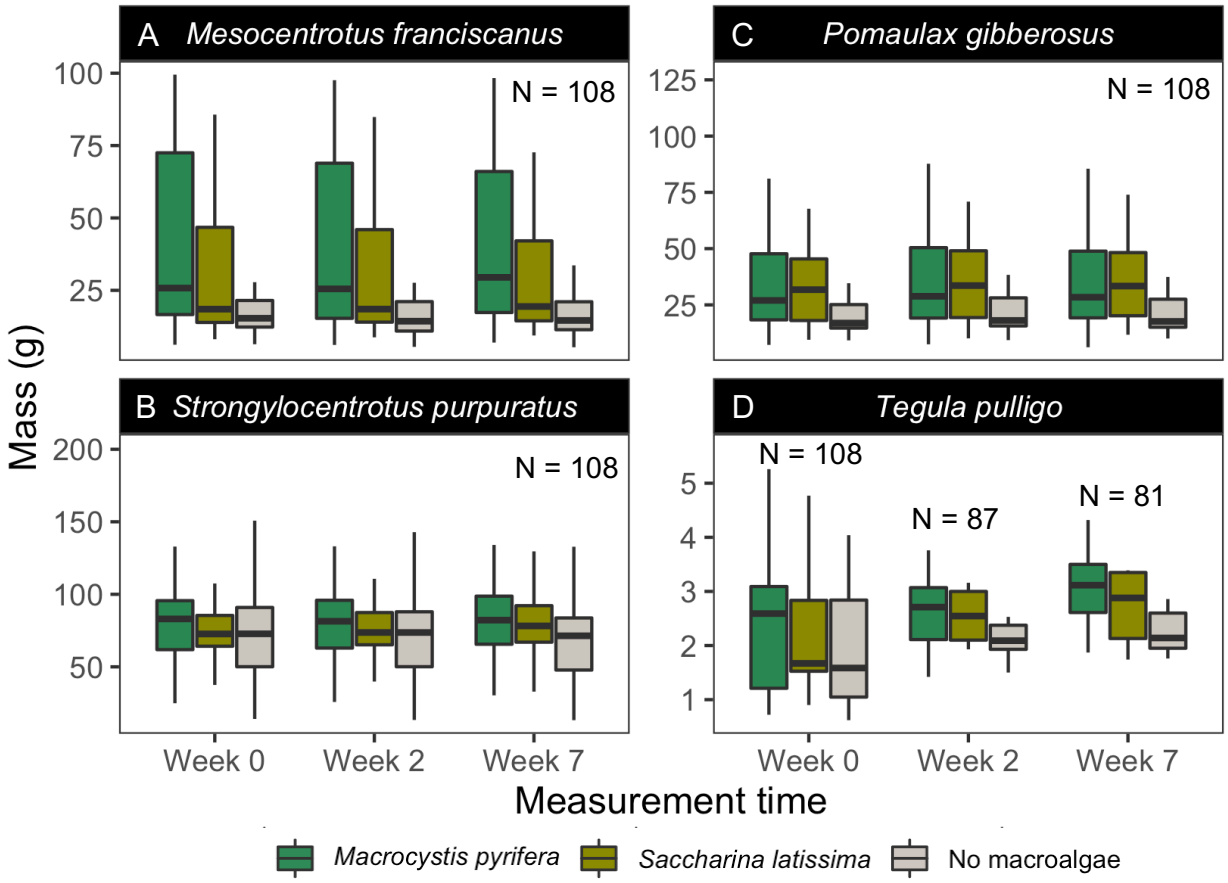

Figure S4. Wet mass of four grazing invertebrate species (A-D) at three time-points of the food treatment period (pre-treatment: Week 0; during treatment: Week 2; post-treatment: Week 7). N = 108 across treatments for each of the 4 species at each measurement point, unless otherwise indicated (some individuals of *Tegula pulligo* were lost during treatment). Due to inadvertent, systematic bias in the allocation of individuals of *Mesocentrotus franciscanus* and *Pomaulax gibberosus* to treatments (A and C), the range of individual wet masses was larger in the *Macrocystis pyrifera* and *Saccharina latissima* macroalgae treatments.

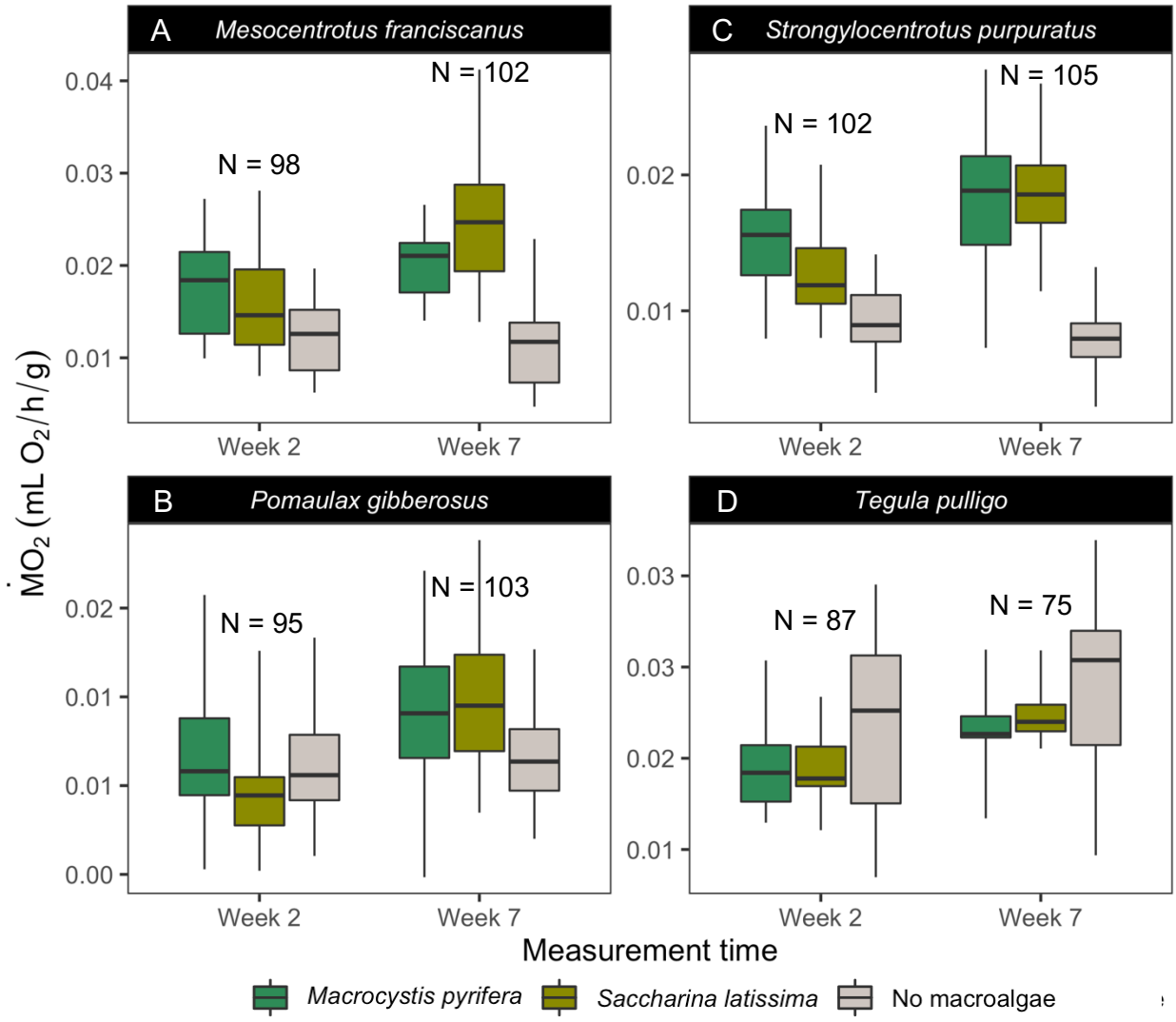

Figure S5. Wet mass-specific oxygen consumption ($\dot{M}O_2$ per unit mass) of four grazing invertebrate species at two measurement time-points (Week 2 and Week 7) along a 7-week food treatment (*Macrocystis pyrifera*, *Saccharina latissima* and no macroalgae). $\dot{M}O_2$ measurements were made at ambient seawater temperatures at time of measurement (9.0°C at Week 2; 10.5°C at Week 7). Boxplots show maximum, minimum and median values, as well as 25th and 75th percentile values. N=432 individuals across all species and treatments.

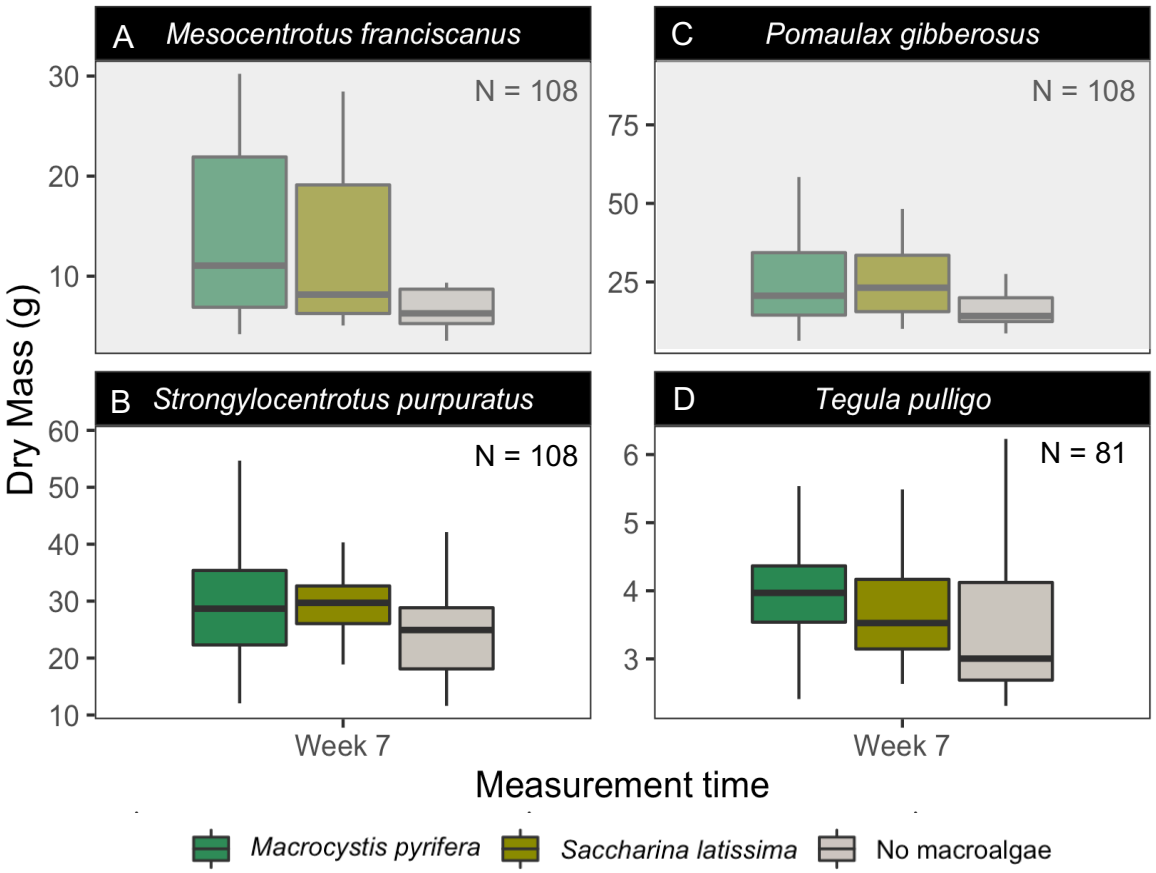

Figure S6. Dry mass of four grazing invertebrate species (A-D) following a 7-week food treatment. N = 108 across treatments for each species (N = 36 per treatment), except for *Tegula pulligo* where N = 81 (some individuals were lost during treatment). Dry mass differences across treatments in *M. franciscanus* (A) and *P. gibberosus* (C) are confounded by initial wet mass differences prior to the start of food treatments (see Week 0 in supplementary figure S4) and are therefore greyed-out.

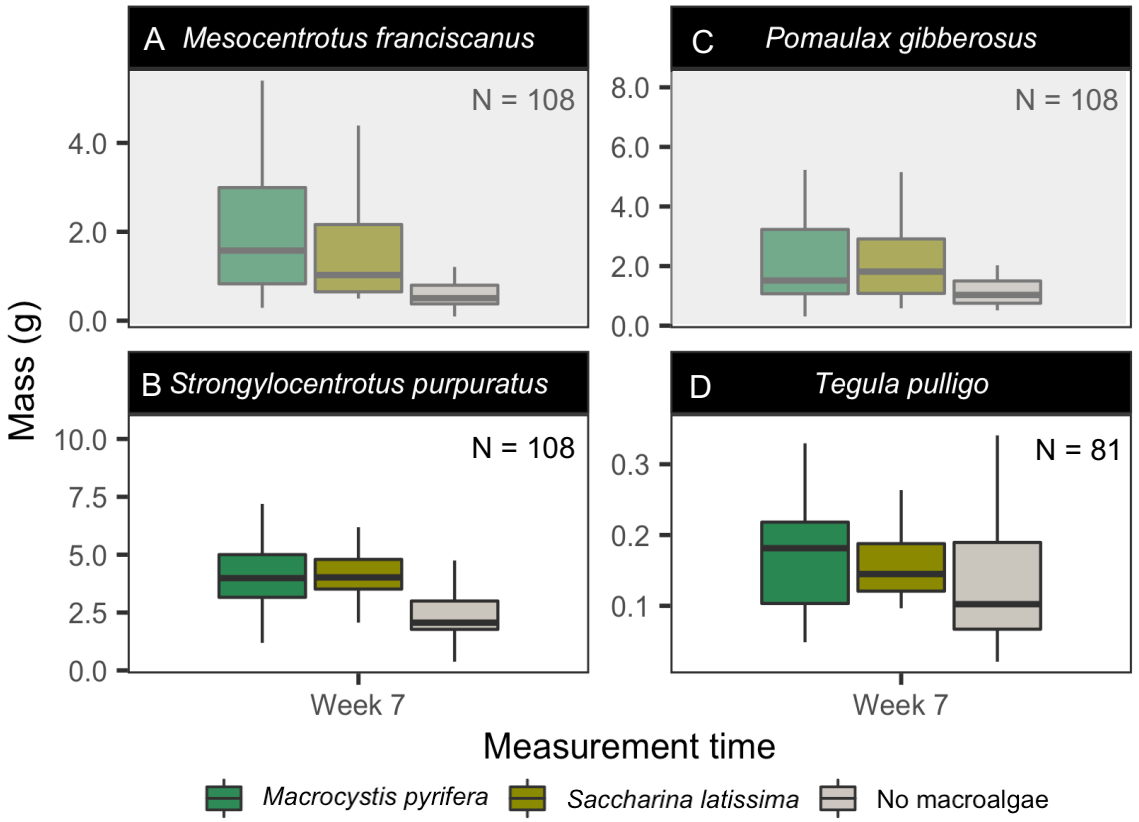

Figure S7. Ash-free dry mass (mass of metabolically active tissue) of four grazing invertebrate species (A-D) following a 7-week food treatment. N = 108 across treatments for each species (N = 36 per treatment and species), except for *Tegula pulligo* where N = 81 (some individuals were lost during treatment). Dry mass differences across treatments in *M. franciscanus* (A) and *P. gibberosus* (C) are confounded by initial wet mass differences prior to the start of food treatments (see Week 0 in supplementary figure S4) and are therefore greyed-out.

Table S1. Chemical composition of two species of kelp. Values were extracted from the literature (references provided in square brackets). A range of values are given where multiple measurements or different values from several studies are available. DM = dry mass.

	Macrocystis pyrifera	***Saccharina latissima***
Protein (g/kg DM)	110.0 - 330.0 [1, 2]	30.0 - 140.0 [4, 5, 6]
Gross energy (MJ/kg)	9.0 [3]	10.8 – 11.1 [4, 5, 6]
Iodine (g/kg DM)	2.0 [1, 2]	3.6 - 6.3 [4, 5, 6]
Calcium (g/kg DM)	11.6 – 16.6 [3]	9.6 – 10.0 [3]
Phosphorus (g/kg DM)	2.6 – 3.2 [3]	2.2 – 3.1 [3]
Potassium (g/kg DM)	44.8 – 112.3 [3]	52.5 [3]
Sodium (g/kg DM)	17.1 – 56.7 [3]	33.0 [3]
Magnesium (g/kg DM)	16.2 – 61.8 [3]	5.1 – 7.4 [3]

Table S2. Timing of oxygen consumption ($\dot{M}O_2$) measurements after two- and seven weeks of a caged food experiment. Individual $\dot{M}O_2$ was quantified for all organisms held under one of three food treatments.

Treatment	**Treatment Replicate**	**Date of $\dot{M}O_2$ measurement – Week 2**	**Date of $\dot{M}O_2$ measurement – Week 7**
Saccharina latissima	Cage #1	08-April-2021	13-May-2021
Saccharina latissima	Cage #2	09-April-2021	14-May-2021
Saccharina latissima	Cage #3	10-April-2021	15-May-2021
Macrocystis pyrifera	Cage #4	08-April-2021	13-May-2021
Macrocystis pyrifera	Cage #5	09-April-2021	14-May-2021
Macrocystis pyrifera	Cage #6	10-April-2021	15-May-2021
No macroalgae	Cage #7	08-April-2021	13-May-2021
No macroalgae	Cage #8	09-April-2021	14-May-2021
No macroalgae	Cage #9	10-April-2021	15-May-2021

Table S3. Summary of Shapiro-Wilk normality test of absolute and mass-independent oxygen consumption ($\dot{M}O_2$) values for each grazer species. Bold text indicates species and $\dot{M}O_2$ measurement time-points (Week 2 and Week 7) where data failed the normality test (i.e., $p < 0.05$).

Response	Species	*W-statistic*		*p*-value	
		Week 2	**Week 7**	**Week 2**	**Week 7**
Absolute $\dot{M}O_2$	***Mesocentrotus franciscanus***	**0.935**	**0.936**	**<0.001**	**<0.001**
	Strongylocentrotus purpuratus	0.983	0.983	0.209	0.212
	Pomaulax gibberosus	**0.925**	**0.917**	**<0.001**	**<0.001**
	Tegula pulligo	0.946	0.975	0.146	0.748
Mass-independent $\dot{M}O_2$	***Mesocentrotus franciscanus***	**0.956**	0.989	**0.003**	0.660
	Strongylocentrotus purpuratus	0.996	**0.904**	0.988	**<0.001**
	Pomaulax gibberosus	0.979	**0.963**	0.191	**0.008**
	Tegula pulligo	0.982	0.955	0.904	0.321

Table S4. Summary statistics of Wilcoxon post-hoc test for sensitivity analysis of absolute oxygen consumption values ($\dot{M}O_2$) across three food treatments in *M. franciscanus* and *P. gibberosus* subsets. Because of initial wet mass differences (prior to treatment start) across food treatments in these two species, a subset with the largest individuals removed was selected for analysis. A Wilcox post-hoc test was computed for non-parametric data following a Kruskal-Wallis test (Week 2: $X^2(2, N = 96) = 15.98$, $p = <0.001$ and Week 7: $X^2(2, N = 97) = 40.55$, $p = <0.001$ for *M. franciscanus*; and Week 2: $X^2(2, N = 76) = 3.44$, $p = 0.179$ and Week 7: $X^2(2, N = 78) = 14.76$, $p = <0.001$ for *P. gibberosus*). The three treatments levels were: a) *Macrocystis pyrifera* (MP), b) *Saccharina latissima* (SL) and c) no macroalgae (NM).

Species	Time	Treatments	*Z*-statistic	*p*-value	Adjusted *p*-value
Mesocentrotus franciscanus	Week 2	MP vs SL	471	0.061	0.182
		MP vs NM	740	<0.001	<0.001
		SL vs NM	572	0.035	0.035
	Week 7	MP vs SL	353	0.431	1.000
		MP vs NM	806	<0.001	<0.001
		SL vs NM	980	<0.001	<0.001
Pomaulax gibberosus	Week 2	MP vs SL	192	0.476	1.000
		MP vs NM	294	0.090	0.270
		SL vs NM	355	0.224	0.672
	Week 7	MP vs SL	168	0.197	0.591
		MP vs NM	476	0.029	0.086
		SL vs NM	523	<0.001	<0.001

Table S5. Summary statistics of differences in absolute and mass-independent oxygen consumption ($\dot{M}O_2$) values across three food treatments (*Macrocystis pyrifera*, *Saccharina latissima* and no macroalgae). A separate model was run for each grazing invertebrate species and measurement time-point (Week 2 and Week 7). A non-parametric Kruskal-Wallis test was conducted where data failed to meet normality assumptions (see table S2). NAs indicate model data met parametric test assumptions, with one-way ANOVA summary statistics presented in table S6. A sensitivity test was run for *M. franciscanus* and *P. gibberosus*, with a subset where the largest individuals were removed, to account for initial wet mass differences across treatments in these two species.

Response	Species	Statistic	Time-point	
			Week 2	**Week 7**
Absolute $\dot{M}O_2$	***Mesocentrotus franciscanus***	Chi-squared (X^2) value	19.78	43.72
		d.f.	2	2
		p-value	<0.001	<0.001
	Strongylocentrotus purpuratus	Chi-squared (X^2) value	*NA*	*NA*
		d.f.	*NA*	*NA*
		p-value	*NA*	*NA*
	Pomaulax gibberosus	Chi-squared (X^2) value	7.87	21.41
		d.f.	2	2
		p-value	0.019	<0.001
	Tegula pulligo	Chi-squared (X^2) value	*NA*	*NA*
		d.f.	*NA*	*NA*
		p-value	*NA*	*NA*
Mass-independent $\dot{M}O_2$	***Mesocentrotus franciscanus***	Chi-squared (X^2) value	4.56	*NA*
		d.f.	2	*NA*
		p-value	0.102	*NA*
	Strongylocentrotus purpuratus	Chi-squared (X^2) value	*NA*	57.54
		d.f.	*NA*	2
		p-value	*NA*	<0.001
	Pomaulax gibberosus	Chi-squared (X^2) value	*NA*	3.46
		d.f.	*NA*	2
		p-value	*NA*	0.177
	Tegula pulligo	Chi-squared (X^2) value	*NA*	*NA*
		d.f.	*NA*	*NA*
		p-value	*NA*	*NA*

Table S6. Summary statistics of differences in absolute and mass-independent oxygen consumption values across three food treatments (*Macrocystis pyrifera*, *Saccharina latissima* and no macroalgae). A separate one-way ANOVA was run for each grazing invertebrate species. NAs indicate model data did not meet parametric test assumptions, with Kruskal-Wallis summary statistics presented in table S5.

	Species	Time		DF	Sum of Squares	Mean Squares	*F*-value	*p*-value
Absolute $\dot{M}O_2$	***Strongylocentrotus purpuratus***	**Week 2**	Treatment	2	4.407	2.204	19.38	<0.001
			Residuals	98	11.145	0.114		
		Week 7	Treatment	2	17.18	8.588	62.71	<0.001
			Residuals	101	13.83	0.137		
	Tegula pulligo	**Week 2**	Treatment	2	<0.001	<0.001	0.78	0.470
			Residuals	26	0.003	<0.001		
		Week 7	Treatment	2	<0.001	<0.001	1.69	0.207
			Residuals	23	<0.001	<0.001		
Mass-independent $\dot{M}O_2$	***Mesocentrotus franciscanus***	**Week 2**	Treatment	*NA*	*NA*	*NA*	*NA*	*NA*
			Residuals	*NA*	*NA*	*NA*		
		Week 7	Treatment	2	1.392	0.696	90.42	<0.001
			Residuals	94	0.723	0.008		
	Strongylocentrotus purpuratus	**Week 2**	Treatment	2	3.259	1.630	27.45	<0.001
			Residuals	98	5.813	0.059		
			Treatment	*NA*	*NA*	*NA*	*NA*	*NA*

	Week 7	Residuals	*NA*	*NA*	*NA*		
Pomaulax gibberosus	**Week 2**	Treatment	2	0.043	0.021	2.21	0.117
		Residuals	78	0.755	0.010		
	Week 7	Treatment	*NA*	*NA*	*NA*	*NA*	*NA*
		Residuals	*NA*	*NA*	*NA*		
Tegula pulligo	**Week 2**	Treatment	2	<0.001	<0.001	0.428	0.656
		Residuals	26	0.003	<0.001		
	Week 7	Treatment	2	<0.001	<0.001	1.016	0.378
		Residuals	23	0.004	<0.001		

Table S7. Summary statistics of Wilcox post-hoc tests to identify differences in absolute and mass-independent $\dot{M}O_2$ values across three food treatments in grazing invertebrates. A Wilcox post-hoc test was computed for non-parametric data following a Kruskal-Wallis test (Kruskal-Wallis results reported in table S4). The three treatments levels were: a) *Macrocystis pyrifera* (MP), b) *Saccharina latissima* (SL) and c) no macroalgae (NM).

	Species	Time	Treatments	*Z*-statistic	*p*-value	Adjusted *p*-value
Absolute $\dot{M}O_2$	***Mesocentrotus franciscanus***	Week 2	MP vs SL	613	0.058	0.175
			MP vs NM	886	<0.001	<0.001
			SL vs NM	712	0.002	0.007
		Week 7	MP vs SL	561	0.833	1.000
			MP vs NM	1099	<0.001	<0.001
			SL vs NM	1033	<0.001	<0.001
	Pomaulax gibberosus	Week 2	MP vs SL	406	0.431	1.000
			MP vs NM	517	0.013	0.040
			SL vs NM	619	0.026	0.078
		Week 7	MP vs SL	456	0.463	1.000
			MP vs NM	871	<0.001	0.002
			SL vs NM	913	<0.001	<0.001
Mass-independent $\dot{M}O_2$	***Mesocentrotus franciscanus***	Week 2	MP vs SL	576	0.031	0.093
			MP vs NM	628	0.120	0.360
			SL vs NM	480	0.801	1.000
	Strongylocentrotus purpuratus	Week 7	MP vs SL	577	0.548	1.000
			MP vs NM	1089	<0.001	<0.001
			SL vs NM	1109	<0.001	<0.001
	Pomaulax gibberosus	Week 7	MP vs SL	478	0.983	1.000
			MP vs NM	721	0.076	0.227
			SL vs NM	647	0.171	0.513

Table S8. Summary statistics of Tukey's post-hoc tests to identify differences in absolute and mass-independent $\dot{M}O_2$ values across three food treatments in grazing invertebrates. A Tukey's post-hoc test was computed for parametric data following one-way ANOVAs (ANOVA results reported in table S6). The difference between means of treatment pairs are given, together with lower and upper 95th confidence intervals (CI). The three treatments levels were: a) *Macrocystis pyrifera* (MP), b) *Saccharina latissima* (SL) and c) no macroalgae (NM).

	Species	Time	Treatments	Mean difference	Lower 95th CI	Upper 95th CI	*p*-value
Absolute $\dot{M}O_2$	***Strongylocentrotus purpuratus***	Week 2	MP vs SL	-0.17	-0.37	0.02	0.097
			MP vs NM	-0.51	-0.70	-0.31	<0.001
			SL vs NM	-0.33	-0.53	-0.14	<0.001
		Week 7	MP vs SL	0.03	-0.18	0.24	0.951
			MP vs NM	-0.86	-1.07	-0.65	<0.001
			SL vs NM	-0.89	-1.10	-0.67	<0.001
	Tegula pulligo	Week 2	MP vs SL	-0.0003	-0.01	0.01	0.999
			MP vs NM	-0.01	-0.02	0.01	0.550
			SL vs NM	-0.005	-0.02	0.01	0.543
		Week 7	MP vs SL	0.01	-0.01	0.03	0.688
			MP vs NM	-0.01	-0.03	0.01	0.669
			SL vs NM	-0.01	-0.03	0.004	0.180
Mass-independent $\dot{M}O_2$	***Mesocentrotus franciscanus***	Week 7	MP vs SL	0.05	0.002	0.11	0.037
			MP vs NM	-0.22	-0.27	-0.17	<0.001
			SL vs NM	-0.28	-0.33	-0.22	<0.001
	Strongylocentrotus purpuratus	Week 2	MP vs SL	-0.18	-0.32	-0.04	<0.001
			MP vs NM	-0.44	-0.58	-0.30	<0.001
			SL vs NM	-0.26	-0.40	-0.12	<0.001
	Pomaulax gibberosus	Week 2	MP vs SL	-0.02	-0.09	0.04	0.711
			MP vs NM	0.03	-0.03	0.10	0.452
			SL vs NM	0.05	-0.01	0.12	0.099

Table S9. Summary statistics of differences in body mass (wet, dry and ash-free dry mass (AFDM)) of grazing invertebrate species across three food treatments (*Macrocystis pyrifera*, *Saccharina latissima* and no macroalgae). A separate model was run for each grazing invertebrate species, at each measurement time-point (Week 0, 2 and 7). Differences in wet mass were compared at three time-points (Week 0, 2 and 7), whilst dry mass and ash-free dry mass were obtained after the food treatment had ended. Because of initial wet mass differences across treatments in *M. franciscanus* and *P. gibberosus* at Week 0, no treatment comparisons of dry mass or AFDM were made for these two species (grey text). A non-parametric Kruskal-Wallis test was conducted because data failed to meet normality assumptions.

	Species	Statistic	Kruskal-Wallis test		
			Week 0	Week 2	Week 7
Wet mass (g)	*Mesocentrotus franciscanus*	Chi-squared (X^2)	8.917	9.752	13.938
		d.f.	2	2	2
		p-value	0.01	0.008	<0.001
	Strongylocentrotus purpuratus	Chi-squared (X^2)	0.588	0.928	3.640
		d.f.	2	2	2
		p-value	0.745	0.629	0.162
	Pomaulax gibberosus	Chi-squared (X^2)	9.701	9.791	10.604
		d.f.	2	2	2
		p-value	0.008	0.007	0.005
	Tegula pulligo	Chi-squared (X^2)	4.071	15.487	15.916
		d.f.	2	2	2
		p-value	0.131	<0.001	<0.001
Dry mass (g)	***Strongylocentrotus purpuratus***	Chi-squared (X^2)			6.877
		d.f.			2
		p-value			0.032
	Tegula pulligo	Chi-squared (X^2)			7.394
		d.f.			2
		p-value			0.025
AFDM (g)	***Strongylocentrotus purpuratus***	Chi-squared (X^2)			30.456
		d.f.			2
		p-value			<0.001
	Tegula pulligo	Chi-squared (X^2)			8.607
		d.f.			2
		p-value			0.014

Table S10. Summary statistics of Wilcox post-hoc test to identify differences in body mass across food treatments in grazing invertebrate species following a Kruskal-Wallis test. Differences in wet mass were compared at three time-points (Week 0, 2 and 7), whilst dry mass and ash-free dry mass were obtained after the food treatment had ended. A Wilcox post-hoc test was only computed if the Kruskal-Wallis test indicated significant treatment differences (see table S9). Because of initial wet mass differences across treatments in *M. franciscanus* and *P. gibberosus* at Week 0 (see table S9), no treatment comparisons of dry mass or AFDM were made for these two species (grey text). The three treatments levels were: a) *Macrocystis pyrifera* (MP), b) *Saccharina latissima* (SL) and c) no macroalgae (NM).

	Species	Time	Treatments	*Z*-statistic	*p*-value	Adjusted *p*-value
Wet mass (g)	***Mesocentrotus franciscanus***	Week 0	MP vs SL	799	0.090	0.271
			MP vs NM	908	0.004	0.011
			SL vs NM	770	0.172	0.516
		Week 2	MP vs SL	773	0.162	0.486
			MP vs NM	911	0.003	0.008
			SL vs NM	822	0.05	0.150
		Week 7	MP vs SL	818	0.056	0.166
			MP vs NM	959	<0.001	0.001
			SL vs NM	846	0.026	0.077
	Pomaulax gibberosus	Week 0	MP vs SL	638	0.915	1.000
			MP vs NM	871	0.012	0.035
			SL vs NM	902	0.004	0.012
		Week 2	MP vs SL	641	0.942	1.000
			MP vs NM	874	0.011	0.034
			SL vs NM	902	0.004	0.012
		Week 7	MP vs SL	606	0.788	1.000
			MP vs NM	867	0.013	0.040
			SL vs NM	901	0.002	0.005
	Tegula pulligo	Week 2	MP vs SL	458	0.165	0.495
			MP vs NM	606	<0.001	0.003

			SL vs NM	706	0.001	0.004
		Week 7	MP vs SL	388	0.192	0.576
			MP vs NM	501	0.002	0.005
			SL vs NM	663	<0.001	0.002
Dry mass (g)	***Strongylocentrotus purpuratus***	Week 7	MP vs SL	626	0.81	1.000
			MP vs NM	801	0.086	0.258
			SL vs NM	890	0.006	0.018
	Tegula pulligo		MP vs SL	440	0.225	0.675
			MP vs NM	484	0.028	0.082
			SL vs NM	777	0.029	0.086
AFDM (g)	***Strongylocentrotus purpuratus***	Week 7	MP vs SL	605	0.634	1.000
			MP vs NM	1022	<0.001	<0.001
			SL vs NM	1114	<0.001	<0.001
	Tegula pulligo		MP vs SL	406	0.515	1.000
			MP vs NM	488	0.023	0.069
			SL vs NM	813	0.008	0.025

References:

1. Zimmerman, R.C. & Kremer, J.N. (1986). In situ growth and chemical composition of the giant kelp, *Macrocystis pyrifera*: response to temporal changes in ambient nutrient availability. *Mar. Ecol. Prog. Ser.*, 27, 277–285.
2. Smith, J.L., Summers, G. & Wong, R. (2010). Nutrient and heavy metal content of edible seaweeds in New Zealand. *New Zeal. J. Crop Hortic. Sci.*, 38, 19–28.
3. Corino, C., Modina, S.C., Di Giancamillo, A., Chiapparini, S. & Rossi, R. (2019). Seaweeds in Pig Nutrition. *Animals*, 9, 1126.

4. Biancarosa, I., Belghit, I., Bruckner, C.G., Liland, N.S., Waagbø, R., Amlund, H., *et al.* (2018). Chemical characterization of 21 species of marine macroalgae common in Norwegian waters: benefits of and limitations to their potential use in food and feed. *J. Sci. Food Agric.*, 98, 2035–2042.
5. Sharma, S., Neves, L., Funderud, J., Mydland, L.T., Øverland, M. & Horn, S.J. (2018). Seasonal and depth variations in the chemical composition of cultivated *Saccharina latissima*. *Algal Res.*, 32, 107–112.
6. Krogdahl, Å., Jaramillo-Torres, A., Ahlstrøm, Ø., Chikwati, E., Aasen, I.-M. & Kortner, T.M. (2021). Protein value and health aspects of the seaweeds *Saccharina latissima* and *Palmaria palmata* evaluated with mink as model for monogastric animals. *Anim. Feed Sci. Technol.*, 276, 114902.

Chapter 4 - Tropicalization of Temperate Reef Fish Communities Facilitated by Urchin Grazing and Diversity of Thermal Affinities.

This chapter formed the basis of the publication:

Schuster, J. M., Stuart-Smith, R. D., Edgar, G. J. and Bates, A. E., 2022. Tropicalization of temperate reef fish communities facilitated by urchin grazing and diversity of thermal affinities. Global Ecology and Biogeography, 31(5), pp.995-1005.

4.1 Abstract

Global declines in structurally complex habitats are reshaping both land- and sea-scapes in directions that affect biological communities' responses to warming. Here, we test whether widespread loss of kelp habitats through sea urchin overgrazing systematically changes sensitivity of fish communities to warming. Community thermal affinity shifts related to habitat were assessed by simulating and comparing fish communities from 2,271 surveys across 15 ecoregions. We find that fishes in kelp and urchin barrens differ in realized thermal affinities and range sizes, but only in regions where species pools have high variability in species' thermal affinities. Barrens on warm-temperate reefs host relatively more warm-affinity fish species than neighbouring kelp beds, highlighting acceleration of tropicalization processes facilitated by urchin herbivory. By contrast, proportionally more cool-affinity fishes colonize barrens at high temperate latitudes, contributing to community lags with ocean warming in these regions. Our findings implicate urchins as drivers of ecological change, in part by affecting biological resilience to warming.

4.2 Introduction

Biodiversity and the distribution of species are rapidly re-structuring in response to contemporary climate change (Poloczanska *et al.* 2013; Blowes *et al.* 2019; Kennedy *et al.* 2019). In the ocean, species are tracking warming waters, leading to population declines in areas where warming exceeds thermal thresholds, and population increases in locations where warming allows colonization into sites that were previously too cold (Pinsky *et al.* 2013) – a process often termed "tropicalization" in temperate regions. Moreover, studies in terrestrial systems suggest habitat alteration can favour particular species (Barnagaud *et al.* 2012; Nowakowski *et al.* 2018; Platts *et al.* 2019), leading to assemblages that are less sensitive to extreme heat or cold (Williams *et al.* 2019). Thus, habitat change may lead to significant shifts in types of species present, which can facilitate or dampen the progression of tropicalization. This may also be true for shallow marine systems, where various human activities have tipped ecosystems towards declines of biogenic habitat formers (e.g. kelps, seagrasses and corals; Airoldi *et al.* 2008; Ling *et al.* 2018).

In shallow rocky reef habitats, sea urchins are strong agents of habitat change (Dayton 1985; Filbee-Dexter & Scheibling 2014; Ling *et al.* 2015). Urchins can reach high densities and form feeding fronts that over-graze kelp forests and macroalgal beds, leaving behind barren rock devoid of macrophytes (here referred to as 'urchin barrens'). Barrens expansion can be indirectly driven by over-exploitation of natural predators (e.g. lobster and sea otters) through trophic cascades (Jessup *et al.* 2004; Pederson & Johnson 2006; Bonaviri *et al.* 2009;

Sangil *et al.* 2012). Urchin barrens are unique environments because they represent areas that would be kelp-dominated in the absence of urchin disturbance. By contrast, areas that are naturally devoid of kelp because of other mechanisms than urchin overgrazing, such as hydrodynamics, pollution or sandy substrate, pose long-term and persistent limits to the existence of kelps and their associated communities. Once formed, urchin barrens can persist for decades as urchins switch their feeding to encrusting algae, drift algae and biofilms, thus inhibiting kelp regrowth (Harrold & Reed 1985), and creating distinct habitats that can be spatially and temporally extensive (Watanuki *et al.* 2010). Newly formed barrens have distinctive physical and chemical characteristics related to the absence of kelp, including reduced habitat complexity and shade, increased sedimentation rates and wave exposure (Reed & Foster 1984; Rosman *et al.* 2013), and reduced availability of food and 3D-structure that provides refugia for other reef animals.

Consequently, barren habitats present different 'environmental filters' (Kraft *et al.* 2015) for fauna in temperate zones than habitats comprising large erect macroalgae (hereafter referred to simply as 'kelp'). For example, as kelp transitions to barrens, few species of epibenthic invertebrates persist at high numbers, while kelp-specialists, such as the kelp perch *Brachyistius frenatus*, are lost (Miller *et al.* 2018). Indeed, fish and invertebrate communities can be markedly different in barrens and kelp (Ling 2008), both in terms of community diversity and structure, despite the lack of physical barriers to movement between immediately adjacent habitats. This local community turnover due to habitat modification has the

potential to interact with climate-driven species range shifts. For instance, range expanding warm-affinity species may prefer barren habitat that more closely resembles tropical and subtropical reefs that lack large fleshy macroalgae (e.g., Bates *et al.* 2014).

Kelp beds and barrens may further select for species with different traits. For example, the range-extending sea urchin, *Centrostephanus rodgersii,* facilitates colonization of species more typical of warmer waters, which also have traits that lead to persistence in barrens, such as suspension feeding invertebrates (Bates *et al.* 2017). Sessile colonizers of bare rock may also then attract more mobile benthic invertivores than found in kelp. In contrast, barrens may select against herbivores that specialize on kelp, or species dependent on the erect structure of kelp that extends into the water column. Open questions are whether different barren-forming urchin species drive a systematic shift towards assemblages with relatively warmer-affinity species (compared to adjacent kelp beds), and how shifts in the types of species present in each habitat lead to different expectations of community-level sensitivity to environmental variability (Burrows *et al.* 2019).

Here, our overall objective is to investigate if habitat modification influences warming-driven range shifts in temperate rocky reef ecosystems. Specifically, we quantify how the creation of barrens by sea urchins in areas that would otherwise host kelp modifies the 'thermal composition' of rocky reef fish communities across 15 temperate ecoregions. To investigate changes in different elements of fish thermal composition, we assess community level metrics based on the thermal

affinities of the fishes surveyed on reefs, including the mean (community temperature index, CTI), and variation of thermal affinities among species (community thermal diversity, CTDiv), as well as the breadth of temperatures occupied by species across their range (community thermal range, CTR). We refer to the term 'thermal composition' to describe the distribution of thermal affinities (measured as CTI, CTDiv and CTR) in a fish community (Fig 4.1). We first simulate how differences in CTI of fish communities may manifest between barren and kelp habitats for different species pool compositions with varying levels of CTI sensitivity (high, medium or low). Theory predicts CTI sensitivity (i.e., how responsive CTI is to changes in local temperature) depends on the response diversity typified by thermal affinities and average species' thermal range breadths (STRs) in a regional species pool (Burrows *et al.* 2019). Our simulations aim to identify under which scenario of CTI sensitivity a difference in CTI could be expected between adjacent barrens and kelp habitats. We predict differences between the two habitats when the initial response diversity is high, i.e. high diversity of thermal affinities and narrow average thermal range breadths. We then test whether barren formation can facilitate a relative warming ('tropicalization') of fish communities in 15 ecoregions with varying CTI sensitivity. We expect a warming signature (CTI increase) for barrens fish communities relative to adjacent kelp beds, driven by an influx of warm-affinity species typical of kelp-free lower latitudes. Assuming, on average, lower species diversity at barrens (Edwards & Konar 2020; Pinna *et al.* 2020), we expect lower community thermal diversity (diversity of warm- and cold-affinity species), and a shift towards communities dominated by more widespread,

thermal generalists (with broad thermal ranges; greater CTR). Because patterns in thermal diversity may, for example, link to differences in feeding strategy or water column position, we run a supplementary analysis to test whether thermal composition changes are associated with, or occur independently of, overall community changes (change in species abundance, species richness) or functional richness. Finally, we explore the vulnerability of communities in different regions to tropicalization signals, based on combined CTI sensitivity and warming exposure.

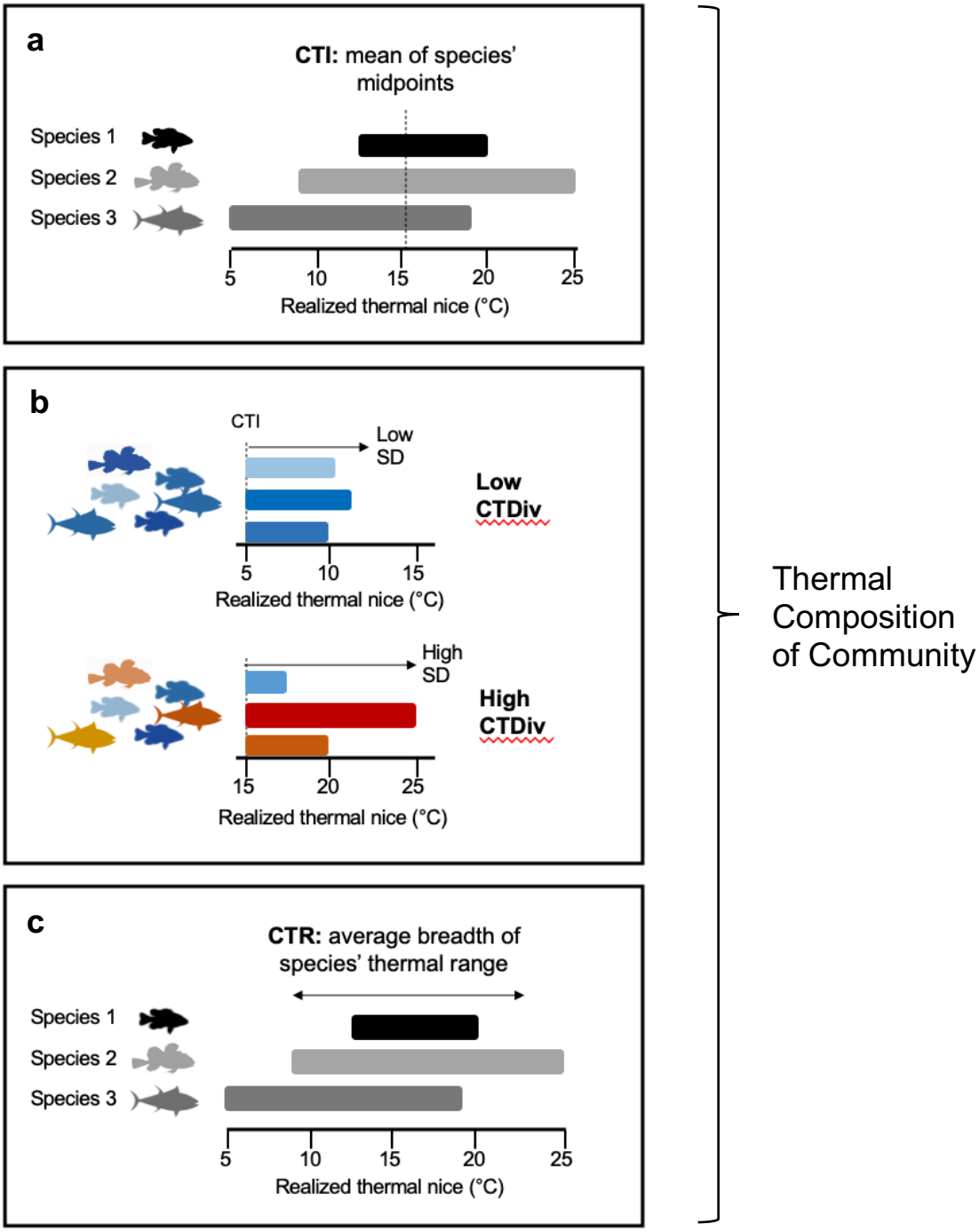

Figure 4.1 Conceptual illustration of Community Temperature Index (CTI; box a), community thermal diversity (CTDiv; box b) and community thermal range (CTR; box c). CTI is calculated as the average thermal affinity (STI) of all species in a local community. The CTDiv (Burrows *et al.* 2019) score indicates the variation of thermal affinities among species in a community and is calculated as the standard

deviation (SD) of STIs. Communities with a mix of cold- (blue) and warm-affinity (red) species have a high score and those containing species with similar thermal affinities have a low score. The CTR represents the average breadth of species' thermal ranges (STRs).

4.3 Methods

4.3.1 Survey data

Standardized quantitative surveys of reef fishes and invertebrates were conducted by trained SCUBA divers through the Reef Life Survey (RLS) program. Full details of the methods are provided in (Edgar & Stuart-Smith 2009; Edgar *et al.* 2020) and in an online methods manual (http://www.reeflifesurvey.com). In brief, each survey quantified species abundance along a 50 m transect line, with size and counts of fishes recorded within 5 m on each side of the line (500 m^2). Large mobile invertebrates (>2.5 cm maximum body length), including urchins, were counted in 1 m bands on each side of the same transect lines (100 m^2). For habitat classification, twenty photo-quadrats were taken 50 cm above the substrate along each transect (Edgar *et al.* 2020).

We restricted our study to temperate latitudes (23.5 – 50.0° latitude, North and South) where kelp forests and barren forming sea urchins co-occur (supplementary table S1), to compare areas with kelp to areas that lack kelp but could potentially support kelp if not for urchin overgrazing. Within this latitudinal band, only ecoregions with surveys that fulfilled the following two criteria were included: 1) barren-forming urchin species were present (barren-forming species classified by expert opinion, see supplementary table S2) and 2) kelp was present, as evident

from the habitat photo-quadrats and literature. We further restricted our analysis to surveys with habitat photo-quadrats available, for habitat classification to ensure only the highest quality data are included (see below). Out of 13,754 global surveys (as of January 2021) this resulted in 2,271 unique survey transects across 15 temperate ecoregions (Spalding *et al.* 2007). In the supplementary material (supplementary table S12 and figure S9), we present a sensitivity analysis based on the full data that also include temperate ecoregions where no habitat-photo-quadrats are available (19 ecoregions, 5,996 surveys).

Each survey was classified as barren or kelp by combining urchin densities and kelp cover from the photo-quadrats. Photo-quadrats were scored using a grid overlay of 5 points per image with 100 points per transect (detailed description of habitat scores provided in (Stuart-Smith *et al.* 2018, 2021; Edgar *et al.* 2020). Surveys hosting densities of barren-forming sea urchin species exceeding 2 m^{-2} and with canopy-forming macroalgae cover below 50% were classified as 'barrens'. This urchin density threshold represents the density of urchins needed to maintain a barren once formed, where barrens can persist even at relatively low urchin densities due to recurrent scraping of bedrock that precludes turf formation, and increased sedimentation preventing kelp recovery (Ling *et al.* 2015, see Fig 1 in the paper by Krumhansl *et al.* 2016). Surveys with over 50% cover of canopy-forming macroalgae cover and low urchin densities (less than 2 urchins per m^{-2}) were classified as 'kelp'. By combining urchin densities and kelp cover we ensure that surveys on patchy habitat, or surveys representing neither kelps nor urchin

barrens, are excluded (e.g., sites with low urchin densities that also lack significant kelp cover). While this approach reduced the number of surveys included in our analysis, it ensured that only those surveys with definitive barrens or kelp habitat were considered in our main analysis. In the supplementary material, we test whether tropicalization signals also emerge in areas that are naturally bare (i.e. lacking significant kelp with low urchin densities) based on 400 surveys (added to the 2,271 barren and kelp surveys), where kelp cover and urchin densities are below 50% and 2 urchins m^{-2}, respectively (results presented in supplementary figure S5a and table S7).

We also designed a sensitivity analysis to test the robustness of using our urchin density threshold, and found our results and main conclusions are robust to variation in this threshold (see supplementary figure S7). To maintain a broad spatial balance so barren and kelp sites in the same region could be contrasted, ecoregions with only one habitat type (e.g., all surveys are in barrens) were removed. Consequently, some prominent kelp-urchin systems, such as the Gulf of Maine, were not included in the analysis.

4.3.2 Community temperature metrics and thermal affinity

We constructed the realized thermal range of all species recorded on selected RLS surveys based on global occurrence data. RLS records were combined with records from the Global Biodiversity Information Facility (GBIF: http://www.gbif.org) for the same species, with GBIF records attributed to 'human observations' (as identified in GBIF meta-data) since 1981 at depths <30 m. The thermal ranges

included all global RLS surveys for full geographic range coverage, rather than the latitudinally restricted barren-kelp subset. This resulted in 570,646 occurrences of 3,120 species.

Weekly mean satellite sea surface temperature (SST) data (one-degree grid, NOAA Optimum Interpolation (OI) SST V2, 1981-present) were matched to each occurrence location. At each location, temperature at time of survey, as well as the annual mean, maximum and minimum were extracted. Species realized thermal range breadth (STR) was calculated as the lower and upper percentile (5^{th} and 95^{th} percentile) of temperatures experienced across a species geographic range. The midpoint of the thermal range was used to estimate the Species Thermal Index (STI).

We computed three community temperature indices (visually illustrated in Fig 4.1) for fish communities to contrast realized thermal composition in barrens and kelps. First, the Community Temperature Index (CTI) was calculated as the average thermal affinity (STI) of all species in a local community. Second, the Community Thermal Diversity (CTDiv; Burrows *et al.* 2019) score – a metric describing variation of thermal affinities among species in a community – was calculated as the standard deviation of STIs in a local community. Communities with a mix of cold- and warm-affinity species have a high score and those containing species with similar thermal affinities have a low score. Third, the Community Thermal Range (CTR) was calculated as the average breadth of species' thermal ranges (STRs).

To interpret community level trends, species were classified as relatively warm or cold-affinity species, relative to others included in the surveyed region. In each ecoregion, the lower and upper quartiles (25^{th} or 75^{th} percentile) of each ecoregional species pool thermal midpoint were used to classify species as the warmest or coldest in their region (supplementary table S3). A sensitivity test for this threshold was run to confirm patterns are robust (see supplementary figure S8) when using lower and upper deciles (10^{th} and 90^{th} percentile).

Ecoregional species pools with diverse thermal affinities (large standard deviations of thermal midpoints) and narrow thermal ranges are more sensitive to large-scale restructuring under temperature change, as observed through shifts in CTI values (Burrows *et al.* 2019). To establish theoretical expectations for a possible habitat effect, we used aggregated ecoregional fish species lists, representing all species that could occur in any given habitat or site within an ecoregion, in a simulation of differences in CTI across barrens and kelp under four scenarios of CTI sensitivity (following the approach of Edwards & Konar 2020): scenario a) species pool with high diversity of STIs and narrow STRs; scenario b) high diversity of STIs and wide STRs; scenario c) low diversity of STIs and narrow STRs; and scenario d) low diversity of STIs and wide STRs. Sensitivity to CTI change is high in scenario (a), medium in scenarios (b) and (c), and low in scenario (d). The diversity of STIs (sdSTI) was calculated as standard deviation of species' thermal midpoints in each ecoregional species pool, and STR was the average breadth of species' thermal ranges in each pool. We used generalized additive model analyses to describe the

overall response of CTI to the distribution of species' thermal properties (sdSTI and STR), habitat and temperature in all species' pools (see supplementary table S4). We simulated potential habitat effects (barren (>2 urchins per m^2) vs kelp (<2 urchins per m^2)) on CTI values for each of the four scenarios (a-d), using different combinations of high or low STRs and sdSTIs for each scenario. Habitat effects were simulated over a temperature range of 8 to 28°C, and values of STR and sdSTI were manipulated over ranges of 5-19 and 1-4, respectively. These expectations were then tested using data on local-scale fish communities from adjacent sites with different habitats, across all study regions. We assigned a CTI sensitivity score of high, medium or low to each ecoregion included in our analysis, based on the thermal characteristics of species observed within each region. Globally, the diversity of STIs (sdSTI) ranged from scores of 1-4, whilst STRs ranged from 6-20°C, thus, ecoregions with sdSTIs of > 2 and STRs of < 13 were assigned high CTI sensitivity; those with sdSTIs of > 2 and STR > 13 or sdSTIs of < 2 and STR < 13 were assigned medium CTI sensitivity (matching scenarios b and c, respectively), and those with sdSTIs < 2 and STRs > 13 were considered ecoregions with low CTI sensitivity.

4.3.3 Statistical modelling

To test for differences in community temperature metrics, richness and abundance across barrens and kelp sites, we used linear mixed effects models and generalized additive mixed models with the packages 'nlme' and 'mgcv' in R (R Core Team 2014) using the functions 'lme' and 'gamm' (Wood 2011; Pinheiro *et*

al. 2015). Nested random effects of realm, ecoregion, latitudinal bins (1x1 degree grid) and survey site were included to account for variation in the response variables due to the non-random spatial structure of the data. Realms and ecoregions are defined per Spalding *et al.* 2007. The random effect for survey site ("SiteCode" in the RLS database) accounts for temporal replicates where a single site was repeatedly surveyed across time. Habitat (barren or kelp) was included in all models to test for habitat-dependent variation in the response of interest, with survey temperature and depth as covariates. Survey temperature (satellite SST extracted at time of survey as described in section 3.2) was used instead of latitude to assess the tropicalization gradient away from the tropics, as temperature-latitude relationships vary between ocean basins. Model fit was visually inspected to ensure test assumptions were met, and model results were compared with different distribution families (poisson, quasi-poisson and negative binomial, all with a log-link function) versus transformation of response data (log and square-root) to ensure results were robust to the modelling approach.

4.4 Results

As predicted from theory, simulations indicate community-level tropicalization is most likely with barren formation in areas where CTI sensitivity and temperature are high (Fig 4.2; 'High' CTI sensitivity scenario). By contrast, impacts of barren formation on tropicalization are expected to be small in areas with low to medium CTI sensitivity (Fig 4.2; 'Low' and 'Medium' CTI sensitivity scenarios). Indeed, analysis of observed fish communities in the 7 ecoregions with high CTI sensitivity confirmed that urchin barrens in warm temperate zones (> 20ºC) support reef

communities with a higher proportion of warm-affinity fish species relative to kelp beds, with different gradients in CTI from cool temperate (< 15ºC) to warm temperate regions depending on the habitat (Fig 4.3a, supplementary table S5). On average, CTI differed by -0.3, -0.3, 0.09 and 0.8ºC between barrens and kelps at survey temperatures of 10, 15, 20 and 25ºC, respectively. The relatively higher CTI in barrens from warm temperate regions is due to a combination of more warm-affinity species and fewer cold-affinity species (Fig 4.4a, supplementary table S6), whilst the opposite signal (fewer warm-affinity species and more cold-affinity species) leads to relatively 'cooler' communities in barrens in colder regions (Fig 4.4b, supplementary table S6). Consequently, the thermal composition of fish communities in kelps varies less along a latitudinal gradient than in urchin barren habitats (along the same gradient). Reef sites at which the habitat is naturally bare (i.e. surveys lacking significant kelp cover and with low urchin densities) also showed relatively higher CTI values in warm temperate regions, relative to kelp, however differences are more pronounced at urchin barrens (supplementary figure S5a and table S7).

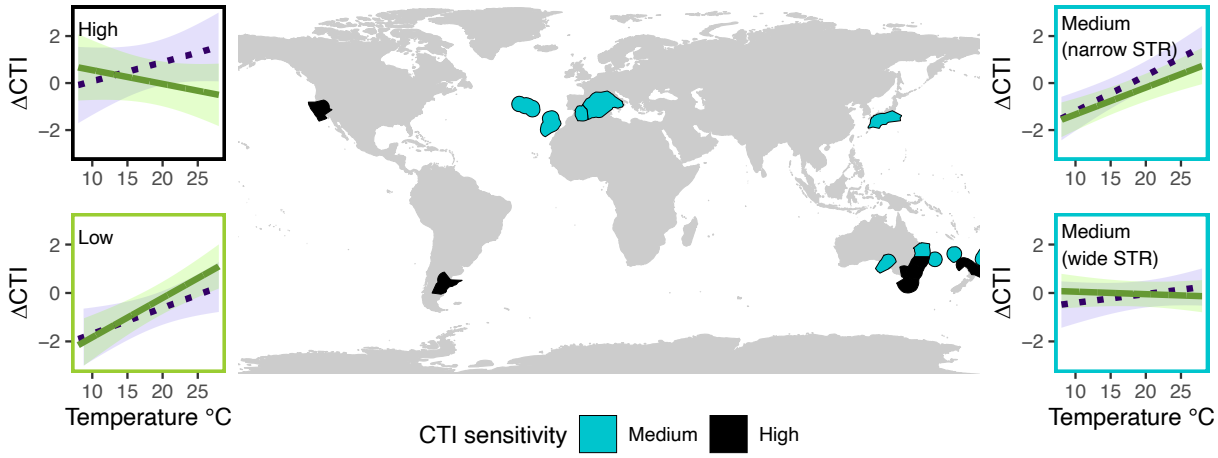

Figure 4.2 Map of temperate ecoregions (23.5 - 50° latitude) with surveyed shallow rocky reef sites hosting sea urchin barrens or kelp beds. Polygons on the map show the ecoregions included in this analysis, with colours indicating their relative CTI sensitivity. A CTI sensitivity score (high, medium or low) was assigned based on the composition of the ecoregional species pool (average species' thermal range (STR) and diversity of thermal affinities (sdSTI); see methods; (Burrows *et al.* 2019)). Plots on the left and right side of the map show differences in community temperature index in kelp beds (green solid lines) and sea urchin barrens (purple dotted lines) under four simulated scenarios of CTI sensitivity.

The overall thermal composition of rocky reef communities differs between barren and kelp habitats across temperate regions and along a gradient from the warm sub-tropics to cool temperate regions. Overall, barrens tend to host fish communities with higher thermal diversity than kelp beds (Fig 4.3b) in areas where CTI sensitivity is high. We also found a slight increase in thermal range breadths for fishes recorded on barrens in warm-temperate regions (Fig 4.3c), suggesting that barren communities with higher CTIs consist of species with particularly broad thermal ranges in these zones. As predicted, in ecoregions with medium CTI

sensitivity, difference in thermal diversity between barrens and kelp are small (Fig 4.3d-f). At 10ºC, CTI in barrens was predicted to be 1.1-2.3ºC below average, whilst the CTI of communities in kelps was predicted as 0.1-1.2ºC below average (in medium CTI sensitivity regions). At 25ºC, barrens CTI was predicted to increase 0.1-0.7ºC from the mean, while CTI in kelps was predicted to change by -0.1 to 0.5ºC. CTI differences between habitats were likely not generally related to differences in overall species abundance and richness, as they were overall similar for barren and kelp habitats (supplementary figure 1a-b). However, functional richness was relatively lower for fishes at barrens at the coldest and warmest edges of temperate latitudes (supplementary figure 1c; see supplementary material for full details).

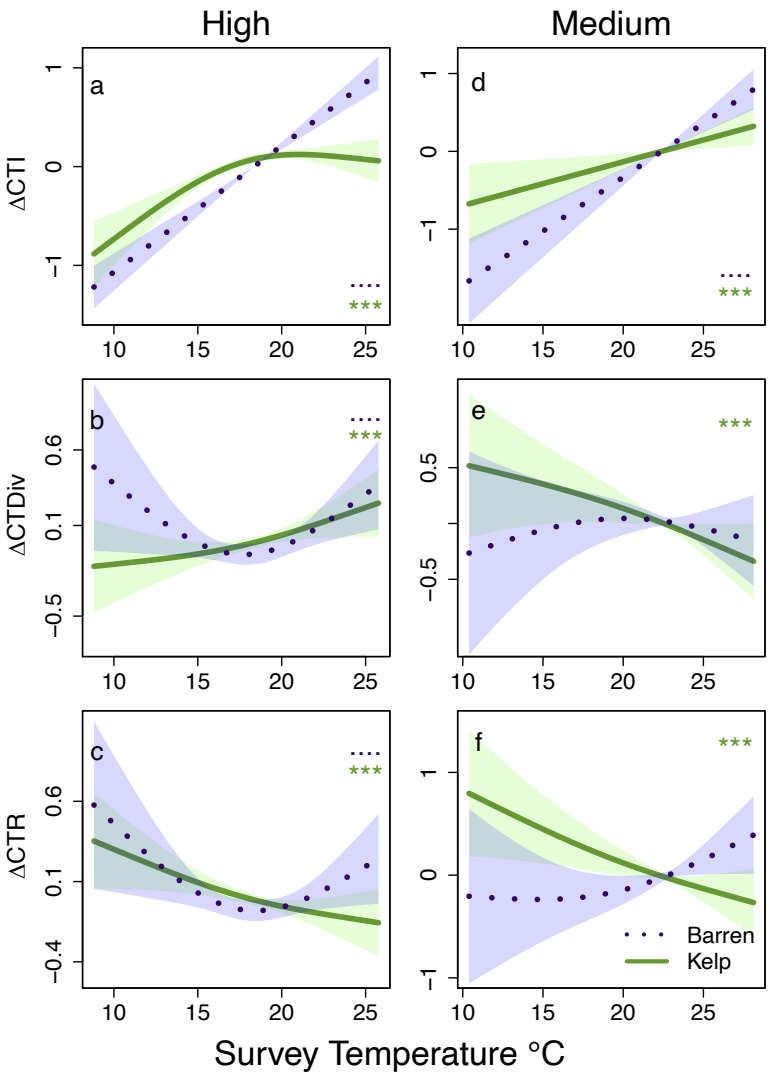

Figure 4.3 Differences in community temperature index (CTI), community thermal diversity (CTDiv) and community thermal range (CTR) for fish communities at barrens and in kelp beds across temperate rocky reefs spanning a temperature gradient. Trends are modelled separately for ecoregions with high CTI sensitivity (left column; a-c) and medium CTI sensitivity (right column, d-f). The CTI sensitivity score was assigned to each ecoregion on the basis of its sdSTI and STR (see methods). Lines indicate trends of barrens (dotted purple line) vs kelp (solid green line) relative to the mean. A symbol is included in the top or bottom right corner of each panel when trends are significant, relative to the mean, i.e., purple dots indicating a significant difference at barrens, and green asterisks indicate kelp sites are significantly different. Shaded areas are 95% confidence intervals predicted by GAMMs. All fixed effects are scaled for coefficient comparison. CTI values differed significantly across ecoregions which masked local CTI differences due to habitat. Raw values are shown in supplementary figure S5. See supplementary material table S5 for model summary tables.

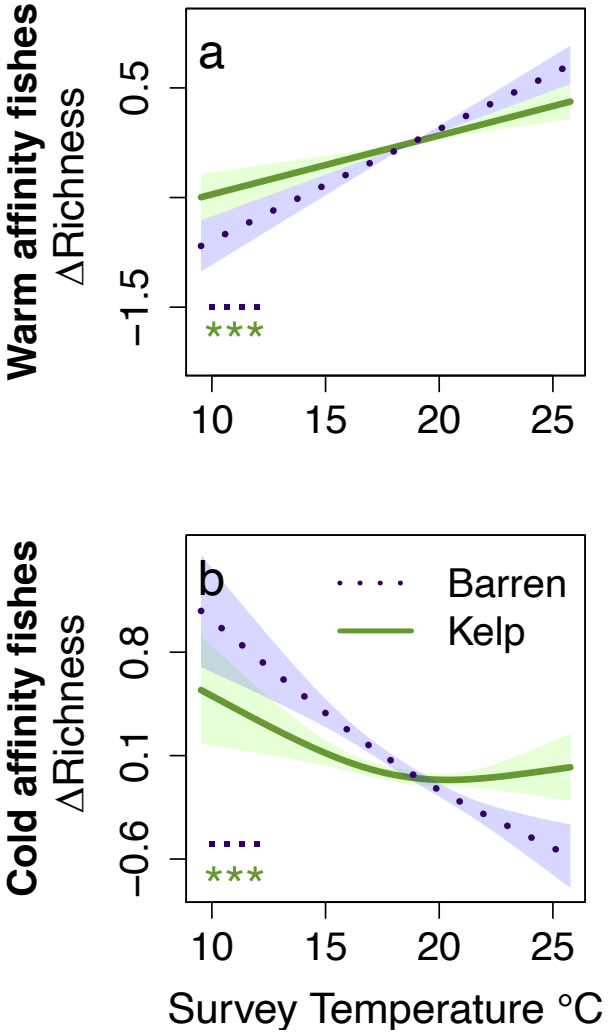

Figure 4.4 Differences in species richness of warm (a) and cold (b) affinity fishes (relative to the mean) contrasted for barren and kelp sites across temperate rocky reefs. Differences in richness at sites with high CTI sensitivity (matching Fig 4.3a-c) are shown here. Lines indicate trends of barrens (dotted purple line) vs kelp (solid green line) relative to the mean. A symbol is included in the bottom left corner of each panel when trends are significant, relative to the mean, i.e., purple dots indicating a significant difference at barrens, and green asterisks indicate kelp sites are significantly different. Shaded areas are 95% confidence intervals predicted by GAMMs. All fixed effects are scaled for coefficient comparison. Richness values differed significantly across ecoregions which masked local richness differences due to habitat. See supplementary material table S6 for model summary tables.

4.5 Discussion

Urchins play a key role in restructuring entire reef communities through dramatic habitat change, with secondary impacts on supported food and habitat resources. Moreover, urchin barrens are expanding due to the removal of top predators which leads to an increase in local urchin populations and geographic range extensions of species as new thermal niches are available (Ling 2008; Filbee-Dexter & Scheibling 2014; Ling *et al.* 2015). Here we highlight that urchin barrens support fish communities with distinct structures that affect their potential resistance and resilience to climate change. In regions where the species pool has high thermal diversity, the formation of barrens also has the potential to strongly influence the sensitivity of the fish community to climate driven temperature changes. We find that urchin barrens and kelp beds host fish communities with distinct patterns of thermal composition (based on CTI) and different sensitivities to environmental stress. Specifically, barrens formed by urchins are associated with both positive and negative shifts in the community temperature index (CTI) of fishes across temperate rocky reefs, depending on context.

We find that kelp covered reefs may be more resistant to temperature-associated changes in fish community structure. This is because urchin barrens are associated with relatively increased tropicalization of fish communities at the equatorward edge of ecoregions included in our analysis – locations that are most sensitive to thermal change. Such regions are also experiencing increasing populations of herbivorous fishes (Vergés *et al.* 2014, 2016), which could further exacerbate the stability of kelp-free states and the corresponding outcomes for the

fish thermal structure that we have found. By contrast, fish communities inhabiting barrens in cool temperate regions show the opposite CTI response (i.e., relatively lower CTI at barrens compared to kelp covered reefs). In addition, the thermal composition of fishes in kelp beds deviates less across a temperature gradient (CTI values are more similar across warm- and cold-temperate regions).

The response of biological communities to thermal composition change (CTI change) depends on the composition of regional species pools (Burrows *et al.* 2019). Our simulations demonstrate habitat change can locally shift the composition of warmer and cooler affinity species when the regional species pool is composed of species with narrow thermal ranges and diverse thermal affinities. Areas with an observed species pool that is similar to simulated thermal affinities and ranges under a high CTI sensitivity scenario showed clear tropicalization signals. In other regions, where species pools have lower thermal diversity and more species with broad thermal ranges, we find no significant tropicalization signal, matching expectations from simulations. Nonetheless, trends in medium CTI sensitivity regions are directionally similar (comparing Fig 4.3a and 4.3b), indicating that similar processes may occur there but are less pronounced. Although no regions with low CTI sensitivity are included in our data, simulations suggest such regions may be relatively resistant to habitat-related tropicalization signals, but this needs to be verified as data become available. We identify regions in the temperate North Pacific, temperate Australasia and temperate South America as particularly vulnerable to urchin barren-related thermal composition

change (Fig 4.3, Table 4.1). In ecoregions in the temperate North Pacific (California) and temperate Australasia (Table 4.1), urchin barrens display stronger tropicalization signals than neighbouring kelp beds, a signal independent of any potential temperature differences between adjacent barrens and kelps. These regions are undergoing rapid warming (supplementary figure S6; Lima & Wethey 2012), leaving local communities particularly vulnerable to exacerbated tropicalization. In Northern Patagonia (temperate South America), fishes inhabiting barrens are inferred to have shifted towards cooler communities, relative to those in kelps, which may result in lagged responses to warming seas. By contrast, many regions in the Mediterranean appear to be more resilient to urchin barren-facilitated tropicalization of fish communities, despite clear warming signals, due to the relatively low response diversity of the species pool in this region. This finding highlights the importance of considering both exposure and sensitivity to environmentally driven community changes, otherwise vulnerability will be under- or over-estimated. We further note that our ability to detect sensitive regions in the global North is limited by lower data coverage in the Northern, compared to Southern Hemisphere, requiring future work.

Table 4.1 Vulnerability of fish communities to thermal diversity change with urchin driven seascape change (barren formation) in temperate ecoregions. Exposure to warming based on NOAA dOISST.v2.1 (1982-2019), calculated as mean±sd degree change for each ecoregion (updated from 30). The most vulnerable ecoregions to urchin-associated tropicalization signals are indicated by grey shading.

Realm	Ecoregion	CTI sensitivity	Warming exposure (°C)
Temperate Northern Pacific	Northern California	High	+0.05 ± 0.04
	Central Kuroshio Current	Medium	+0.22 ± 0.12
Temperate Northern Atlantic	Alboran Sea	Medium	+0.29 ± 0.04
	Azores Canaries Madeira	Medium	+0.25 ± 0.06
	Western Mediterranean	Medium	+0.34 ± 0.05
Central Indo-Pacific	Lord Howe and Norfolk Islands	Medium	+0.16 ± 0.03
Temperate Australasia	Bassian	High	+0.23 ± 0.06
	Cape Howe	High	+0.30 ± 0.07
	Manning-Hawkesbury	High	+0.22 ± 0.05
	South Australian Gulfs	Medium	+0.21 ± 0.03
	Three Kings-North Cape	High	+0.17 ± 0.03
	Kermadec Island	Medium	+0.20 ± 0.02
	Northeastern New Zealand	High	+0.16 ± 0.02
	Tweed-Moreton	Medium	+0.18 ± 0.04
Temperate South America	North Patagonian Gulfs	High	+0.11 ± 0.4

We find that habitat modification correlates with both positive and negative responses in community thermal diversity, a result that may explain why some communities do not match warming expectations with climate lag (Doak & Morris

2010; Bertrand *et al.* 2011). In pelagic and shelf systems, where fishes typically occupy large depth ranges, thermal community composition change can be buffered by fishes moving into deeper waters to track temperature (Burrows *et al.* 2019). In contrast, shallow reef fishes are typically more closely associated with their habitat and constrained to shallow waters, with depth changes far less likely or even possible (Sunday *et al.* 2012; Stuart-Smith *et al.* 2017). Thus, we do not expect depth to play a substantial and general ecological role through temperature refugia for the shallow reef fish communities investigated here. Regardless, CTDiv and CTR both decreased with depth (supplementary table S5), suggesting that species found at deeper reefs are less tolerant of extreme temperatures. The depth effect may be due to an interaction with species richness. In any case, shallow reef fish communities appear strongly shaped by sensitivity to temperature, making them a responsive model group for CTI change.

Tropicalization of fish communities involves a restructuring of thermal affinities at subtropical barrens through the influx of tropical (warm-affinity) fish species and simultaneous loss of colder affinity fishes (Vergés *et al.* 2019). In warmer temperate regions, barrens may offer preferential habitat for range-shifting tropical fish species that come from adjacent tropical regions with few large fleshy macroalgal beds. The expansion of barrens could therefore further facilitate the ongoing tropicalization of temperate fish communities (Poloczanska *et al.* 2013; Hyndes *et al.* 2016; Vergés *et al.* 2019) driven by contemporary oceanographic and climatic changes. However, elevated local diversity of fishes through increases

in tropical species may be limited beyond the warm temperate regions where seasonal temperature minima pose physiological constraints and set a poleward range limit for species typical of warmer waters (Kimball *et al.* 2004; Urian *et al.* 2011). Interestingly, signals of fish community tropicalization also emerge in areas that are naturally devoid of kelp with low urchin densities (e.g., due to hydrodynamics or sandy substrate), albeit tropicalization signals there are not as strong as in urchin barrens (supplementary figure S5a).

Towards the cold edge of temperate regions, a loss of warm-affinity species is associated with a downward shift of fish CTI at barrens. The richness of ectothermic predators (higher carnivores) and herbivorous fishes generally decreases with latitude (Edgar *et al.* 2017; Grady *et al.* 2019). Among those carnivores that do extend into colder waters are fishes such as gadid cod and sebastid rockfish, many of which utilize kelp during juvenile stages. The removal of critical kelp habitat through urchins may thus further constrain warm-distributed carnivores in cold regions that are vulnerable to predation as juveniles settling in exposed barrens. However, adult sit-and-wait predators may benefit from the open space created in barrens.

A key question that arises from our results is whether the observed changes in the thermal composition in the fish communities relate to systematic changes in the functional composition of the community. Indeed, significant functional diversity shifts with marine habitat and land-use change have been described (Flynn *et al.* 2009; Laliberté *et al.* 2010; Clavel *et al.* 2011; Richardson *et al.* 2017; Cáceres *et*

al. 2020). Whilst overall diversity is often reduced at barrens (Pinna *et al.* 2020), certain groups can take advantage of barren conditions. For instance, sea stars commonly display strong associations with barren habitats (Scheibling & Lauzon-Guay 2007). In Australia, barren formation facilitates the colonization of sessile species from warmer, kelp-free habitats (Bates *et al.* 2017), which use the settlement space created through kelp removal. Some invertivore fishes may benefit from barren conditions, as kelp loss enables access to large invertebrate prey, however, those feeding on amphipods or small invertebrates living on kelp may be disadvantaged at barrens. Despite only small changes in individual trophic groups (supplementary figure S2-4, supplementary table S9-10), our supplementary analysis indicates strongly reduced overall functional richness at barrens relative to kelp, at the most tropical and polar-edge of the temperate band (see supplementary analysis and supplementary figure S1 and table S8). Detecting individual functional group changes is limited in our supplementary analysis (supplementary tables S9-10 and figures S2-4) due to the spatial scale of fish surveys (500 m^2) potentially being too broad to capture small-scale patch dynamics often observed in urchin grazing (e.g. 5 m^2) and/or an inability to match up timing of surveys with various stages of habitat modification (i.e., fresh versus established barrens). Nonetheless, detecting reduced functional richness in barrens warrants further analysis, as functional changes due to barren formation likely have important implications for community resilience and ecosystem service provisioning. Future research into the dynamics of functional group changes at a finer scale may also reveal other ecologically important signals.

Variation in the habitat-dependent tropicalization signal with the composition of the regional species pool has important conservation implications. While other mechanisms can lead to kelp loss and habitat change in rocky reefs, including heatwaves (Scheibling *et al.* 2013), storm events (Edwards 2004), overfishing and invasive species (Krumhansl *et al.* 2016), urchins play a pivotal role in maintaining persistent bare substrate and preventing kelp recovery. Regardless of the mechanism leading to kelp loss, habitat preservation and restoration may offer important opportunities for building climate resilience in seascapes. As such, managing barren-forming urchin populations, either directly through carefully regulated harvesting, or indirectly through large-scale fishing restrictions on urchin predators, could be particularly effective in regions identified here as most vulnerable. Even so, our analysis was limited to ecoregions where both barren and kelp habitats were observed. Other vulnerable regions likely existed for which paired, standardised fish data from barrens and kelp were not available. Nonetheless, protecting vulnerable kelps will require a combination of global efforts to reduce ocean warming and local management strategies that are ecology-informed and aim to preserve healthy ecosystems (i.e., sea urchin density reduction, not complete removal).

Here we implicate barren-forming sea urchins as drivers of seascape change that correlates with community tropicalization in fishes. Directional shifts towards warmer communities with human-induced land use change are well documented in terrestrial habitats (e.g., birds, amphibians and terrestrial vertebrates;

Barnagaud *et al.* 2012; Nowakowski *et al.* 2018; Williams *et al.* 2019), and are linked to local temperature changes that result from habitat change (e.g., removal of shading). Thus, we demonstrate that barren-forming sea urchins are drivers of seascape change in a manner that is analogous to deforestation by humans. The removal of underwater forests can drive both negative and positive CTI responses, and thus alter how fish communities respond to warming signals. Our findings further imply directional community responses can occur as a by-product of habitat changes independent of local habitat temperatures. In the case of kelp-to-barren transitions, local urchin population management (including carefully regulated commercial harvesting) could be a powerful tool for increasing climate resilience of coastal biological systems.

4.6 References

Airoldi, L., Balata, D. & Beck, M. (2008). The Gray Zone: Relationships between habitat loss and marine diversity and their applications in conservation. *J. Exp. Mar. Bio. Ecol.*, 366, 8–15.

Barnagaud, J.-Y., Devictor, V., Jiguet, F., Barbet-Massin, M., Le Viol, I. & Archaux, F. (2012). Relating Habitat and Climatic Niches in Birds. *PLoS One*, 7, e32819.

Bates, A., Barrett, N., Stuart-Smith, R., Holbrook, N., Thompson, P. & J. Edgar, G. (2014). Resilience and signatures of tropicalisation in reef fish communities. *Nat. Clim. Chang.*, 4, 62–67.

Bates, A.E., Stuart-smith, R.D., Barrett, N.S. & Edgar, G.J. (2017). Biological interactions both facilitate and resist climate-related functional change in temperate reef communities. *Proc. R. Soc. B Biol. Sci.*, 284.

Bertrand, R., Lenoir, J., Piedallu, C., Riofrío-Dillon, G., de Ruffray, P., Vidal, C., *et al.* (2011). Changes in plant community composition lag behind climate warming in lowland forests. *Nature*, 479, 517–520.

Blowes, S.A., Supp, S.R., Antão, L.H., Bates, A., Bruelheide, H., Chase, J.M., *et al.* (2019). The geography of biodiversity change in marine and terrestrial assemblages. *Science (80-.).*, 366, 339–345.

Bonaviri, C., T, V.F., Badalamenti, F., Gianguzza, P., M, D.L. & Riggio, S. (2009). Fish versus starfish predation in controlling sea urchin populations in Mediterranean rocky shores . *Mar. Ecol. Prog. Ser.*, 382, 129–138.

Burrows, M.T., Bates, A.E., Costello, M.J., Edwards, M., Edgar, G.J., Fox, C.J., *et al.* (2019). Ocean community warming responses explained by thermal affinities and temperature gradients. *Nat. Clim. Chang.*, 9, 959–963.

Cáceres, I., Ibarra-García, E.C., Ortiz, M., Ayón-Parente, M. & Rodríguez-Zaragoza, F.A. (2020). Effect of fisheries and benthic habitat on the ecological and functional diversity of fish at the Cayos Cochinos coral reefs (Honduras). *Mar. Biodivers.*, 50, 9.

Clavel, J., Julliard, R. & Devictor, V. (2011). Worldwide decline of specialist species: toward a global functional homogenization? *Front. Ecol. Environ.*, 9, 222–228.

Dayton, P.K. (1985). Ecology of Kelp Communities. *Annu. Rev. Ecol. Syst.*, 16, 215–245.

Doak, D.F. & Morris, W.F. (2010). Demographic compensation and tipping points in climate-induced range shifts. *Nature*, 467, 959–962.

Edgar, G., Cooper, A., Baker, S., Barker, W., Barrett, N., Becerro, M., *et al.* (2020). Reef Life Survey: Establishing the ecological basis for conservation of shallow marine life. *Biol. Conserv.*

Edgar, G.J., Alexander, T.J., Lefcheck, J.S., Bates, A.E., Kininmonth, S.J.,

Thomson, R.J., *et al.* (2017). Abundance and local-scale processes contribute to multi-phyla gradients in global marine diversity. *Sci. Adv.*, 3, e1700419.

Edgar, G.J. & Stuart-Smith, R.D. (2009). Ecological effects of marine protected areas on rocky reef communities—a continental-scale analysis. *Mar. Ecol. Prog. Ser.*, 388, 51–62.

Edwards, M.S. (2004). Estimating scale-dependency in disturbance impacts: El Niños and giant kelp forests in the northeast Pacific. *Oecologia*, 138, 436–447.

Edwards, M.S. & Konar, B. (2020). Trophic downgrading reduces spatial variability on rocky reefs. *Sci. Rep.*, 10, 18079.

Filbee-Dexter, K. & Scheibling, R. (2014). Sea urchin barrens as alternative stable states of collapsed kelp ecosystems. *Mar. Ecol. Prog. Ser.*, 495, 1–25.

Flynn, D.F.B., Gogol-Prokurat, M., Nogeire, T., Molinari, N., Richers, B.T., Lin, B.B., *et al.* (2009). Loss of functional diversity under land use intensification across multiple taxa. *Ecol. Lett.*, 12, 22–33.

Grady, J.M., Maitner, B.S., Winter, A.S., Kaschner, K., Tittensor, D.P., Record, S., *et al.* (2019). Metabolic asymmetry and the global diversity of marine predators. *Science (80-.).*, 363.

Harrold, C. & Reed, D.C. (1985). Food Availability, Sea Urchin Grazing, and Kelp Forest Community Structure. *Ecology*, 66, 1160–1169.

Hyndes, G.A., Heck Jr., K.L., Vergés, A., Harvey, E.S., Kendrick, G.A., Lavery, P.S., *et al.* (2016). Accelerating Tropicalization and the Transformation of Temperate Seagrass Meadows. *Bioscience*, 66, 938–948.

Jessup, D.A., Miller, M., Ames, J., Harris, M., Kreuder, C., Conrad, P.A., *et al.* (2004). Southern Sea Otter as a Sentinel of Marine Ecosystem Health. *Ecohealth*, 1, 239–245.

Kennedy, C.M., Oakleaf, J.R., Theobald, D.M., Baruch-Mordo, S. & Kiesecker, J. (2019). Managing the middle: A shift in conservation priorities based on the global human modification gradient. *Glob. Chang. Biol.*, 25, 811–826.

Kimball, M., Miller, J., Whitfield, P. & Hare, J. (2004). Thermal tolerance and potential distribution of invasive lionfish (*Pterois volitans/miles* complex) on the east coast of the United States. *Mar. Ecol. Prog. Ser.*, 283, 269–278.

Kraft, N.J.B., Adler, P.B., Godoy, O., James, E.C., Fuller, S. & Levine, J.M. (2015). Community assembly, coexistence and the environmental filtering metaphor. *Funct. Ecol.*, 29, 592–599.

Krumhansl, K.A., Okamoto, D.K., Rassweiler, A., Novak, M., Bolton, J.J., Cavanaugh, K.C., *et al.* (2016). Global patterns of kelp forest change over the past half-century. *Proc. Natl. Acad. Sci.*, 113, 13785 LP – 13790.

Laliberté, E., Wells, J.A., DeClerck, F., Metcalfe, D.J., Catterall, C.P., Queiroz, C., *et al.* (2010). Land-use intensification reduces functional redundancy and response diversity in plant communities. *Ecol. Lett.*, 13, 76–86.

Lima, F.P. & Wethey, D.S. (2012). Three decades of high-resolution coastal sea surface temperatures reveal more than warming. *Nat. Commun.*, 3, 704.

Ling, S.D. (2008). Range expansion of a habitat-modifying species leads to loss of taxonomic diversity: a new and impoverished reef state. *Oecologia*, 156, 883–894.

Ling, S.D., Davey, A., Reeves, S.E., Gaylard, S., Davies, P.L., Stuart-Smith, R.D., *et al.* (2018). Pollution signature for temperate reef biodiversity is short and simple. *Mar. Pollut. Bull.*, 130, 159–169.

Ling, S.D., Scheibling, R.E., Rassweiler, A., Johnson, C.R., Shears, N., Connell, S.D., *et al.* (2015). Global regime shift dynamics of catastrophic sea urchin overgrazing. *Philos. Trans. R. Soc. B Biol. Sci.*, 370, 20130269.

Miller, R.J., Lafferty, K.D., Lamy, T., Kui, L., Rassweiler, A. & Reed, D.C. (2018).

Giant kelp, *Macrocystis pyrifera*, increases faunal diversity through physical engineering. *Proc. R. Soc. B Biol. Sci.*, 285, 20172571.

Nowakowski, A.J., Frishkoff, L.O., Thompson, M.E., Smith, T.M. & Todd, B.D. (2018). Phylogenetic homogenization of amphibian assemblages in human-altered habitats across the globe. *Proc. Natl. Acad. Sci.*, 115, E3454 LP-E3462.

Pederson, H.G. & Johnson, C.R. (2006). Predation of the sea urchin *Heliocidaris erythrogramma* by rock lobsters (*Jasus edwardsii*) in no-take marine reserves. *J. Exp. Mar. Bio. Ecol.*, 336, 120–134.

Pinheiro, J., Bates, D., DebRoy, S., Sarkar, D. & Team, R. (2015). nlme: linear and nonlinear mixed effects models.

Pinna, S., Piazzi, L., Ceccherelli, G., Castelli, A., Costa, G., Curini-Galletti, M., *et al.* (2020). Macroalgal forest vs sea urchin barren: Patterns of macro-zoobenthic diversity in a large-scale Mediterranean study. *Mar. Environ. Res.*, 159, 104955.

Pinsky, M.L., Worm, B., Fogarty, M.J., Sarmiento, J.L. & Levin, S.A. (2013). Marine Taxa Track Local Climate Velocities. *Science (80-.).*, 341, 1239 LP – 1242.

Platts, P.J., Mason, S.C., Palmer, G., Hill, J.K., Oliver, T.H., Powney, G.D., *et al.* (2019). Habitat availability explains variation in climate-driven range shifts across multiple taxonomic groups. *Sci. Rep.*, 9, 15039.

Poloczanska, E.S., Brown, C.J., Sydeman, W.J., Kiessling, W., Schoeman, D.S., Moore, P.J., *et al.* (2013). Global imprint of climate change on marine life. *Nat. Clim. Chang.*, 3, 919–925.

R Core Team. (2014). R: a language and environment for statistical computing.

Reed, D.C. & Foster, M.S. (1984). The Effects of Canopy Shadings on Algal Recruitment and Growth in a Giant Kelp Forest. *Ecology*, 65, 937–948.

Richardson, L.E., Graham, N.A.J., Pratchett, M.S. & Hoey, A.S. (2017). Structural complexity mediates functional structure of reef fish assemblages among coral habitats. *Environ. Biol. Fishes*, 100, 193–207.

Rosman, J.H., Denny, M.W., Zeller, R.B., Monismith, S.G. & Koseff, J.R. (2013). Interaction of waves and currents with kelp forests (*Macrocystis pyrifera*): Insights from a dynamically scaled laboratory model. *Limnol. Oceanogr.*, 58, 790–802.

Sangil, C., Clemente, S., Martín-García, L. & Hernández, J.C. (2012). No-take areas as an effective tool to restore urchin barrens on subtropical rocky reefs. *Estuar. Coast. Shelf Sci.*, 112, 207–215.

Scheibling, R. & Lauzon-Guay, J.-S. (2007). Feeding aggregations of sea stars (*Asterias* spp. and *Henricia sanguinolenta*) associated with sea urchin (*Strongylocentrotus droebachiensis*) grazing fronts in Nova Scotia. *Mar. Biol.*, 151, 1175–1183.

Scheibling, R.E., Feehan, C.J. & Lauzon-Guan, J.-S. (2013). Climate change, disease and the dynamics of a kelp-bed ecosystem in Nova Scotia. In: *Climate change: past, present and future perspectives, a global synthesis from the Atlantic.* (eds. Fernández-Palacios, J.M., Nascimento, L., Hernández, C.J., Clemente, S., González, A. & Díaz-González, J.P.). Servicio de Publicaciones, Universidad de La Laguna, S/C de Tenerife, pp. 361–387.

Spalding, M., Fox, H., Allen, G., Davidson, N., Ferdaña, Z., Finlayson, M., *et al.* (2007). Marine Ecoregions of the World: A Bioregionalization of Coastal and Shelf Areas. *Bioscience*, 57, 573–583.

Stuart-Smith, R.D., Brown, C.J., Ceccarelli, D.M. & Edgar, G.J. (2018). Ecosystem restructuring along the Great Barrier Reef following mass coral bleaching. *Nature*, 560, 92–96.

Stuart-Smith, R.D., Edgar, G.J. & Bates, A.E. (2017). Thermal limits to the

geographic distributions of shallow-water marine species. *Nat. Ecol. Evol.*, 1, 1846–1852.

Stuart-Smith, R.D., Mellin, C., Bates, A.E. & Edgar, G.J. (2021). Habitat loss and range shifts contribute to ecological generalisation amongst reef fishes. *Nat. Ecol. Evol.*, 5, 656–662.

Sunday, J.M., Bates, A.E. & Dulvy, N.K. (2012). Thermal tolerance and the global redistribution of animals. *Nat. Clim. Chang.*, 2, 686.

Urian, A.G., Hatle, J.D. & Gilg, M.R. (2011). Thermal constraints for range expansion of the invasive green mussel, *Perna viridis*, in the southeastern United States. *J. Exp. Zool. Part A Ecol. Genet. Physiol.*, 315, 12–21.

Vergés, A., Doropoulos, C., Malcolm, H.A., Skye, M., Garcia-Pizá, M., Marzinelli, E.M., *et al.* (2016). Long-term empirical evidence of ocean warming leading to tropicalization of fish communities, increased herbivory, and loss of kelp. *Proc. Natl. Acad. Sci.*, 113, 13791 LP – 13796.

Vergés, A., McCosker, E., Mayer-Pinto, M., Coleman, M.A., Wernberg, T., Ainsworth, T., *et al.* (2019). Tropicalisation of temperate reefs: Implications for ecosystem functions and management actions. *Funct. Ecol.*, 33, 1000–1013.

Vergés, A., Steinberg, P.D., Hay, M.E., Poore, A.G.B., Campbell, A.H., Ballesteros, E., *et al.* (2014). The tropicalization of temperate marine ecosystems: climate-mediated changes in herbivory and community phase shifts. *Proc. R. Soc. B Biol. Sci.*, 281.

Watanuki, A., Aota, T., Otsuka, E., Kawai, T., Iwahashi, Y., Kuwahara, H., *et al.* (2010). Restoration of kelp beds on an urchin barren: removal of sea urchins by citizen divers in southwestern Hokkaido. *Bull. Fish. Res. Agen*, 32, 83–87.

Williams, J.J., Bates, A.E. & Newbold, T. (2019). Human-dominated land uses favour species affiliated with more extreme climates, especially in the tropics. *Ecography (Cop.).*, 43, 391–405.

Wood, S.N. (2011). Fast stable restricted maximum likelihood and marginal likelihood estimation of semiparametric generalized linear models. *J. R. Stat. Soc. Ser. B (Statistical Methodol.*, 73, 3–36.

4.7 Appendix C – Supplementary analysis for Chapter 4

C1 Supplementary Methods

C1.1 Functional richness

Because a likely consequence of thermal diversity restructuring are functional changes we conducted a supplementary analysis of functional richness and trophic restructuring. To test for differences in functional richness, fishes were classified into trophic groups: benthic invertivores, planktivores, omnivores, herbivores and carnivores, and activity groups (position in the water column): demersal, benthic, pelagic site-attached and pelagic non-site attached. Functional group assignments were based on those used for (Stuart-Smith *et al.* 2013, 2018), based on information from FishBase (http://www.fishbase.org/) and SeaLifeBase (http://www.sealifebase.org/) and expert opinion. Functional richness was calculated for each community based on multiple traits (trophic group, activity group, maximum length, gregariousness and diel activity (day/night)) using the package 'FD' in R (Laliberté & Legendre 2010; Laliberté *et al.* 2014).

C2 Supplementary Results

The CTI differences between habitats observed in Fig 3 were not likely a direct result of differences in the overall abundance and species richness in the two

habitats. At the global scale of the analysis, the total abundance and number of species were similar for fishes at barrens and kelp (supplementary figure 1a-b), however, functional richness (supplementary figure 1c) is significantly lower for barrens-associated fishes towards the coldest and warmest edges of temperate latitudes. Trends of individual trophic groups and activity groups were not significant (supplementary figure S2-3).

C3 Supplementary Discussion

Significant functional diversity shifts with land-use change have been described (Flynn *et al.* 2009; Laliberté *et al.* 2010; Clavel *et al.* 2011) and our supplementary analysis finds evidence of reduced functional richness at barrens relative to kelp at the polar-edge of the temperate band (supplementary figure 1c). This trend is evident despite overall species' abundance and richness similarity amongst barrens and kelp, and only small, non-significant changes in individual trophic or activity groups. Perhaps species losses cannot be generalized for barren formation, but instead, barrens homogenize and thereby reduce functional richness, for example through a shift towards more benthic species. The dynamics of functional group changes are also likely variable between regions and sites, and our relatively coarse-scale characterization to detect general trends has almost certainly overlooked some ecologically important signals driven by fish-habitat associations. Nonetheless, a general pattern of functional richness loss is evident at barrens close to the tropics and polar regions, suggesting barrens present different 'environmental filters', with locally varying 'filtering dynamics'. Contributing

to this are an influx in demersal and omnivorous or herbivorous species at the warm and cold edge of temperate barrens (supplementary figure S2-3).

C4 References

Clavel, J., Julliard, R. & Devictor, V. (2011). Worldwide decline of specialist species: toward a global functional homogenization? *Front. Ecol. Environ.*, 9, 222–228.

Flynn, D.F.B., Gogol-Prokurat, M., Nogeire, T., Molinari, N., Richers, B.T., Lin, B.B., *et al.* (2009). Loss of functional diversity under land use intensification across multiple taxa. *Ecol. Lett.*, 12, 22–33.

Laliberté, E. & Legendre, P. (2010). A distance-based framework for measuring functional diversity from multiple traits. *Ecology*, 91, 299–305.

Laliberté, E., Legendre, P. & Shipley, B. (2014). FD: measuring functional diversity from multiple traits, and other tools for functional ecology. *R Packag. version 1.0-12*.

Laliberté, E., Wells, J.A., DeClerck, F., Metcalfe, D.J., Catterall, C.P., Queiroz, C., *et al.* (2010). Land-use intensification reduces functional redundancy and response diversity in plant communities. *Ecol. Lett.*, 13, 76–86.

Lima, F.P. & Wethey, D.S. (2012). Three decades of high-resolution coastal sea surface temperatures reveal more than warming. *Nat. Commun.*, 3, 704.

Stuart-Smith, R.D., Bates, A.E., Lefcheck, J.S., Duffy, J.E., Baker, S.C., Thomson, R.J., *et al.* (2013). Integrating abundance and functional traits reveals new global hotspots of fish diversity. *Nature*, 501, 539–542.

Stuart-Smith, R.D., Brown, C.J., Ceccarelli, D.M. & Edgar, G.J. (2018). Ecosystem restructuring along the Great Barrier Reef following mass coral bleaching. *Nature*, 560, 92–96.

4.8 Appendix D – Supplementary figures and tables for Chapter 4

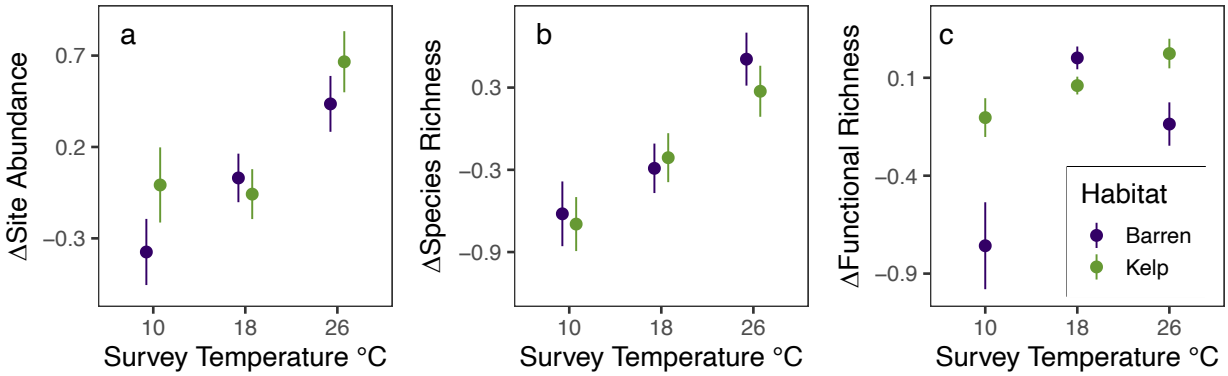

Figure S1 Predicted differences in overall fish species abundance (a), species richness (b) and functional richness (c) relative to the mean contrasted for urchin barrens and kelp beds. Error bars show 95% confidence intervals.

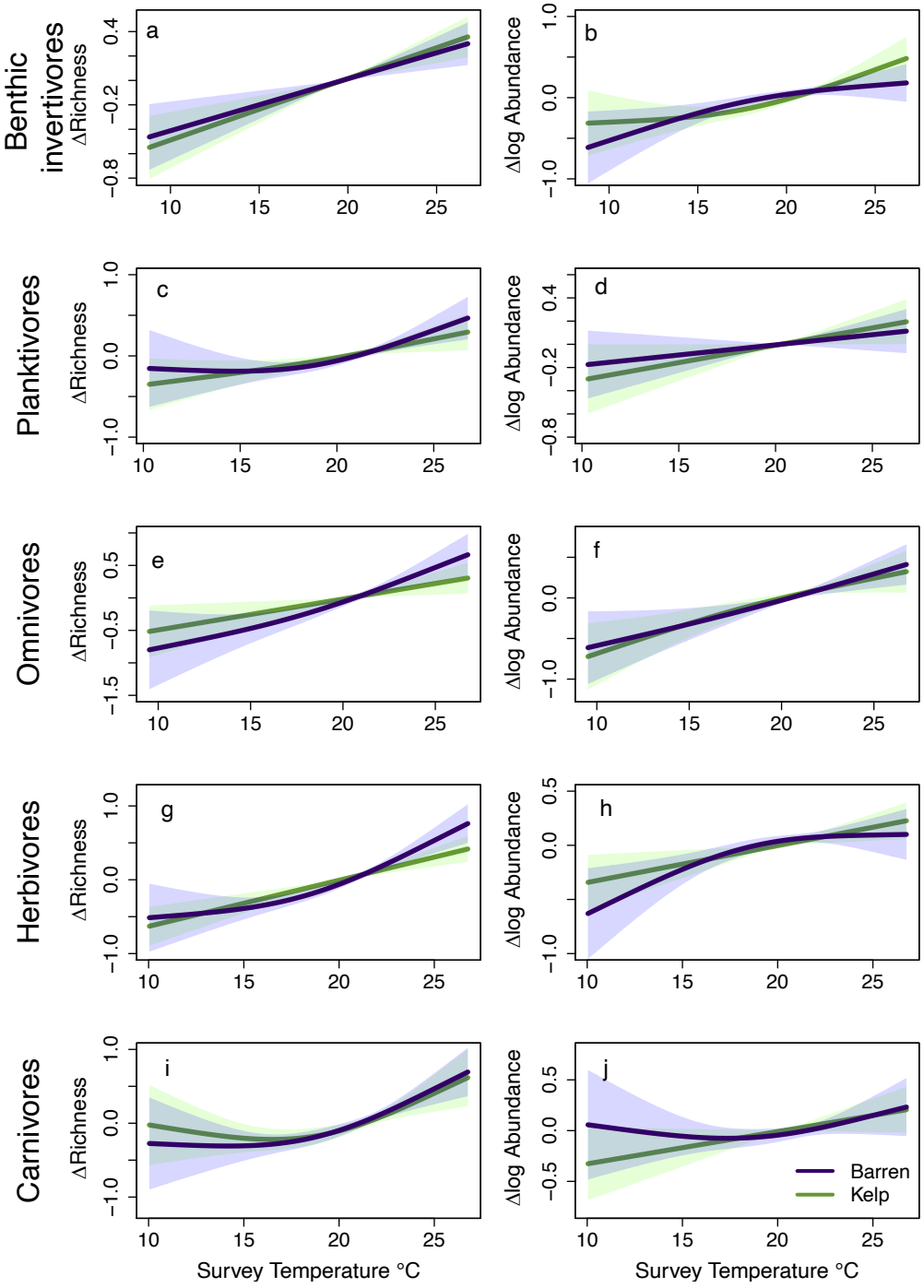

Figure S2 Trends in richness and abundance of fish trophic groups at barrens and kelp sites across temperate rocky reefs. Lines indicate trends of barren vs kelp sites relative to the mean. Trends are not significantly different between barrens and kelp. Shaded areas are 95% confidence intervals predicted by GAMMs. All fixed effects are scaled for coefficient comparison.

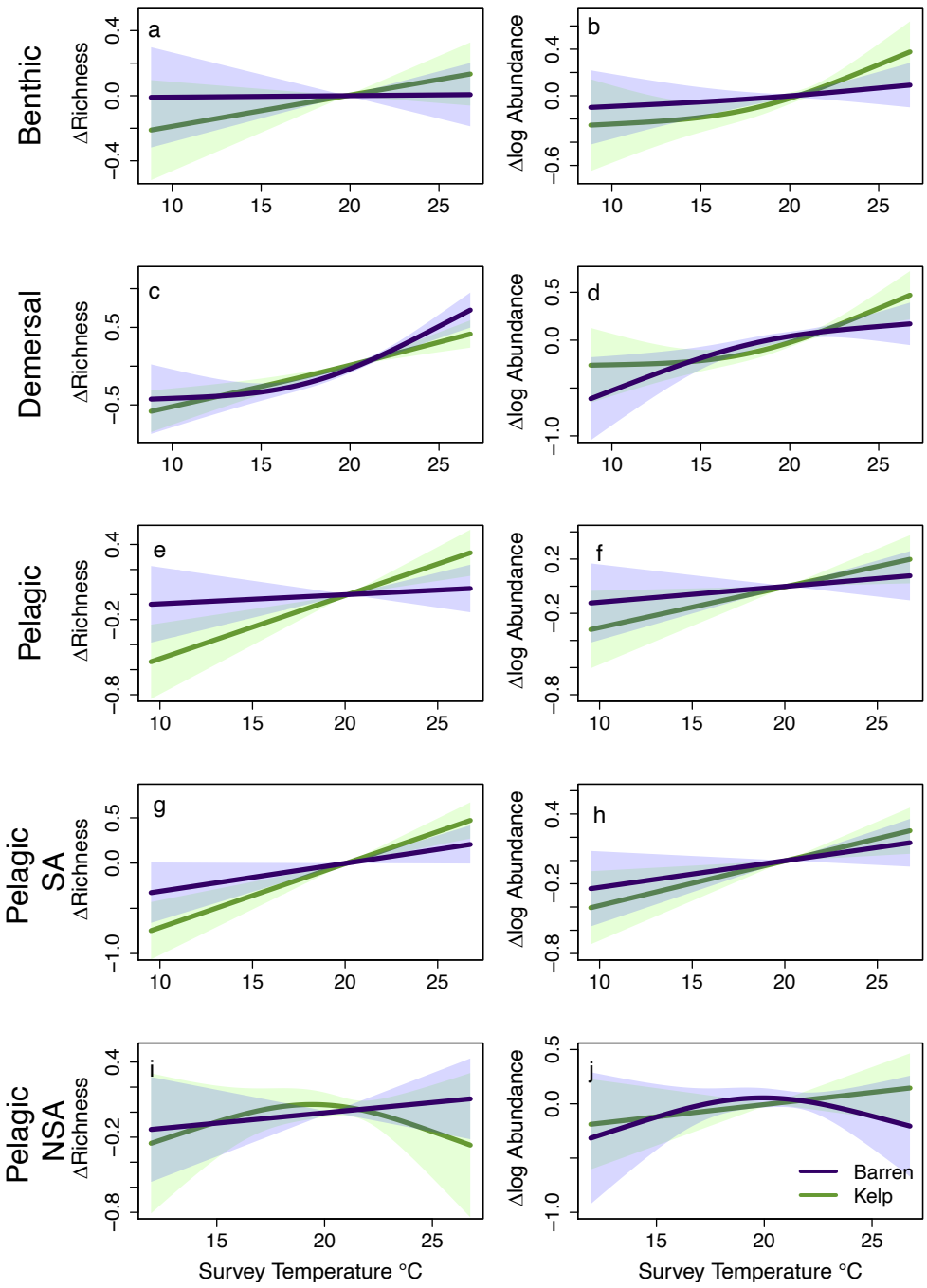

Figure S3 Trends in richness and abundance of fish activity groups at barrens and kelp sites across temperate rocky reefs. Pelagic SA = pelagic site attached, pelagic NSA = pelagic, non-site attached. Lines indicate trends of barren vs kelp sites relative to the mean. Trends are not significantly different between barrens and kelp. Shaded areas are 95% confidence intervals predicted by GAMMs. All fixed effects are scaled for coefficient comparison.

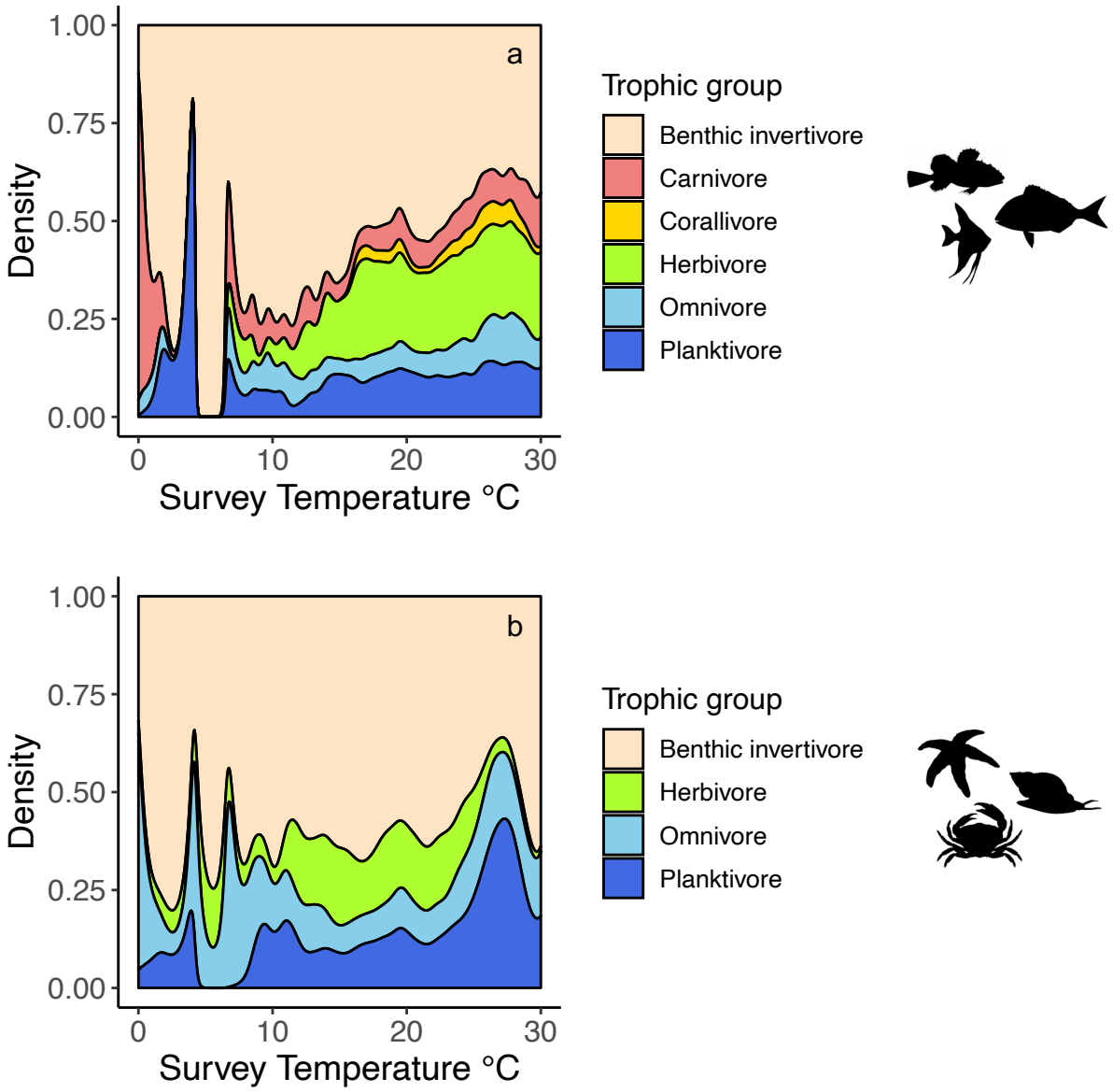

Figure S4 Distribution of trophic groups across temperature (proportion of species counts per trophic group at each survey temperature) in fishes (a) and invertebrates (b). All Reef Life Survey data (data downloaded 25.01.2019, n=12005 surveys, 96 ecoregions) are included here, regardless of latitude or urchin presence to show global functional group distributions.

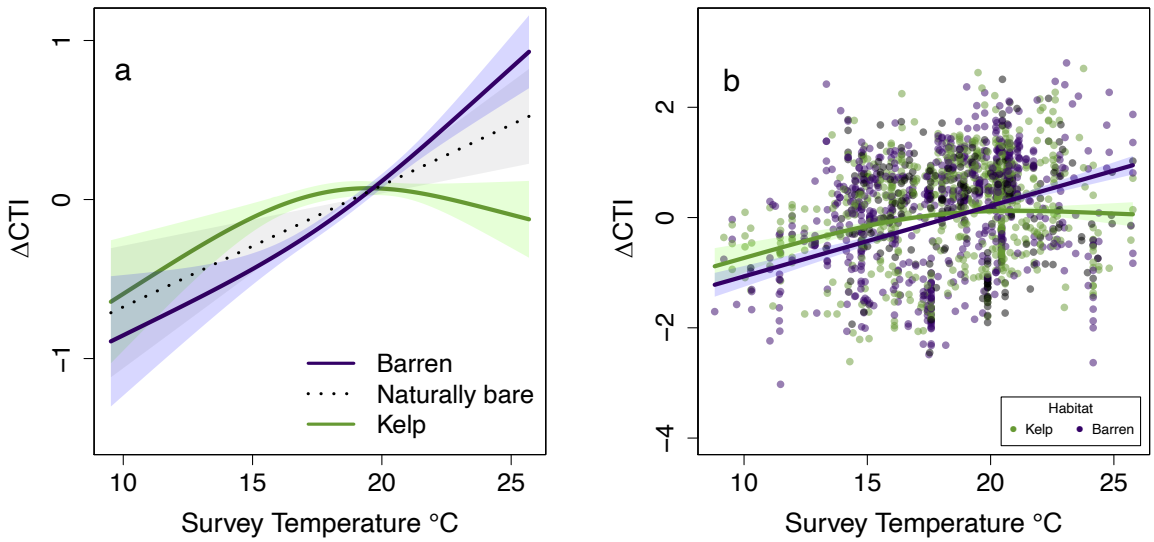

Figure S5 Changes in community temperature index (CTI) for fish communities at urchin barrens, naturally bare areas (sites lacking significant kelp and with low urchin densities) and in kelp beds across temperate rocky reefs spanning a temperature gradient (a). Changes in community temperature index (CTI) for fish communities at urchin barrens and kelp beds with raw data points (b). Trends are modelled for ecoregions with high CTI sensitivity (corresponding to figure 3a in the main text). Lines indicate trends of barrens (purple solid line), naturally bare areas (black dotted line) and kelp (green solid line), relative to the mean. Lines in (b) are the original trends reported in figure 3a of the main manuscript, albeit on a larger y-axis scale to show observed CTI values (data points). Shaded areas are 95% confidence intervals predicted by GAMMs. All fixed effects are scaled for coefficient comparison. See supplementary material table S7 for model summary tables.

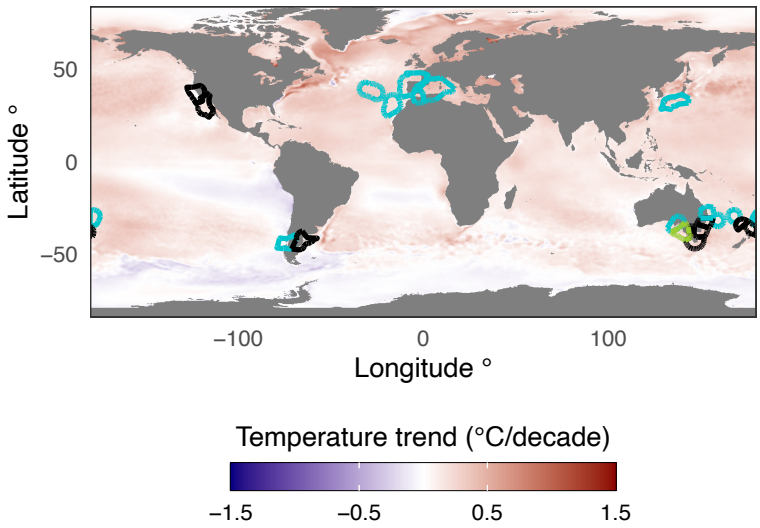

Figure S6 Map of temperate ecoregions (23.5 - 50° latitude, North and South) with shallow rocky reef sites that are highly sensitive to thermal diversity change (black outlined ecoregions; high CTI sensitivity), medium CTI sensitive (turquoise ecoregions) or low CTI sensitive (green ecoregion). Purple-red gradient shows oceanic warming or cooling trends (degrees °C per decade) based on NOAA dOISST.v2.1 (1982-2019) (Lima & Wethey 2012).

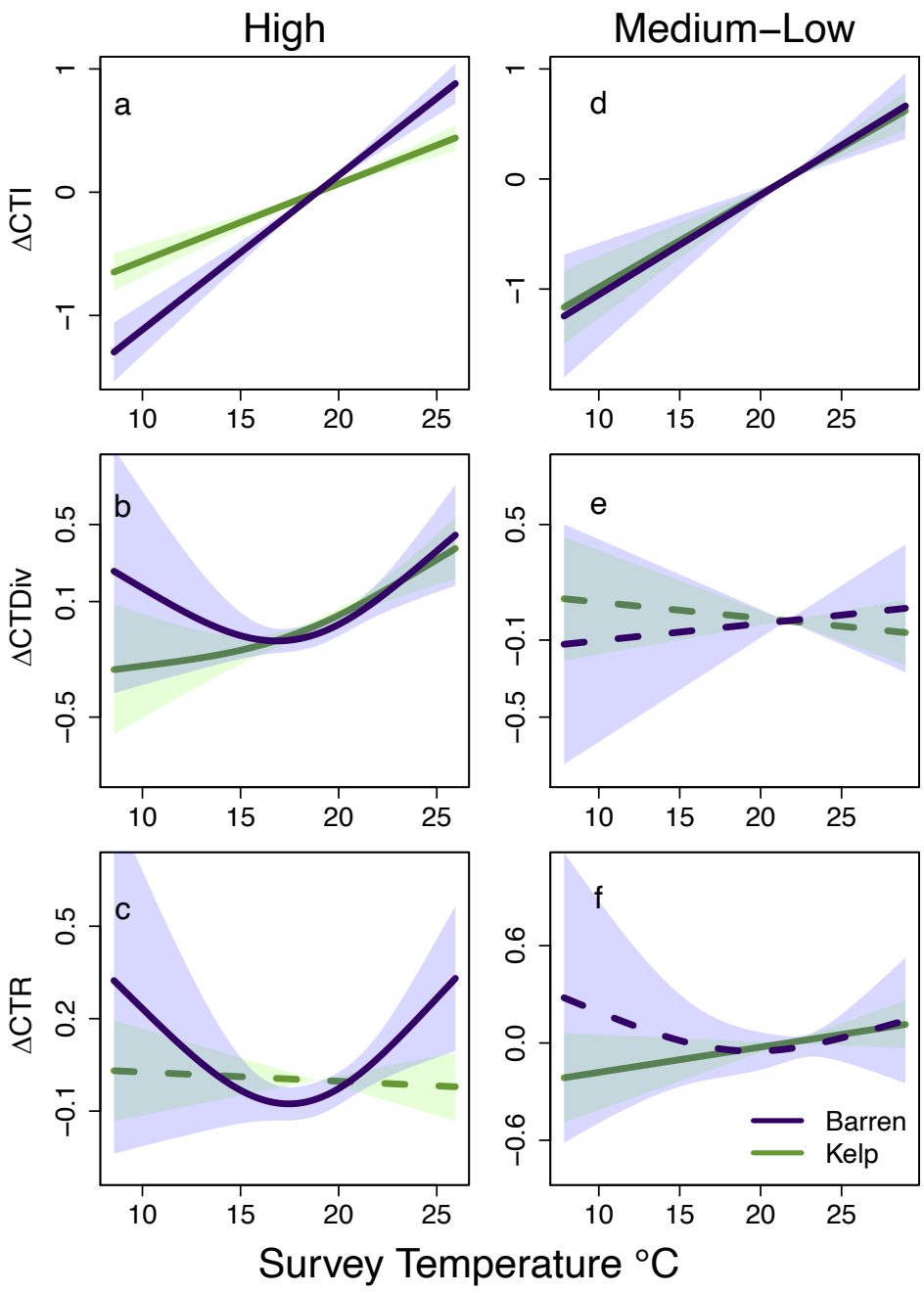

Figure S7 Sensitivity analysis showing changes in CTI, CTDiv and CTR for fish communities at barrens and in kelp beds across temperate rocky reefs are robust to a higher urchin density threshold for classifying sites (3 urchins per m^2). Trends reported in the main manuscript are robust to the higher threshold used here (i.e. compare Figure 3 with supplementary figure S7). We fitted the same model but with a higher urchin density threshold to classify sites for this sensitivity analysis. Lines indicate trends of barren vs kelp sites relative to the mean. Shaded areas

are 95% confidence intervals predicted by GAMMs. All fixed effects are scaled for coefficient comparison.

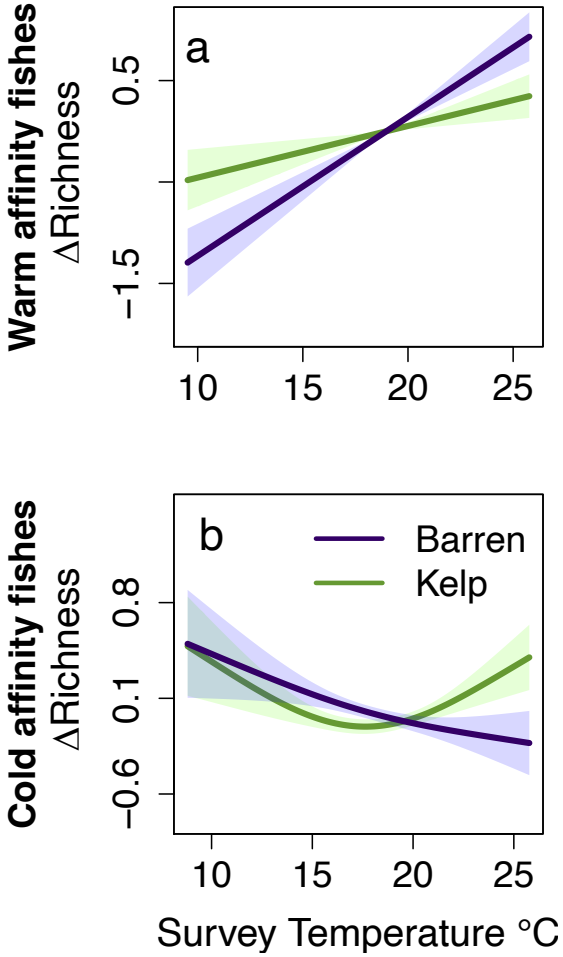

Figure S8 Sensitivity analysis of threshold for selecting species with warmest or coldest thermal midpoint in each ecoregion. Here, upper and lower deciles (10th and 90th percentile) were used to classify fishes as warm or cold affinity. Trends are overall consistent with those reported in the main manuscript (upper and lower quartiles), albeit differences are smaller as fewer fish fall into the warm or cold affinity category when upper and lower deciles are used and fewer samples are available to detect differences.
A and B show changes in richness of fish communities at barrens and in kelp beds across temperate rocky reefs. Lines indicate trends of barren vs kelp sites relative to the mean. Shaded areas are 95% confidence intervals predicted by GAMMs. All fixed effects are scaled for coefficient comparison.

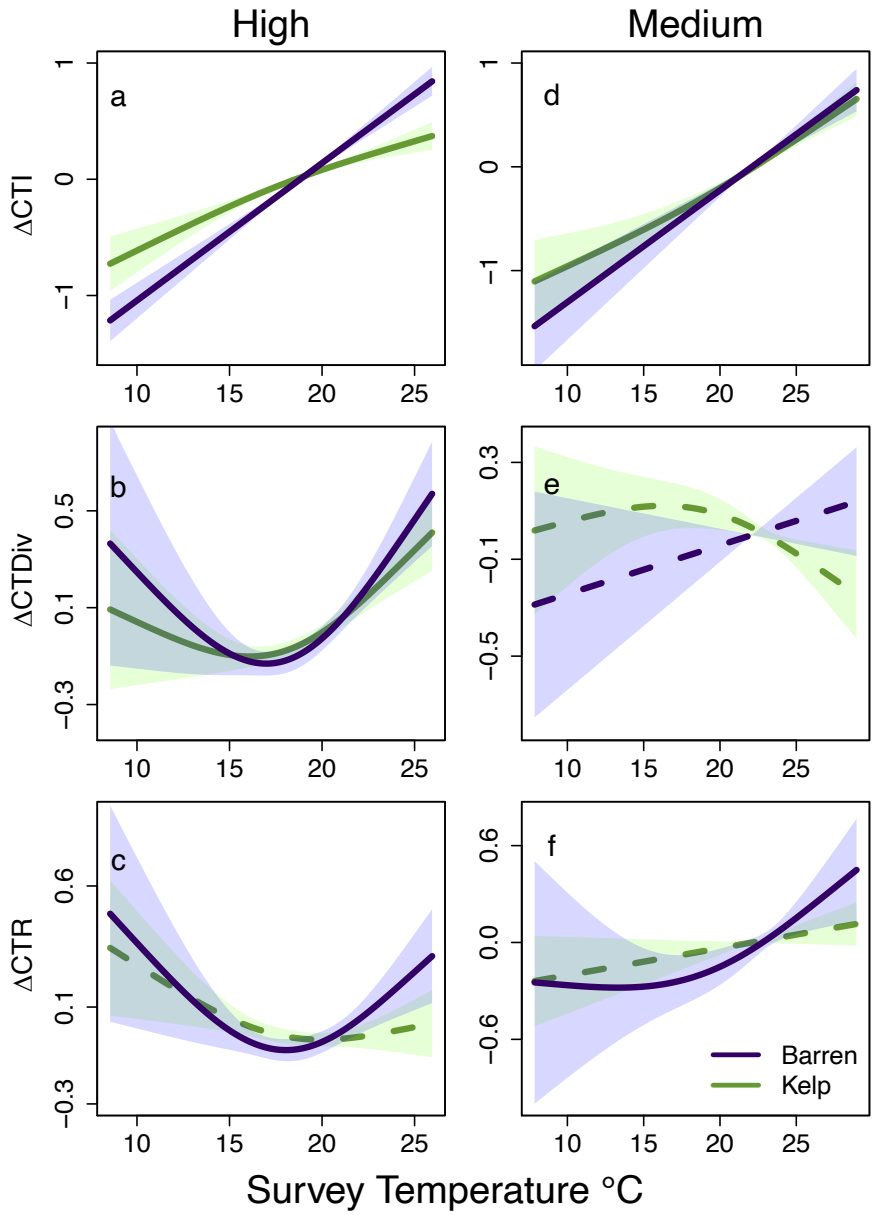

Figure S9 Sensitivity analysis of results to using full dataset (19 ecoregions, 5,996 surveys) with better Northern Hemisphere coverage. Differences in community temperature index (CTI), community thermal diversity (CTDiv) and community thermal range (CTR) for fish communities at barrens and in kelp beds across temperate rocky reefs spanning a temperature gradient. Trends are modelled separately for ecoregions with high CTI sensitivity (left column; a-c) and medium CTI sensitivity (right column, d-f). Lines indicate trends of barrens vs kelp relative to the mean, with solid lines for significant trends, dotted for non-significant. Shaded areas are 95% confidence intervals predicted by GAMMs. All fixed effects

are scaled for coefficient comparison. See supplementary material table S12 for model summary tables.

Table S1 Barren and kelp survey sites included in our analysis. Only sites in temperate latitudes (23.5 – 50.0° latitude, North and South) where kelp forests and barren forming sea urchins occur were included.

Ecoregion	# of kelp surveys	# of barren surveys	Total # surveys	Depth range of surveys (m)	Temporal span
Alboran Sea	8	25	33	2-10	2013-14
Azores Canaries Madeira	14	8	22	5-18	2011-15
Bassian	360	70	430	1-24	2008-18
Cape Howe	370	258	628	1-20	2008-18
Central Kuroshio Current	7	4	11	3-6	2010-12
Kermadec Island	4	10	14	7-19	2012-13
Lord Howe and Norfolk Islands	82	156	238	1-20	2006-18
Manning-Hawkesbury	135	211	346	1-29	2008-18
North Patagonian Gulfs	5	10	15	4-18	2012
Northeastern New Zealand	78	33	111	2-22	2008-12
Northern California	5	7	12	7-14	2010
South Australian Gulfs	302	7	309	2-12	2008-18
Three Kings-North Cape	9	2	11	6-15	2012
Tweed-Moreton	6	63	69	4-15	2008-18
Western Mediterranean	15	7	22	4-18	2015

Table S2 Urchin species observed across temperate RLS transects. Species are scored as barren forming or non-barren forming (grey-shaded), with only surveys with barren formers included in analysis. Urchin are scored by expert opinion and based on the literature (numbers in parentheses in the final column provide relevant references confirming species is a barren former). Maximum survey abundance refers to the highest number of individual urchins recorded during a single survey.

Species name	Genus	# Survey occurrences	Max urchin abundance (# per survey)	Barren former (Y/N)
Arbacia dufresnii	Arbacia	45	4110	Y
Arbacia lixula	Arbacia	430	1056	Y (1)
Arbacia stellata	Arbacia	1	2	Y
Centrostephanus rodgersii	Centrostephanus	3311	2408	Y (1)
Centrostephanus tenuispinus	Centrostephanus	296	229	Y
Diadema africanum	Diadema	67	535	Y
Diadema antillarum	Diadema	204	950	Y (1)
Diadema mexicanum	Diadema	482	905	Y (2)
Diadema palmeri	Diadema	5	3	Y (3)
Diadema savignyi	Diadema	801	1690	Y (3)
Diadema setosum	Diadema	330	889	Y (3)
Echinometra mathaei	Echinometra	1263	2300	Y
Echinometra vanbrunti	Echinometra	115	2074	Y
Echinus esculentus	Echinus	30	7895	Y (4)
Eucidaris thouarsii	Eucidaris	177	580	Y
Evechinus chloroticus	Evechinus	161	943	Y (1)
Heliocidaris crassispina	Heliocidaris	18	1433	Y (5)
Heliocidaris erythrogramma	Heliocidaris	1932	3398	Y (1)
Heliocidaris tuberculata	Heliocidaris	536	850	Y
Loxechinus albus	Loxechinus	22	2720	Y (1)
Mesocentrotus franciscanus	Mesocentrotus	56	1090	Y (6)
Mesocentrotus nudus	Mesocentrotus	15	754	Y
Paracentrotus lividus	Paracentrotus	506	971	Y (1)
Pseudechinus magellanicus	Pseudechinus	15	1200	Y
Pseudocentrotus depressus	Pseudocentrotus	4	6	Y
Strongylocentrotus droebachiensis	Strongylocentrotus	37	12670	Y (1)
Strongylocentrotus intermedius	Strongylocentrotus	6	815	Y
Strongylocentrotus pallidus	Strongylocentrotus	3	435	Y

Strongylocentrotus purpuratus	Strongylocentrotus	48	8050	Y (1)
Temnopleurus alexandri	Temnopleurus	12	8	Y
Temnopleurus reevesii	Temnopleurus	1	1	Y
Temnopleurus toreumaticus	Temnopleurus	12	14	Y
Tripneustes depressus	Tripneustes	79	42	Y
Tripneustes gratilla	Tripneustes	479	671	Y (7)
Tripneustes ventricosus	Tripneustes	7	201	Y
Amblypneustes elevatus	Amblypneustes	37	8	N
Amblypneustes grandis	Amblypneustes	2	1	N
Amblypneustes ovum	Amblypneustes	170	88	N
Amblypneustes pallidus	Amblypneustes	4	11	N
Amblypneustes spp.	Amblypneustes	46	9	N
Asthenosoma varium	Asthenosoma	1	1	N
Astropyga pulvinata	Astropyga	22	6	N
Astropyga spp.	Astropyga	1	1	N
Austrocidaris canaliculata	Austrocidaris	4	1150	N
Breynia australasiae	Breynia	3	7	N
Centrostephanus coronatus	Centrostephanus	158	650	N
Chondrocidaris gigantea	Chondrocidaris	3	4	N
Echinocardium spp.	Echinocardium	1	1	N
Echinometra lucunter	Echinometra	36	110	N
Echinometra spp.	Echinometra	3	276	N
Echinometra viridis	Echinometra	104	2850	N
Echinoneus cyclostomus	Echinoneus	1	1	N
Echinostrephus aciculatus	Echinostrephus	1092	2200	N
Echinostrephus molaris	Echinostrephus	52	576	N
Echinothrix calamaris	Echinothrix	158	281	N
Echinothrix diadema	Echinothrix	76	70	N
Eucidaris metularia	Eucidaris	8	4	N
Eucidaris tribuloides	Eucidaris	37	25	N
Goniocidaris impressa	Goniocidaris	24	97	N
Goniocidaris spp.	Goniocidaris	2	3	N
Goniocidaris tubaria	Goniocidaris	231	42	N
Hesperocidaris asteriscus	Hesperocidaris	227	260	N
Heterocentrotus mamillatus	Heterocentrotus	4	1	N
Heterocentrotus mammillatus	Heterocentrotus	20	78	N
Heterocentrotus trigonarius	Heterocentrotus	1	40	N
Holopneustes inflatus	Holopneustes	37	18	N
Holopneustes porosissimus	Holopneustes	97	21	N

Holopneustes purpurascens	Holopneustes	48	80	N
Lytechinus pictus	Lytechinus	9	43	N
Lytechinus williamsi	Lytechinus	21	138	N
Mespilia globulus	Mespilia	3	12	N
Microcyphus annulatus	Microcyphus	2	2	N
Parasalenia gratiosa	Parasalenia	2	391	N
Parechinus angulosus	Parechinus	24	3970	N
Phyllacanthus imperialis	Phyllacanthus	27	26	N
Phyllacanthus irregularis	Phyllacanthus	556	33	N
Phyllacanthus longispinus	Phyllacanthus	43	26	N
Phyllacanthus parvispinus	Phyllacanthus	1277	244	N
Prionocidaris australis	Prionocidaris	1	1	N
Prionocidaris callista	Prionocidaris	88	46	N
Pseudoboletia indiana	Pseudoboletia	114	107	N
Pseudoboletia maculata	Pseudoboletia	2	4	N
Salmacis sphaeroides	Salmacis	14	63	N
Sphaerechinus granularis	Sphaerechinus	189	170	N
Sterechinus neumayeri	Sterechinus	8	3370	N
Toxopneustes pileolus	Toxopneustes	33	72	N
Toxopneustes roseus	Toxopneustes	64	60	N

Table S3 Species thermal affinity was classified as relatively warm (above upper (75^{th}) quartile) or cold (below lower (25^{th}) quartile). Thresholds were individually calculated for each ecoregional species pool to identify the relatively warmest and coldest species in each region.

	Fishes	
Ecoregion	**Lower Quartile Threshold °C**	**Upper Quartile Threshold °C**
Alboran Sea	16.39	17.97
Azores Canaries Madeira	18.80	24.14
Bassian	15.87	18.49
Cape Howe	18.65	19.85
Central Kuroshio Current	22.46	23.37
Kermadec Island	19.79	21.38
Lord Howe and Norfolk Islands	21.38	22.49
Manning-Hawkesbury	19.68	20.36
North Patagonian Gulfs	12.69	13.17
Northeastern New Zealand	14.81	18.86
Northern California	16.78	22.54
South Australian Gulfs	17.92	18.61
Three Kings-North Cape	15.18	18.38
Tweed-Moreton	20.28	22.76
Western Mediterranean	16.35	17.67

Table S4 Summary table for simulation model of response of fish CTI to the distribution of species' thermal properties (diversity of STI (sdSTI) and species thermal ranges (STR)), habitat (barrens vs kelp) and temperature. We fit a generalized additive mixed model (GAMM, mgcv package) with the function gamm in R. Random effects of site nested in latitude nested in ecoregion are included to account for the spatial structure of the data. 's' indicates fixed effects (Depth of survey) modelled with penalized regression splines (GAM component), and sdSTI, STR, temperature and habitat as covariates (fixed effect, LME component). Interaction effects of temperature*habitat*sdSTI and temperature*habitat*STR were also included in the model. AIC = Akaine information criterion; Std. error = standard error; Edf = Estimated degrees of freedom; Ref. df = reference degree of freedom (prior to deductions).

Random effects

~1| Ecoregion:	0.194
~1| Ecoregion/Latitude:	0.615
~1| Ecoregion/Latitude/Site Code:	0.610
Residual:	0.580
AIC:	12683.38

LME	**Estimated value**	**Std. Error**	**DF**	**t-value**	**p-value**
Intercept	-3.343	1.133	4605	-2.950	0.003
STR	-0.003	0.091	16	-0.027	0.978
sdSTI	0.665	0.408	16	1.632	0.122
Temperature	0.192	0.055	4605	3.494	<0.001
Kelp	0.050	0.994	4605	0.051	0.959
Temperature*Kelp	-0.037	0.048	4605	-0.779	0.436
STR*Temperature	-0.003	0.005	4605	0.682	0.495
STR*Kelp	-0.067	0.070	4605	-0.995	0.340
sdSTI*Temperature	-0.024	0.018	4605	-1.309	0.191
sdSTI*Kelp	0.539	0.315	4605	1.712	0.087
STR*Temperature*Kelp	0.007	0.004	4605	1.761	0.078
sdSTI*Temperature*Kelp	-0.034	0.015	4605	-2.291	0.022
Depth	-0.265	0.171	4605	-1.552	0.121
GAM	**Edf**	**Ref. df**		**F-value**	**p-value**
s(Depth)	6.02	6.02		9.586	<0.001

Table S5 Summary table for statistical tests of response of fish CTI (a,b), CTDiv (c,d) and CTR (e,f) in ecoregions that are highly sensitive (a, c, e) or medium sensitive (b, d, f) to CTI change. We fit generalized additive mixed models (GAMM, mgcv package) with the function gamm in R. Random effects of site nested in latitude nested in ecoregion are included to account for the spatial structure of the data. 's' indicates fixed effects (Temperature at time of survey) modelled with penalized regression splines (GAM component) for barren and kelp sites, and a Depth covariate (fixed effect, LME component). Fixed effects were scaled for coefficient comparison. AIC = Akaine information criterion; Std. error = standard error; Edf = Estimated degrees of freedom; Ref. df = reference degree of freedom (prior to deductions). We ran models with different distribution families (gaussian, quasipoisson) and transformed response data to ensure patterns are consistent. Separate models for barrens and kelp were also fit to check for consistent patterns.

a) Fish CTI in Ecoregions with High CTI sensitivity

Random effects	
~1| Ecoregion:	0.264
~1| Ecoregion/Latitude:	0.744
~1| Ecoregion/Latitude/Site Code:	0.418
Residual:	0.530
AIC:	3016.67

LME	**Estimated value**	**Std. Error**	**DF**	**t-value**	**p-value**
Intercept	-0.105	0.202	994	-0.521	0.603
Depth	0.035	0.024	994	1.476	0.140
GAM	**Edf**	**Ref. df**		**F- value**	**p-value**
s(Temperature:Kelp)	1.92	1.92		12.98	<0.001
s(Temperature:Barren)	1.00	1.00		127.31	<0.001

b) Fish CTI in Ecoregions with Medium CTI sensitivity

Random effects	
~1| Ecoregion:	0.207
~1| Ecoregion/Latitude:	0.445
~1| Ecoregion/Latitude/Site Code:	0.636
Residual:	0.517
AIC:	1496.28

LME	**Estimated value**	**Std. Error**	**DF**	**t-value**	**p-value**
Intercept	0.001	0.140	480	0.007	0.995

Depth	-0.045	0.040	480	-1.140	0.255
GAM	**Edf**	**Ref. df**		**F-value**	**p-value**
s(Temperature:Kelp)	1.00	1.00		6.93	0.009
s(Temperature:Barren)	1.00	1.00		37.45	<0.001

c) Fish CTDiv in High CTI sensitivity ecoregions

Random effects

~1| Ecoregion:	0.001
~1| Ecoregion/Latitude:	0.549
~1| Ecoregion/Latitude/Site Code:	0.410
Residual:	0.695
AIC:	3686.02

LME	**Estimated value**	**Std. Error**	**DF**	**t-value**	**p-value**
Intercept	0.127	0.129	994	0.979	0.327
Depth	-0.108	0.028	994	-3.830	<0.001
GAM	**Edf**	**Ref. df**		**F-value**	**p-value**
s(Temperature:Kelp)	1.37	1.37		4.59	0.048
s(Temperature:Barren)	1.86	1.86		4.04	0.037

d) Fish CTDiv in Medium CTI sensitivity ecoregions

Random effects

~1| Ecoregion:	0.144
~1| Ecoregion/Latitude:	0.281
~1| Ecoregion/Latitude/Site Code:	0.595
Residual:	0.753
AIC:	1887.06

LME	**Estimated value**	**Std. Error**	**DF**	**t-value**	**p-value**
Intercept	0.002	0.108	480	0.017	0.986
Depth	0.025	0.049	480	0.509	0.612
	Edf	**Ref. df**		**F-value**	**p-value**
s(Temperature:Kelp)	1.23	1.23		4.07	0.057
s(Temperature:Barren)	1.47	1.47		0.39	0.673

e) Fish CTR in High CTI sensitivity ecoregions

Random effects

~1| Ecoregion:	0.032
~1| Ecoregion/Latitude:	0.837
~1| Ecoregion/Latitude/Site Code:	0.307
Residual:	0.678
AIC:	3524.03

LME	**Estimated value**	**Std. Error**	**DF**	**t-value**	**p-value**
Intercept	0.282	0.189	994	1.489	1.367
Depth	-0.076	0.026	994	-2.960	0.003
GAM	**Edf**	**Ref. df**		**F- value**	**p-value**
s(Temperature:Kelp)	1.40	1.40		3.55	0.027
s(Temperature:Barren)	1.86	1.86		2.68	0.060

f) Fish CTR in Medium CTI sensitivity ecoregions

Random effects

~1| Ecoregion:	0.157
~1| Ecoregion/Latitude:	0.277
~1| Ecoregion/Latitude/Site Code:	0.592
Residual:	0.657
AIC:	1728.16

LME	**Estimated value**	**Std. Error**	**DF**	**t-value**	**p-value**
Intercept	-0.157	0.108	480	-1.457	0.146
Depth	-0.091	0.045	480	-2.021	0.044
GAM	**Edf**	**Ref. df**		**F- value**	**p-value**
s(Temperature:Kelp)	1.29	1.29		4.70	0.016
s(Temperature:Barren)	1.52	1.52		3.38	0.136

Table S6 Summary table for statistical tests of response of warm- and cold- affinity fishes (a,b). Differences in warm- and cold- affinity fishes was modelled for ecoregions that are highly sensitive to CTI change, where significant differences in community thermal diversity were found. We fit generalized additive mixed models (GAMM, mgcv package) with the function gamm in R. Random effects of site nested in latitude nested in ecoregion are included to account for the spatial structure of the data. 's' indicates fixed effects (Temperature at time of survey) modelled with penalized regression splines (GAM component) for barren and kelp sites, and a Depth covariate (fixed effect, LME component). Fixed effects were scaled for coefficient comparison. AIC = Akaine information criterion; Std. error = standard error; Edf = Estimated degrees of freedom; Ref. df = reference degree of freedom (prior to deductions). We ran models with different distribution families (gaussian, quasipoisson) and transformed response data to ensure patterns are consistent. Separate models for barrens and kelp were also fit to check for consistent patterns.

a) Richness of warm affinity fishes

Random effects

~1| Ecoregion:	1.140
~1| Ecoregion/Latitude:	0.623
~1| Ecoregion/Latitude/Site Code:	0.368
Residual:	0.563
AIC:	2757.90

LME	**Estimated value**	**Std. Error**	**DF**	**t-value**	**p-value**
Intercept	0.187	0.464	833	0.403	0.687
Depth	-0.018	0.026	833	-0.693	0.488
GAM	**Edf**	**Ref. df**		**F-value**	**p-value**
s(Temperature:Kelp)	1.00	1.00		22.39	<0.001
s(Temperature:Barren)	1.00	1.00		64.91	<0.001

b) Richness of cold affinity fishes

Random effects

~1| Ecoregion:	<0.001
~1| Ecoregion/Latitude:	0.968
~1| Ecoregion/Latitude/Site Code:	0.346
Residual:	0.501
AIC:	2104.01

LME	**Estimated value**	**Std. Error**	**DF**	**t-value**	**p-value**
Intercept	0.260	0.222	730	1.173	0.241
Depth	-0.008	0.024	730	-0.340	0.734

GAM	Edf	Ref. df	F-value	p-value
s(Temperature:Kelp)	1.82	1.82	3.23	0.024
s(Temperature:Barren)	1.56	1.56	40.36	<0.001

Table S7 Summary table for statistical tests of response of fish CTI at urchin barren, naturally bare and kelp covered sites, in ecoregions that are highly sensitive to CTI change. We fit generalized additive mixed models (GAMM, mgcv package) with the function gamm in R. Random effects of site nested in latitude nested in ecoregion are included to account for the spatial structure of the data. 's' indicates fixed effects (Temperature at time of survey) modelled with penalized regression splines (GAM component) for barren and kelp sites, and a Depth covariate (fixed effect, LME component). Fixed effects were scaled for coefficient comparison. AIC = Akaine information criterion; Std. error = standard error; Edf = Estimated degrees of freedom; Ref. df = reference degree of freedom (prior to deductions). We ran models with different distribution families (gaussian, quasipoisson) and transformed response data to ensure patterns are consistent. Separate models for barrens and kelp were also fit to check for consistent patterns.

a) Fish CTI in Ecoregions with High CTI sensitivity at urchin barren, naturally bare and kelp covered sites

Random effects

~1| Ecoregion:	0.070
~1| Ecoregion/Latitude:	0.610
~1| Ecoregion/Latitude/Site Code:	0.325
Residual:	0.533
AIC:	2374.65

LME	Estimated value	Std. Error	DF	t-value	p-value
Intercept	0.023	0.151	832	0.156	0.876
Depth	-0.006	0.023	832	-0.249	0.804
GAM	**Edf**	**Ref. df**		**F-value**	**p-value**
s(Temperature:Kelp)	1.89	1.89		4.17	0.009
s(Temperature:Barren)	1.62	1.62		70.32	<0.001
s(Temperature:NaturallyBare)	1.00	1.00		12.29	<0.001

Table S8 Summary table for statistical tests of response of fish (1a-c) abundance, species richness and functional richness. We fit generalized additive mixed models (GAMM, mgcv package) with the function gamm in R. Random effects of site nested in latitude nested in ecoregion are included to account for the spatial structure of the data. 's' indicates fixed effects (Temperature at time of survey) modelled with penalized regression splines (GAM component) for barren and kelp sites, and a Depth covariate (fixed effect, LME component). Fixed effects were scaled for coefficient comparison. AIC = Akaine information criterion; Std. error = standard error; Edf = Estimated degrees of freedom; Ref. df = reference degree of freedom (prior to deductions). We ran models with different distribution families (gaussian, quasipoisson) and transformed response data to ensure patterns are consistent.

a) Total abundance of fishes at site

Random effects

~1| Ecoregion:	0.357
~1| Ecoregion/Latitude:	0.473
~1| Ecoregion/Latitude/Site Code:	0.600
Residual:	0.716
AIC:	5785.84

LME	**Estimated value**	**Std. Error**	**DF**	**t-value**	**p-value**
Intercept	0.058	0.131	1477	0.443	0.657
Depth	0.069	0.027	1477	2.551	0.011
GAM	**Edf**	**Ref. df**		**F-value**	**p-value**
s(Temperature:Kelp)	1.90	1.90		16.58	<0.001
s(Temperature:Barren)	1.00	1.00		15.76	<0.001

b) Species richness of fishes at site

Random effects

~1| Ecoregion:	0.648
~1| Ecoregion/Latitude:	0.263
~1| Ecoregion/Latitude/Site Code:	0.380
Residual:	0.559
AIC:	4501.64

LME	**Estimated value**	**Std. Error**	**DF**	**t-value**	**p-value**
Intercept	-0.177	0.178	1477	-0.996	0.319
Depth	0.079	0.020	1477	4.089	0.000
GAM	**Edf**	**Ref. df**		**F-value**	**p-value**

s(Temperature:Kelp)	1.00	1.00	48.59	<0.001
s(Temperature:Barren)	1.81	1.81	45.84	<0.001

c) Functional richness of fishes at site

Random effects

~1| Ecoregion:	0.079
~1| Ecoregion/Latitude:	0.061
~1| Ecoregion/Latitude/Site Code:	0.395
Residual:	0.898
AIC:	6247.34

LME	**Estimated value**	**Std. Error**	**DF**	**t-value**	**p-value**
Intercept	0.016	0.040	1460	0.393	0.694
Depth	0.097	0.025	1460	3.891	<0.001
GAM	**Edf**	**Ref. df**		**F-value**	**p-value**
s(Temperature:Kelp)	1.00	1.00		4.71	0.030
s(Temperature:Barren)	1.94	1.94		7.93	<0.001

Table S9 Summary table for statistical tests of response of fish (1a-j) trophic groups. We fit generalized additive mixed models (GAMM, mgcv package) with the function gamm in R. Random effects of site nested in latitude nested in ecoregion are included to account for the spatial structure of the data. 's' indicates fixed effects (Temperature at time of survey) modelled with penalized regression splines (GAM component) for barren and kelp sites, and a Depth covariate (fixed effect, LME component). Fixed effects were scaled for coefficient comparison. AIC = Akaine information criterion; Std. error = standard error; Edf = Estimated degrees of freedom; Ref. df = reference degree of freedom (prior to deductions). We ran models with different distribution families (gaussian, quasipoisson) and transformed response data to ensure patterns are consistent. Separate models for barrens and kelp were also fit to check for consistent patterns.

1) FISHES

a) Trends in richness of benthic invertivores at barren and kelp sites

Random effects

~1| Ecoregion:	0.595
~1| Ecoregion/Latitude:	0.320
~1| Ecoregion/Latitude/Site Code:	0.414
Residual:	0.615
AIC:	3824.66

LME	Estimated value	Std. Error	DF	t-value	p-value
Intercept	-0.158	0.175	1092	-0.904	0.366
Depth	0.077	0.024	1092	3.226	0.001
GAM	**Edf**	**Ref. df**		**F-value**	**p-value**
s(Temperature:Kelp)	1.00	1.00		18.16	<0.001
s(Temperature:Barren)	1.00	1.00		11.86	<0.001

b) Trends in richness of planktivores at barren and kelp sites

Random effects

~1| Ecoregion:	0.723
~1| Ecoregion/Latitude:	0.156
~1| Ecoregion/Latitude/Site Code:	0.326
Residual:	0.668
AIC:	3179.90

LME	Estimated value	Std. Error	DF	t-value	p-value
Intercept	-0.116	0.207	871	-0.560	0.576
Depth	0.065	0.025	871	2.594	0.010
GAM	**Edf**	**Ref. df**		**F- value**	**p-value**
s(Temperature:Kelp)	1.24	1.24		7.403	0.008
s(Temperature:Barren)	1.72	1.72		9.91	0.003

c) Trends in richness of omnivores at barren and kelp sites

Random effects

~1| Ecoregion:	0.380
~1| Ecoregion/Latitude:	0.236
~1| Ecoregion/Latitude/Site Code:	0.327
Residual:	0.812
AIC:	2672.70

LME	Estimated value	Std. Error	DF	t-value	p-value
Intercept	-0.020	0.139	601	-0.143	0.886
Depth	0.019	0.035	601	0.530	0.596
GAM	**Edf**	**Ref. df**		**F-value**	**p-value**
s(Temperature:Kelp)	1.00	1.00		6.68	0.010
s(Temperature:Barren)	1.43	1.43		15.24	<0.001

d) Trends in richness of herbivores at barren and kelp sites

Random effects

~1| Ecoregion:	0.544
~1| Ecoregion/Latitude:	0.178
~1| Ecoregion/Latitude/Site Code:	0.411
Residual:	0.670
AIC:	3696.25

LME	Estimated value	Std. Error	DF	t-value	p-value
Intercept	-0.264	0.168	1013	-1.572	0.116
Depth	-0.05	0.026	1013	-1.855	0.064
GAM	**Edf**	**Ref. df**		**F-value**	**p-value**
s(Temperature:Kelp)	1.00	1.00		22.98	<0.001
s(Temperature:Barren)	1.78	1.78		28.82	<0.001

e) Trends in richness of carnivores at barren and kelp sites

Random effects

~1| Ecoregion:	0.488
~1| Ecoregion/Latitude:	0.319
~1| Ecoregion/Latitude/Site Code:	0.246
Residual:	0.801
AIC:	2791.51

LME	Estimated value	Std. Error	DF	t-value	p-value
Intercept	0.020	0.155	622	0.131	0.896
Depth	0.173	0.032	622	5.359	0.000
GAM	**Edf**	**Ref. df**		**F-value**	**p-value**
s(Temperature:Kelp)	1.82	1.82		7.03	0.011
s(Temperature:Barren)	1.77	1.77		14.05	<0.000

f) Trends in abundance of benthic invertivores at barren and kelp sites

Random effects

~1| Ecoregion:	0.196
~1| Ecoregion/Latitude:	0.340
~1| Ecoregion/Latitude/Site Code:	0.552
Residual:	0.639
AIC:	4103.56

LME	Estimated value	Std. Error	DF	t-value	p-value
Intercept	-0.075	0.092	1092	-0.820	0.412

Depth	0.035	0.027	1092	1.318	0.188
GAM	**Edf**	**Ref. df**		**F-value**	**p-value**
s(Temperature:Kelp)	1.67	1.67		11.75	0.001
s(Temperature:Barren)	1.55	1.55		4.58	0.010

g) Trends in abundance of planktivores at barren and kelp sites

Random effects

~1| Ecoregion:	0.779
~1| Ecoregion/Latitude:	0.268
~1| Ecoregion/Latitude/Site Code:	0.404
Residual:	0.667
AIC:	3268.53

LME	**Estimated value**	**Std. Error**	**DF**	**t-value**	**p-value**
Intercept	-0.016	0.226	871	-0.07	0.943
Depth	0.179	0.027	871	6.567	0.000
GAM	**Edf**	**Ref. df**		**F- value**	**p-value**
s(Temperature:Kelp)	1.00	1.00		4.03	0.045
s(Temperature:Barren)	1.00	1.00		1.42	0.233

h) Trends in abundance of omnivores at barren and kelp sites

Random effects

~1| Ecoregion:	0.639
~1| Ecoregion/Latitude:	0.266
~1| Ecoregion/Latitude/Site Code:	0.399
Residual:	0.617
AIC:	2260.98

LME	**Estimated value**	**Std. Error**	**DF**	**t-value**	**p-value**
Intercept	0.142	0.209	601	0.679	0.497
Depth	-0.036	0.030	601	-1.203	0.230
GAM	**Edf**	**Ref. df**		**F-value**	**p-value**
s(Temperature:Kelp)	1.34	1.34		8.80	<0.001
s(Temperature:Barren)	1.15	1.15		10.48	0.001

i) Trends in abundance of herbivores at barren and kelp sites

Random effects

~1| Ecoregion:	0.690

~1| Ecoregion/Latitude:	0.344
~1| Ecoregion/Latitude/Site Code:	0.502
Residual:	0.567
AIC:	3403.47

LME	**Estimated value**	**Std. Error**	**DF**	**t-value**	**p-value**
Intercept	-0.142	0.213	1013	-0.668	0.505
Depth	-0.077	0.026	1013	-3.017	0.003
GAM	**Edf**	**Ref. df**		**F-value**	**p-value**
s(Temperature:Kelp)	1.00	1.00		7.24	0.007
s(Temperature:Barren)	1.72	1.72		4.10	0.012

j) Trends in abundance of carnivores at barren and kelp sites

Random effects

~1| Ecoregion:	0.393
~1| Ecoregion/Latitude:	0.307
~1| Ecoregion/Latitude/Site Code:	0.356
Residual:	0.738
AIC:	2701.76

LME	**Estimated value**	**Std. Error**	**DF**	**t-value**	**p-value**
Intercept	-0.198	0.132	623	-1.497	0.135
Depth	0.009	0.032	623	0.276	0.783
GAM	**Edf**	**Ref. df**		**F- value**	**p-value**
s(Temperature:Kelp)	1.00	1.00		3.30	0.070
s(Temperature:Barren)	1.56	1.56		1.90	0.305

Table S10 Summary table for statistical tests of response of fish (1a-j) activity groups. We fit generalized additive mixed models (GAMM, mgcv package) with the function gamm in R. Random effects of site nested in latitude nested in ecoregion are included to account for the spatial structure of the data. 's' indicates fixed effects (Temperature at time of survey) modelled with penalized regression splines (GAM component) for barren and kelp sites, and a Depth covariate (fixed effect, LME component). Fixed effects were scaled for coefficient comparison. AIC = Akaine information criterion; Std. error = standard error; Edf = Estimated degrees of freedom; Ref. df = reference degree of freedom (prior to deductions). We ran models with different distribution families (gaussian, quasipoisson) and transformed response data to ensure patterns are consistent. Separate models for barrens and kelp were also fit to check for consistent patterns.

a) Trends in richness of benthic fishes at barren and kelp sites

Random effects

~1| Ecoregion:	0.566
~1| Ecoregion/Latitude:	0.244
~1| Ecoregion/Latitude/Site Code:	0.343
Residual:	0.789
AIC:	3727.92

LME	**Estimated value**	**Std. Error**	**DF**	**t-value**	**p-value**
Intercept	0.116	0.166	880	0.701	0.484
Depth	0.024	0.023	880	0.873	0.383
GAM	**Edf**	**Ref. df**		**F- value**	**p-value**
s(Temperature:Kelp)	1.00	1.00		1.89	0.17
s(Temperature:Barren)	1.00	1.00		0.00	0.95

b) Trends in richness of demersal fishes at barren and kelp sites

Random effects

~1| Ecoregion:	0.694
~1| Ecoregion/Latitude:	0.251
~1| Ecoregion/Latitude/Site Code:	0.393
Residual:	0.571
AIC:	3566.63

LME	**Estimated value**	**Std. Error**	**DF**	**t-value**	**p-value**
Intercept	-0.267	0.194	1088	-1.374	0.170
Depth	0.057	0.022	1088	2.563	0.011
GAM	**Edf**	**Ref. df**		**F-value**	**p-value**
s(Temperature:Kelp)	1.16	1.16		23.32	<0.001
s(Temperature:Barren)	1.83	1.83		31.49	<0.001

c) Trends in richness of pelagic fishes at barren and kelp sites

Random effects

~1| Ecoregion:	0.168
~1| Ecoregion/Latitude:	0.190
~1| Ecoregion/Latitude/Site Code:	0.322
Residual:	0.898
AIC:	5761.70

LME	Estimated value	Std. Error	DF	t-value	p-value
Intercept	-0.105	0.073	1520	-1.431	0.153
Depth	0.077	0.027	1520	2.859	0.004
GAM	**Edf**	**Ref. df**		**F-value**	**p-value**
s(Temperature:Kelp)	1.00	1.00		13.11	<0.001
s(Temperature:Barren)	1.00	1.00		0.26	0.611

d) Trends in richness of site attached pelagic fishes at barren and kelp sites

Random effects

~1| Ecoregion:	0.287
~1| Ecoregion/Latitude:	0.146
~1| Ecoregion/Latitude/Site Code:	0.497
Residual:	0.751
AIC:	3853.12

LME	Estimated value	Std. Error	DF	t-value	p-value
Intercept	-0.183	0.102	926	-1.796	0.073
Depth	0.075	0.029	926	2.580	0.010
GAM	**Edf**	**Ref. df**		**F-value**	**p-value**
s(Temperature:Kelp)	1.00	1.00		22.24	<0.001
s(Temperature:Barren)	1.00	1.00		3.83	0.051

e) Trends in richness of non-site attached pelagic fishes at barren and kelp sites

Random effects

~1| Ecoregion:	0.257
~1| Ecoregion/Latitude:	0.116
~1| Ecoregion/Latitude/Site Code:	0.218

Residual: 0.940
AIC: 1678.03

LME	Estimated value	Std. Error	DF	t-value	p-value
Intercept	-0.023	0.106	306	-0.219	0.827
Depth	0.126	0.04	306	2.830	0.005
GAM	**Edf**	**Ref. df**		**F- value**	**p-value**
s(Temperature:Kelp)	1.59	1.59		0.53	0.54
s(Temperature:Barren)	1.00	1.00		0.43	0.51

f) Trends in abundance of benthic fishes at barren and kelp sites

Random effects
~1| Ecoregion: 0.530
~1| Ecoregion/Latitude: 0.291
~1| Ecoregion/Latitude/Site Code: 0.396
Residual: 0.660
AIC: 3424.76

LME	Estimated value	Std. Error	DF	t-value	p-value
Intercept	0.176	0.159	880	1.107	0.269
Depth	-0.043	0.027	880	-1.615	0.107
GAM	**Edf**	**Ref. df**		**F- value**	**p-value**
s(Temperature:Kelp)	1.60	1.60		7.19	0.013
s(Temperature:Barren)	1.10	1.10		0.84	0.407

g) Trends in abundance of demersal fishes at barren and kelp sites

Random effects
~1| Ecoregion: 0.741
~1| Ecoregion/Latitude: 0.356
~1| Ecoregion/Latitude/Site Code: 0.579
Residual: 0.557
AIC: 3776.18

LME	Estimated value	Std. Error	DF	t-value	p-value
Intercept	0.031	0.150	1088	0.205	0.837
Depth	0.097	0.025	1088	3.826	<0.001
GAM	**Edf**	**Ref. df**		**F-value**	**p-value**
s(Temperature:Kelp)	1.72	1.72		11.65	0.001
s(Temperature:Barren)	1.59	1.59		4.62	0.009

h) Trends in abundance of pelagic fishes at barren and kelp sites

Random effects
~1| Ecoregion: 0.374
~1| Ecoregion/Latitude: 0.193
~1| Ecoregion/Latitude/Site Code: 0.313
Residual: 0.808
AIC: 5360.09

LME	Estimated value	Std. Error	DF	t-value	p-value
Intercept	-0.196	0.121	1520	-1.625	0.104
Depth	0.028	0.025	1520	1.120	0.263
GAM	**Edf**	**Ref. df**		**F-value**	**p-value**
s(Temperature:Kelp)	1.00	1.00		5.01	0.025
s(Temperature:Barren)	1.00	1.00		0.72	0.397

i) Trends in abundance of site attached pelagic fishes at barren and kelp sites

Random effects
~1| Ecoregion: 0.448
~1| Ecoregion/Latitude: 0.194
~1| Ecoregion/Latitude/Site Code: 0.488
Residual: 0.700
AIC: 3683.01

LME	Estimated value	Std. Error	DF	t-value	p-value
Intercept	-0.133	0.143	926	-0.931	0.352
Depth	0.071	0.028	926	2.515	0.012
GAM	**Edf**	**Ref. df**		**F- value**	**p-value**
s(Temperature:Kelp)	1.00	1.00		6.68	0.010
s(Temperature:Barren)	1.00	1.00		2.22	0.136

j) Trends in abundance of non-site attached pelagic fishes at barren and kelp sites

Random effects
~1| Ecoregion: 0.333
~1| Ecoregion/Latitude: 0.252
~1| Ecoregion/Latitude/Site Code: 0.418
Residual: 0.775
AIC: 1554.64

LME	Estimated value	Std. Error	DF	t-value	p-value
Intercept	-0.029	0.132	306	-2.220	0.027
Depth	-0.055	0.045	306	-1.229	0.220

GAM	Edf	Ref. df	F- value	p-value
s(Temperature:Kelp)	1.00	1.00	0.82	0.365
s(Temperature:Barren)	1.62	1.62	0.57	0.506

Table S11 Ecoregional species richness for fishes, with number of species that only occur in barrens or in kelp (kelp specialists), and total number of species (both habitat specialists and those occurring in both habitats).

	Fish		
Ecoregion	**Barren unique**	**Kelp unique**	**Total**
	# of species		
Alboran Sea	33	4	**91**
Azores Canaries Madeira	5	14	**86**
Bassian	15	56	**185**
Cape Howe	69	54	**372**
Central Kuroshio Current	39	14	**98**
Kermadec Island	10	5	**63**
Lord Howe and Norfolk Islands	61	117	**504**
Manning-Hawkesbury	73	68	**469**
North Patagonian Gulfs	4	0	**12**
Northeastern New Zealand	14	11	**88**
Northern California	5	5	**30**
South Australian Gulfs	1	110	**165**
Three Kings-North Cape	9	6	**34**
Tweed-Moreton	148	71	**503**
Western Mediterranean	10	13	**87**

Table S12 Sensitivity analysis of pattern stability when using the full dataset (19 ecoregions, 5996 sites), as compared to the highest quality data set presented in the analysis of the main manuscript. Summary table for statistical tests of response of fish CTI (a,b), CTDiv (c,d) and CTR (e,f) in ecoregions that are highly sensitive (a, c, e) or medium sensitive (b, d, f) to CTI change. We fit generalized additive mixed models (GAMM, mgcv package) with the function gamm in R. Random effects of site nested in latitude nested in ecoregion are included to account for the spatial structure of the data. 's' indicates fixed effects (Temperature at time of survey) modelled with penalized regression splines (GAM component) for barren and kelp sites, and a Depth covariate (fixed effect, LME component). Fixed effects were scaled for coefficient comparison. AIC = Akaine information criterion; Std. error = standard error; Edf = Estimated degrees of freedom; Ref. df = reference degree of freedom (prior to deductions). We ran models with different distribution families (gaussian, quasipoisson) and transformed response data to ensure patterns are consistent. Separate models for barrens and kelp were also fit to check for consistent patterns. Separate Southern and Northern Hemisphere models and results are provided on GitHub.

a) Fish CTI in Ecoregions with High CTI sensitivity

Random effects

~1| Ecoregion:	0.252
~1| Ecoregion/Latitude:	0.716
~1| Ecoregion/Latitude/Site Code:	0.463
Residual:	0.590
AIC:	7033.42

LME	Estimated value	Std. Error	DF	t-value	p-value
Intercept	-0.110	0.182	2734	-0.602	0.5470
Depth	-0.040	0.018	2734	-2.219	0.0266
GAM	**Edf**	**Ref. df**		**F- value**	**p-value**
s(Temperature:Kelp)	1.60	1.60		45.66	<0.001
s(Temperature:Barren)	1.00	1.00		184.53	<0.001

b) Fish CTI in Ecoregions with Medium CTI sensitivity

Random effects

~1| Ecoregion:	0.107
~1| Ecoregion/Latitude:	0.495
~1| Ecoregion/Latitude/Site Code:	0.736
Residual:	0.586
AIC:	5367.72

LME	Estimated value	Std. Error	DF	t-value	p-value

Intercept	0.284	0.106	1751	2.685	0.0073
Depth	-0.111	0.023	1751	-4.783	<0.000
GAM	**Edf**	**Ref. df**		**F-value**	**p-value**
s(Temperature:Kelp)	1.51	1.51		55.22	<0.001
s(Temperature:Barren)	1.00	1.00		51.81	<0.001

c) Fish CTDiv in High CTI sensitivity ecoregions

Random effects

~1| Ecoregion:	0.055
~1| Ecoregion/Latitude:	0.510
~1| Ecoregion/Latitude/Site Code:	0.514
Residual:	0.724
AIC:	8349.75

LME	**Estimated value**	**Std. Error**	**DF**	**t-value**	**p-value**
Intercept	0.095	0.117	2734	0.814	0.416
Depth	-0.092	0.022	2734	-4.232	<0.000
GAM	**Edf**	**Ref. df**		**F-value**	**p-value**
s(Temperature:Kelp)	1.90	1.90		16.55	<0.001
s(Temperature:Barren)	1.92	1.92		16.20	<0.001

d) Fish CTDiv in Medium CTI sensitivity ecoregions

Random effects

~1| Ecoregion:	<0.001
~1| Ecoregion/Latitude:	0.137
~1| Ecoregion/Latitude/Site Code:	0.561
Residual:	0.824
AIC:	6440.61

LME	**Estimated value**	**Std. Error**	**DF**	**t-value**	**p-value**
Intercept	0.050	0.045	1751	1.123	0.262
Depth	0.055	0.023	1751	2.074	0.0382
GAM	**Edf**	**Ref. df**		**F-value**	**p-value**
s(Temperature:Kelp)	1.77	1.77		4.921	0.051
s(Temperature:Barren)	1.00	1.00		1.516	0.218

e) Fish CTR in High CTI sensitivity ecoregions

Random effects
~1| Ecoregion: 0.075
~1| Ecoregion/Latitude: 0.795
~1| Ecoregion/Latitude/Site Code: 0.403
Residual: 0.656
AIC: 7583.05

LME	Estimated value	Std. Error	DF	t-value	p-value
Intercept	0.265	0.171	2734	1.552	0.121
Depth	-0.140	0.019	2734	-7.364	0.0000
GAM	**Edf**	**Ref. df**		**F-value**	**p-value**
s(Temperature:Kelp)	1.81	1.81		2.056	0.078
s(Temperature:Barren)	1.90	1.90		5.870	0.006

f) Fish CTR in Medium CTI sensitivity ecoregions

Random effects
~1| Ecoregion: <0.001
~1| Ecoregion/Latitude: 0.231
~1| Ecoregion/Latitude/Site Code: 0.702
Residual: 0.721
AIC: 6088.17

LME	Estimated value	Std. Error	DF	t-value	p-value
Intercept	0.100	0.061	1751	1.644	0.1003
Depth	-0.109	0.026	1751	-4.148	<0.000
GAM	**Edf**	**Ref. df**		**F-value**	**p-value**
s(Temperature:Kelp)	1.00	1.00		2.928	0.087
s(Temperature:Barren)	1.59	1.59		6.884	0.020

References

1. K. Filbee-Dexter, R. Scheibling, Sea urchin barrens as alternative stable states of collapsed kelp ecosystems. *Mar. Ecol. Prog. Ser.* **495**, 1–25 (2014).

2. P. W. Glynn, El Niño warming, coral mortality and reef framework destruction by echinoid bioerosion in the eastern Pacific. *Galaxea,* **7**, 129-160 (1988).

3. N. Muthiga, T. McClanahan, Ecology of Diadema. *Dev. Aquacul. Fish. Sci.* **37**, 205–225 (2007).

4. N. S. Jones, J. M. Kain, Subtidal algae colonization following the removal of *Echinus. Helgoländer Wissenschaftliche Meeresuntersuchungen*. **15**, 460-466 (1967).

5. J. D. Urriago Suarez, J. C. Y. Wong, C. P. Dumont and J.-W. Qiu, High density and secondary production but variable recruitment of a sea urchin in subtidal barren areas of Hong Kong. *Reg. Stud. Mar. Sci.* **48**, 102017 (2021).

6. P. E. Parnell, J. T. Fumo, C. E. Lennert-Cody, S. C. Schroeter and P. K. Dayton, Sea urchin behaviour in a Southern California kelp forest: food, fear, behavioural niches and scaling up individual behaviour. *J. Shellfish Res.* **36**, 529-543 (2017).

7. J. P. Valentine, G. J. Edgar, Impacts of a population outbreak of the urchin *Tripneustes gratilla* amongst Lord Howe Island coral communities. *Coral Reefs*, **29**, 399-410 (2010).

Chapter 5 - Rapid Fish Community Response to Two Severe Marine Heat Events in the Pacific.

5.1 Abstract

Marine heatwaves can cause rapid ecological change, and these extreme heat events are becoming more frequent and severe. When heatwaves disturb or eliminate biogenic habitats, such as kelp forests, local species must respond to both heatwave-related temperature extremes and the loss of habitat and food (e.g., kelp). Here, I test whether two severe Pacific heatwaves, the 1997 – 98 El Niño and 2014 – 16 simultaneous Heat Blob and El Niño, drive fish community changes in a kelp forest ecosystem in the same direction as expected with longer gradual warming signals. Community thermal affinity shifts in response to the heatwaves were assessed using long-term monitoring data from the Channel Islands National Park in California, USA. I compared fish communities from 16 permanent monitoring sites across five islands, that represent kelp forests and sea urchin barrens over heatwave event phases, including recovery. Species observed during both heatwaves have warmer realized thermal affinities and larger range sizes. However, trajectories of recovery differed across the two heatwaves. Fish communities returned to a pre-event state (or similar) after the El Niño, but not after the Heat Blob, which was more severe in magnitude and duration. In addition, sites that are sea urchin barrens or patchy habitat tended to host species with warmer thermal affinities and broader thermal ranges, relative to kelp forested sites.

Therefore, my results suggest that declines in kelp and expanding sea urchin populations may facilitate fish heatwave-related tropicalization processes. Heatwaves restructure shallow reef fish communities towards a more tropical composition, in part by facilitating sea urchin population increases and shrinking kelp habitats that strengthen the biological resilience of communities to heat stress.

5.2 Introduction

In the ocean, many mobile species may escape climate warming or heatwaves by tracking their preferred thermal window. This can lead to population increases or introductions of warmer-affinity (more tropical) species in areas where warming allows colonization, creating 'tropicalization' signals in historically cooler areas (Pinsky *et al.* 2013). Species occurrence data combined with the range of temperatures they experience across their geographic range (realized thermal niches) can thus enable powerful predictions of biodiversity change (i.e., determining winners or losers) during acute heatwave events (Day *et al.* 2018) or as the climate gradually warms (Burrows *et al.* 2019). Furthermore, local gains and losses of species with different thermal affinities (warm or cold) can drive changes in community structure (Burrows *et al.* 2019).

Whole-community responses to temperature change can be evaluated with community metrics based on species' thermal affinities (e.g., Day *et al.* 2018; Burrows *et al.* 2019; Stuart-Smith *et al.* 2021; Schuster *et al.* 2022). Such community-level metrics have revealed signatures of ocean warming through space (Cheung *et al.* 2013; Stuart-Smith *et al.* 2015) and time (Bates *et al.* 2014), as well as during extreme heatwave events (Day *et al.* 2018). Applications of community-level metrics reveal, for example, that generalist tropical reef fishes (with broad thermal ranges and few specific habitat requirements) extend further into subtropical and temperate regions than specialists (Stuart-Smith *et al.* 2021). Another global analysis of shallow rocky reef fish communities reveals that signatures of gradual ocean warming can be habitat-dependent, with stronger

signals of fish tropicalization in sea urchin barrens than neighbouring kelp forests (Schuster *et al.* 2022).

Less clear is whether shorter-term events, such as marine heatwaves and El Niños, can drive habitat-dependent community restructuring in similar directions as found by Schuster *et al*. (2022). Marine heatwaves are discrete events marked by the acute onset of anomalously warm temperatures (Holbrook *et al.* 2019; Oliver *et al.* 2019). El Niño events are the warm phase of the El Niño-Southern Oscillation (ENSO), where weakened trade winds push warm waters towards the west coast of the Americas (Bjerknes 1966; Yang *et al.* 2018). Both marine heatwaves and El Niño's are events of anomalously warm water temperatures (marine heat events, thereafter). Species with warmer-affinities may move into an area during a heat anomaly and increase in abundance, while cool-affinity species may decline (e.g., Day *et al.* 2018). Such heat anomaly-related tropicalization signals may be temporary, followed by recovery as temperatures normalize after extreme events. Thus, there may be greater potential for recovery towards a pre-event state (or similar), where warm water species disappear again (Day *et al.* 2018). Individual species and communities will have different responses to warm water events, depending on their sensitivity to a given heat event. Some species may benefit from heat events, increasing in biomass or frequency, while others are negatively impacted (Bates *et al.* 2014; Vergés *et al.* 2014; Wernberg *et al.* 2016), and these responses may correspond with species' thermal affinities.

Habitat status can facilitate or dampen tropicalization processes by favouring particular species (Bates *et al.* 2014, 2017; Vergés *et al.* 2014; Schuster *et al.* 2022). For example, macroalgae may colonize newly available reef space after heat event-related mass coral mortalities, which in turn can attract more tropical, herbivorous fishes (Vergés *et al.* 2014). Similarly, simulations and observational data from 15 temperate ecoregions show that sea urchin barrens host relatively more warm-affinity fishes than neighbouring kelp beds in regions where species pools have high response diversity, because forested areas appear to resist range-expanding tropical species that prefer barren reefs (Schuster *et al.* 2022). Overgrazing of kelps by sea urchins can thus accelerate tropicalization processes across space, and similar patterns may emerge through time during marine heat events. In northern California, sea urchin populations increased 30-fold relative to historic numbers during a heatwave (Rogers-Bennett & Catton 2019), intensifying grazing pressure on kelps. Rocky reef habitats may thus transition from kelp forests to high urchin density barrens as a heatwave unfolds, potentially modifying community responses to the heatwave. Understanding community responses to heatwaves is thus particularly compelling in areas of biogenic habitat, where communities respond directly to a heatwave or indirectly to associated habitat loss.

Kelp forests along the northeast Pacific coast support biodiversity hotspots (Graham 2004). Giant kelp, *Macrocystis pyrifera*, is a dominant biogenic habitat former in ecosystems from central California, USA to central Baja California Sur, Mexico and supports many species that rely on these forests for habitat and food.

While kelp forests are resilient to short-term warming events, multiple severe events spanning months to years have driven kelp decline (Edwards 2004). For example, the 1997 – 98 El Niño, one of the strongest El Niño's ever recorded in the Pacific northeast, resulted in near-total loss of all giant kelp forests throughout half of the species' range. Fisheries stock assessments from the Southern Pacific reported decreased anchovy biomass, while sardines and mackerels increased during the El Niño (Ñiquen & Bouchon 2004). Another record-breaking marine heat event occurred in the northeast Pacific between the winter of 2013-14 and mid-2016, bringing anomalously warm water temperatures of over +2.5°C (Bond *et al.* 2015; Di Lorenzo & Mantua 2016). The latter event, presented as a combined Heat Blob and El Niño, hereafter referred to as the 'Heat Blob', led to biomass decreases and range shifts of commercial fish stocks (e.g., anchovy and salmon; Arafeh-Dalmau *et al.* 2019; Cheung & Frölicher 2020), and shifted productive kelp forests to unproductive sea urchin barrens across the northeast Pacific (Di Lorenzo & Mantua 2016; Rogers-Bennett & Catton 2019). Ecosystems in the Pacific northeast have thus experienced two severe heat events and kelp deforestation at a variety of scales over the last few decades which allows investigation of interactions between acute ocean warming and kelp loss.

A long-term kelp forest monitoring program has been maintained at the Channel Islands National Park, California, USA, to track changes in species abundance and diversity since 1982. These islands are surrounded by extensive and productive kelp forests that support diverse communities. Yet, these forests have shown

declines due to climatic stress and grazing pressure by sea urchins (Tegner & Dayton 1987, 1991; Rogers-Bennett & Catton 2019). Consequently, the 16 monitoring sites across five of the Channel Islands cover a broad range of environmental conditions, habitat types and biological assemblages.

Several heatwave events have occurred in the park during the historical monitoring period (Fig 5.1), offering an excellent opportunity to investigate community responses to heat events and across habitat types (kelp forests versus urchin barrens) in fishes. In particular, the park's location in an area of biogeographic transition where the biotas of central and southern California meet (Winant & Bratkovich 1981; Caselle *et al.* 2015; Freedman *et al.* 2020), creates an ecological mixing zone. The major ocean currents affecting the Bight are the California Current, an eastern boundary current that brings cold, fresh and nutrient poor water from northern latitudes, and the California Undercurrent, which originates further south, carrying warm and nutrient rich water (Gelpi & Norris 2008). The Bight forms a biological transition zone from temperate species typical of California to cooler, northern species. Therefore, many species are at their Northern or Southern range limits and likely have different sensitivities to temperature changes, thus leading to community re-shuffling. In addition, the Southern and Northern Pacific are sensitive to temperature-related changes in community composition (Burrows *et al.* 2019; Schuster *et al.* 2022), because the response diversity of the species pools is high in these regions (i.e., high diversity of thermal affinities and narrow average thermal range breadths across species).

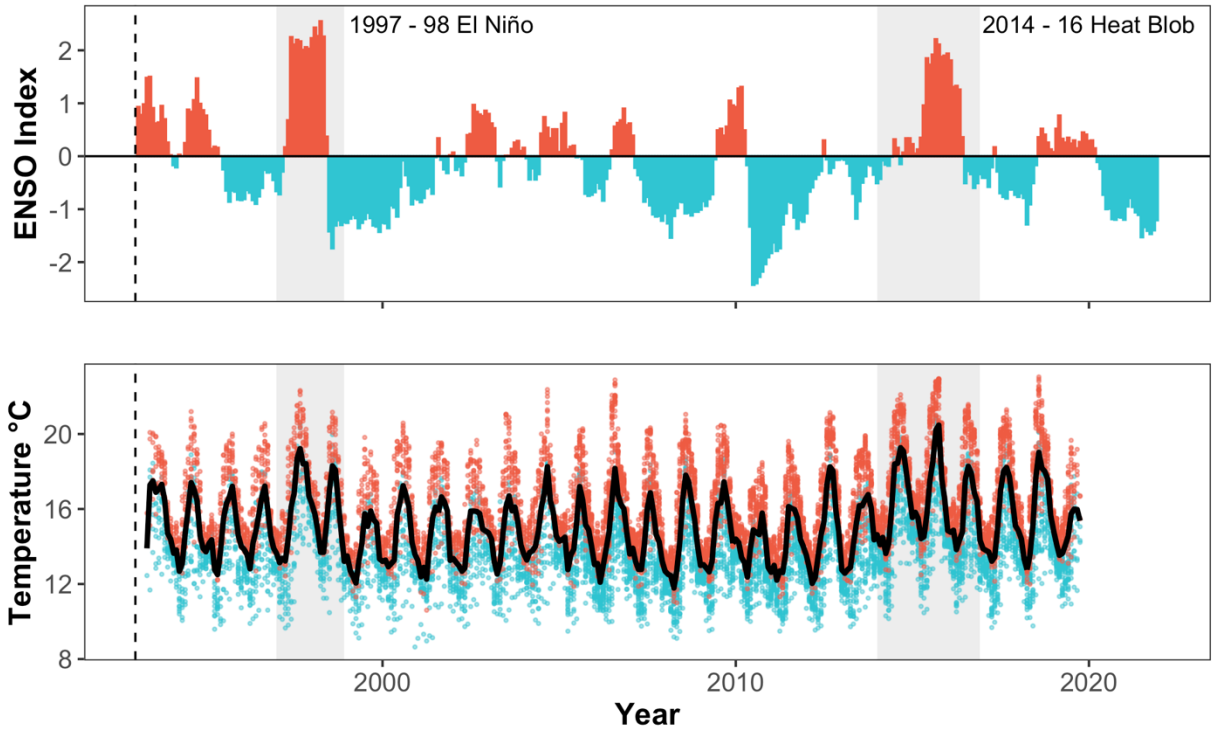

Figure 5.1 Time-series of ENSO index values (A) and in situ daily mean temperatures (B) recorded in the Channel Islands (CI) National Park, California, USA. The multivariate ENSO index tracks shifts between warm El Niño oceanographic conditions (positive values; red) and cold La Niña years (negative values; blue). Daily mean temperatures (black line), as well as daily maximum (red dots) and daily minimum (blue dots) are shown in B, starting in 1993 when in situ temperature monitoring began (marked by vertical dashed line). Grey shaded areas mark two extreme marine heat events that occurred in the Park since monitoring began.

In the present chapter, my overall objective is to investigate fish community responses to marine heat events, including recovery, and whether community response differs across kelp forested sites and sites that are sea urchin barrens. Specifically, I quantify how two severe marine heat events (the 1997 – 98 El Niño and the 2014 – 16 Heat Blob) modify the 'thermal composition' (see Fig 1 in

Schuster *et al.* 2022) of reef fish communities in the Channel Islands. To quantify changes in the thermal composition of the fish community, I assess three community-level metrics based on the thermal affinities of the fishes observed at 16 sites in the park, including the mean (community temperature index: CTI) and variation of thermal affinities among species (community thermal diversity: CTDiv), as well as the range of temperatures occupied by species across their global range (community thermal range: CTR). First, I quantify how the three components of thermal composition, i.e., CTI, CTDiv and CTR, differ during each marine heat event, relative to a 3-year period prior to and after each event across all sites. I predict a warming signature for fish communities during heat event years (CTI increase) driven by an influx of warm-affinity fishes, but subsequent return to pre-event CTI values as warm anomalies subside after the marine heat events. I furthermore expect lower diversity of warm- and cold-affinity species (CTDiv decrease) and a shift towards communities dominated by more widespread thermal generalists (with broad thermal ranges; i.e., greater CTR). Second, I quantify changes in the individual abundance and occurrence frequency of 13 indicator fish species and sea urchins for each marine heat event, and test whether the events are associated with changes in functional trait distribution in the fish assemblages of the Channel Islands. I expect negative trends (abundance and frequency declines) in indicator fish species that have cold-affinities, and positive trends in warm-affinity fish species. I predict increases in sea urchin densities due to their relative heat tolerance (Hardy *et al.* 2014; Minuti *et al.* 2022) and release from predator pressure. Finally, I test whether changes in community thermal

composition during and after a marine heat event are amplified at urchin barren sites, relative to kelp forest sites. I predict stronger signals of CTI increase at sites that are barrens, relative to those that are forested, because tropicalization signals (CTI increases) are accelerated at sea urchin barrens relative to neighbouring kelp forest sites in regions where CTI sensitivity is high (Schuster *et al.* 2022).

5.3 Methods

Analyses were completed using data from the Channel Islands National Park's kelp forest monitoring program (KFMP), described in more detail below. The KFMP has been ongoing since 1982 to present (2022), with comprehensive fish surveys starting in 1996, a period that includes two of the strongest ENSO events on record. I used data from two discrete time periods which span these two events (1994 – 2001 and 2010 – 2019) to explore fish community response to two severe marine heat events occurring during the afore mentioned periods: 1) a large-scale El Niño in 1997 – 98 and 2) the 2014 – 16 Pacific Heat Blob and simultaneous El Niño.

5.3.1 Channel Islands National Park's kelp forest monitoring program (KFMP)

Annual surveys of the diversity and abundance or density of fishes, invertebrates and macroalgae have been conducted in the Channel Islands for almost four decades by the National Park Service (KFMP). Sixteen permanent transects on reef sites on five islands have been continuously monitored since 1986 (some since 1982), providing the longest set of fishery independent data along the Pacific west coast. Each site was sampled at least once per year in the summer (May to October), using non-invasive sampling by scuba divers. A range of monitoring

protocols are used to represent the variety of organisms and physical habitats that are present. A full description of the monitoring techniques and revisions of the protocols are detailed in (Davis *et al.* 1996; Kushner *et al.* 2013), and described in brief below. For each site and sampling year, I aggregated the data for each species to produce an abundance measure based on total counts. All data were standardized to account for protocol or sampling area changes in accordance with the KFMP data protocols (Kushner *et al.* 2013).

To investigate fish community responses to marine heat events overall, and across habitat types, I used data from two fish monitoring protocols: (1) Roving Diver Fish Counts (RDFC) and (2) Visual Fish Transects (VFT). The RDFC protocol determines the species richness and abundance of all fishes along a 100m transect line, with 122 fish species observed as of 2021. Prior to 2003, abundances of each fish species were recorded by category (single, few, common or many), with whole fish counts recorded thereafter. The VFT protocol determines the abundance of 13 selected indicator fish species along the transect line. The KFMP indicator species were selected to represent a cross section of the ecological roles present in the park's kelp forests (i.e., species that are threatened or endangered, legally harvested, common or characteristic of entire communities). Monitoring of the entire fish community (RDFC) only began in 1996, thus, I used the VFT data (which started in 1985) to supplement my analysis for earlier years and to investigate whether indicator fishes respond synchronously with the whole fish community.

To contrast community responses to marine heat events across habitat types, I classified each site as (1) kelp forest, (2) sea urchin barren, or (3) mixed and patchy habitat by combining kelp stipe counts and sea urchin densities. *Macrocystis pyrifera* stipes were counted along the fixed transect lines, with the number of adult stipes (>1m above the bottom) counted. Sea urchin densities were quantified using 1 x 1 m quadrats, and mean densities per m^2 were calculated across 20 quadrats (1985 – 1995) and 12 quadrats (1996 to present) at each site. Due to the dynamic nature of kelp forest ecosystems, sites were classified based on their state (kelp versus urchin dominated) in the three years prior to each marine heat event. Sites hosting densities of barren-forming sea urchins exceeding $4/m^2$ and fewer than 80 adult *Macrocystis* stipes were classified as 'barrens'. Sites with more than 80 adult kelp stipes during each of the 3 years prior, and low sea urchin densities (<4 urchins/m^2) were classified as 'kelp'. The urchin density threshold represents the density of sea urchins needed to form and maintain barrens, and adult kelp stipe counts are a good estimator of a healthy, canopy-forming kelp forest. By combining stipe counts and urchin densities, I was able to identify sites that are patchy or represent neither kelps nor urchin barrens ('mixed' sites, hereafter). The final site classifications prior to each event is provided in supplementary table S1. I ran a sensitivity analysis to test the robustness of using the above sea urchin and kelp thresholds and found that the results and main conclusions are robust to using a higher threshold (six urchins per m^2 and 100 kelp stipes; see supplementary figure S1 and table S10).

To further verify the above site classifications, I also used data from the Random Point Contacts (RPCs) protocol, which estimates substrate composition (sand, cobble or rock) and percent cover of macroalgae (including kelp) and selected invertebrate taxa along the transects (see supplementary table S2). I first collapsed the substrate data into seven categories: sand, cobble, rock, bare substrate (devoid of any apparent living organisms), coralline algae, macroalgae and kelp (order Laminariales), after removing macro-invertebrate observations (e.g., barnacles, cup corals, brittle stars) that have no clear association with kelp or barren habitat states (see supplementary table S2). I then calculated the total % cover of each substrate category for every survey (see supplementary figure S2). I constructed site-by-substrate matrices and used non-metric multidimensional scaling (NMDS) to distinguish differences in substrate composition across the 16 monitored sites (Fig 5.2). I evaluated whether sites classified as kelp forest, sea urchin barrens or mixed, patchy sites show distinct patterns of substrate dissimilarity based on NMDS plots.

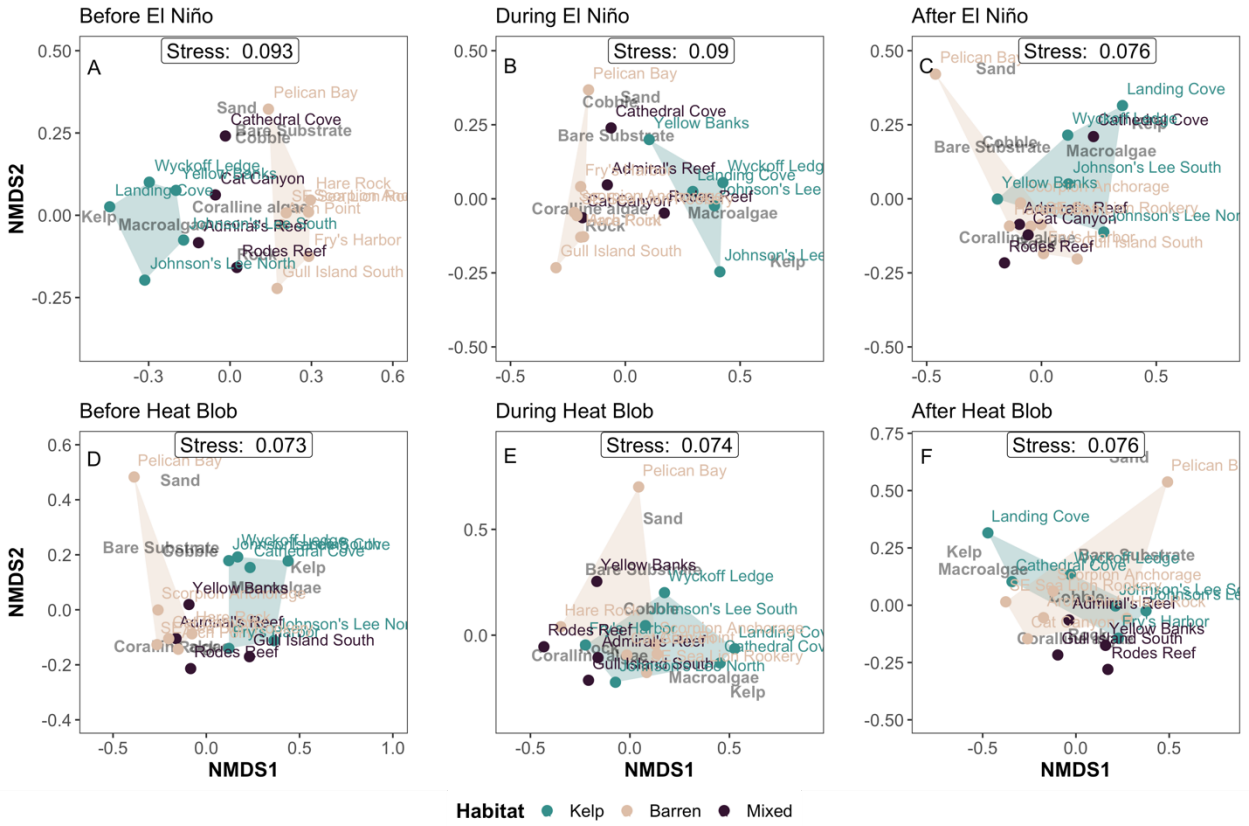

Figure 5.2 Non-metric multidimensional scaling (NMDS) ordination plots illustrating substrate-cover differences among 16 permanent monitoring sites in the Channel Islands National Park. Substrate composition (% cover of rock, sand, cobble, bare substrate, coralline algae, macroalgae and kelp) across sites is shown for two marine heat events: the 1997 – 98 El Niño (top row) and 2014 – 16 Heat Blob (bottom row), before (A, D), during (B, E) and after (C, F) each event. Each site was classified as a sea urchin barren (brown shading) or kelp forest (green shading) based on both sea urchin densities and kelp densities in the three years prior to each event. Sites that are barren are distinct from sites that are forested based on substrate NMDS plots (see A and D), although some sites undergo changes (i.e., kelp loss) during and after the event, reducing differences between barrens and kelp classified sites.

5.3.2. Community temperature metrics and thermal affinity

I constructed the realized thermal range of all species recorded in the Channel Islands monitoring program based on global occurrence data. Channel Island species records were matched to the same species reported in the Global

Biodiversity Information Facility (GBIF; http://www.gbif.org) database. I extracted GBIF records attributed to 'human observations' using the function 'occ' from the 'spocc' package in R (Chamberlain 2021), and included records at depths <30 m to select for occurrences where SST would match experienced *in situ* temperatures. This resulted in a total of 40,869 occurrences for the 122 species from the Channel Islands. I then matched weekly mean satellite sea surface temperature (SST) data (1° grid, NOAA Optimum Interpolation [OI] SST V2, 1981–present) to each occurrence location. For each location, four temperature metrics were extracted: the temperature at time of the survey, and the annual mean, maximum and minimum for the location. These data were then matched with species and community-level temperature metrices for each location, as described in Schuster *et al.* (2022). In brief, I first calculated each species realized thermal range breadth (STR; lower (5th) and upper (95th) percentiles of temperatures experienced across their geographic range) and estimated the species thermal index (STI; midpoint of the thermal range) (Burrows *et al.* 2019). I then computed three community temperature indices for site-level fish communities to contrast realized thermal composition across event phases of two marine heat events. The community temperature index (CTI) was calculated as the average thermal affinity (STI) of all fishes at a site. The community thermal diversity (CTDiv; Burrows *et al.*, 2019) score was the standard deviation of STIs in a local community. CTDiv is the variation of thermal affinities among species in a community, where communities with a mix of cold-and warm-affinity species have a high score, and those containing species with similar thermal affinities have a low score. The community

thermal range (CTR) was calculated as the average breadth of thermal ranges (STRs) across all species in a community. I calculated separate community temperature indices for the indicator fish communities (using VFT data) and the whole community (RDFC data).

Finally, I classified species as having a relatively warm- or cold-affinity, compared to those observed in the Channel Islands, to interpret community-level trends. The lower and upper quartiles (25th or 75th percentiles) of the species' pool of thermal midpoints were used to classify species as the warmest or coldest in their region. I also classified the most extreme warm- or cold-affinity fishes based on lower and upper deciles (10th and 90th percentile) to test the robustness of findings to the selected threshold (see supporting figure S3).

5.3.3 Functional trait classification

To test for differences in functional richness, fishes were classified into trophic groups (benthic invertivores, planktivores, omnivores, herbivores and carnivores) and level of activity, based on their position in the water column (benthic, demersal or pelagic). Trait classifications were based on information from FishBase (http://www.fishbase.org/) (Stuart-Smith *et al.* 2013, 2018; Schuster *et al.* 2022). The richness of fishes (number of species) in each trophic and activity group was calculated for each survey, based on the whole community data (RDFC data).

5.3.4 Statistical modelling

To test for differences in community temperature metrics and richness of fishes across phases of two marine heat events, I used linear mixed effects models (LME)

with the package 'nlme' in R (R Core Team 2014) using the function 'lme' (Atkin *et al.* 2015; Pinheiro *et al.* 2015). I included nested random effects of island and site to account for variation in the response variables due to the non-random spatial structure of the data and for temporal replicates where a single site was surveyed more than once a year. Event status (before, during or after event) was included in all models to test for marine heat event-dependent variation in the response of interest, where event years (i.e., 1997 – 98 for the El Niño and 2014 – 16 for the Heat Blob) were set as the basis-level, and contrasted with the three years before and after the event, respectively. Depth was included as a covariate. To test for habitat-dependent variation in community thermal diversity, I ran separate models of the same structure described above for each habitat type (kelp, barren and mixed habitat). A variance function was included to model heteroscedasticity among the five islands. Model fit was inspected visually to ensure test assumptions were met.

5.4 Results

5.4.1 Community thermal diversity

Fish communities shifted towards a relatively more tropicalized assemblage structure during the two discrete marine heat events in the Channel Islands National Park observed here. Annual monitoring of fish communities revealed community compositions with relatively higher CTI values during both the 1997 – 98 El Niño (Fig 5.3A, D) and 2014 – 16 Heat Blob (Fig 5.4A, D), relative to the three years prior to each marine heat events (see supplementary table S3). This shift towards relatively higher CTI during marine heat event years was evident when

calculating CTI values for the entire fish community (Fig 5.3D; Fig 5.4D, supplementary table S2), but also emerged within a subset of indicator fishes (Fig 5.3A; Fig 5.4A, supplementary table S3), although the effect was marginal (p = 0.055) for indicator fishes during the 1997 – 98 El Niño (see supplementary table S4). While both events were distinguished with relatively higher CTI during the event period, the trajectory of fish community recovery after each marine heat event differed (see Fig 5.3D vs Fig 5.4D). After the El Niño, fish CTI was lower than during the event, for both the whole fish community and the indicator species, and returned to pre-event CTI values. By contrast, following the Heat Blob, whole-community fish CTI was higher in the 3-year period after the Blob than it was during the Blob (see supplementary table S2), thus, CTI increased as the Heat Blob unfolded, and then continued to increase after the Blob vanished. Average CTI of the whole fish community was 19.8 ± 0.76 (°C, mean ± sd) before the El Niño, rose to 20.1 ± 0.73 during the El Niño, and subsequently declined to 19.9 ± 0.56 after the event. Whole fish community CTI was 19.3 ± 0.63 (mean ± sd) before the Heat Blob, rising to 19.7 ± 0.65 during the Blob, and continued to increase to 20.0 ± 0.62 after the event. Changes in CTI values coincided with changes in mean *in situ* temperatures recorded in the park. During the El Niño, temperatures were warmer by 0.8 to 1.2 °C, while temperatures increased by 1.6 to 2.0 °C during the Heat Blob (Table 5.1).

Table 5.1 *In situ* temperatures recorded before (3-years), during and after (3-years) two severe marine heat events in the Channel Islands National Park, CA, USA. Daily temperature values were averaged across each event phase. Sd = standard deviations. Temperature changes were calculated from event phase averages (event rise = change in mean temperature during event, relative to the three years prior; event fall = change in mean temperature in the three years after the event, relative to the event).

Event	Island	Temperature (mean ± sd; °C)			Temperature Change (°C)	
		Before Event	During Event	After Event	Event Rise	Event Fall
1997 – 98 El Niño	Santa Barbara	15.9 ± 1.69	16.9 ± 2.07	15.3 ± 1.96	+1.1	-1.6
	Anacapa	15.5 ± 1.98	16.7 ± 2.32	15.3 ± 1.97	+1.2	-1.4
	Santa Cruz	14.8 ± 1.84	15.8 ± 2.29	14.5 ± 1.87	+1.0	-1.3
	Santa Rosa	13.9 ± 1.40	14.9 ± 2.01	13.6 ± 1.46	+1.0	-1.3
	San Miguel	13.4 ± 1.40	14.3 ± 2.12	12.7 ± 1.51	+0.9	-1.6
	All Islands	14.79 ± 1.92	15.80 ± 2.37	14.4 ± 2.02	+1.0	-1.4
2014 – 16 Heat Blob	Santa Barbara	15.3 ± 1.99	17.3 ± 1.94	16.3 ± 2.02	+2.0	-1.0
	Anacapa	15.2 ± 2.15	17.0 ± 2.33	16.0 ± 2.34	+1.8	-1.0
	Santa Cruz	14.8 ± 2.17	16.5 ± 2.38	15.6 ± 2.34	+1.7	-0.9
	Santa Rosa	13.4 ± 1.62	15.1 ± 1.84	14.3 ± 1.66	+1.7	-0.8
	San Miguel	12.9 ± 1.64	14.5 ± 1.94	13.7 ± 1.70	+1.6	-0.8
	All Islands	14.56 ± 2.15	16.35 ± 2.34	15.39 ± 2.26	+1.8	-1.0

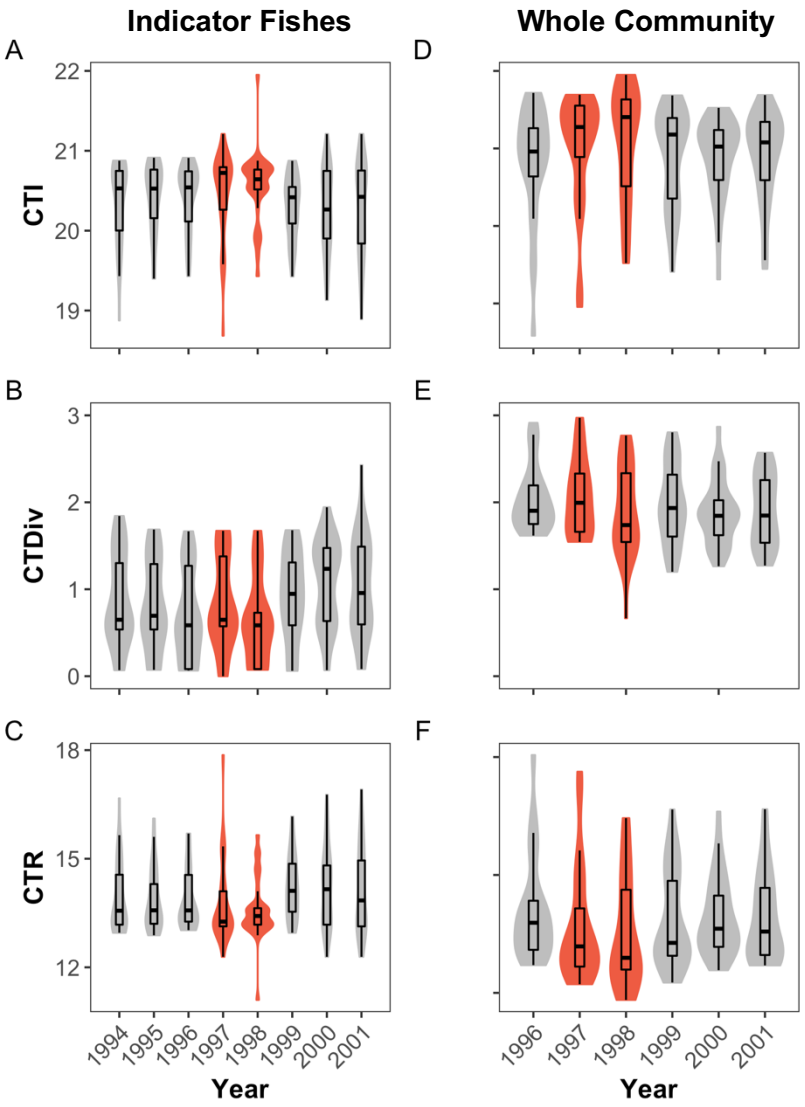

Figure 5.3 Differences in community temperature index (CTI; first row), community thermal diversity (CTDiv; second row) and community thermal range (CTR; third row) for fish communities observed before, during and after the 1997 – 98 El Niño. Community thermal diversity was contrasted for a 3-year period prior to the event, the event years (red shading) and a 3-year period after to the event. The first column (A-C) shows CTI, CTDiv and CTR values of indicator fish species assemblages (13 species monitored). The second column (D-F) shows CTI, CTDiv and CTR values of all fish species observed at the Channel Islands (note: monitoring of the whole fish community started in 1996, i.e., only one year prior to the El Niño event). Boxplots show maximum, minimum and median values, as well as 25th and 75th percentile values.

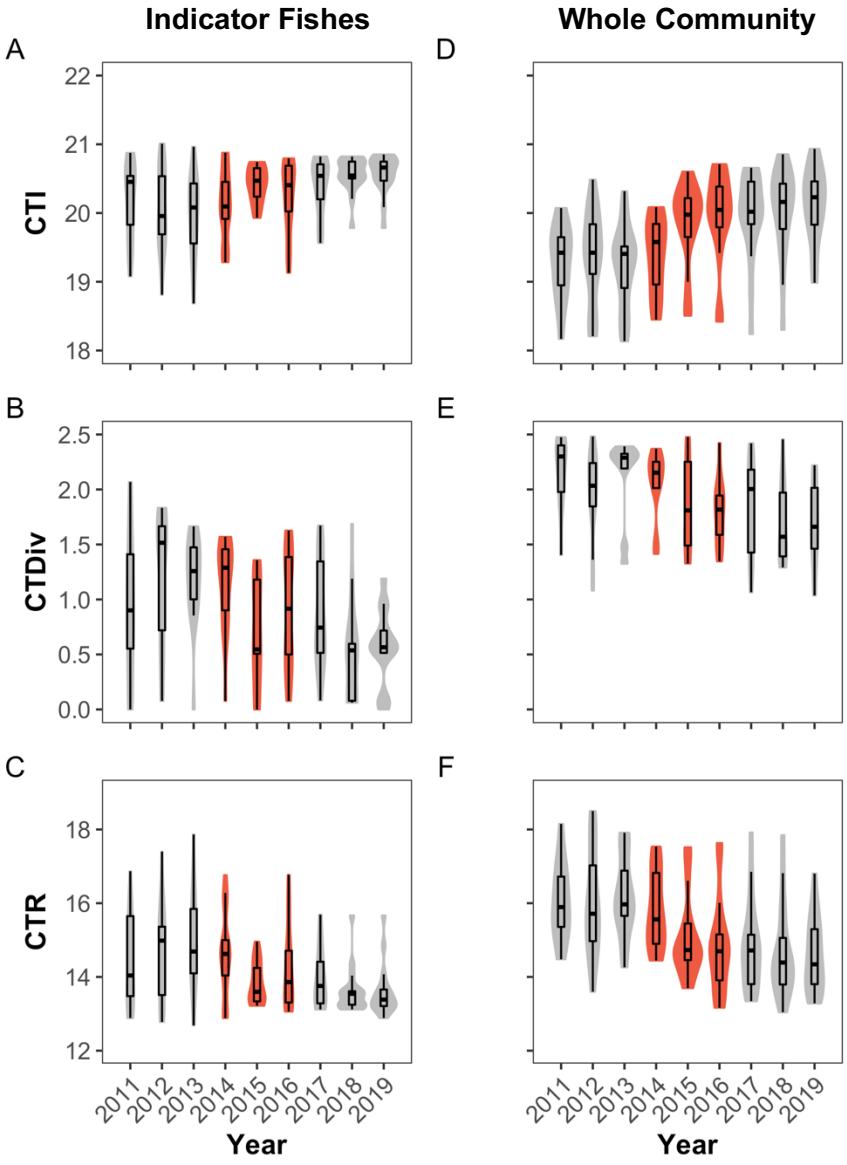

Figure 5.4 Differences in community temperature index (CTI; first row), community thermal diversity (CTDiv; second row) and community thermal range (CTR; third row) for fish communities observed before, during and after the 2014 – 16 Heat Blob. Community thermal diversity was contrasted for a 3-year period prior to the event, the event years (red shading) and a 3-year period after to the event. The first column (A-C) shows CTI, CTDiv and CTR values of indicator fish species assemblages (13 species monitored). The second column (D-F) shows CTI, CTDiv and CTR values of all fish species observed at the Channel Islands. Boxplots show maximum, minimum and median values, as well as 25th and 75th percentile values.

The relatively higher CTI during the El Niño was attributable to relatively greater increases in warm-affinity species versus cold-affinity species (Fig 5.6A; supplementary figure S3), whereby richness increased, respectively, by 75% and 35%. Even so, the overall species richness of the fish community was similar in the three years prior to the El Niño and during the El Niño, but richness was higher after the El Niño than during the event (supplementary table S4). Losses in generalist species (that are neither warm- nor cold affinity) may explain the absence of change in overall richness. CTI declined in the three years following the El Niño, relative to the event years, because of a 4-fold increase in cold-affinity fishes, although some warm-affinity fishes also appeared (Fig 5.6B). By contrast, the relatively higher CTI during the Heat Blob, compared to the three years prior, is due to the presence of 33% more warm-affinity fishes but 50% fewer cold-affinity fishes (Fig 5.6C; supplementary table S4), but with no overall difference in species richness (supplementary table S3f). The richness of warm-affinity fishes remained high after the Heat Blob (i.e., no significant difference between Heat Blob years and the three years following the Blob), while 47% fewer cold-affinity fishes were present after the Blob, resulting in even higher CTI values after the Blob. This loss of cold-affinity fishes also aligned with lower overall fish richness after the Heat Blob (supplementary table S4f).

The overall thermal composition of fish communities differed between time periods of two marine heat events. Heat event years were associated with lower thermal diversity (Fig 5.8B) and smaller thermal range breadths (Fig 5.8C) in those species found during surveys, relative to the three years prior of each event (supplementary table S2), suggesting that whole fish communities with higher CTIs consist of more similar, warm-affinity species with narrower thermal ranges, on average (supplementary figure S4). The thermal diversity and range breadth of indicator fish assemblages remained unchanged during the El Niño, but was also lower during the Heat Blob (Fig 5.9B, C; supplementary table S3), matching the response of the whole fish community. Changes in the thermal composition of the whole fish community differed as each marine heat event subsided, where thermal diversity remained low, but CTR returned to higher values following the El Niño, while both thermal diversity and thermal range breadths were lower after the Heat Blob, relative to Blob years (Fig 5.8B, C). Thus, the El Niño resulted in an overall loss of thermal diversity that persisted past the heat event years, and a temporary decline in range breadths, albeit some broader ranged species returned following the event. In the indicator assemblages (Fig 5.9B, C), thermal diversity and thermal range breadths were higher after the El Niño than during, but did not change after the Heat Blob (i.e., remained lower than before the Blob).

5.4.2 Individual species responses

Three species of fish were observed exclusively during the 1997 – 98 El Niño, but not in the three years prior to or after the event: *Icelinus tenuis* (spotfin sculpin), *Atherinopsis californiensis* (jack smelt) and *Apogon quadalupensis* (cardinal fish).

All three species were rare, with the warm-affinity *A. quadalupensis* recorded only twice throughout the entire time-series, both instances in 1998. By contrast, three relatively cold-affinity fish species were not observed during the El Niño years, but were frequent before and after the event: *Sebastes rastrelliger* (grass rockfish), *Sebastes auriculatus* (brown rockfish) and *Stereolepis gigas* (giant sea bass). No species of fish appeared or disappeared entirely during the 2014 – 16 Heat Blob.

5.4.2.1 Fish indicator species and sea urchins

All 13 species of indicator fishes were observed before, during and after both heat events, but their frequency of occurrence varied across the 16 sites monitored (Fig 5.5). The identities of species responding strongly to either event were variable. For example, *Rhacochilus vacca*, a cold-affinity species, occurred less frequently (observed at ≤ 25% of sites) during the El Niño (Fig 5.5A). Two cool-affinity rockfishes, *Sebastes mystinus* and *Sebastes serranoides* increased in frequency after the El Niño, from ≤ 25% to 50-75% and 25-50% site presence, respectively.

By contrast, frequency of occurrence changed more strongly among warm-affinity species during the Heat Blob (Fig 5.5B), including: *Hypsypos rubicundus, Paralabrax clathratus, Semicossyphus pulcher, O. californica, Halichoeres semicinctus,* but also two colder-affinity species *Chromis punctipinnis* and *Embiotoca jacksoni.* Furthermore, *S. atrovirens*, *S. mystinus* and *Embiotoca lateralis* were found at fewer sites during and after the Heat Blob.

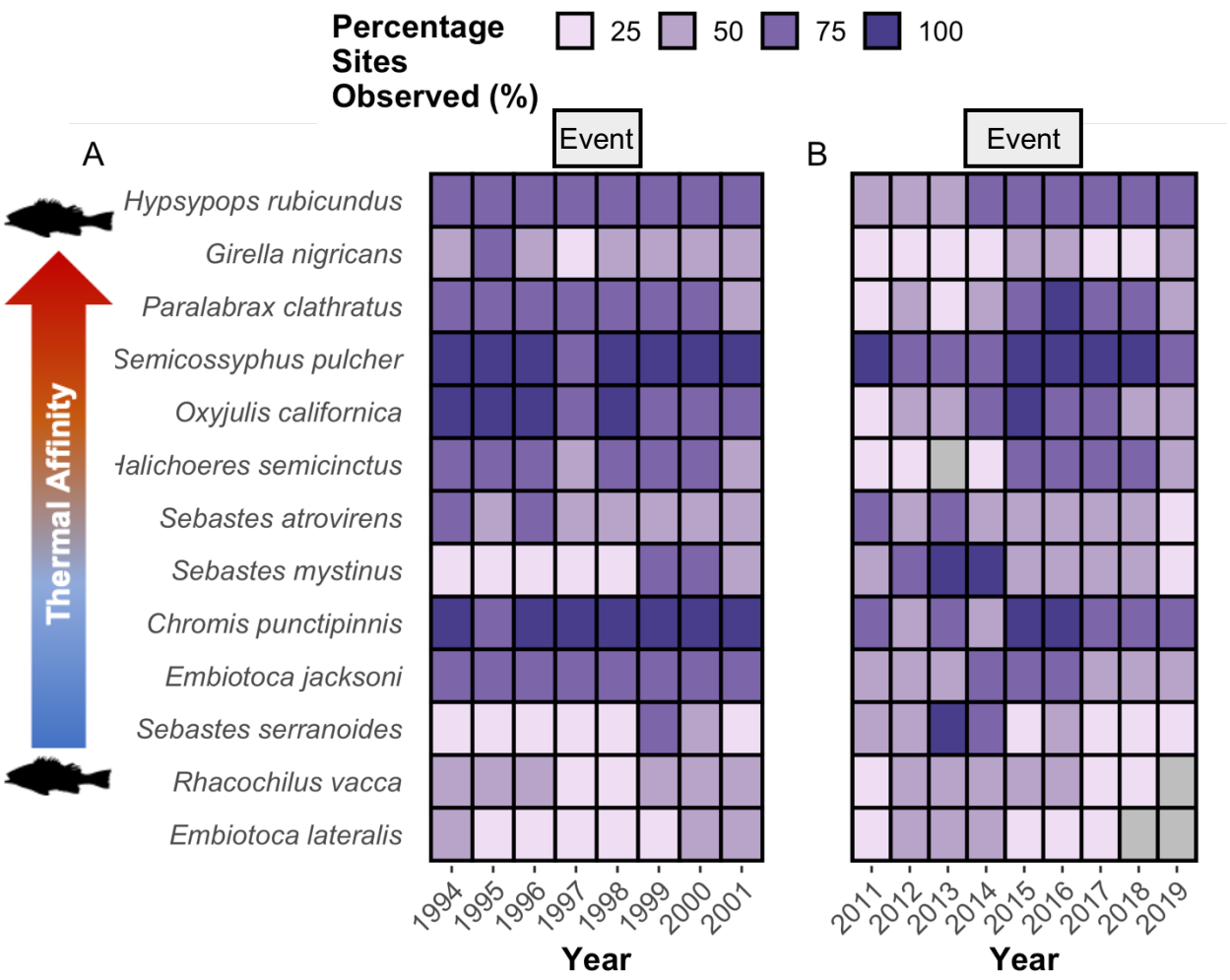

Figure 5.5 Heatmap of the occurrence frequency of 13 indicator fish species across 16 sites in the Channel Islands before, during and after two marine heat events: the 1997 – 98 El Niño (A) and the 2014 – 16 Heat Blob (B). Individual fish species are organized by thermal affinity, with the warmest-affinity species near the top, and coolest affinity species at the bottom. Occurrence frequencies three years prior and three years after each event are shown. Tile shading indicates the percentage of sites (out of 16) a species was observed at in a given year, with occurrences bins for occurrences at 0-25% of sites, 25-50% of sites, 50-75% of sites and 75-100% of sites. Grey shaded tiles indicate a species was absent at all sites during that year.

The relative abundance of several indicator fishes also changed during and after the El Niño (Fig 5.6A-B). Notably, *S. pulcher, S. atrovirens* and *R. vacca* declined during the event by 65%, 25% and 28%, respectively, across all islands (Fig 5.6A). Strong losses (> 100%) were also observed at individual islands, in particular at the western-most islands, where cold-water fishes such as *S. atrovirens*, *C. punctipinnis* and *E. lateralis* showed significant declines. The period after the El Niño (Fig 5.6B) was marked by mostly positive percentage changes in fish abundance, with significant increases overall in *S. pulcher, S. mystinus, S. serranoides* and *R. vacca,* of which the latter three have cold-affinities. Strong abundance increases of predominantly cold-affinity fishes were also evident at the western-most and central islands after the El Niño.

During the Heat Blob, several warm-affinity fishes were observed in higher abundances than in the three years prior, including *H. rubicundus, P. clathratus, S. pulcher, O. californica* and *H. semicinctus*. A 20-100% increase in the abundance of each of these species occurred predominantly across the eastern-most and central islands (Fig 5.6C). Three cold-affinity fishes declined in abundance during the Blob by 63%, 59% and 41% overall: *S. mystinus, S. serranoides* and *E. lateralis*. Fish abundances remained overall similar or declined in the three years after the Heat Blob, relative to the marine heat events years (Fig 5.6D).

Fish abundance changes observed during each heat event occurred in different affinity groups. The El Niño was characterized by mostly declines in cold-affinity fish abundances during the event, but much higher numbers of cold-affinity fishes

after the event. The Heat Blob, by contrast, was characterized by more abundant warm-affinity fishes during the event and simultaneous declines in the abundance of cold-affinity fishes, with the latter further decreasing in numbers after the Blob.

Sea urchin density increases were associated with both heat events, albeit with different timings. Increases in sea urchin densities, by 20-100% overall, were observed in the three years after the El Niño, relative to the El Niño years. The strongest sea urchin increases (>100%) were observed in red (*Mesocentrotus franciscanus*) and purple (*Strongylocentrotus purpuratus*) sea urchins. By contrast, sea urchins responded more rapidly to the Heat Blob than the earlier El Niño, with significant changes in urchin abundance evident during the heat event years (rather than trailing the event, as was the case in the earlier El Niño). Crowned sea urchin (*Centrostephanus coronatus*) abundances were significantly higher (by 55%) during the Heat Blob than in the three years prior, while red sea urchins declined, with abundances that were 76% lower overall, >100% lower at the three eastern-most islands, but 56% higher at Santa Rosa Island. Notably, purple sea urchins increased in abundance by >165% at the two western-most islands, relative to the Heat Blob years.

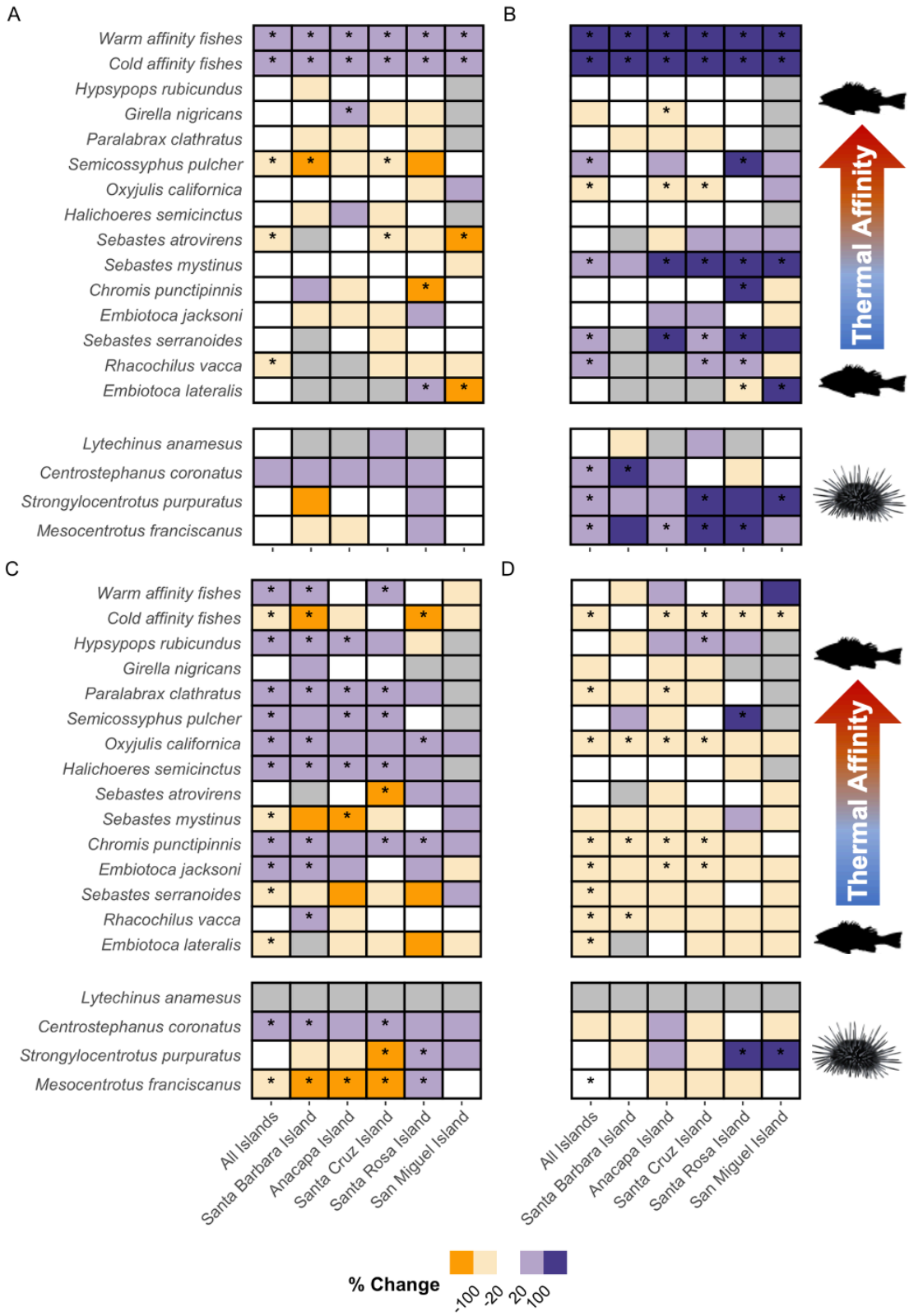

Figure 5.6 Percentage change in warm-affinity and cold-affinity fishes, 13

individual indicator fish species and four sea urchin species across all islands, and for individual islands. Percent change was calculated for each location from the pre-event period to the event period (first column, A and C) and from the event period to the post-event period (second column, B and D). Abundance responses to two marine heat events are shown: the 1997 – 98 El Niño (A-B) and the 2014 – 16 Heat Blob (C-D). Individual fish species are organized by thermal affinity, with the warmest-affinity species near the top, and coolest affinity species at the bottom. Percent change was calculated from model estimates of individual fish abundances across event periods, using linear mixed effects models. Tile colours indicate binned % abundance change values, with little change (-20 to 20% change) in white, moderate declines in light orange (-20 to -100), moderate increases in light purple (20 to 100), strong declines (greater than -100%) in orange and strong increases (greater than 100%) in purple. Tiles are shaded in grey where abundance data was insufficient for model fitting (mostly zeros or complete absence at a given island).

5.4.3 Habitat-specific tropicalization signals

During the 1997 – 98 El Niño, sites that were sea urchin barrens or patchy, mixed-habitat sites supported fish communities with a higher proportion of warm-affinity species, leading to stronger tropicalization signals indicated by higher CTI values (Fig 5.7B; Fig 5.8A; supplementary table S5). By contrast, kelp forested sites showed no change in the proportion of warm- or cold-affinity species (i.e., no CTI change) during the El Niño. In the indicator species assemblages, a similar pattern emerged, although CTI change during the El Niño was most pronounced at barrens, while CTI remained stable at patchy and kelp forested sites (Fig 5.7A; Fig 5.9A; supplementary table S6). Barrens tend to host fish communities with lower thermal diversity and lower thermal range breadths (Fig 5.8B, C) compared to forested sites during heat event years, suggesting barren communities consisted of more similar, warm-specialist species. In the three years after the El Niño, an influx of cold-affinity species supported communities with lower CTI values across

all habitat types. The fish community responded differently to the 2014 – 16 Heat Blob, with strong signals of tropicalization (i.e., higher CTI) in all habitat types associated with the Blob, and no sign of community recovery, as CTI values continued to rise after the Blob subsided across barrens, patchy and kelp forest sites (Fig 5.7D; Fig 5.8A; Fig 5.9A). Overall, comprehensive fish community monitoring revealed that rapid fish community tropicalization during heat events can be habitat-type dependent, but signals are event-specific.

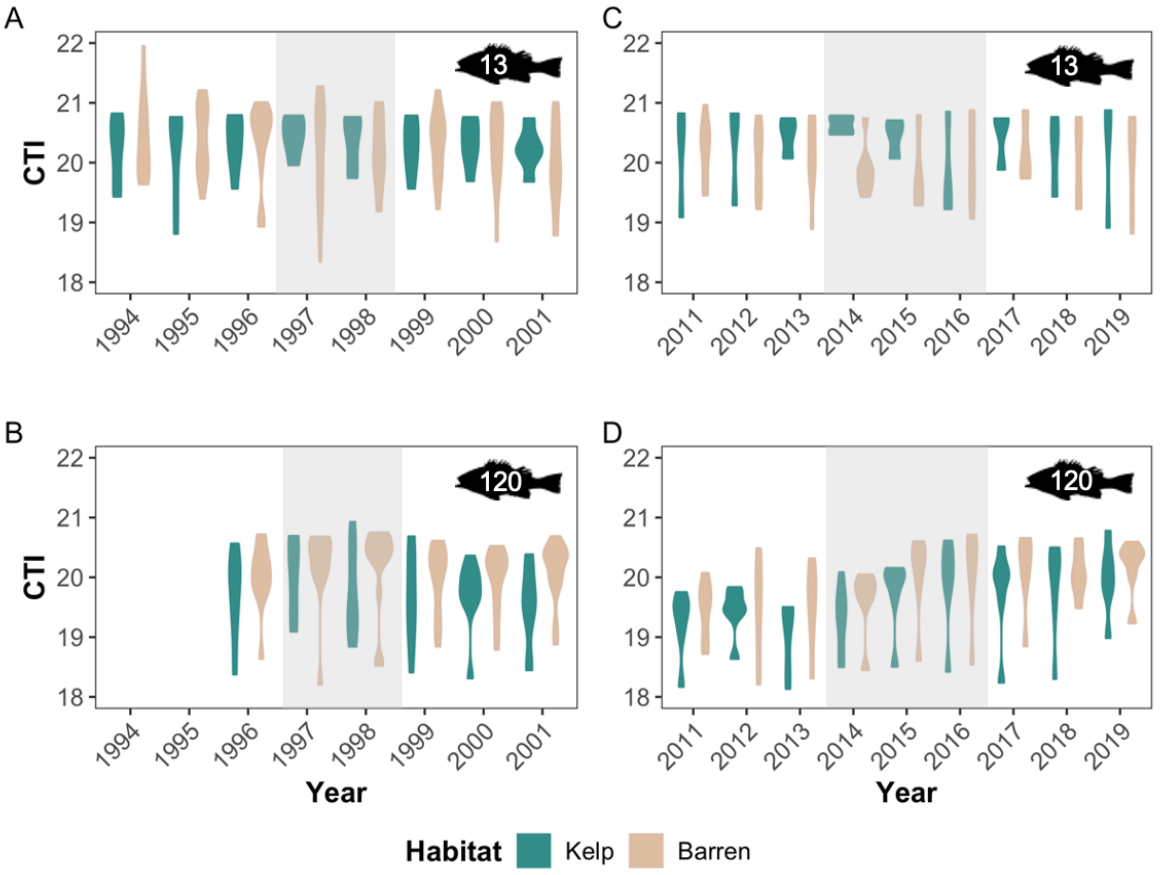

Figure 5.7 Annual differences in community temperature index (CTI) between kelp forested sites (green) and sea urchin barren sites (brown) in the Channel Islands

National Park before, during and after the 1997 – 98 El Niño (A, B) and the 2014 – 16 Heat Blob (C, D). Event years are highlighted by the grey boxes. CTI was calculated for assemblages of 13 indicator fishes (top row) and for the whole fish community (bottom row, >120 fish species observed). Note: monitoring of the whole fish community started in 1996, i.e., only one year prior to the El Niño event.

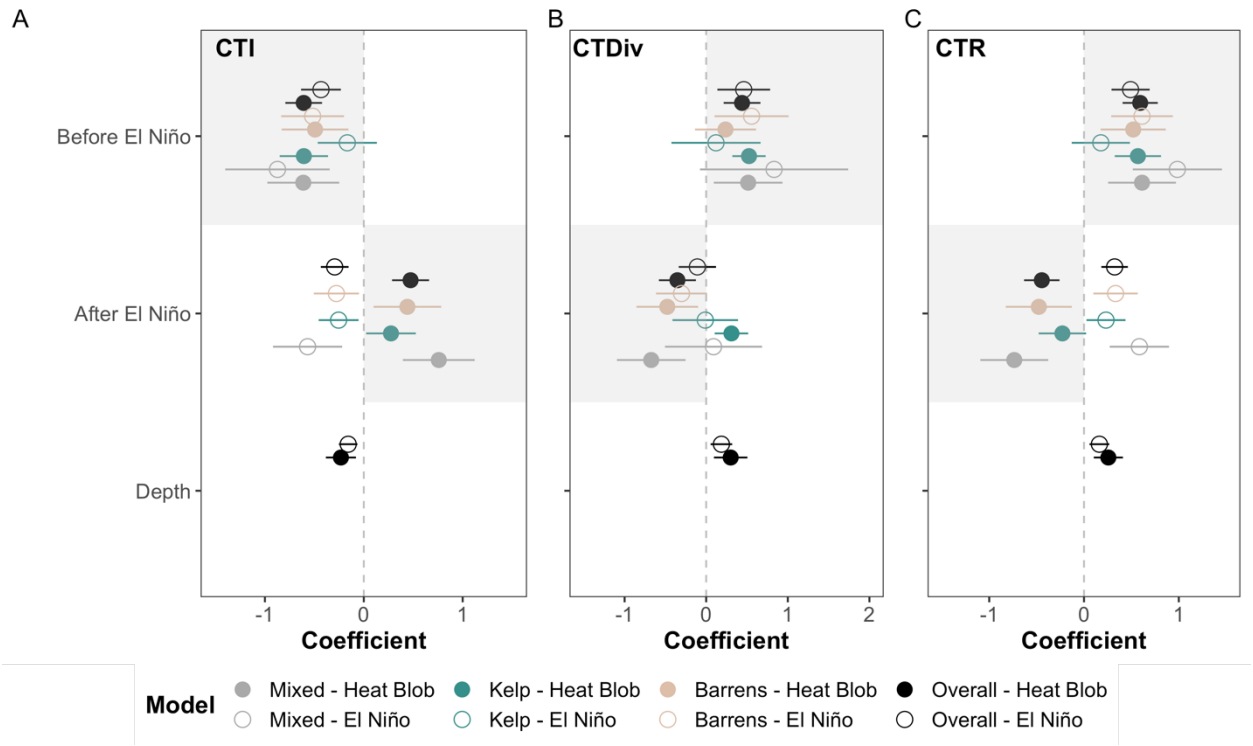

Figure 5.8 Coefficient plots from linear mixed-effect models contrasting the community temperature index (CTI; A), community thermal diversity (CTDiv; B) and community thermal ranges (CTR; C) of the pre-event period (3 years prior to event) and post-event period (3 years after event) to the event period, respectively. CTI, CTDiv and CTR were calculated based on the composition of the whole fish community. Open symbols show model coefficients for the 1997 – 98 El Niño, and filled symbols show coefficients for the 2014 – 16 Heat Blob. An overall (global; black symbols) model was fit for each response, as well as a habitat specific model (brown symbols for sea urchin barrens; green symbols for kelp forests and grey symbols for mixed or patchy habitats). In A, grey shaded areas denote community-level tropicalization signals associated with the event (i.e., lower CTI before the event means a shift towards a more tropical community during the event, and

higher CTI after the event, compared to the event period, means further community tropicalization). In B and C, grey shaded areas show a loss in community thermal diversity and contraction of community thermal ranges associated with the event (i.e., higher CTDiv or CTR before the event mean less thermally diverse communities or communities with smaller thermal ranges, on average, during the event. Lower CTDiv or CTR after the event suggest further declines in CTDiv and CTR, or lack of community recovery). Depth was included as a covariate in all models.

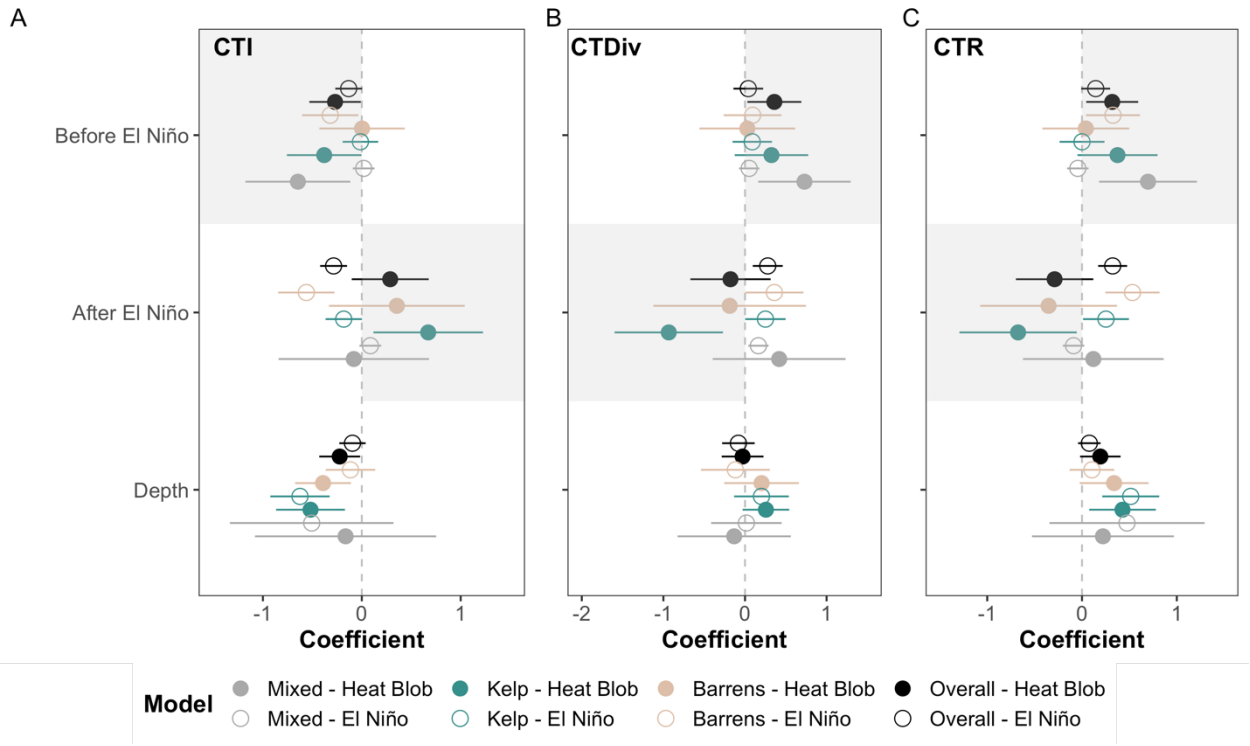

Figure 5.9 Coefficient plots from linear mixed-effect models contrasting the community temperature index (CTI; A), community thermal diversity (CTDiv; B) and community thermal ranges (CTR; C) of the pre-event period (3 years prior to event) and post-event period (3 years after event) to the event period, respectively. CTI, CTDiv and CTR were calculated based on the composition of the indicator species assemblage (13 species). Open symbols show model coefficients for the 1997–98 El Niño, and filled symbols show coefficients for the 2014–16 Heat Blob. An overall (global; black symbols) model was fit for each response, as well as a habitat specific model (brown symbols for sea urchin barrens; green symbols for kelp forests and grey symbols for mixed or patchy habitats). In A, grey shaded areas

denote community-level tropicalization signals associated with the event (i.e., lower CTI before the event means a shift towards a more tropical community during the event, and higher CTI after the event, compared to the event period, means further community tropicalization). In B and C, grey shaded areas show a loss in community thermal diversity and contraction of community thermal ranges associated with the event (i.e., higher CTDiv or CTR before the event mean less thermally diverse communities or communities with smaller thermal ranges, on average, during the event. Lower CTDiv or CTR after the event suggest further declines in CTDiv and CTR, or lack of community recovery). Depth was included as a covariate in all models.

5.4.4 Trait change

Differences in CTI across heat event phases were related to changes in the richness of certain trait groups (supplementary table S8-9), with some consistencies across both events. Both heat events were marked by an increase in benthic fishes, relative to the years prior, with benthic fish richness staying high after the events. Similarly, demersal fishes increased in richness after both events, relative to the pre-event and event phases. After the El Niño, more species of carnivorous fishes were also observed than before or during. During the Heat Blob, herbivorous fishes also increased, while the richness of carnivore and invertivore fishes was lower after the Blob than before and during.

5.5 Discussion

Here, I found that marine heat events can rapidly restructure fish communities in directions consistent with tropicalization and alter the types and characteristics of fishes present for years. Indeed, heat events can have strong ecological impacts and restructure reef communities, either by directly altering the abundance and

distribution of species, or through secondary impacts related to changes in biogenic habitats which I observed here (Smale *et al.* 2013; Oliver *et al.* 2019; Smale 2020).

The two severe heat events that recently impacted the Pacific Northeast (the 1997 – 98 El Niño and the 2014 – 16 Heat Blob) supported fish communities with distinctive thermal compositions. For both events, years of anomalously high seawater temperatures (i.e., marine heat event years) were associated with increases in the community thermal index (CTI) of fishes, relative to the years prior to each event. Overall, marine heat events led to temperature-associated changes in fish community structure, with increased tropicalization during heat event years. Indeed, the Northeast Pacific is vulnerable to changes in thermal community composition (such as CTI change) because of its diverse regional species pool and warming exposure (Burrows *et al.* 2019; Schuster *et al.* 2022). Therefore, observed community composition changes were in line with predictions for this region during two separate events, highlighting that other vulnerable regions (e.g., Southern Australia) are likely to undergo similar community changes during heat events.

During both heat events, community thermal diversity (CTDiv) and thermal ranges (CTR) initially declined. However, increases in both CTDiv and CTR were evident as the El Niño subsided, but not following the Heat Blob (i.e., both CTDiv and CTR continued to decline). Overall, communities shifted towards a composition with more similar species that have narrow, warm-water distributions. The synchronous response of CTDiv and CTR indicates that community tropicalization occurred

through a loss of cold-affinity fishes with broad thermal ranges (which were relatively unique), while those warm-affinity species that were gained had relatively narrower thermal ranges.

Overall, I found that marine heat events can accelerate tropicalization processes, at least temporarily, during both heat events. Fish community tropicalization (CTI increases) involved an influx of more tropical (warm-affinity) fishes and simultaneous decline of cold-affinity fishes. However, gains of warm-affinity fishes played a relatively larger role (compared to losses of cold-affinity fishes). For example, during the El Niño (1997 – 1998), cold-affinity fishes that were lost were only those species with the most extreme cold-affinities, such as *Scorpaenichthys marmoratus* (cabezon), while several warm-affinity fishes were gained. This finding supports that warm temperature anomalies during the marine heat events allowed species with warmer temperature distributions to take advantage of sites with atypically warmer waters. For instance, warm-affinity *Caulolatilus princeps* (ocean whitefish) and *Paralabrax clathratus* (kelp bass), were observed at more sites and in higher abundances during the Heat Blob than before. By contrast, extreme temperatures may have also driven other species to decline in abundance (through emigration or mortality).

While fish species responded to warmer waters in directions consistent with their thermal distributions, the long-term impacts of marine heat events depends on whether the system recovers (Suryan *et al.* 2021). Here, I found a different trajectory of recovery following the El Niño in comparison to the Heat Blob. While

the community thermal composition returned to a pre-heat event state after the El Niño, no recovery was evident after the Heat Blob (at least for the period observed). After the El Niño, the climate of the northeast Pacific rapidly transitioned into a cool-phase, driven by winds that strengthened upwelling (Peterson & Schwing 2003). As a consequence, tropicalization signals did not last beyond the El Niño years, with some of the more tropical species disappearing, while cold-affinity fishes increased four-fold, lowering CTI values again. By contrast, the years following the Heat Blob were marked by continued increases in CTI values, and thus increases in the relative numbers of warm-affinity species. This trend continued despite a drop in seawater temperatures after the Blob subsided, albeit temperatures were still on average 1°C higher than before the Blob. The lack of community recovery following the heat event is likely due to the unmatched spatial and temporal magnitude and severity of this event. The Heat Blob was 2-10 times longer than any other marine heat event recorded globally in the last decade, lasting through all four seasons over several years (Hobday *et al.* 2018; Suryan *et al.* 2021). These findings are therefore consistent with those of previous work showing that reef fish community structures initially track extreme temperature anomalies during marine heat events (Day *et al.* 2018), but furthermore show that heat event recovery, and thus long-term event impact, is idiosyncratic.

Overall, my findings demonstrate that expanding sea urchin barrens support fish communities with distinct structures that alter their resilience to long-term warming (Schuster *et al.* 2022), and to marine heat events in some cases. I found that fish

communities at kelp forested sites appear more resilient (no CTI change) to heat event-induced tropicalization processes in some cases, compared to urchin barrens and patchy, mixed-habitat sites (higher CTI). However, the capacity of kelp forests to limit tropicalization processes may depend on the intensity and duration of the event. For example, while barrens and patchy sites hosted relatively more warm-affinity fishes than kelp sites during the El Niño, sites of any habitat type showed similarly strong tropicalization signals during the Heat Blob, an event that was more severe in magnitude and duration of warm anomalies. Furthermore, large-scale kelp declines occurred during the Heat Blob at several monitoring sites in the park, which had historically stable kelp forests (e.g., Johnson's Lee South and Johnson's Lee North; see supplementary figure S2). Fewer intact kelp forested sites persisted as the Blob progressed to buffer against tropicalization processes. In fact, previously robust kelp forests collapsed into unproductive urchin barrens along 350 km of coastline in northern California in 2014 (Rogers-Bennett & Catton 2019). Thus, as the system entered the Heat Blob, communities had already experienced numerous environmental and biological disturbances that acted as filters and altered the initial state of the biological system (Kraft *et al.* 2015), which may have impacted response diversity and resilience (Beisner *et al.* 2003; Bates *et al.* 2019). In any case, the capacity of kelp forests to provide resilience to tropicalization processes may be impeded by heat event-related increases in urchin densities, as recorded here. High sea urchin numbers further erode forest persistence and can prevent kelp recovery from heat stress (Hart & Scheibling 1988; Rogers-Bennett & Catton 2019). Ongoing tropicalization of temperate

regions may thus be accelerated by marine heat events, sea urchin barren expansion (i.e., kelp loss), or both (Hyndes *et al.* 2016; Vergés *et al.* 2019; Bosch *et al.* 2022; Schuster *et al.* 2022). The same patterns of community tropicalization are emerging repeatedly across space (Cheung *et al.* 2013; Stuart-Smith *et al.* 2015; Burrows *et al.* 2019; Schuster *et al.* 2022) and time, at different temporal scales (acute, extreme events (Day *et al.* 2018) and long-term (Bates *et al.* 2014, 2017)), indicating that space-for-time substitutions are well suited to capture tropicalization processes.

Heat event-related decline of kelp forests (Rogers-Bennett & Catton 2019) can open up foraging space of benthic animals that are usually sheltered by kelp. Changes in thermal composition in the fish communities related to systematic changes in the functional composition of the community. I found increases in benthic fishes during and after both heat events, and increases in demersal fishes after each event. Tropical herbivores that increased during the Blob may also benefit from increased availability of turf algae after kelp removal. In a warming hotspot in Australia, tropical invertivores (Smith *et al.* 2021) and herbivores (Bates *et al.* 2014; Smith *et al.* 2021) are increasing over time, and following large-scale kelp loss (Smith *et al.* 2021). Combined with heat event-related thermal stress, loss of canopy kelp appears to be a major restructuring driver of the fish assemblages in the Channel Islands. For example, *Sebastes atrovirens* declined in occurrence frequency and abundance, and is a canopy-dweller that depends on water-column habitat provided by *Macrocystis pyrifera* (Graham 2004). Previous work also shows

that of the species commonly observed in the Channel Islands, 36% occur more often in forested areas than deforested areas, and 25 species are exclusive to kelp forest sites (Graham 2004).

My findings add to the body of research documenting biological changes following marine heat events, supporting that full recovery of communities and ecosystems after a severe heat event is unlikely. Beyond fish community tropicalization signals demonstrated here, tropical pyrosomes (pelagic tunicates) expanded their range into the northeast Pacific during the Blob (Sutherland *et al.* 2018), microzooplankton communities shifted towards more gelatinous taxa (Brodeur *et al.* 2019) and disease outbreaks nearly extirpated predatory sea stars such as *Pycnopodia helianthoides* (Harvell *et al.* 2022). Sea star wasting disease and associated sea star die-offs have driven further ecosystem changes because *P. helianthoides* is a major sea urchin predator (Moitoza & Phillips 1979; Eckert *et al.* 1999). Indeed, sea urchin densities increased significantly in the Channel Islands after both heat events, especially at the western-most (warmest) islands, which may relate to the loss of species which feed on urchins or graze larval recruits. Trophic cascades, where sea star declines resulted in exploding urchin populations and collapse of kelp forests, were recorded throughout the northeast Pacific following the Heat Blob (Schultz *et al.* 2016; Miner *et al.* 2018; Suryan *et al.* 2021).

Marine heat events, such as the 1997 – 98 El Niño and 2014 – 16 Heat Blob, are emerging as powerful drivers of marine community and ecosystem change, with longer-term impacts that extend beyond the event duration. While anthropogenic

climate change and associated slow warming is gradually reorganizing the dynamics of life on the planet, extreme events can rapidly restructure communities in similar directions. Here, I demonstrate accelerated community tropicalization during two separate heat events, with different trajectories of recovery related to event magnitude and environmental conditions as each event subsided. Furthermore, the prevalence of sea urchin barrens can exacerbate tropicalization processes during marine heat events, while healthy, intact kelp forests may buffer against tropicalization to some extent. Long-term monitoring programs, such as the Channel Islands National Park program, are critical to observe, assess, understand and eventually predict the ecological consequences of heat events.

5.6 References

Arafeh-Dalmau, N., Montaño-Moctezuma, G., Martínez, J.A., Beas-Luna, R., Schoeman, D.S. & Torres-Moye, G. (2019). Extreme Marine Heatwaves Alter Kelp Forest Community Near Its Equatorward Distribution Limit. *Front. Mar. Sci.*, 6.

Atkin, O.K., Bloomfield, K.J., Reich, P.B., Tjoelker, M.G., Asner, G.P., Bonal, D., *et al.* (2015). Global variability in leaf respiration in relation to climate, plant functional types and leaf traits. *New Phytol.*, 206, 614–636.

Bates, A.E., Barrett, N.S., Stuart-Smith, R.D., Holbrook, N.J., Thompson, P.A. & Edgar, G.J. (2014). Resilience and signatures of tropicalization in protected reef fish communities. *Nat. Clim. Chang.*, 4, 62–67.

Bates, A.E., Cooke, R.S.C., Duncan, M.I., Edgar, G.J., Bruno, J.F., Benedetti-Cecchi, L., *et al.* (2019). Climate resilience in marine protected areas and the 'Protection Paradox.' *Biol. Conserv.*, 236, 305–314.

Bates, A.E., Stuart-smith, R.D., Barrett, N.S. & Edgar, G.J. (2017). Biological

interactions both facilitate and resist climate-related functional change in temperate reef communities. *Proc. R. Soc. B Biol. Sci.*, 284.

Beisner, B.E., Haydon, D.T. & Cuddington, K. (2003). Alternative stable states in ecology. *Front. Ecol. Environ.*, 1, 376–382.

Bjerknes, J. (1966). A possible response of the atmospheric Hadley circulation to equatorial anomalies of ocean temperature. *Tellus*, 18(4), 820-829.

Bond, N.A., Cronin, M.F., Freeland, H. & Mantua, N. (2015). Causes and impacts of the 2014 warm anomaly in the NE Pacific. *Geophys. Res. Lett.*, 42, 3414–3420.

Bosch, N.E., McLean, M., Zarco-Perello, S., Bennett, S., Stuart-Smith, R.D., Vergés, A., *et al.* (2022). Persistent thermally-driven shift in the functional trait structure of herbivorous fishes: evidence of top-down control on the rebound potential of temperate seaweed forests? *Glob. Chang. Biol.*, 28, 2296–2311.

Brodeur, R.D., Auth, T.D. & Phillips, A.J. (2019). Major Shifts in Pelagic Micronekton and Macrozooplankton Community Structure in an Upwelling Ecosystem Related to an Unprecedented Marine Heatwave. *Front. Mar. Sci.*, 6, 1–15.

Burrows, M.T., Bates, A.E., Costello, M.J., Edwards, M., Edgar, G.J., Fox, C.J., *et al.* (2019). Ocean community warming responses explained by thermal affinities and temperature gradients. *Nat. Clim. Chang.*, 9, 959–963.

Caselle, J.E., Rassweiler, A., Hamilton, S.L. & Warner, R.R. (2015). Recovery trajectories of kelp forest animals are rapid yet spatially variable across a network of temperate marine protected areas. *Sci. Rep.*, 5, 14102.

Chamberlain, S. (2021). spocc: Interface to species occurrence data sources.

Cheung, W.W.L. & Frölicher, T.L. (2020). Marine heatwaves exacerbate climate change impacts for fisheries in the northeast Pacific. *Sci. Rep.*, 10, 6678.

Cheung, W.W.L., Watson, R. & Pauly, D. (2013). Signature of ocean warming in global fisheries catch. *Nature*, 497, 365–368.

Davis, G., Richards, D. & Kushner, D. (1996). *Kelp forest monitoring design review.* Channel Islands National Park, California, USA.

Day, P.B., Stuart-Smith, R.D., Edgar, G.J. & Bates, A.E. (2018). Species' thermal ranges predict changes in reef fish community structure during 8 years of extreme temperature variation. *Divers. Distrib.*, 24, 1036–1046.

Eckert, G.L., Engle, J.M. & Kushner, D.J. (1999). Sea star disease and population declines at the Channel Islands. *Proc 5th Calif. Isl. Symp.*, 5, 390–393.

Edwards, M.S. (2004). Estimating scale-dependency in disturbance impacts: El Niños and giant kelp forests in the northeast Pacific. *Oecologia*, 138, 436–447.

Freedman, R.M., Brown, J.A., Caldow, C. & Caselle, J.E. (2020). Marine protected areas do not prevent marine heatwave-induced fish community structure changes in a temperate transition zone. *Sci. Rep.*, 10, 21081.

Gelpi, C.G. & Norris, K.E. (2008). Seasonal temperature dynamics of the upper ocean in the Southern California Bight. *J. Geophys. Res. Ocean.*, 113, 1–18.

Graham, M.H. (2004). Effects of Local Deforestation on the Diversity and Structure of Southern California Giant Kelp Forest Food Webs. *Ecosystems*, 7, 341–357.

Hardy, N.A., Lamare, M., Uthicke, S., Wolfe, K., Doo, S., Dworjanyn, S., *et al.* (2014). Thermal tolerance of early development in tropical and temperate sea urchins: inferences for the tropicalization of eastern Australia. *Mar. Biol.*, 161, 395–409.

Hart, M.W. & Scheibling, R.E. (1988). Heat waves, baby booms, and the destruction of kelp beds by sea urchins. *Mar. Biol.*, 99, 167–176.

Harvell, C.D., Montecino-Latorre, D., Caldwell, J.M., Burt, J.M., Bosley, K., Keller, A., *et al.* (2022). Disease epidemic and a marine heat wave are associated with the continental-scale collapse of a pivotal predator (*Pycnopodia helianthoides*). *Sci. Adv.*, 5, eaau7042.

Hobday, A.J., Oliver, E.C.J., Gupta, A. Sen, Benthuysen, J.A., Burrows, M.T., Donat, M.G., *et al.* (2018). Categorizing and naming marine heatwaves. *Oceanography*, 31, 162–173.

Holbrook, N.J., Scannell, H.A., Gupta, A. Sen, Benthuysen, J.A., Feng, M., Oliver, E.C.J., *et al.* (2019). A global assessment of marine heatwaves and their drivers. *Nat. Commun.*, 10, 1–13.

Hyndes, G.A., Heck Jr., K.L., Vergés, A., Harvey, E.S., Kendrick, G.A., Lavery, P.S., *et al.* (2016). Accelerating Tropicalization and the Transformation of Temperate Seagrass Meadows. *Bioscience*, 66, 938–948.

Kraft, N.J.B., Adler, P.B., Godoy, O., James, E.C., Fuller, S. & Levine, J.M. (2015). Community assembly, coexistence and the environmental filtering metaphor. *Funct. Ecol.*, 29, 592–599.

Kushner, D.J., Rassweiler, A., McLaughlin, J.P. & Lafferty, K.D. (2013). A multi-decade time series of kelp forest community structure at the California Channel Islands. *Ecology*, 94, 2655.

Di Lorenzo, E. & Mantua, N. (2016). Multi-year persistence of the 2014/15 North Pacific marine heatwave. *Nat. Clim. Chang.*, 6, 1042–1047.

Miner, C.M., Burnaford, J.L., Ambrose, R.F., Antrim, L., Bohlmann, H., Blanchette, C.A., *et al.* (2018). Large-scale impacts of sea star wasting disease (SSWD) on intertidal sea stars and implications for recovery. *PLoS One*, 13, e0192870.

Minuti, J.J., Byrne, M., Campbell, H., Hemraj, D.A. & Russell, B.D. (2022). Live-fast-die-young: Carryover effects of heatwave-exposed adult urchins on the development of the next generation. *Glob. Chang. Biol.*, n/a.

Moitoza, D.J. & Phillips, D.W. (1979). Prey defense, predator preference, and nonrandom diet: The interactions between *Pycnopodia helianthoides* and two species of sea urchins. *Mar. Biol.*, 53, 299–304.

Ñiquen, M. & Bouchon, M. (2004). Impact of El Niño events on pelagic fisheries in Peruvian waters. *Deep Sea Res. Part II Top. Stud. Oceanogr.*, 51, 563–574.

Oliver, E.C.J., Burrows, M.T., Donat, M.G., Sen Gupta, A., Alexander, L. V, Perkins-Kirkpatrick, S.E., *et al.* (2019). Projected Marine Heatwaves in the 21st Century and the Potential for Ecological Impact. *Front. Mar. Sci.*, 6, 1–12.

Peterson, W.T. & Schwing, F.B. (2003). A new climate regime in northeast pacific ecosystems. *Geophys. Res. Lett.*, 30.

Pinheiro, J., Bates, D., DebRoy, S., Sarkar, D. & Team, R. (2015). nlme: linear and nonlinear mixed effects models.

Pinsky, M.L., Worm, B., Fogarty, M.J., Sarmiento, J.L. & Levin, S.A. (2013). Marine Taxa Track Local Climate Velocities. *Science (80-.).*, 341, 1239 LP – 1242.

R Core Team. (2014). R: a language and environment for statistical computing.

Rogers-Bennett, L. & Catton, C.A. (2019). Marine heat wave and multiple stressors tip bull kelp forest to sea urchin barrens. *Sci. Rep.*, 9, 15050.

Schultz, J.A., Cloutier, R.N. & Côté, I.M. (2016). Evidence for a trophic cascade on rocky reefs following sea star mass mortality in British Columbia. *PeerJ*, 4, e1980.

Schuster, J.M., Stuart-Smith, R.D., Edgar, G.J. & Bates, A.E. (2022). Tropicalization of temperate reef fish communities facilitated by urchin grazing and diversity of thermal affinities. *Glob. Ecol. Biogeogr.*, 31, 995–1005.

Smale, D.A. (2020). Impacts of ocean warming on kelp forest ecosystems. *New Phytol.*, 225, 1447–1454.

Smale, D.A., Burrows, M.T., Moore, P., Connor, N.O. & Hawkins, S.J. (2013). Threats and knowledge gaps for ecosystem services provided by kelp forests : a northeast Atlantic perspective, 2090.

Smith, S.M., Malcolm, H.A., Marzinelli, E.M., Schultz, A.L., Steinberg, P.D. & Vergés, A. (2021). Tropicalization and kelp loss shift trophic composition and lead to more winners than losers in fish communities. *Glob. Chang. Biol.*, 27, 2537–2548.

Stuart-Smith, R.D., Bates, A.E., Lefcheck, J.S., Duffy, J.E., Baker, S.C., Thomson, R.J., *et al.* (2013). Integrating abundance and functional traits reveals new global hotspots of fish diversity. *Nature*, 501, 539–542.

Stuart-Smith, R.D., Brown, C.J., Ceccarelli, D.M. & Edgar, G.J. (2018). Ecosystem restructuring along the Great Barrier Reef following mass coral bleaching. *Nature*, 560, 92–96.

Stuart-Smith, R.D., Edgar, G.J., Barrett, N.S., Kininmonth, S.J. & Bates, A.E. (2015). Thermal biases and vulnerability to warming in the world's marine fauna. *Nature*, 628, 88–104.

Stuart-Smith, R.D., Mellin, C., Bates, A.E. & Edgar, G.J. (2021). Habitat loss and range shifts contribute to ecological generalisation amongst reef fishes. *Nat. Ecol. Evol.*, 5, 656–662.

Suryan, R.M., Arimitsu, M.L., Coletti, H.A., Hopcroft, R.R., Lindeberg, M.R., Barbeaux, S.J., *et al.* (2021). Ecosystem response persists after a prolonged marine heatwave. *Sci. Rep.*, 11, 6235.

Sutherland, K.R., Sorensen, H.L., Blondheim, O.N., Brodeur, R.D. & Galloway, A.W.E. (2018). Range expansion of tropical pyrosomes in the northeast Pacific Ocean. *Ecology*, 99, 2397–2399.

Tegner, M.J. & Dayton, P. (1991). Sea urchins, El Ninos, and the long term stability of Southern California kelp forest communities. *Mar. Ecol. Prog. Ser.*, 77, 49–63.

Tegner, M.J. & Dayton, P.K. (1987). El Nino effects on southern California kelp forest communities. *Adv. Ecol. Res.*, 17, 243–279.

Vergés, A., McCosker, E., Mayer-Pinto, M., Coleman, M.A., Wernberg, T., Ainsworth, T., *et al.* (2019). Tropicalisation of temperate reefs: Implications for ecosystem functions and management actions. *Funct. Ecol.*, 33, 1000–1013.

Vergés, A., Steinberg, P.D., Hay, M.E., Poore, A.G.B., Campbell, A.H., Ballesteros, E., *et al.* (2014). The tropicalization of temperate marine ecosystems: climate-mediated changes in herbivory and community phase shifts. *Proc. R. Soc. B Biol. Sci.*, 281.

Wernberg, T., Bennett, S., Babcock, R.C., de Bettignies, T., Cure, K., Depczynski, M., *et al.* (2016). Climate-driven regime shift of a temperate marine ecosystem. *Science (80)*, 353, 169–172.

Winant, C.D. & Bratkovich, A.W. (1981). Temperature and Currents on the Southern California Shelf: A Description of the Variability. *J. Phys. Oceanogr.*, 11, 71–86.

Yang, S., Li, Z., Yu, J. Y., Hu, X., Dong, W., & He, S. (2018). El Niño–Southern Oscillation and its impact in the changing climate. *National Science Review*, 5(6), 840-857.

5.7 Appendix E – Supplementary figures and tables for Chapter 5

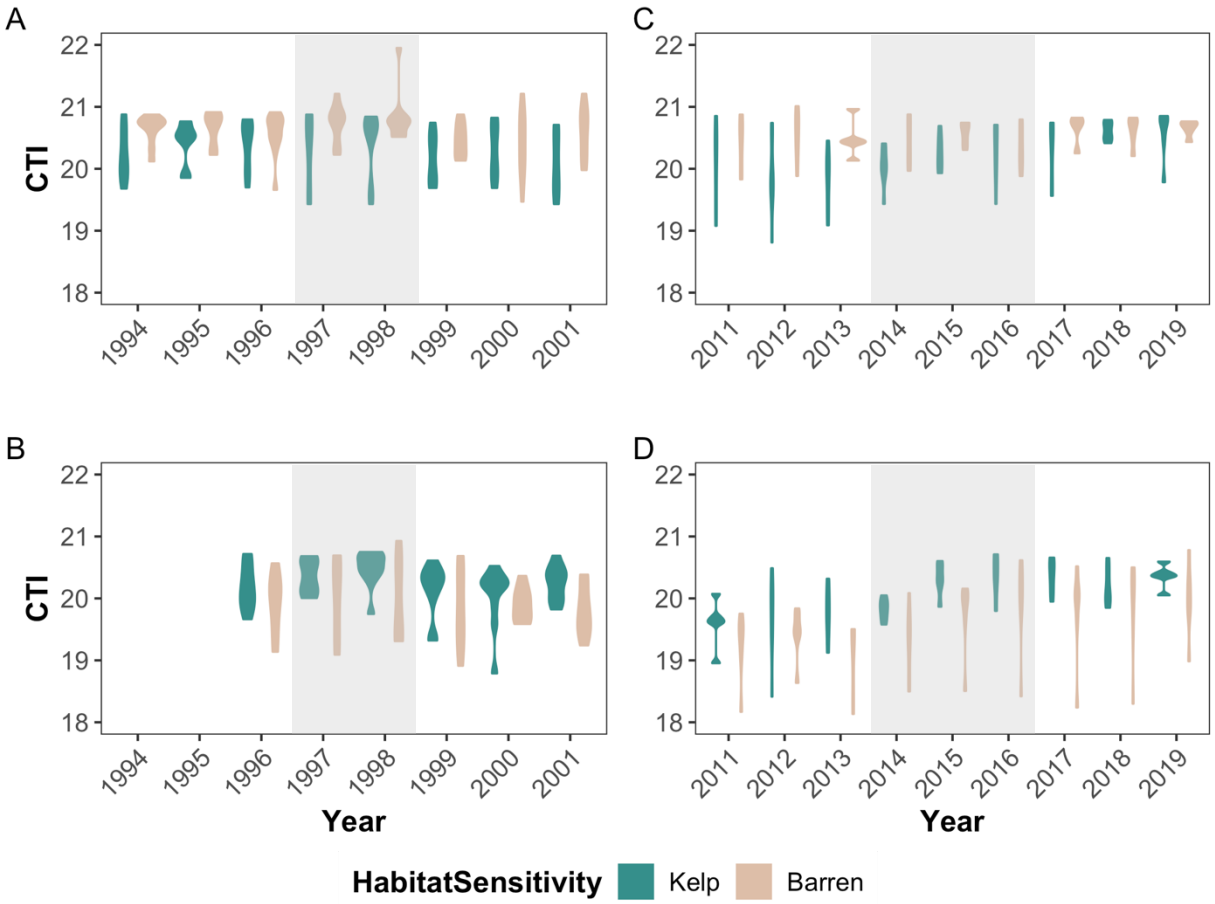

Figure S1. Sensitivity analysis showing annual differences in community temperature index (CTI) between kelp forested sites (green) and sea urchin barren sites (brown) in the Channel Islands National Park before, during and after the 1997-98 El Niño (A, B) and the 2014-16 Heat Blob (C, D). CTI changes across event phases are robust to a higher urchin density and kelp stipe threshold (6 urchins per m^2 and 80 stipes per site) used here (i.e., compare to Figure 3.7). CTI was calculated for assemblages of 13 indicator fishes (top row) and for the whole fish community (bottom row, >120 fish species observed). Event years are highlighted by the grey boxes. Note: monitoring of the whole fish community started in 1996, i.e., only one year prior to the El Niño event.

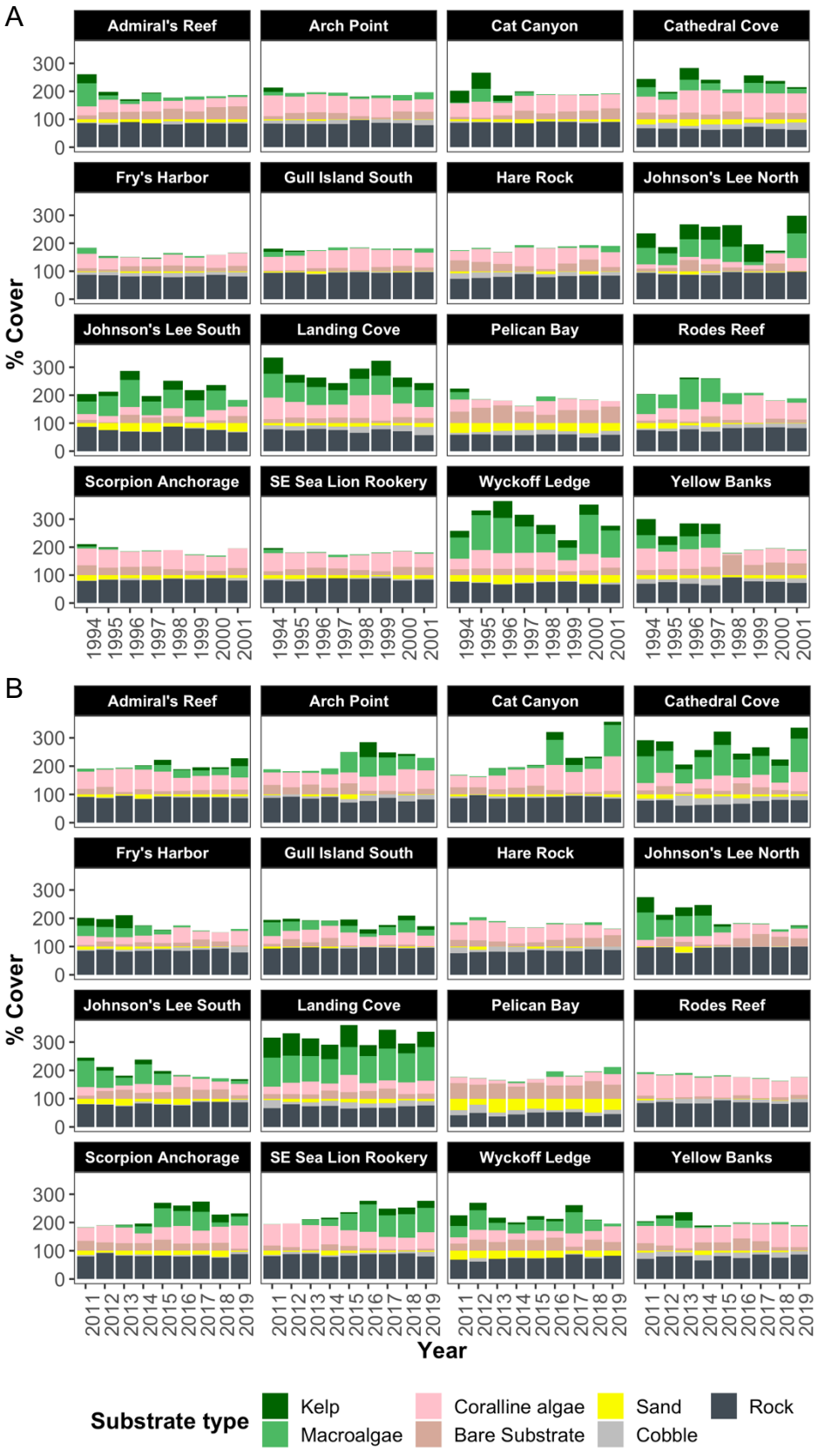
A
Admiral's Reef
Arch Point
Cat Canyon
Cathedral Cove
Fry's Harbor
Gull Island South
Hare Rock
Johnson's Lee North
Johnson's Lee South
Landing Cove
Pelican Bay
Rodes Reef
Scorpion Anchorage
SE Sea Lion Rookery
Wyckoff Ledge
Yellow Banks
% Cover
0
100
200
300
1994
1995
1996
1997
1998
1999
2000
2001
B
2011
2012
2013
2014
2015
2016
2017
2018
2019
Year
Substrate type
Kelp
Macroalgae
Coralline algae
Bare Substrate
Sand
Cobble
Rock

Figure S2. Substrate composition at the 16 long-term monitoring sites in the Channel Islands National Park, California, USA in the years before, during and after the 1997-98 El Niño (A) and the 2014-16 Heat Blob (B). Percent cover of each substrate category is shown for three years before and after each event. See table S1 for a full list of monitored substrates and algae species and how they were subsequently classified into the 7 categories shown here.

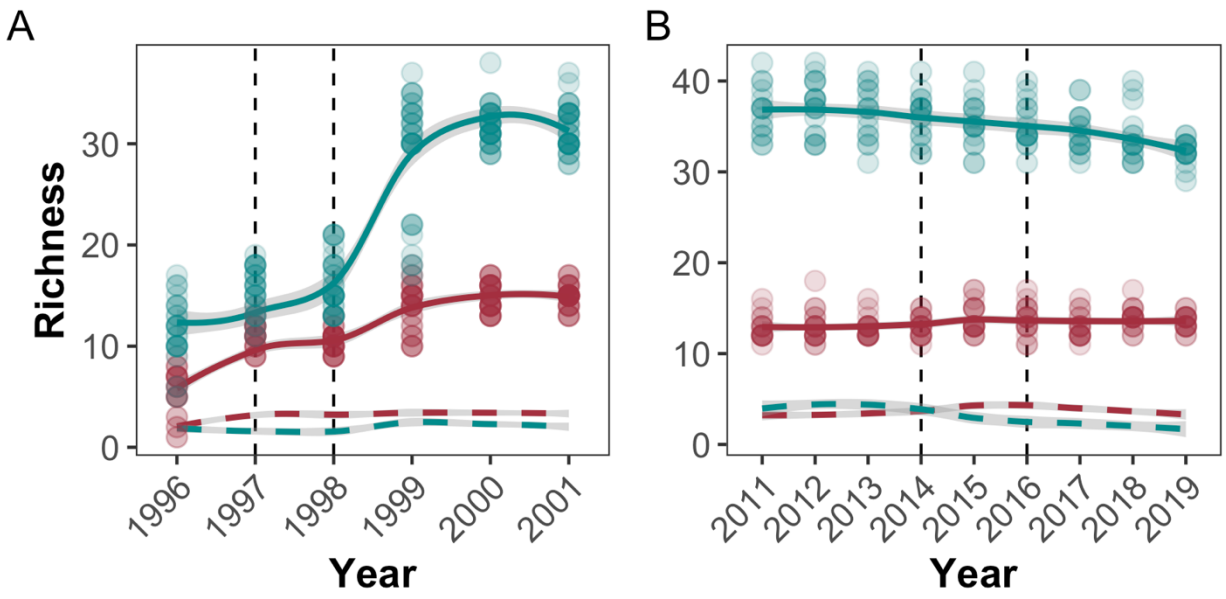

Figure S3. Changes in species richness of warm-affinity (red lines and dots) and cold-affinity fishes (blue lines and dots) across event periods of two severe heat events in the Channel Islands National Park: the 1997-98 El Niño (A) and the 2014-16 Heat Blob (B). Solid lines show the richness of warm- and cold-affinity fishes when classified based on upper and lower quantiles (25th and 75th percentile), dashed lines show richness of extreme warm- and cold-affinity fishes, classified based on upper and lower deciles (10th and 90th percentile). Lines show richness trends of each group over time, fitted by linear mixed effects models (LME). Shaded areas are 95% confidence intervals predicted by LMEs. Dashed black vertical lines mark the start and end of each heat event period.

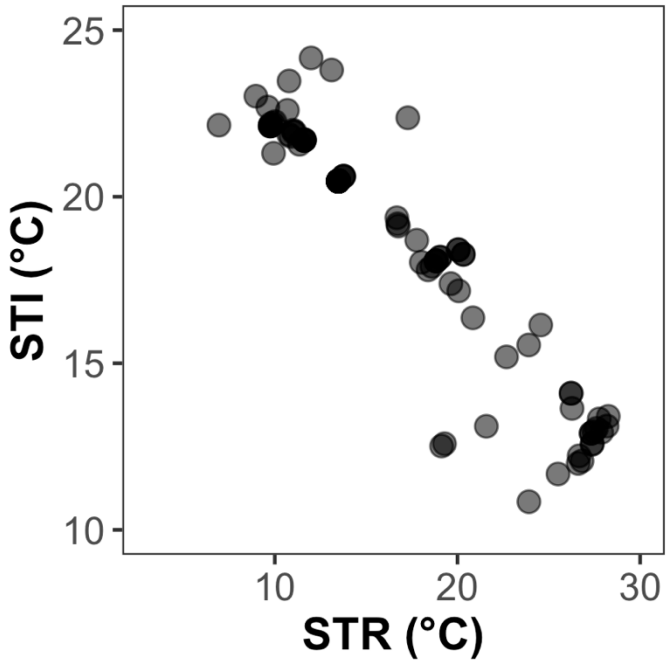

Figure S4. Relationship between species thermal index (STI; midpoint of species' thermal range) and species thermal ranges (STR) of fishes observed in the Channel Islands National Park's monitoring program. Each data point represents a unique species (N = 94). Species with warmer affinities have relatively narrow thermal ranges, while species with colder affinities have relatively broad thermal ranges.

Table S1. Habitat classification of the 16 long-term monitoring sites in the Channel Islands National Park, California, USA. We combined sea urchin densities and adult *Macrocystis* kelp stipe counts to classify sites as healthy kelp forests ('kelp'), sea urchin barrens ('barren') and sites that are neither, or patchy ('mixed'). Sites were classified based on urchin densities and stipe counts in the 3 years prior to the 1997-98 El Niño and the 2014-16 Heat Blob.

Island	Site Name	Event	Habitat classification
Santa Barbara Island	Cat Canyon	El Niño	Mixed
		Heat Blob	Barren
	SE Sea Lion Rookery	El Niño	Barren
		Heat Blob	Barren
	Arch Point	El Niño	Barren
		Heat Blob	Barren
Anacapa Island	Admiral's Reef	El Niño	Mixed
		Heat Blob	Mixed
	Cathedral Cove	El Niño	Mixed
		Heat Blob	Kelp
	Landing Cove	El Niño	Kelp
		Heat Blob	Kelp
Santa Cruz Island	Yellow Banks	El Niño	Kelp
		Heat Blob	Mixed
	Gull Island South	El Niño	Barren
		Heat Blob	Mixed
	Fry's Harbor	El Niño	Barren
		Heat Blob	Kelp
	Pelican Bay	El Niño	Barren
		Heat Blob	Barren
	Scorpion Anchorage	El Niño	Barren
		Heat Blob	Barren
Santa Rosa Island	Rodes Reef	El Niño	Mixed
		Heat Blob	Mixed
	Johnson's Lee North	El Niño	Kelp
		Heat Blob	Kelp
	Johnson's Lee South	El Niño	Kelp
		Heat Blob	Kelp
San Miguel Island	Wyckoff Ledge	El Niño	Kelp
		Heat Blob	Kelp

	Hare Rock	El Niño	Barren
		Heat Blob	Barren

Table S2. Organisms sampled by the Random Point Contacts (RPCs) protocol in the Channel Islands National Park. Species and common names are shown as recorded by the RPCs protocol. The third column provides the final substrate categories assigned for this analysis. Invertebrates and microscopic plants (e.g., diatoms) were excluded from habitat classification. Macroalgae within the order Laminariales were classified as 'Kelp'.

Species Name	Common Name	Substrate category
Algae		
green algae		Macroalgae
other brown algae		Macroalgae
Desmarestia spp.	acid weed	Macroalgae
Cystoseira spp.	bladder chain kelp	Macroalgae
Macrocystis pyrifera	giant kelp	Kelp
Eisenia arborea	southern sea palm	Kelp
Pterygophora californica	California sea palm	Kelp
Laminaria farlowii	oar weed	Kelp
Sargassum horneri	Sargassum	Macroalgae
other red algae		Macroalgae
articulated coralline algae		Coralline algae
encrusting coralline algae		Coralline algae
Gelidium spp.	agar weed	Macroalgae
Gigartina spp.	sea tongue	Macroalgae
miscellaneous plants	e.g. diatoms, Phyllospadix, etc.	Excluded
Invertebrates		
Astrangia lajollaensis	La Jolla cup coral	Excluded
Balanophyllia elegans	orange cup coral	Excluded
Diopatra ornata	ornate tube worm	Excluded
Phragmatopoma californica	colonial sand-tube worm	Excluded
Serpulorbis squamigerus	scaled tube snail	Excluded

Corynactis californica	strawberry anemone	Excluded
Diaperoecia californica	southern staghorn bryozoan	Excluded
Pachythyone rubra	red sea cucumber	Excluded
Ophiothrix spiculata	spiny brittle star	Excluded
other bryozoans		Excluded
tunicates		Excluded
sponges		Excluded
miscellaneous invertebrates		Excluded
Bare	No cover; devoid of living organisms	Bare Substrate
Substrate		
rock	larger than fist-sized	Rock
cobble	free-moving, less than fist-sized	Cobble
sand	sediment you can push finger in up to first knuckle	Sand

Table S3. Summary table for statistical tests of response of whole-community fish CTI (a, b), CTDiv (c,d) and CTR (e, f). We fit linear mixed effect models (LME, mgcv package) with the function lme in R. Random effects of site nested in island are included to account for the spatial structure of the data. Heat event status (before, during and after event) was included as a fixed effect, with years before and after the event contrasted against event years. A depth covariate was also included. Fixed effects were scaled for coefficient comparison. A variance function was included to model heteroscedasticity among the 5 islands. AIC = Akaine information criterion; Std. error = standard error.

g) **1997-98 El Niño Fish CTI**

Random effects

~1| Island:	1.132
~1| Island/Site:	0.130
Residual:	0.572
AIC:	268.36

Variance function

Santa Barbara Island	1.000
Anacapa Island	0.618
Santa Cruz Island	0.626
Santa Rosa Island	0.815
San Miguel Island	1.100

LME	Estimated value	Std. Error	DF	t-value	p-value
Intercept	-0.005	0.511	155	-0.009	0.993
Before El Niño	-0.433	0.103	155	-4.217	<0.001
After El Niño	-0.294	0.072	155	-4.107	<0.001
Depth	-0.158	0.048	10	-3.306	0.008

b) 2014-16 Heat Blob Fish CTI

Random effects

~1| Island:	0.885
~1| Island/Site:	0.244
Residual:	0.562
AIC:	266.56

Variance function

Santa Barbara Island	1.000
Anacapa Island	0.779
Santa Cruz Island	0.929

Santa Rosa Island 0.792
San Miguel Island 0.702

LME	Estimated value	Std. Error	DF	t-value	p-value
Intercept	-0.116	0.406	130	-0.286	0.776
Before Heat Blob	-0.608	0.095	130	-6.412	<0.001
After Heat Blob	0.473	0.096	130	4.952	<0.001
Depth	-0.232	0.078	10	-2.981	0.014

c) 1997-98 El Niño Fish CTDiv

Random effects
~1| Island: 0.802
~1| Island/Site: 0.156
Residual: 1.002
AIC: 429.03

Variance function
Santa Barbara Island 1.000
Anacapa Island 0.690
Santa Cruz Island 0.663
Santa Rosa Island 0.837
San Miguel Island 0.433

LME	Estimated value	Std. Error	DF	t-value	p-value
Intercept	0.162	0.374	155	0.433	0.666
Before El Niño	0.460	0.165	155	2.792	0.006
After El Niño	-0.108	0.117	155	-0.931	0.354
Depth	0.187	0.068	10	2.762	0.020

d) 2014-16 Heat Blob Fish CTDiv

Random effects
~1| Island: 0.675
~1| Island/Site: 0.338
Residual: 0.872
AIC: 334.21

Variance function
Santa Barbara Island 1.000
Anacapa Island 0.700

Santa Cruz Island 0.762
Santa Rosa Island 0.591
San Miguel Island 0.428

LME	Estimated value	Std. Error	DF	t-value	p-value
Intercept	0.098	0.326	130	0.301	0.764
Before Heat Blob	0.439	0.115	130	3.822	<0.001
After Heat Blob	-0.353	0.116	130	-3.048	0.003
Depth	0.300	0.105	10	2.865	0.017

e) 1997-98 El Niño Fish CTR

Random effects
~1| Island: 1.000
~1| Island/Site: 0.622
Residual: 0.703
AIC: 267.19

Variance function
Santa Barbara Island 1.000
Anacapa Island 0.622
Santa Cruz Island 0.703
Santa Rosa Island 0.872
San Miguel Island 1.169

LME	Estimated value	Std. Error	DF	t-value	p-value
Intercept	-0.026	0.505	155	-0.051	0.959
Before El Niño	0.491	0.103	155	4.781	<0.001
After El Niño	0.323	0.071	155	4.520	<0.001
Depth	0.162	0.053	10	3.033	0.013

f) 2014-16 Heat Blob Fish CTR

Random effects
~1| Island: 0.872
~1| Island/Site: 0.251
Residual: 0.579
AIC: 266.13

Variance function
Santa Barbara Island 1.000

Anacapa Island	0.812
Santa Cruz Island	0.852
Santa Rosa Island	0.753
San Miguel Island	0.683

LME	Estimated value	Std. Error	DF	t-value	p-value
Intercept	0.106	0.401	130	0.265	0.792
Before Heat Blob	0.593	0.095	130	6.257	<0.001
After Heat Blob	-0.445	0.096	130	-4.663	<0.001
Depth	0.257	0.079	10	3.269	0.008

Table S4. Summary table for statistical tests of response of indicator fish species CTI (a, b), CTDiv (c,d) and CTR (e, f). We fit linear mixed effect models (LME, mgcv package) with the function lme in R. Random effects of site nested in island are included to account for the spatial structure of the data. Heat event status (before, during and after event) was included as a fixed effect, with years before and after the event contrasted against event years. A depth covariate was also included. Fixed effects were scaled for coefficient comparison. A variance function was included to model heteroscedasticity among the 5 islands. AIC = Akaine information criterion; Std. error = standard error.

a) 1997-98 El Niño Indicator Fish CTI

<u>Random effects</u>

~1| Island:	0.924
~1| Island/Site:	0.213
Residual:	0.426
AIC:	451.47

<u>Variance function</u>

Santa Barbara Island	1.000
Anacapa Island	0.585
Santa Cruz Island	1.347
Santa Rosa Island	1.768
San Miguel Island	2.176

LME	Estimated value	Std. Error	DF	t-value	p-value
Intercept	0.063	0.423	235	0.149	0.882

Before El Niño	-0.133	0.069	235	-1.926	0.055
After El Niño	-0.285	0.069	235	-4.107	<0.001
Depth	-0.094	0.068	10	-1.387	0.196

b) 2014-16 Heat Blob Indicator Fish CTI

Random effects

~1| Island:	0.544
~1| Island/Site:	0.260
Residual:	0.531
AIC:	364.82

Variance function

Santa Barbara Island	1.000
Anacapa Island	1.021
Santa Cruz Island	1.203
Santa Rosa Island	1.983
San Miguel Island	1.870

LME	Estimated value	Std. Error	DF	t-value	p-value
Intercept	-0.090	0.272	131	-0.330	0.742
Before Heat Blob	-0.244	0.129	131	-1.898	0.059
After Heat Blob	0.463	0.132	131	3.509	<0.001
Depth	-0.185	0.090	10	-2.060	0.066

c) 1997-98 El Niño Indicator Fish CTDiv

Random effects

~1| Island:	0.576
~1| Island/Site:	0.327
Residual:	0.385
AIC:	589.70

Variance function

Santa Barbara Island	1.000
Anacapa Island	1.054
Santa Cruz Island	2.377
Santa Rosa Island	2.562
San Miguel Island	2.715

LME	Estimated value	Std. Error	DF	t-value	p-value
Intercept	-0.071	0.284	234	-0.250	0.803
Before El Niño	0.040	0.093	234	0.432	0.666
After El Niño	0.279	0.094	234	2.974	0.003
Depth	-0.081	0.102	10	-0.795	0.445

d) 2014-16 Heat Blob Indicator Fish CTDiv

Random effects

~1| Island:	<0.001
~1| Island/Site:	0.405
Residual:	0.871
AIC:	330.32

Variance function

Santa Barbara Island	1.000
Anacapa Island	0.784
Santa Cruz Island	0.874
Santa Rosa Island	1.315
San Miguel Island	1.482

LME	Estimated value	Std. Error	DF	t-value	p-value
Intercept	-0.178	0.158	95	-1.123	0.264
Before Heat Blob	0.360	0.169	95	2.132	0.036
After Heat Blob	-0.178	0.251	95	-0.709	0.480
Depth	-0.029	0.131	10	-0.225	0.826

e) 1997-98 El Niño Indicator Fish CTR

Random effects

~1| Island:	0.908
~1| Island/Site:	0.174
Residual:	0.401
AIC:	478.99

Variance function

Santa Barbara Island	1.000
Anacapa Island	0.783
Santa Cruz Island	1.515
Santa Rosa Island	1.895

San Miguel Island 2.528

LME	Estimated value	Std. Error	DF	t-value	p-value
Intercept	-0.079	0.415	235	-0.189	0.850
Before El Niño	0.145	0.078	235	1.868	0.063
After El Niño	0.323	0.078	235	4.147	<0.001
Depth	0.077	0.061	10	1.269	0.233

f) 2014-16 Heat Blob Indicator Fish CTR

Random effects

~1| Island: 0.486
~1| Island/Site: 0.319
Residual: 0.634
AIC: 307.64

Variance function

Santa Barbara Island 1.000
Anacapa Island 0.903
Santa Cruz Island 1.041
Santa Rosa Island 1.749
San Miguel Island 1.669

LME	Estimated value	Std. Error	DF	t-value	p-value
Intercept	-0.089	0.257	98	-0.348	0.729
Before Heat Blob	0.319	0.140	98	2.277	0.025
After Heat Blob	-0.289	0.208	98	-1.387	0.169
Depth	0.193	0.109	10	1.772	0.107

Table S5. Summary table for statistical tests of response of warm- and cold- affinity fishes (a-d) and overall fish richness (e-f). We fit linear mixed effect models (LME, mgcv package) with the function lme in R. Random effects of site nested in island are included to account for the spatial structure of the data. Heat event status (before, during and after event) was included as a fixed effect, with years before and after the event contrasted against event years. A depth covariate was also included. Fixed effects were scaled for coefficient comparison. A variance function was included to model heteroscedasticity among the 5 islands. AIC = Akaine information criterion; Std. error = standard error.

a) 1997-98 El Niño – Richness of warm affinity fishes

Random effects

~1| Island:	0.147
~1| Island/Site:	0.172
Residual:	0.407
AIC:	224.89

Variance function

Santa Barbara Island	1.000
Anacapa Island	0.715
Santa Cruz Island	0.888
Santa Rosa Island	1.215
San Miguel Island	1.376

LME	Estimated value	Std. Error	DF	t-value	p-value
Intercept	-0.383	0.096	155	-3.971	<0.001
Before El Niño	-1.378	0.094	155	-14.729	<0.001
After El Niño	1.026	0.065	155	15.734	<0.001
Depth	-0.104	0.054	10	-1.930	0.083

b) 1997-98 El Niño – Richness of cold affinity fishes

Random effects

~1| Island:	0.220
~1| Island/Site:	0.115
Residual:	0.383
AIC:	144.71

Variance function

Santa Barbara Island	1.000
Anacapa Island	0.726
Santa Cruz Island	0.751
Santa Rosa Island	0.721

San Miguel Island 1.029

LME	Estimated value	Std. Error	DF	t-value	p-value
Intercept	-0.822	0.112	155	-7.358	<0.001
Before El Niño	-0437	0.075	155	-5.839	<0.001
After El Niño	1.680	0.052	155	32.174	<0.001
Depth	-0.058	0.039	10	-1.494	0.169

c) 2014-16 Heat Blob – Richness of warm affinity fishes

Random effects
~1| Island: 0.403
~1| Island/Site: <0.001
Residual: 0.926
AIC: 425.61

Variance function
Santa Barbara Island 1.000
Anacapa Island 1.213
Santa Cruz Island 1.029
Santa Rosa Island 0.802
San Miguel Island 0.764

LME	Estimated value	Std. Error	DF	t-value	p-value
Intercept	0.024	0.220	130	0.109	0.913
Before El Niño	-0.369	0.177	130	-2.088	0.039
After El Niño	0.008	0.178	130	0.046	0.963
Depth	-0.113	0.078	10	-1.443	0.180

d) 2014-16 Heat Blob – Richness of cold affinity fishes

Random effects
~1| Island: 0.591
~1| Island/Site: 0.203
Residual: 0.580
AIC: 369.47

Variance function
Santa Barbara Island 1.000
Anacapa Island 1.057
Santa Cruz Island 1.371

Santa Rosa Island 1.534
San Miguel Island 1.208

LME	Estimated value	Std. Error	DF	t-value	p-value
Intercept	0.132	0.288	130	0.457	0.648
Before El Niño	0.416	0.140	130	2.967	0.004
After El Niño	-0.648	0.141	130	-4.587	<0.001
Depth	0.004	0.083	10	0.043	0.967

e) 1997-98 El Niño – Overall fish richness

Random effects
~1| Island: 0.633
~1| Island/Site: 0.367
Residual: 0.697
AIC: 430.12

Variance function
Santa Barbara Island 1.000
Anacapa Island 0.837
Santa Cruz Island 1.102
Santa Rosa Island 1.136
San Miguel Island 0.944

LME	Estimated value	Std. Error	DF	t-value	p-value
Intercept	-0.161	0.314	155	-0.512	0.610
Before El Niño	0.030	0.172	155	0.177	0.860
After El Niño	0.262	0.120	155	2.182	0.031
Depth	-0.338	0.113	10	-3.003	0.013

f) 2014-16 Heat Blob – Overall fish richness

Random effects
~1| Island: 0.401
~1| Island/Site: 0.358
Residual: 0.760
AIC: 381.87

Variance function
Santa Barbara Island 1.000

Anacapa Island 0.937
Santa Cruz Island 1.112
Santa Rosa Island 0.741
San Miguel Island 1.053

LME	Estimated value	Std. Error	DF	t-value	p-value
Intercept	0.152	0.227	130	0.670	0.504
Before El Niño	0.234	0.145	130	1.616	0.108
After El Niño	-0.816	0.146	130	-5.585	<0.001
Depth	-0.117	0.116	10	-1.01	0.335

Table S6. Summary table for statistical tests of response of whole-community fish CTI across habitat types: sea urchin barrens (a, d), kelp forested sites (b, e) and patchy, mixed-habitat sites (c, f). We fit linear mixed effect models (LME, mgcv package) with the function lme in R. Random effects of site nested in island are included to account for the spatial structure of the data. Heat event status (before, during and after event) was included as a fixed effect, with years before and after the event contrasted against event years. A depth covariate was also included. Fixed effects were scaled for coefficient comparison. A variance function was included to model heteroscedasticity among the 5 islands. AIC = Akaine information criterion; Std. error = standard error.

a) 1997-98 El Niño – Fish CTI response in sea urchin barrens

Random effects
~1| Island: 1.367
~1| Island/Site: 0.266
Residual: 0.751
AIC: 156.21
Variance function
Santa Barbara Island 1.000
Santa Cruz Island 0.515
San Miguel Island 0.960
Number of Sites: 7

LME	Estimated value	Std. Error	DF	t-value	p-value
Intercept	-0.225	0.807	71	-0.279	0.781
Before El Niño	-0.518	0.162	71	-3.196	0.002
After El Niño	-0.277	0.116	71	-2.382	0.020

b) 1997-98 El Niño – Fish CTI response in kelp forests

Random effects
~1| Island: 1.202
~1| Island/Site: 0.073
Residual: 0.223
AIC: 82.55
Variance function
Anacapa Island 1.000
Santa Cruz Island 1.483
San Rosa Island 1.939
San Miguel Island 2.374
Number of Sites: 5

LME	Estimated value	Std. Error	DF	t-value	p-value
Intercept	0.139	0.609	45	0.228	0.821
Before El Niño	-0.167	0.153	45	-1.093	0.280
After El Niño	-0.255	0.103	45	-2.472	0.017

c) 1997-98 El Niño – Fish CTI response in mixed, patchy habitat

Random effects
~1| Island: 1.122
~1| Island/Site: <0.001
Residual: 0.504
AIC: 87.23
Variance function
Santa Barbara Island 1.000
Anacapa Island 1.002
San Rosa Island 0.988
Number of Sites: 4

LME	Estimated value	Std. Error	DF	t-value	p-value
Intercept	0.358	0.664	35	0.539	0.593
Before El Niño	-0.873	0.270	35	-3.239	0.003
After El Niño	-0.569	0.178	35	-3.186	0.003

d) 2014-16 Heat Blob – Fish CTI response in sea urchin barrens

Random effects
~1| Island: 1.123

~1| Island/Site: 0.183
Residual: 0.618
AIC: 118.64
Variance function
Santa Barbara Island 1.000
Santa Cruz Island 0.818
San Miguel Island 0.647
Number of Sites: 6

LME	Estimated value	Std. Error	DF	t-value	p-value
Intercept	-0.280	0.665	47	-0.422	0.675
Before El Niño	-0.493	0.172	47	-2.866	0.006
After El Niño	0.441	0.174	47	-2.529	0.015

e) 2014-16 Heat Blob – Fish CTI response in kelp forests

Random effects
~1| Island: 0.981
~1| Island/Site: 0.337
Residual: 0.475
AIC: 99.96
Variance function
Anacapa Island 1.000
Santa Cruz Island 0.550
San Rosa Island 1.012
San Miguel Island 0.754
Number of Sites: 6

LME	Estimated value	Std. Error	DF	t-value	p-value
Intercept	-0.034	0.520	48	-0.065	0.948
Before El Niño	-0.606	0.125	48	-4.861	<0.001
After El Niño	-0.275	0.128	48	2.147	0.037

f) 2014-16 Heat Blob – Fish CTI response in mixed, patchy habitat

Random effects
~1| Island: 0.847
~1| Island/Site: 0.181
Residual: 0.384
AIC: 78.58

Variance function

Anacapa Island	1.000
Santa Cruz Island	1.529
San Rosa Island	1.082
Number of Sites:	4

LME	Estimated value	Std. Error	DF	t-value	p-value
Intercept	-0.091	0.514	31	-0.177	0.861
Before El Niño	-0.612	0.185	31	-3.303	0.002
After El Niño	0.758	0.185	31	4.093	<0.001

Table S7. Summary table for statistical tests of response of indicator fish CTI across habitat types: sea urchin barrens (a, d), kelp forested sites (b, e) and patchy, mixed-habitat sites (c, f). We fit linear mixed effect models (LME, mgcv package) with the function lme in R. Random effects of site nested in island are included to account for the spatial structure of the data. Heat event status (before, during and after event) was included as a fixed effect, with years before and after the event contrasted against event years. A depth covariate was also included. Fixed effects were scaled for coefficient comparison. A variance function was included to model heteroscedasticity among the 5 islands. AIC = Akaine information criterion; Std. error = standard error.

a) 1997-98 El Niño – Indicator Fish CTI response in sea urchin barrens

Random effects

~1| Island:	1.130
~1| Island/Site:	0.280
Residual:	0.545
AIC:	238.17

Variance function

Santa Barbara Island	1.000
Santa Cruz Island	1.061
San Miguel Island	1.567
Number of Sites:	7

LME	Estimated value	Std. Error	DF	t-value	p-value
Intercept	0.149	0.676	102	0.220	0.826
Before El Niño	-0.319	0.145	102	-2.202	0.029
After El Niño	-0.560	0.145	102	-3.862	<0.001

b) 1997-98 El Niño – Indicator Fish CTI response in kelp forests

Random effects	
~1| Island:	0.419
~1| Island/Site:	0.733
Residual:	0.160
AIC:	155.80
Variance function	
Anacapa Island	1.000
Santa Cruz Island	3.652
San Rosa Island	3.960
San Miguel Island	5.917
Number of Sites:	5

LME	Estimated value	Std. Error	DF	t-value	p-value
Intercept	0.111	0.405	72	0.273	0.786
Before El Niño	-0.014	0.092	72	-0.156	0.877
After El Niño	-0.183	0.094	72	-1.953	0.055

c) 1997-98 El Niño – Indicator Fish CTI response in mixed, patchy habitat

Random effects	
~1| Island:	1.059
~1| Island/Site:	<0.001
Residual:	0.092
AIC:	83.03
Variance function	
Santa Barbara Island	1.000
Anacapa Island	4.298
San Rosa Island	12.460
Number of Sites:	4

LME	Estimated value	Std. Error	DF	t-value	p-value
Intercept	0.358	0.664	35	0.539	0.593
Before El Niño	-0.873	0.270	35	-3.239	0.003
After El Niño	-0.569	0.178	35	-3.186	0.003

d) 2014-16 Heat Blob – Indicator Fish CTI response in sea urchin barrens

Random effects
~1| Island: 0.760
~1| Island/Site: 0.337
Residual: 0.556
AIC: 144.23
Variance function
Santa Barbara Island 1.000
Santa Cruz Island 1.344
San Miguel Island 2.107
Number of Sites: 6

LME	Estimated value	Std. Error	DF	t-value	p-value
Intercept	-0.343	0.499	47	-0.688	0.495
Before El Niño	0.036	0.212	47	0.171	0.865
After El Niño	0.427	0.223	47	1.921	0.061

e) 2014-16 Heat Blob – Indicator Fish CTI response in kelp forests

Random effects
~1| Island: 0.458
~1| Island/Site: 0.325
Residual: 0.540
AIC: 139.61
Variance function
Anacapa Island 1.000
Santa Cruz Island 0.587
San Rosa Island 1.664
San Miguel Island 1.831
Number of Sites: 6

LME	Estimated value	Std. Error	DF	t-value	p-value
Intercept	-0.148	0.303	48	-0.487	0.628
Before El Niño	-0.386	0.173	48	-2.233	0.030
After El Niño	0.862	0.179	48	4.8199	<0.001

f) 2014-16 Heat Blob – Indicator Fish CTI response in mixed, patchy habitat

Random effects
~1| Island: <0.001

~1| Island/Site: 0.562
Residual: 0.596
AIC: 105.09
Variance function
Anacapa Island 1.000
Santa Cruz Island 0.994
San Rosa Island 1.960
Number of Sites: 4

LME	Estimated value	Std. Error	DF	t-value	p-value
Intercept	0.175	0.337	32	0.520	0.607
Before El Niño	-0.686	0.261	32	-2.629	0.013
After El Niño	0.217	0.261	32	0.831	0.412

Table S8. Summary table for statistical tests of response of fish trophic groups to two heat events. We fit linear mixed effect models (LME, mgcv package) with the function lme in R. Random effects of site nested in island are included to account for the spatial structure of the data. Heat event status (before, during and after event) was included as a fixed effect, with years before and after the event contrasted against event years. A depth covariate was also included. Fixed effects were scaled for coefficient comparison. A variance function was included to model heteroscedasticity among the 5 islands. AIC = Akaine information criterion; Std. error = standard error.

a) 1997-98 El Niño – Planktivore fish richness

Random effects
~1| Island: 0.465
~1| Island/Site: 0.522
Residual: 0.600
AIC: 423.20

Variance function
Santa Barbara Island 1.000
Anacapa Island 1.036
Santa Cruz Island 1.137
Santa Rosa Island 1.563
San Miguel Island 1.016

LME	Estimated value	Std. Error	DF	t-value	p-value
Intercept	0.025	0.264	155	0.095	0.924
Before El Niño	0.286	0.162	155	1.762	0.080
After El Niño	-0.220	0.115	155	-1.914	0.057
Depth	-0.305	0.146	10	-2.090	0.063

b) 1997-98 El Niño – Herbivore fish richness

Random effects

~1| Island:	0.366
~1| Island/Site:	0.570
Residual:	0.487
AIC:	319.86

Variance function

Santa Barbara Island	1.000
Anacapa Island	1.487
Santa Cruz Island	1.591
Santa Rosa Island	1.406

LME	Estimated value	Std. Error	DF	t-value	p-value
Intercept	0.094	0.261	115	0.360	0.719
Before El Niño	0.046	0.181	115	0.255	0.799
After El Niño	-0.248	0.126	115	-1.962	0.052
Depth	-0.357	0.170	10	-2.089	0.066

c) 1997-98 El Niño – Invertivore fish richness

Random effects

~1| Island:	0.622
~1| Island/Site:	0.315
Residual:	0.671
AIC:	432.13

Variance function

Santa Barbara Island	1.000
Anacapa Island	0.839
Santa Cruz Island	1.134
Santa Rosa Island	1.143

San Miguel Island 1.382

LME	Estimated value	Std. Error	DF	t-value	p-value
Intercept	-0.070	0.307	155	-0.228	0.819
Before El Niño	-0.005	0.173	155	-0.028	0.977
After El Niño	0.031	0.121	155	0.259	0.796
Depth	-0.412	0.102	10	-4.023	0.002

d) 1997-98 El Niño – Carnivore fish richness

Random effects
~1| Island: 0.776
~1| Island/Site: 0.273
Residual: 0.572
AIC: 381.89

Variance function
Santa Barbara Island 1.000
Anacapa Island 0.831
Santa Cruz Island 1.279
Santa Rosa Island 1.249
San Miguel Island 0.902

LME	Estimated value	Std. Error	DF	t-value	p-value
Intercept	-0.291	0.364	154	-0.799	0.425
Before El Niño	0.225	0.147	154	1.528	0.128
After El Niño	0.570	0.103	154	5.532	<0.001
Depth	0.079	0.089	10	0.887	0.398

e) 2014-16 Heat Blob – Planktivore fish richness

Random effects
~1| Island: 0.379
~1| Island/Site: 0.484
Residual: 0.580
AIC: 398.49

Variance function
Santa Barbara Island 1.000
Anacapa Island 1.221
Santa Cruz Island 1.570

Santa Rosa Island 1.608
San Miguel Island 1.388

LME	Estimated value	Std. Error	DF	t-value	p-value
Intercept	-0.058	0.238	128	-0.242	0.809
Before El Niño	0.097	0.154	128	0.631	0.529
After El Niño	-0.126	0.155	128	-0.816	0.416
Depth	-0.197	0.145	10	-1.369	0.204

f) 2014-16 Heat Blob – Herbivore fish richness

Random effects
~1| Island: <0.001
~1| Island/Site: 0.128
Residual: 0.969
AIC: 338.07

Variance function
Santa Barbara Island 1.000
Anacapa Island 0.782
Santa Cruz Island 0.958
Santa Rosa Island 1.131
San Miguel Island 2.005

LME	Estimated value	Std. Error	DF	t-value	p-value
Intercept	0.171	0.149	98	1.149	0.253
Before El Niño	-0.554	0.208	98	-2.660	0.009
After El Niño	0.111	0.205	98	0.539	0.591
Depth	-0.276	0.093	10	-2.954	0.016

g) 2014-16 Heat Blob – Invertivore fish richness

Random effects
~1| Island: 0.353
~1| Island/Site: 0.418
Residual: 1.013
AIC: 392.98

Variance function

Santa Barbara Island	1.000
Anacapa Island	0.675
Santa Cruz Island	0.830
Santa Rosa Island	0.565
San Miguel Island	0.723

LME	Estimated value	Std. Error	DF	t-value	p-value
Intercept	0.152	0.219	130	0.693	0.490
Before El Niño	0.098	0.148	130	0.661	0.510
After El Niño	-0.670	0.149	130	-4.493	<0.001
Depth	-0.193	0.128	10	-1.506	0.163

d) 2014-16 Heat Blob – Carnivore fish richness

Random effects

~1| Island:	0.340
~1| Island/Site:	0.367
Residual:	0.837
AIC:	367.18

Variance function

Santa Barbara Island	1.000
Anacapa Island	0.930
Santa Cruz Island	0.843
Santa Rosa Island	0.805
San Miguel Island	0.547

LME	Estimated value	Std. Error	DF	t-value	p-value
Intercept	0.221	0.225	130	0.985	0.326
Before El Niño	0.086	0.135	130	0.637	0.525
After El Niño	-0.745	0.136	130	-5.468	<0.001
Depth	0.227	0.113	10	2.014	0.072

Table S9. Summary table for statistical tests of response of fish activity groups to two marine heat events. We fit linear mixed effect models (LME, mgcv package) with the function lme in R. Random effects of site nested in island are included to account for the spatial structure of the data. Heat event status (before, during and after event) was included as a fixed effect, with years before and after the event

contrasted against event years. A depth covariate was also included. Fixed effects were scaled for coefficient comparison. A variance function was included to model heteroscedasticity among the 5 islands. AIC = Akaine information criterion; Std. error = standard error.

a) 1997-98 El Niño – Benthic fish richness

Random effects

~1| Island:	0.505
~1| Island/Site:	0.296
Residual:	0.743
AIC:	444.57

Variance function

Santa Barbara Island	1.000
Anacapa Island	0.825
Santa Cruz Island	1.105
Santa Rosa Island	1.252
San Miguel Island	0.791

LME	Estimated value	Std. Error	DF	t-value	p-value
Intercept	-0.100	0.259	155	-0.386	0.699
Before El Niño	-0.425	0.180	155	-2.368	0.019
After El Niño	0.090	0.126	155	0.717	0.475
Depth	-0.383	0.099	10	-3.886	0.003

b) 1997-98 El Niño – Demersal fish richness

Random effects

~1| Island:	0.380
~1| Island/Site:	0.418
Residual:	0.940
AIC:	457.76

Variance function

Santa Barbara Island	1.000
Anacapa Island	0.598
Santa Cruz Island	0.894
Santa Rosa Island	0.840
San Miguel Island	0.754

LME	Estimated value	Std. Error	DF	t-value	p-value
Intercept	-0.350	0.227	155	-1.544	0.125

Before El Niño	0.172	0.187	155	0.918	0.360
After El Niño	0.561	0.129	155	4.344	<0.001
Depth	-0.077	0.125	10	-0.617	0.551

c) 1997-98 El Niño – Pelagic fish richness

Random effects
~1| Island: 0.863
~1| Island/Site: 0.460
Residual: 0.489
AIC: 343.80

Variance function
Santa Barbara Island 1.000
Anacapa Island 1.183
Santa Cruz Island 1.009
Santa Rosa Island 1.641
San Miguel Island 1.217

LME	Estimated value	Std. Error	DF	t-value	p-value
Intercept	-0.014	0.413	142	-0.035	0.973
Before El Niño	0.143	0.139	142	1.027	0.306
After El Niño	-0.049	0.101	142	-0.487	0.627
Depth	-0.144	0.132	10	-1.095	0.299

d) 2014-16 Heat Blob – Benthic fish richness

Random effects
~1| Island: 0.366
~1| Island/Site: 0.369
Residual: 0.819
AIC: 401.37

Variance function
Santa Barbara Island 1.000
Anacapa Island 1.156
Santa Cruz Island 1.056
Santa Rosa Island 0.799
San Miguel Island 0.754

LME	Estimated value	Std. Error	DF	t-value	p-value
Intercept	0.024	0.220	130	0.111	0.912
Before El Niño	0.140	0.156	130	0.899	0.370
After El Niño	-0.429	0.157	130	-2.735	0.007
Depth	-0.231	0.119	10	-1.943	0.081

e) 2014-16 Heat Blob – Demersal fish richness

Random effects

~1| Island:	0.333
~1| Island/Site:	0.439
Residual:	0.835
AIC:	374.54

Variance function

Santa Barbara Island	1.000
Anacapa Island	0.802
Santa Cruz Island	0.856
Santa Rosa Island	0.779
San Miguel Island	0.849

LME	Estimated value	Std. Error	DF	t-value	p-value
Intercept	0.202	0.212	130	0.949	0.345
Before El Niño	0.146	0.142	130	1.031	0.305
After El Niño	-0.848	0.143	130	-5.920	<0.001
Depth	0.112	0.129	10	0.869	0.405

f) 2014-16 Heat Blob – Pelagic fish richness

Random effects

~1| Island:	0.335
~1| Island/Site:	0.511
Residual:	0.758
AIC:	395.94

Variance function

Santa Barbara Island	1.000
Anacapa Island	0.930
Santa Cruz Island	1.171
Santa Rosa Island	1.126
San Miguel Island	0.994

LME	Estimated value	Std. Error	DF	t-value	p-value
Intercept	0.197	0.229	125	0.863	0.390
Before El Niño	-0.162	0.163	125	-0.991	0.323
After El Niño	-0.557	0.163	125	-3.431	<0.001
Depth	-0.050	0.150	10	-0.331	0.748

Table S10. Summary table for sensitivity of statistical tests for response of whole-community fish CTI across habitat types: sea urchin barrens (a, d), kelp forested sites (b, e) and patchy, mixed-habitat sites (c, f). To test the robustness of overall results to the habitat classification threshold, we applied a higher threshold (6 urchins per m^2 and 100 kelp stipes) for classifying sites as barren or kelp. We fit linear mixed effect models (LME, mgcv package) with the function lme in R. Random effects of site nested in island are included to account for the spatial structure of the data. Marine heat event status (before, during and after event) was included as a fixed effect, with years before and after the event contrasted against event years. A depth covariate was also included. Fixed effects were scaled for coefficient comparison. A variance function was included to model heteroscedasticity among the 5 islands. AIC = Akaine information criterion; Std. error = standard error.

a) 1997-98 El Niño – Fish CTI response in sea urchin barrens

Random effects	
~1| Island:	0.178
~1| Island/Site:	0.439
Residual:	1.105
AIC:	162.64
Variance function	
Santa Barbara Island	1.000
Santa Cruz Island	0.595

LME	Estimated value	Std. Error	DF	t-value	p-value
Intercept	0.422	0.298	51	1.454	0.152
Before El Niño	-0.774	0.314	51	-2.460	0.017
After El Niño	-0.648	0.226	51	-2.865	0.006

b) 1997-98 El Niño – Fish CTI response in kelp forests

Random effects	
~1| Island:	0.989
~1| Island/Site:	0.087
Residual:	0.328
AIC:	90.88
Variance function	
Anacapa Island	1.000
Santa Cruz Island	1.503
Santa Rosa Island	1.938

LME	Estimated value	Std. Error	DF	t-value	p-value
Intercept	0.475	0.587	37	0.809	0.424
Before El Niño	0.133	0.238	37	0.559	0.579
After El Niño	-0.381	0.157	37	-2.420	0.021

c) 1997-98 El Niño – Fish CTI response in mixed, patchy habitat

Random effects	
~1| Island:	0.952
~1| Island/Site:	0.200
Residual:	0.325
AIC:	88.37
Variance function	
Santa Barbara Island	1.000
Anacapa Island	0.944
Santa Cruz Island	0.516
Santa Rosa Island	0.893
San Miguel Island	1.518

LME	Estimated value	Std. Error	DF	t-value	p-value
Intercept	0.261	0.438	63	0.597	0.552
Before El Niño	-0.496	0.104	63	-4.761	<0.001
After El Niño	-0.176	0.073	63	-2.402	0.019

d) 2014-16 Heat Blob – Fish CTI response in sea urchin barrens

Random effects	
~1| Island:	0.117
~1| Island/Site:	0.279
Residual:	0.822

AIC: 127.35
Variance function
Santa Barbara Island 1.000
Santa Cruz Island 0.912

LME	Estimated value	Std. Error	DF	t-value	p-value
Intercept	0.245	0.254	39	0.964	0.341
Before El Niño	-0.955	0.284	39	-3.365	0.002
After El Niño	0.304	0.289	39	1.052	0.299

e) 2014-16 Heat Blob – Fish CTI response in kelp forests

Random effects
~1| Island: 0.981
~1| Island/Site: 0.337
Residual: 0.475
AIC: 99.96
Variance function
Anacapa Island 1.000
Santa Cruz Island 0.550
San Rosa Island 1.012
San Miguel Island 0.754

LME	Estimated value	Std. Error	DF	t-value	p-value
Intercept	-0.034	0.520	48	-0.065	0.948
Before El Niño	-0.606	0.125	48	-4.861	<0.001
After El Niño	0.275	0.128	48	2.147	0.037

f) 2014-16 Heat Blob – Fish CTI response in mixed, patchy habitats

Random effects
~1| Island: 0.881
~1| Island/Site: 0.162
Residual: 0.329
AIC: 86.42
Variance function
Anacapa Island 1.000
Santa Cruz Island 1.686
San Rosa Island 1.229
San Miguel Island 0.987

LME	Estimated value	Std. Error	DF	t-value	p-value
Intercept	-0.210	0.458	39	-0.459	0.649
Before El Niño	-0.427	0.143	39	-2.991	0.005
After El Niño	0.772	0.143	39	5.414	<0.001

Chapter 6 – Overview, Synthesis and Future Directions

6.1 Overview

Understanding the factors that determine the abundance and distribution of organisms is a central goal of ecology. Community assembly is shaped by environmental factors that constrain individuals and species, as well as intra- and interspecific interactions and competition (MacArthur & Wilson 1967; Connor & Simberloff 1979; Strong *et al.* 1979). However, deciphering the precise ecological dynamics of community assembly is complex, especially in light of multifaceted environmental change. Trait-based approaches have improved our ability to disentangle community assembly and functioning (e.g., Lavorel & Garnier 2002; Kraft *et al.* 2008; Cadotte *et al.* 2009; Lebrija-Trejos *et al.* 2010), and community response to environmental change (Suding *et al.* 2008; Litchman *et al.* 2012; Green *et al.* 2022), by replacing taxonomic identities with individual or species attributes that link to organism physiology, functioning and behaviour (Steneck & Dethier 1994; Lavorel *et al.* 1997; Lambers *et al.* 2006). Trait-based approaches provide mechanistic insights into the trait-environment relationships that underpin the broad-scale geographic patterns of individuals and species that, in turn, form assemblages (McGill *et al.* 2006). This is because traits reflect phenotypic adaptations to different environments that promote fitness (Whittaker 1972). Resolving patterns of trait-environment relationships and intra- and inter-specific trait variation along environmental gradients can build predictive frameworks of community assembly in a changing world (Laughlin *et al.* 2012; Violle *et al.* 2012).

Even so, traditional traits approaches are limited because these approaches commonly assign broad ecological categories that can be inconsistent and imprecise (Funk *et al.* 2017; Mouillot *et al.* 2021).

Trait-based approaches that center around organism energetics are emerging as a promising framework to overcome some of the limitations of low-resolution, categorical traits (e.g., Anderson & Jetz 2005; Killen *et al.* 2010; Auer *et al.* 2018; Healy *et al.* 2019; Brandl *et al.* 2022). All organisms on Earth must acquire and assimilate free energy to fuel maintenance, growth and reproduction (Brown *et al.* 2004). Where, when and how energy can be obtained depends on environmental conditions (Hutchinson 1957; Hall *et al.* 1992), as well as interactions and competition (Clarke 1992; DeAngelis 1995; Seth *et al.* 2013; Brown *et al.* 2018). Thus, energy-based traits may lead to improved understanding of community assembly and functioning and allow predictions of how organisms respond to environmental change (Brandl *et al.* 2022).

My thesis demonstrates that abiotic environmental filters (temperature, habitat type and food availability) select for distinct traits that relate to energetics at multiple levels of biological organization. I show that the distribution of energetic traits (e.g., routine metabolic rate) varies predictably across environmental gradients in individuals and populations (Chapter 2 and Chapter 3). This work is novel because it demonstrates that populations host distinct phenotypes quantifiable as energetic units, and how these units use free energy relates to environmental conditions and change. In addition, I show that community assembly patterns can be deciphered based on realized niche traits that explain vulnerability to environmental change

(Chapter 4 and Chapter 5). Although energetic traits were not measured explicitly in Chapter 4 and Chapter 5, observed shifts in niche trait distribution (e.g., thermal affinities) under varying environmental conditions may be energetically underpinned. This is because species with defined environmental niches (e.g., warm vs. cold temperature affinity) are exposed to unique environmental conditions (e.g., warmer temperatures and less seasonal variation in the tropics compared to temperate regions) that impose distinct energetic regimes. Overall, this thesis provides new evidence that energy- and niche-based traits can provide a framework for understanding and predicting community assembly and response to environmental change that is applicable across numerous ecological contexts.

6.2 Chapter summaries

In Chapter 2 (Schuster *et al.* 2022), I tested whether adjacent sea urchin barrens and kelp beds select for individuals with certain energetic traits, creating distinct populations. I measured the temperature dependence of mass-independent oxygen consumption (routine metabolic rate) in green sea urchins from neighbouring barren and kelp habitats. I found that sea urchins from kelp habitats consumed more oxygen than sea urchins from barrens, across a nearly 30ºC temperature range. Sea urchins from kelp habitats were also less sensitive to increases in temperature. Thus, sea urchins from barren and kelp habitats of comparable body masses represent different energetic units. A question emerged from the results of Chapter 2: what drives physiological differences across habitat types mechanistically? Because food directly fuels metabolism, but macroalgae

food resources are scarce in sea urchin barrens, I hypothesized that food is the most likely driver of detected physiological differences.

In Chapter 3, I assessed if distinct physiologies in grazers from barren and kelp habitats could emerge due to low availability and quality of food using an experimental approach. I tested the energetic consequences of the loss of canopy-forming kelps as a food source by quantifying mass-independent oxygen consumption in two sea urchin species and two gastropod species. Specifically, I tested whether food type or food restriction alter the metabolic performance of grazing invertebrates, and whether lack of high-quality food impairs grazers ability to respond to environmental temperature stress. I found that both species of sea urchin depressed their metabolic rates after restricted food provisioning, while the gastropod species did not. Urchins were also more resistant to heat stress than the gastropods, although food type and availability had no strong impact on heat resistance in any of the species. Chapters 2 and 3 revealed that habitat type and food availability can select for certain energetic traits among individuals and populations. Chapter 3 also suggests that trait selection varies across species (e.g., two urchins depressed metabolism during macroalgae restrictions, but two gastropods did not). Next, I asked if habitat type filters for species with distinct niche traits, and in turn alters community assembly.

In Chapter 4 (Schuster *et al.* 2022), I broadened my perspective from populations to communities, and tested whether the signatures of climate warming occur differently in fish communities inhabiting kelp-covered reefs than those in sea urchin barrens. I quantified species realized thermal niches to calculate

community-level sensitivity to climate warming across habitat types in 15 temperate ecoregions. I found that fish communities differ in realized thermal affinities and range sizes between kelp and barren habitats, but only in regions where species pools have high response diversity. Barrens host relatively more warm-affinity fish species than neighbouring kelp habitats, highlighting that expanding sea urchin populations that overgraze kelps facilitate tropicalization processes in temperate regions. This work highlights that sea urchins are agents of seascape change, which 'filters' species towards assemblage structures that are more vulnerable to warming.

In Chapter 5, I tested whether large-scale patterns of habitat-dependent community tropicalization hold true through time. I quantified community changes during and after two severe marine heat events in a kelp forest ecosystem in the Pacific Northwest. I used species realized thermal niches to assess whether communities shift towards a more tropicalized composition during heat event years, mirroring community responses to long-term, gradual warming. I also tested whether heat event responses differ across reef sites that are kelp forested, and those that are sea urchin barrens. I found relatively more warm-affinity fishes during heat events, creating tropicalization signals that emerged more clearly at sites that are barrens than kelp. This work supports that marine heat events that occur in climatic transition zones, where northern (cool) and southern (warm) species mix, can trigger short-term tropicalization processes that mirror, and potentially accelerate, climate change driven range shifts of tropical species into temperate regions.

6.3 Synthesis

Looking across the chapters of the present thesis provides insights into energetic and niche trait restructuring across biological levels of organization (individual to community) in response to environmental change. I demonstrate trait restructuring in a system of sea urchin driven seascape change (Fig 6.1) and highlight below how several of the mechanisms at play in this particular system are also drivers of change in other terrestrial and aquatic systems. Sea urchins can overgraze habitat-forming kelps, creating barren reef seascapes that are devoid of macroalgae (Filbee-Dexter & Scheibling 2014; Filbee-Dexter & Wernberg 2018). Thus, kelp habitats transition from complex, food rich reefs to 'flat', food-deprived reefs (Filbee-Dexter & Scheibling 2014; Filbee-Dexter & Wernberg 2018). These sea urchin barrens support populations and communities with distinct trait distributions. For example, in Chapter 2, physiological traits varied across sea urchin populations found in barren and kelp-covered habitats. Sea urchins that inhabit kelp beds had higher metabolic rates across a range of temperatures tested, reached higher maximum metabolic rates, and were less sensitive to increases in temperature (Chapter 2). Sea urchins from barrens and kelp habitats thus represent distinct energetic units. Energy and nutrient intake (i.e., food) fuel metabolism, which ultimately controls all higher-order physiological and functional processes (Brown *et al.* 2004; Huey & Kingsolver 2019; Norin & Metcalfe 2019). Thus, the paucity of food (especially macroalgae/kelp) in barren seascapes is likely an important driver, setting energetic constraints on what types of individuals can persist there. Indeed, I found that two species of sea urchins enter a state of lowered metabolic rates

following prolonged macroalgae restrictions (Chapter 3). By contrast, urchins that were continuously fed macroalgae showed consistent metabolic performance over time. These findings mirror population-level differences from Chapter 2, that is, sea urchins from kelp beds, and those fed on macroalgae or kelp, had higher metabolic performance than sea urchins from barrens, and those that were unfed. Together, these findings highlight that loss of high quality food (kelp) alters physiological performance, and constrains what traits are present on rocky reef habitats. This work is novel because I demonstrate that habitat type and food resources select distinct phenotypes in the wild. This has broad implications given that food resource limitations and habitat degradation occur in many ecosystems and contexts. For example, mammal and bird predators are impacted by collapsed forage fish populations (Beverton 1990; Cury *et al.* 2011; Essington *et al.* 2015). Similarly, rapid declines in tropical arthropods (including insects) due to climate warming drive synchronous declines in their lizard, frog and bird predators (Lister & Garcia 2018). In addition, many complex habitats are threatened: forests are logged (Laurance 1999; Kreutzweiser et al. 2008), coral reefs are degrading (Hughes 1994; Pandolfi et al. 2003), and wetlands are converted for agricultural use (Lougheed et al. 2008; Davidson 2014).

Interestingly, not all species exhibited distinct physiological traits in response to food limitations (i.e., no population-level variation in two gastropod species in Chapter 3). Selection of phenotypes with lower metabolic performance and thus lower net energy gain in food limited or degraded environments could ultimately

move populations towards lower growth and fitness (Huey & Kingsolver 2019). By contrast, high metabolic rates demand more energy consumption, which can necessitate heightened activity (Nilsson 2002; Pettersen *et al.* 2016), with possible consequences for interactions with other species. For example, populations of two interacting species may respond in opposite directions, or at different rates, which can alter interaction strengths and competition for resource. Selection of certain energetic types, thus, will influence community assembly and functioning.

An open question is how trait filtering across environmental gradients scales up to higher levels of organization. To clarify this, I applied a backwards approach by constructing species' realized niches based on observed distributions in space. I identified which niche traits are filtered among communities from kelp or barren habitats. In Chapter 4, I found sea urchin barrens host fish communities with distinct thermal affinities and range sizes, compared to communities from nearby kelp habitats. The transition from kelp forest to barrens ultimately changes the energetic landscape (where, when and how organisms can acquire and assimilate energy resources) on rocky reefs. It appears that the species that persist in barrens in warm-temperate regions are typical of more tropical regions (i.e., have warmer affinities), perhaps because the energetic and thermal niche adaptations of species typical of tropical coral reefs are better matched for barren conditions than kelp-adapted species. Species with warmer distributions (i.e., more tropical) have more metabolic scope at high temperatures, outcompeting species with cooler distributions that have lower scope at high temperatures (Seth *et al.* 2013). These

same tropical species may prefer barrens because the exposed rock features of barrens are more similar to tropical reefs than kelp-covered areas, which are absent in the tropics.

Other dimensions of species functioning can further explain environmental trait filtering. For example, in Chapter 5, I found that marine heat event-related increases in community temperature index (CTI), which were most pronounced at urchin barrens, relate to increases in benthic fishes. Benthic fish dwell near the seafloor and are generally less consistently active than demersal or pelagic fishes. Fishes living in the water column (demersal/pelagic) have higher standard and maximum metabolic rates than fishes dwelling on the bottom (Killen *et al.* 2016). Moreover, fewer carnivore and invertivore fishes were observed during heat event years in Chapter 5. Previous work shows that in a comparison of two small reef fishes, the species with a more active foraging style and higher proportion of animal prey in its gut has a higher metabolic rate than its less active, herbivorous counterpart (Brandl *et al.* 2021). Links between diet or activity level and metabolism/energetics are well supported (Costa 1993; Clarke 1999; Cruz-Neto & Bozinovic 2004; Fu *et al.* 2009; Killen *et al.* 2016). If different habitat types select for distinct functional traits that are underpinned by energetic traits, then an energy-based framework may be able to explain community dynamics and responses to environmental change. However, further conceptual and empirical advances are needed to clarify these linkages (but see: Brandl *et al.* 2022).

Habitat-dependent assemblage responses to warming (both gradual and acute) emerge throughout this thesis (Fig 6.1). Across a range of scales, I demonstrate that kelp covered reefs may be more resistant to temperature-related changes in population and community structure. For example, differences in responses to warming across habitat types emerged among individuals and populations at the physiological level. In Chapter 2, the metabolic rate of sea urchins from barren habitats was more sensitive to increases in temperature (i.e., higher Q_{10} values) than those from kelp habitats. Surprisingly, in Chapter 3, food availability and quality were weakly linked with heat-sensitivity in two species of sea urchin (but see Future Directions). Moreover, kelp covered reefs appeared more resistant to changes in fish community structure associated with gradual warming, while sea urchin barrens were associated with relatively increased tropicalization of fish communities at the equatorward edge of temperate regions (Chapter 4). In addition, the abundance and occurrence of species with warmer affinities increased in response to two severe marine heat events, and this increase was most pronounced at sea urchin barren sites in Chapter 5. Therefore, the expansion of sea urchin barrens can accelerate tropicalization processes across space, driven by gradual climatic warming (Chapter 4) or over time, in response to acute, extreme heat events (Chapter 5). Similar shifts following land-use change in terrestrial systems are emerging (e.g., Williams *et al.* 2019; Williams & Newbold 2020), but typically are associated with *in situ* warming linked to the land-use change (e.g., loss of shade in deforested areas). Interestingly, directionally similar processes take place following urchin overgrazing of kelps, but independently of

any potential differences in *in situ* temperature between barren and kelp sites. Habitat-dependent assemblage responses emerge clearest in regions with high response diversity among the species pool (i.e., species with high thermal diversity and narrow thermal ranges; Chapter 4), as are often found in biogeographic transition zones (Chapter 5). Overall, I demonstrate that sea urchins hold unique ecological roles within assemblages, by driving seascape change that systematically alters responses of individuals and species to temperature. Invasive species may prove analogous to sea urchins in this context, as many invasive species alter the environment around them (Fei *et al.* 2014).

Protecting and restoring complex habitats, such as kelp forests, may offer important opportunities for building climate resilience in seascapes. Indeed, complex habitats may have similar effects to marine protected areas by preserving phenotypic and response diversity (Bates *et al.* 2019). Overall, my results suggest that healthy (intact) kelp forests can offer spatial refugia against warming over the next few decades, by harbouring more resilient individuals and species in natural systems. Expanding sea urchin barrens, on the other hand, threaten the phenotypes and species that thrive in kelp habitats, eroding the response diversity that insures against environmental disturbance. Protecting and restoring kelp forests, and by extension, other complex, foundational habitats, thus emerges as a conservation and management priority. Management strategies could include actions such as protecting/maintaining existing kelp habitats and restoring kelp forests where they previously existed. Establishing Marine Protected Areas around kelp forests could protect and maintain forests by allowing the recovery of top

predators that naturally control sea urchin populations (Estes *et al.* 1998; Shears & Babcock 2002) and minimizing boat entanglements that dislodge kelp stipes. Additionally, several methods are currently being explored to maintain and restore kelp forests, including, for example, transplanting and seeding kelp (e.g., green gravel (Fredriksen *et al.* 2020)), or grazer control through well-regulated, manual removal of urchins. Past and current efforts towards protecting and restoring kelp forests are reviewed in Layton *et al.* (2020) and Eger *et al.* (2022). Even so, persistence of kelps will ultimately hinge on reducing environmental stressors (cutting carbon emissions and reducing pollution).

High

Habitat Complexity filters traits

Low

Chapter 2

Food availability & quality filters traits

Chapter 3

Physiological Performance

Temperature

Temperature

≠

Kelp and urchin barren habitats host populations with distinct physiologies (Chapter 2). Physiology is altered by food (Chapter 3), which varies across habitat types, and likely is an important environmental filter as kelp forests transition to barrens.

Fundamental traits & niches

Temperature shifts trait patterns in space

Chapter 4

Temperature shifts trait patterns in time

Chapter 5

Species thermal affinities & ranges

Temperature

Temperature

Kelp and urchin barren habitats host communities with distinct realized thermal affinities and range sizes, leading to habitat-dependent sensitivities to warming across large spatial scales (Chapter 4), and through time (Chapter 5)

Realized niches

Figure 6.1 Overview of the main findings reported in this thesis. Sea urchin overgrazing of kelp forests restructures habitats, leading to changes in trait diversity and assemblage structure in shallow marine populations and communities. Traits based on fundamental and realized niches are useful to detect animal responses to habitat and temperature change at different scales of biological organization. Photos of sea urchin barren and kelp forest licenced under CC BY 2.0.

6.3.1 Future directions

This thesis demonstrates that loss of kelp and transition to sea urchin barrens can reshuffle the trait diversity and assemblage structure of shallow reefs. Building on this work, I identify some directions of future research that can improve our understanding of the consequences of complex habitat loss in a warming world.

An important finding of this thesis is that habitat type and warming select for certain phenotypes and species that appear to be linked to energetics (i.e., kelp loss and warming filter for distinct energetic performers). Establishing the generality (across species and ecological contexts) of this pattern is a key future direction. Do populations in less complex, food deprived habitats generally show lower metabolic performance? Is selection of low metabolic rate phenotypes consistent across different species? How does this impact community assembly (competition, predator-prey interactions etc.)? If habitat complexity consistently produces energetic sub-units within species in other systems, these units could be integrated into energy-based forecasting approaches. Energetic models (e.g., the metabolic theory of ecology or dynamic energy budget models) provide promising frameworks for predicting organisms' vulnerability to climate change (Kooijman

1986; Peck & Buckley 2008; Freitas *et al.* 2010; Kearney & White 2012). Yet, most energetic models are average-based, predicting species' mean responses (Saito *et al.* 2021). If energetic sub-units emerge consistently across habitat gradients, such relationships could be integrated into energetic models and explain variation around species' mean responses.

Furthermore, modelling the flow of energy across barren and kelp systems, as well as constructing habitat-specific food webs, would be useful to understand and predict the consequences of kelp loss in terms of productivity. Although previous work has estimated how much productivity is lost due to kelp disappearance *per se* (e.g., Filbee-Dexter & Wernberg 2020; Castorani *et al.* 2021), what is less clear is how the filtering of certain energetic traits among reef inhabitants may alter energy flows across ecosystems.

An additional future goal is to establish whether natural, complex habitats generally provide greater resilience to environmental change than disrupted, low-complexity habitats. That is, do other complex habitats such as coral reefs, seagrass beds or terrestrial forests provide similar protection mechanisms? In terrestrial systems, evidence of the former is emerging (Kampichler *et al.* 2012; De Frenne *et al.* 2013; Williams *et al.* 2019), but gaps remain, especially in the marine realm.

In Chapter 3 I found that food availability and quality can constrain the physiological performance of some grazing invertebrates. Future experimental work could build on the findings of this Chapter and provide greater inference on aspects of this work through some changes in experimental design. For example, tagging individuals in a feeding trial to allow paired observations at various time points of

the same individuals could yield more insights on physiological responses to food limitations without losing information through averaging. Additional response measurements at more time-points along feeding trials (including before feeding trials start, and over longer timespans) could determine the time required for metabolic differences to emerge across treatments. A longer duration of feeding trials may also reveal physiological differences in non-urchin species. Similarly, alternative response measures following food and heat stress treatments may also show larger differences across species and treatments (e.g., condition index, expression of heat shock proteins, growth rates). This could clarify how physiological heat sensitivity is altered across food gradients. Strong links between food availability/quality and temperature sensitivity have been identified in other organisms and contexts (Boersma *et al.* 2008; O'Connor *et al.* 2009; Huey & Kingsolver 2019).

6.4 Final remarks

In this thesis, I have addressed knowledge gaps in how environmental gradients filter the distribution of energetic traits and environmental niches to shape assembly structure. I combined experimental approaches and comprehensive field surveys to quantify how populations and species respond to environmental change. I demonstrated that habitat type, food limitations and temperature select for distinct phenotypes among individuals, populations (Chapter 2 and 3) and species (Chapter 4 and 5). I also show that directional filtering of energetic- and niche traits in low complexity, food depauperate systems has consequences for the resilience of biological systems to environmental disturbance. Human activity

is impacting natural systems across the planet, and understanding the consequences thereof is an era-defining challenge. Frameworks centering around energetic traits and environmental niches applied throughout this thesis help improve our ability to understand and predict changes in biodiversity patterns on Earth.

6.5 References

Anderson, K.J. & Jetz, W. (2005). The broad-scale ecology of energy expenditure of endotherms. *Ecol. Lett.*, 8, 310–318.

Auer, S.K., Dick, C.A., Metcalfe, N.B. & Reznick, D.N. (2018). Metabolic rate evolves rapidly and in parallel with the pace of life history. *Nat. Commun.*, 9, 14.

Bates, A.E., Cooke, R.S.C., Duncan, M.I., Edgar, G.J., Bruno, J.F., Benedetti-Cecchi, L., *et al.* (2019). Climate resilience in marine protected areas and the 'Protection Paradox.' *Biol. Conserv.*, 236, 305–314.

Beverton, R.J.H. (1990). Small marine pelagic fish and the threat of fishing; are they endangered? *J. Fish Biol.*, 37, 5–16.

Boersma, M., Aberle, N., Hantzsche, F., Schoo, K., Wiltshire, K. & Malzahn, A. (2008). Nutritional Limitation Travels up the Food Chain. *Int. Rev. Hydrobiol.*, 93, 479–488.

Brandl, S., Quigley, C.N., Casey, J., Mercière, A., Schiettekatte, N.M.D., Norin, T., *et al.* (2021). Metabolic rates mirror morphological and behavioral differences in two sand-dwelling coral reef gobies. *Mar. Ecol. Prog. Ser.*, 684.

Brandl, S.J., Lefcheck, J.S., Bates, A.E., Rasher, D.B. & Norin, T. (2022). Can metabolic traits explain animal community assembly and functioning? *Biol. Rev.*, n/a.

Brown, J., Hall, C. & Sibly, R. (2018). Equal fitness paradigm explained by a trade-off between generation time and energy production rate. *Nat. Ecol. Evol.*, 2.

Brown, J.H., Gillooly, J.F., Allen, A.P., Savage, V.M. & West, G.B. (2004). Toward a metabolic theory of ecology. *Ecology*, 85, 1771–1789.

Cadotte, M.W., Cavender-Bares, J., Tilman, D. & Oakley, T.H. (2009). Using Phylogenetic, Functional and Trait Diversity to Understand Patterns of Plant Community Productivity. *PLoS One*, 4, e5695.

Castorani, M.C.N., Harrer, S.L., Miller, R.J. & Reed, D.C. (2021). Disturbance structures canopy and understory productivity along an environmental gradient. *Ecol. Lett.*, 24, 2192–2206.

Clarke, R. (1999). Diets and metabolic rates of four Caribbean tube blennies, genus *Acanthemblemaria* (Teleostei: Chaenopsidae). *Bull. Mar. Sci.*, 65, 185–199.

Clarke, R.D. (1992). Effects of microhabitat and metabolic rate on food intake, growth and fecundity of two competing coral reef fishes. *Coral Reefs*, 11, 199–205.

Connor, E.F. & Simberloff, D. (1979). The Assembly of Species Communities: Chance or Competition? *Ecology*, 60, 1132–1140.

Costa, D. (1993). The relationship between reproductive and foraging energetics and the evolution of Pinnipedia. In: *Marine Mammals: Advances in Behavioural and Population Biology*. pp. 293–314.

Cruz-Neto, A.P. & Bozinovic, F. (2004). The Relationship between Diet Quality and Basal Metabolic Rate in Endotherms: Insights from Intraspecific Analysis. *Physiol. Biochem. Zool.*, 77, 877–889.

Cury, P.M., Boyd, I.L., Bonhommeau, S., Anker-Nilssen, T., Crawford, R.J.M., Furness, R.W., *et al.* (2011). Global Seabird Response to Forage Fish

Depletion—One-Third for the Birds. *Science (80-.).*, 334, 1703–1706.

Davidson, N.C. (2014). How much wetland has the world lost? Long-term and recent trends in global wetland area. *Mar. Freshw. Res.*, 65, 934–941.

DeAngelis, D.L. (1995). Relationships Between the Energetics of Species and Large-Scale Species Richness BT - Linking Species & Ecosystems. In: (eds. Jones, C.G. & Lawton, J.H.). Springer US, Boston, MA, pp. 263–272.

Essington, T.E., Moriarty, P.E., Froehlich, H.E., Hodgson, E.E., Koehn, L.E., Oken, K.L., *et al.* (2015). Fishing amplifies forage fish population collapses. *Proc. Natl. Acad. Sci.*, 112, 6648–6652.

Estes, J.A., Tinker, M.T., Williams, T.M. & Doak, D.F. (1998). Killer whale predation on sea otters linking oceanic and nearshore ecosystems. *Science*, 282, 473–476.

Fei, S., Phillips, J. & Shouse, M. (2014). Biogeomorphic Impacts of Invasive Species. *Annu. Rev. Ecol. Evol. Syst.*, 45, 69–87.

Filbee-Dexter, K. & Scheibling, R. (2014). Sea urchin barrens as alternative stable states of collapsed kelp ecosystems. *Mar. Ecol. Prog. Ser.*, 495, 1–25.

Filbee-Dexter, K. & Wernberg, T. (2018). Rise of Turfs: A New Battlefront for Globally Declining Kelp Forests. *Bioscience*, 68, 64–76.

Filbee-Dexter, K. & Wernberg, T. (2020). Substantial blue carbon in overlooked Australian kelp forests. *Sci. Rep.*, 10, 12341.

Fredriksen, S., Filbee-Dexter, K., Norderhaug, K.M., Steen, H., Bodvin, T., Coleman, M.A., *et al.* (2020). Green gravel: a novel restoration tool to combat kelp forest decline. *Sci. Rep.*, 10, 3983.

Freitas, V., Cardoso, J.F.M.F., Lika, K., Peck, M.A., Campos, J., Kooijman, S.A.L.M., *et al.* (2010). Temperature tolerance and energetics: a dynamic energy budget-based comparison of North Atlantic marine species. *Philos. Trans. R. Soc. B Biol. Sci.*, 365, 3553–3565.

De Frenne, P., Rodríguez-Sánchez, F., Coomes, D.A., Baeten, L., Verstraeten, G., Vellend, M., *et al.* (2013). Microclimate moderates plant responses to macroclimate warming. *Proc. Natl. Acad. Sci.*, 110, 18561–18565.

Fu, S.-J., Zeng, L.-Q., Li, X.-M., Pang, X., Cao, Z.-D., Peng, J.-L., *et al.* (2009). The behavioural, digestive and metabolic characteristics of fishes with different foraging strategies. *J. Exp. Biol.*, 212, 2296–2302.

Funk, J.L., Larson, J.E., Ames, G.M., Butterfield, B.J., Cavender-Bares, J., Firn, J., *et al.* (2017). Revisiting the Holy Grail: using plant functional traits to understand ecological processes. *Biol. Rev.*, 92, 1156–1173.

Green, S.J., Brookson, C.B., Hardy, N.A. & Crowder, L.B. (2022). Trait-based approaches to global change ecology: moving from description to prediction. *Proc. R. Soc. B Biol. Sci.*, 289, 20220071.

Hall, C.A.S., Stanford, J.A. & Hauer, F.R. (1992). The Distribution and Abundance of Organisms as a Consequence of Energy Balances along Multiple Environmental Gradients. *Oikos*, 65, 377–390.

Healy, K., Ezard, T.H.G., Jones, O.R., Salguero-Gómez, R. & Buckley, Y.M. (2019). Animal life history is shaped by the pace of life and the distribution of age-specific mortality and reproduction. *Nat. Ecol. Evol.*, 3, 1217–1224.

Huey, R.B. & Kingsolver, J.G. (2019). Climate Warming, Resource Availability, and the Metabolic Meltdown of Ectotherms. *Am. Nat.*, 194, E140–E150.

Hughes, T.P. (1994). Catastrophes, Phase Shifts, and Large-Scale Degradation of a Caribbean Coral Reef. *Science*, 265, 1547–1551.

Hutchinson, G.E. (1957). Concluding Remarks. *Cold Spring Harb. Symp. Quant. Biol.*

Kampichler, C., Van Turnhout, C.A.M., Devictor, V. & Van Der Jeugd, H.P. (2012). Large-scale changes in community composition: determining land use and climate change signals. *PLoS One*, 7, e35272.

Kearney, M.R. & White, C.R. (2012). Testing Metabolic Theories. *Am. Nat.*, 180, 546–565.

Killen, S.S., Atkinson, D. & Glazier, D.S. (2010). The intraspecific scaling of metabolic rate with body mass in fishes depends on lifestyle and temperature. *Ecol. Lett.*, 13, 184–193.

Killen, S.S., Glazier, D.S., Rezende, E.L., Clark, T.D., Atkinson, D., Willener, A.S.T., *et al.* (2016). Ecological Influences and Morphological Correlates of Resting and Maximal Metabolic Rates across Teleost Fish Species. *Am. Nat.*, 187, 592–606.

Kooijman, S.A.L.M. (1986). Energy budgets can explain body size relations. *J. Theor. Biol.*, 121, 269–282.

Kraft, N.J.B., Valencia, R. & Ackerly, D.D. (2008). Functional Traits and Niche-Based Tree Community Assembly in an Amazonian Forest. *Science*, 322, 580–582.

Kreutzweiser, D.P., Hazlett, P.W. & Gunn, J.M. (2008). Logging impacts on the biogeochemistry of boreal forest soils and nutrient export to aquatic systems: A review. *Environ. Rev.*, 16, 157–179.

Lambers, H., Shane, M.W., Cramer, M.D., Pearse, S.J. & Veneklaas, E.J. (2006). Root Structure and Functioning for Efficient Acquisition of Phosphorus: Matching Morphological and Physiological Traits. *Ann. Bot.*, 98, 693–713.

Laughlin, D.C., Joshi, C., van Bodegom, P.M., Bastow, Z.A. & Fulé, P.Z. (2012). A predictive model of community assembly that incorporates intraspecific trait variation. *Ecol. Lett.*, 15, 1291–1299.

Laurance, W.F. (1999). Reflections on the tropical deforestation crisis. *Biol. Conserv.*, 91, 109–117.

Lavorel, S. & Garnier, É. (2002). Predicting changes in community composition and ecosystem functioning from plant traits: revisiting the Holy Grail. *Funct.*

Ecol., 16, 545–556.

Lavorel, S., McIntyre, S., Landsberg, J. & Forbes, T.D.A. (1997). Plant functional classifications: from general groups to specific groups based on response to disturbance. *Trends Ecol. Evol.*, 12, 474–478.

Lebrija-Trejos, E., Pérez-García, E.A., Meave, J.A., Bongers, F. & Poorter, L. (2010). Functional traits and environmental filtering drive community assembly in a species-rich tropical system. *Ecology*, 91, 386–398.

Lister, B.C. & Garcia, A. (2018). Climate-driven declines in arthropod abundance restructure a rainforest food web. *Proc. Natl. Acad. Sci.*, 115, E10397–E10406.

Litchman, E., Edwards, K.F., Klausmeier, C.A. & Thomas, M.K. (2012). Phytoplankton niches, traits and eco-evolutionary responses to global environmental change. *Mar. Ecol. Prog. Ser.*, 470, 235–248.

Lougheed, V.L., Mcintosh, M.D., Parker, C.A. & Stevenson, R.J.A.N. (2008). Wetland degradation leads to homogenization of the biota at local and landscape scales. *Freshw. Biol.*, 53, 2402–2413.

MacArthur, R.H. & Wilson, E.O. (1967). *The theory of island biogeography: monographs in population biology*. Princeton University Press, Princeton.

McGill, B.J., Enquist, B.J., Weiher, E. & Westoby, M. (2006). Rebuilding community ecology from functional traits. *Trends Ecol. Evol.*, 21, 178–185.

Mouillot, D., Loiseau, N., Grenié, M., Algar, A.C., Allegra, M., Cadotte, M.W., *et al.* (2021). The dimensionality and structure of species trait spaces. *Ecol. Lett.*, 24, 1988–2009.

Nilsson, J. (2002). Metabolic consequences of hard work. *Proc. R. Soc. London. Ser. B Biol. Sci.*, 269, 1735–1739.

Norin, T. & Metcalfe, N.B. (2019). Ecological and evolutionary consequences of metabolic rate plasticity in response to environmental change. *Philos. Trans.*

R. Soc. B Biol. Sci., 374, 20180180.

O'Connor, M.I., Piehler, M.F., Leech, D.M., Anton, A. & Bruno, J.F. (2009). Warming and Resource Availability Shift Food Web Structure and Metabolism. *PLOS Biol.*, 7, e1000178.

Pandolfi, J.M., Bradbury, R.H., Sala, E., Hughes, T.P., Bjorndal, K.A., Cooke, R.G., *et al.* (2003). Global Trajectories of the Long-Term Decline of Coral Reef Ecosystems. *Science*, 301, 955–958.

Peck, M.A. & Buckley, L.J. (2008). Measurements of larval Atlantic cod (*Gadus morhua*) routine metabolism: temperature effects, diel differences and individual-based modeling. *J. Appl. Ichthyol.*, 24, 144–149.

Pettersen, A.K., White, C.R. & Marshall, D.J. (2016). Metabolic rate covaries with fitness and the pace of the life history in the field. *Proc. R. Soc. B Biol. Sci.*, 283, 20160323.

Saito, V.S., Perkins, D.M. & Kratina, P. (2021). A Metabolic Perspective of Stochastic Community Assembly. *Trends Ecol. Evol.*, 36, 280–283.

Seth, H., Gräns, A., Sandblom, E., Olsson, C., Wiklander, K., Johnsson, J.I., *et al.* (2013). Metabolic Scope and Interspecific Competition in Sculpins of Greenland Are Influenced by Increased Temperatures Due to Climate Change. *PLoS One*, 8, e62859.

Shears, N.T. & Babcock, R.C. (2002). Marine reserves demonstrate top-down control of community structure on temperate reefs. *Oecologia*, 132, 131–142.

Steneck, R.S. & Dethier, M.N. (1994). A functional group approach to the structure of algal-dominated communities. *Oikos*, 476–498.

Strong, D.R., Szyska, L.A. & Simberloff, D.S. (1979). Test of community-wide character displacement against null hypotheses. *Evolution (N. Y).*, 897–913.

Suding, K.N., Lavorel, S., Chapin Iii, F.S., Cornelissen, J.H.C., Díaz, S., Garnier, E., *et al.* (2008). Scaling environmental change through the community-level:

A trait-based response-and-effect framework for plants. *Glob. Chang. Biol.*, 14, 1125–1140.

Violle, C., Enquist, B.J., McGill, B.J., Jiang, L.I.N., Albert, C.H., Hulshof, C., *et al.* (2012). The return of the variance: intraspecific variability in community ecology. *Trends Ecol. Evol.*, 27, 244–252.

Whittaker, R.H. (1972). Evolution and measurement of species diversity. *Taxon*, 21, 213–251.

Williams, J.J., Bates, A.E. & Newbold, T. (2019). Human-dominated land uses favour species affiliated with more extreme climates, especially in the tropics. *Ecography (Cop.).*, 43, 391–405.

Williams, J.J. & Newbold, T. (2020). Local climatic changes affect biodiversity responses to land use: A review. *Divers. Distrib.*, 26, 76–92.

Appendix F – Biodiversity Surveys of Shallow Rocky Reefs

Reef Life Survey Canada – standardized biodiversity surveys

Over the course of this PhD (2018 to present), I have led a team of scientific divers that form the Canadian branch of Reef Life Survey (RLS; https://reeflifesurvey.com/). Reef Life Survey is an international program in which highly trained scientific divers undertake standardized visual surveys of biodiversity on shallow rocky reefs around the world. RLS Canada was first launched in St. John's, Newfoundland by Dr. Amanda Bates and me in 2018. Since then, I have led survey efforts on the Canadian east (Newfoundland; 2018 to present) and west coast (British Columbia; 2021 to present). The surveys I conduct actively contribute to the global RLS program, through which the data are freely available to the public. Reef Life Survey data has been an integral part of this thesis and is used in Chapters 4 and 5. An overview of the survey metadata is provided in supplementary table S1, and the survey data are included in a full version of this appendix (supplementary tables S2-7), available on GitHub (https://github.com/jmschuster/RLS-Canada-Data.git).

Table S1. Overview of Reef Life Survey transects completed throughout the duration of this PhD (2018 – 2022). Standardized visual surveys were undertaken on shallow rocky reefs (5-10m depth), where mobile invertebrates and fishes were identified, counted and sized, and habitat photos were taken for substrate composition. Numbers of species and individuals indicate the sum of invertebrate and fish counts.

Year	Province	# of surveys	# of species	# of individuals
2018	Newfoundland	5	25	27,441
2019	Newfoundland	13	35	46,511
2020	Newfoundland	16	35	129,937
2021	Newfoundland	5	26	34,355
2021	British Columbia	22	82	18,949
2022	Newfoundland	6	26	16,925
2022	British Columbia	23	102	21,867
Total		**90**	**137**	**295,985**